2023

Source Separation, Frequency Dynamics and Lighting Dependency of Electrophosphenes in Human Vision

Ian Douglas Evans

UNIVERSITY
OF WOLLONGONG
AUSTRALIA

Source Separation, Frequency Dynamics and Lighting Dependency of Electrophosphenes in Human Vision

Ian Douglas Evans

Supervisors:

Rodney J. Croft and Stephen Palmisano

This thesis is presented as part of the requirement for the conferral of the degree:

Doctor of Philosophy

This research has been conducted with the support of the Australian Government Research Training Program Scholarship

University of Wollongong, School of Psychology

March, 2023

ABSTRACT

Exposure to electromagnetic fields (EMF) can produce illusory perceptions of light referred to as phosphenes. Various exposure guidelines around the world use phosphene perception as an indicator that environmental EMF may be affecting the central nervous system, however many of them are based on low quality legacy literature. While exposure guidelines should consider all commonly encountered ambient lighting conditions, there are no studies examining electrophosphenes in commonly encountered mesopic (i.e., dim) lighting conditions. As a result, conclusions drawn from these guidelines may not be reliable or encompass all plausible EMF exposure conditions. Additionally, the roles of the retina and visual cortex in electrophosphene generation have not yet been adequately separated. Given the importance of understanding the effects of EMF exposure on human health, it is crucial to investigate the factors that affect sensitivity to phosphenes in a rigorous and systematic manner. This thesis examined the effects of transcranial electrical stimulation (tES) using different electrode placements, stimulation parameters, and ambient lighting conditions on phosphene detection thresholds using a large sample size, as well as robust experimental and analytical techniques. Detection thresholds across the three experiments (presented in Chapters 2 – 4) showed that up to 74% less current had to be applied to induce phosphenes in mesopic conditions compared to well-lit and dark conditions, indicating that existing guidelines have used relatively insensitive scenarios to determine safe levels of EMF exposure. Lower phosphene detection thresholds in frontal montages suggested that the retina was the most likely source of tES-induced phosphenes. However, the double dissociation analysis in Chapter 3 showed that additional stimulation over the visual cortex lowered the current strength required to induce phosphenes by stimulation near the retina (from 130.7 μA to 87.5 μA). It appears then that electrical stimulation over the cortex can facilitate phosphene detection. Chapter 4 showed that phosphenes were more readily perceived when stimulation was set to specific frequencies in each of the dark (10 Hz), mesopic (16 Hz) and well-lit (20 Hz) conditions. Frequency dependence in these well-lit and dark conditions was in-line with: 1) previously reported dominant electroencephalograph (EEG) frequency bands in the cortex; and 2) sensitivity to stimulation found in rod and cone

photoreceptors in the retina. All three experiments found that stimulation at 16 Hz produced the strongest electrophosphenes in mesopic conditions. While this does not align with any known EEG frequency response in the visual cortex, it closely aligns with the rod-cone phase delay mechanism found in the retina at 15 Hz, suggesting that the frequency component of tES-induced phosphenes may be driven by the frequency dynamics of retinal photoreceptors. Overall, the findings of this thesis indicate that exposure guidelines for EMF need to consider mesopic lighting if they intend to encompass all plausible exposure scenarios. Additionally, tES over the visual cortex can influence phosphene perception. Finally, ambient lighting conditions strongly affect the frequency dynamics and current strength required for tES to produce phosphenes.

CERTIFICATION

I, Ian Douglas Evans, declare that this thesis submitted in fulfilment of the requirements for the conferral of the degree Doctorate of Philosophy, from the University of Wollongong, is wholly my own work unless otherwise referenced or acknowledged. This document has not been submitted for qualifications at any other academic institution.

Ian Douglas Evans

March 23rd, 2023

LIST OF ABBREVIATIONS

AC: Alternating current

AICc: Corrected Akaike's information criteria

CNS: Central nervous system

CSF: Cerebrospinal fluid

DC: Direct current

EEG: Electoencephalogram

EMF: Electromagnetic field(s)

ICNIRP: International Commission on Non-Ionizing Radiation Protection

IEEE: Institute for Electrical and Electronic Engineers

LGN: Lateral geniculate nucleus

PDF: Probability distribution function

REPT: Rapid estimation of phosphene thresholds

RGC: Retinal ganglion cell(s)

tACS: Transcranial alternating current stimulation

tDCS: Transcranial direct current stimulation

tES: Transcranial electrical stimulation

TMS: Transcranial magnetic stimulation

PUBLICATIONS FROM THESIS

Evans, I. D., Palmisano, S., Loughran, S.P., Legros, A. & Croft, R.J. (2019). Frequency-dependent and montage-based differences in phosphene perception thresholds via transcranial alternating current stimulation. *Bioelectromagnetics, 40*, 365-374 (2019). doi:10.1002/bem.22209

Evans, I. D., Palmisano, S., & Croft, R. J. (2021). Retinal and cortical contributions to phosphenes during transcranial electrical current stimulation. *Bioelectromagnetics, 42*(2), 146-158. doi:10.1002/bem.22317

Evans, I. D., Palmisano, S., & Croft, R. J. (2022). Effect of ambient lighting on frequency dependence in transcranial electrical stimulation-induced phosphenes. *Scientific Reports, 12*(1), 7775. doi:10.1038/s41598-022-11755-y

PDF proofs of the original manuscripts for each of these published works can be found in Appendix H (p. 172). The greater part of each of these works is attributable to me as Ph.D candidate. Each supervisor maintained their roles in contributing to experimental designs and editing manuscripts. All recruiting, coding and programming, data collection, data cleaning, data analysis and data reporting are solely the work of the Ph.D candidate, in accordance with the requirements of the Ph.D candidature.

TABLE OF CONTENTS

LIST OF TABLES

LIST OF FIGURES

OVERVIEW

Exposure to electromagnetic fields (EMF) can produce illusory perceptions of light referred to as phosphenes. Various exposure guidelines worldwide use phosphene perception as a sign that environmental exposure to EMF may be affecting the central nervous system (CNS). When considering phosphenes induced by electrical fields, it is important to consider that much of our knowledge of electrophosphenes is based on legacy literature with small sample sizes, using inconsistent experimental and analytical techniques. Exposure guidelines also need to consider all commonly encountered ambient lighting conditions, no studies to date have examined electrophosphenes in dim (a.k.a., mesopic) lighting. It is also commonly assumed that electrophosphenes are the result of stimulating the retina rather than the brain, however this assumption is based on interpretations and/or simulations of other published findings rather than arising from a hypothesis being tested by experiments.

This thesis will attempt to address some of these gaps in knowledge by examining multiple factors that affect sensitivity to phosphenes induced by transcranial electrical stimulation. The primary aims of this thesis were to:

- Confirm the findings of commonly cited but low-quality studies relating to transcranial electrical stimulation frequency and phosphene detection thresholds in photopic (i.e., well-lit) and dark lighting conditions,
- Address the unsettled issue of where phosphenes are generated by separating the contributions of potential cortical and retinal phosphene sources,
- Determine the effects of mesopic lighting on phosphene perception and any related frequency-dependent effects.

Structure

This thesis is separated into five chapters: an introductory chapter, three experimental chapters, and an overall discussion chapter. All three experimental chapters have been published as peer reviewed journal articles (see *Publications From Thesis*, p. vi).

Chapter 1 comprises an introduction to the aims listed above and the concepts relevant to them. This chapter provides a general overview of electromagnetic fields, transcranial electrical stimulation and the factors that change its outcomes, phosphenes and how the visual system produces them, how ambient lighting changes visual processing and phosphene perception, and the psychophysical methods used to measure phosphene perception. The relevant literature is reviewed (and critiqued) within each section.

Chapter 2 is a published study that examines the relationship between transcranial electrical current stimulation frequency and electrode location on phosphene detection thresholds in dim lighting conditions. A fully repeated-measures design with a large sample size was used to examine fifteen stimulation frequencies in both retinally- and cortically-targeted electrode montages.

Chapter 3 is a second published study that expands on the findings of Chapter 2. It examines the relationship between transcranial electrical stimulation and phosphene detection thresholds in mesopic conditions using four different montages and seven frequencies. As in Chapter 2, a fully repeated-measures design with a large sample size was used. This combination of montages provided the opportunity for a double dissociation between montages preferentially targeting either the retina or the visual cortex. The narrower range of frequencies also allowed sufficient testing time to avoid fatigue effects, while still providing opportunities to assess whether the findings outlined in Chapter 2 could be replicated.

Chapter 4 is a third published study that investigates detection thresholds for retinally-targeted electrophosphenes across multiple ambient lighting conditions (photopic, mesopic, and dark) and across five stimulation frequencies. As in previous chapters, a fully repeated-measures design with a large sample size was used, while testing in every combination of conditions was performed twice on separate days to measure test-retest reliability.

Chapter 5 is a general discussion section that summarises and synthesizes the key findings of the three experimental chapters, discussing their implications and limitations, and providing an overall conclusion to the thesis.

1 – General Introduction and Literature Review

1.1: Effects of Electromagnetic Fields in Humans

1.1.1: What is EMF?

Electromagnetic fields (**EMF**) include all types of electromagnetic radiation, such as radio waves, microwaves, infrared radiation, visible light, ultraviolet radiation, X-rays, and gamma rays. At its' core, radiation involves the emission and propagation of energy through any given space in the form of either waves or particles. This ability to redistribute energy is fundamental to the universe in a vast number of ways – for example, infrared EMF is necessary to redistribute heat, sunlight is necessary for much of nature to survive, and technological advances have allowed the use of microwaves and radio waves in everyday life. While there are various types of EMF, each is defined by either its wavelength or frequency, which are related by the equation:

$$f = \frac{v}{\lambda}$$

where f = frequency in Hz, v = speed of the photon through the medium/environment (usually the speed of light or close to it) in metres per second[1], and λ = wavelength in metres. While for all functional purposes wavelength and frequency are interchangeable, individual fields of study tend to discuss EMF in terms of either wavelength or frequency based on whichever measure offers the shortest scale, typically for ease of presentation, measurement and calculation (National Aeronautics and Space Administration, 2013). For example, the infrared spectrum is defined by wavelengths of 10 µm – 1 mm which equate to frequencies of approximately 300 GHz – 30 THz; as a result, infrared astronomers typically report EMF in terms of wavelength (NASA, 2013). Similarly, electrical engineers tend to report EMF in terms of 0 – 60 Hz frequencies rather than the equivalent wavelengths of approximately 5000 kilometres with no upper limit.

[1] Since the photon is a mediator of the electromagnetic force.

As well as differences in frequency and wavelengths, each type of radiation also has its own functions and applications which have proven immensely beneficial to society. However there remain concerns in the general, medical, occupational health, and radiation safety communities regarding their effects on living tissue. Higher frequency ranges of EMF are categorized as *ionizing radiation*. They are capable of separating electrons from atoms, which releases ions whilst breaking the atomic structure (Slovic et al., 1981). This can rapidly damage a broad range of materials such as silicon components in electrical circuitry, and lead to cancer and other detrimental conditions in living beings (Alexander, 2003; Li et al., 2001; Ma & Dressendorfer, 1989; Ward, 1988).

Lower frequencies of EMF (approx. 940 THz and below) are described as *non-ionizing radiation*, as they do not have enough energy to ionize atoms (Wood & Karipidis, 2017). While there are justifiable concerns regarding the increased risk of various cancers or diseases due to ionizing EMF, no biological mechanism for non-ionizing EMF to cause such maladies has been found. However, with sufficient exposure to non-ionizing EMF, it can be dangerous to living beings in other ways.

1.1.2: Effects of Non-ionizing EMF on the Body

Non-ionizing radiation can affect the body in various ways, such as photochemical damage, thermal injury, or electromagnetic interference. The parts of the body that are most sensitive to non-ionizing radiation (and how they are affected) depend on the type of radiation (Kanagasabay, 1982; Omer, 2021). In the high frequency range of non-ionizing radiation, ultraviolet radiation can cause photochemical damage to DNA molecules in skin cells (Narayanan et al., 2010; Panich et al., 2016), while high levels of microwave radiation can cause burns and necrosis of the epidermis and underlying tissues.

At very low frequencies, EMF can also cause electromagnetic interference with tissues that rely on electrochemical operations to function (Miklavčič et al., 2006; Walz, 1995). This can cause muscle tissues to remain contracted, which can be uncomfortable in skeletal muscle tissue, dangerous when affecting the smooth muscle tissues surrounding many internal organs such as the lungs, and potentially fatal in cardiac muscle tissue (Dalziel & Lagen, 1941;

Silversides, 1964). However, with the exception of lightning strikes, natural sources of non-ionizing EMF do not produce sufficient energy to cause these effects. This degree of exposure requires direct stimulation from an EMF source such as direct contact with live electrical wiring or an electrical stimulator set to unnecessarily high amperage. Whilst the consequences for such injuries can be severe, they are relatively straightforward to avoid using appropriate electrical insulation.

Nerve and brain tissues are much more sensitive to low frequency electromagnetic interference than muscle tissues (Adey, 1981; Johnson & Guy, 1972; Saunders & Jefferys, 2007). Their functions can be altered by exposure to EMF of much lower magnitude (Miklavčič et al., 2006). For example, devices such as MRI scanners and power transformers produce stray low frequency EMF outside the device which cannot always be shielded against, particularly in the case of magnetic fields. In practice, simply moving while in proximity to the device during normal operations can produce unwanted sensory effects and vestibular dysfunction (Andreuccetti et al., 2013; Crozier et al., 2007; ICNIRP, 2014; Karpowicz & Gryz, 2013). This sensitivity in nerve fibres creates the risk of low frequency EMF interfering with the central nervous system (**CNS**; Adey, 1981; Johnson & Guy, 1972; Saunders & Jefferys, 2007).

1.1.3: Determining Safe Exposure Levels

Given the role of electrical activity in neural processing, any outside source of interference resulting in changes to the CNS is best avoided where possible. That said, there are many circumstances (particularly occupational) where exposure to EMF is unavoidable. Given the range of potential dangers, it is important to determine what levels of exposure to various types of EMF are acceptable. Determining the safe levels of non-ionizing EMF exposure is not straightforward, as the effects of EMF on human health can vary depending on the frequency and intensity of the EMF at the tissues potentially affected. Guidelines for EMF exposure are set by various national and international health agencies, such as the Institute for Electrical and Electronic Engineers (IEEE) and the International Commission on Non-Ionizing Radiation Protection (ICNIRP). These guidelines are based on a thorough review of the scientific literature on the effects of EMF on human health, and they are updated as new research

becomes available. In general, most experts agree that exposure to EMF at levels below the guidelines set by international health agencies is unlikely to cause adverse health effects (ICNIRP, 2010; IEEE, 2019; Reilly & Hirata, 2016). However, this assumes that available research adequately describes any plausible EMF exposure scenario.

Rather than assess how non-ionizing EMF affects each part of the brain and/or the CNS, some aspects of exposure guidelines use the retina as a model for the CNS (ICNIRP, 2010). The presence of time-varying EMF in the retina can produce illusory perceptions of light referred to as phosphenes, even in complete darkness (including with eyes closed; de Graaf et al., 2017). These phosphenes, referred to as electrophosphenes or magnetophosphenes (depending on how the phosphene was induced; see *1.2.1 – Electrophosphenes and Magnetophosphenes* below) serve as a relatively conservative estimate for demonstrable effects of non-ionizing EMF on the CNS and is considered a valid sign of potential risk of EMF-based interference in the CNS (ICNIRP, 2010).

1.2: Phosphenes

This thesis is focused on understanding the relationship between EMF and phosphenes. Specifically, it examines how electrophosphenes can be induced, the regions of the brain that are involved, how varying the degree of electrical stimulation can affect phosphene perception, and how ambient lighting changes these dynamics. The section below therefore discusses different types of phosphenes, as well as the early research on EMF-phosphene induction and detection. It concludes by outlining reasons for modern interest in EMF-induced phosphenes.

1.2.1: Electrophosphenes and Magnetophosphenes

Phosphenes are perceptions of light caused by mechanical or electromagnetic changes in the visual system, as distinct from perceiving actual light. Mechanically induced phosphenes are witnessed when pressure is applied to the eyeballs (ideally with closed eyelids) and have been reported since approximately 500 BC (Grüsser & Hagner, 1990). Electrophosphenes were first

clinically reported by Charles Le Roy in 1755, a physicist who was experimenting with electricity as a cure for a variety of medical conditions. While attempting to cure a patient of blindness by discharging a Leyden jar into their head, one of the patient's responses was seeing bright flashes of light during the discharge (Le Roy, 1755). Although Le Roy's experiments were the first ever recorded example of the electrical excitability of the visual system, this was not well understood at the time.

Soon after James Clerk Maxwell's discovery that electricity and magnetism were not separate forces (Maxwell, 1873), the existence of magnetophosphenes was also established when Arsonne d'Arsonval (1896) reported symptoms of vertigo, phosphenes, and syncope when patients moved their heads inside an induction coil. Similar findings were made using a variety of coil materials and dimensions, with some variation in the colour of phosphenes and where they appeared in the person's visual field (Dunlap, 1911; Magnusson & Stevens, 1911; 1914). Thompson (1910) reported that simply varying the amount of current in the coil over time also produced magnetophosphenes without requiring the subject to move their head. Barlow and colleagues (1947) reported a similar effect, but with one end of the induction coil near the eyes rather than having the entire head within the coil. They found that phosphenes were perceived if the strength of the magnetic field (and, by extension, the induced current within the head) changed over time. As a result, it was concluded that magnetophosphenes are not induced by the magnetic field itself, but by electrical current generated by changes in the magnetic field (Knighton, 1975a, 1975b; Lövsund et al., 1980). Therefore, while magnetophosphenes and electrophosphenes can be differentiated by what type of EMF is applied, the ultimate cause of phosphene perception is exposure to electric fields.

1.2.2: Initial Electrophosphene Research

Many experiments have focused on studying the causes and properties of electrically-induced phosphenes. After Le Roy (1755) first published his report on electrophosphenes, the initial focus of research was on the perceptual qualities of phosphenes, such as the circumstances under which they were experienced to have colour (Fick, 1892; Motokawa & Ebe, 1952; Neftel, 1878; Pflüger, 1865), whether coloured light affected the perception of phosphenes (Abe, 1951; Kohata et al., 1956; Tukahara & Abe, 1951), and other aspects of the phosphene's

perceptual characteristics (Angelucci, 1890; Du Bois-Raymond, 1848; Fehr, 1911; Mann, 1911; von Helmholtz & Southall, 1924). Over time, inconsistencies in findings emerged due to variations in (or the failure to report) electrode placements and sizes, types of electrical or magnetic fields used, psychophysical methods for determining phosphene detection thresholds, and sample sizes (e.g., some studies might test only a single subject, or did not report the number of subjects tested). Few studies used the same methods, which made direct comparisons across the literature difficult to evaluate ("Survey of the Phosphene Literature", 1956). While more modern research has improved our understanding on some of these matters, many questions regarding the parameters that affect phosphene detection and perception still remain unresolved. With a more systematic approach to studying phosphene perception using consistent methodology and adequate sample sizes, many questions relating to phosphenes could be answered with greater confidence.

1.2.3: Modern Interest in Phosphenes

Exposure guidelines set by both ICNIRP (2010) and IEEE (2019) use data from magnetophosphene research to estimate the induced electrical field produced by time-varying magnetic fields at the retina, as it is generally considered that keeping exposure levels below those that induce phosphenes should also prevent any other EMF-based interference in the brain, and that magnetophosphene experiments typically apply less overall EMF in order to induce phosphenes. IEEE (2019)[2] uses two studies by Lövsund and colleagues (1979; 1980) to estimate the minimum magnetic flux density required to induce phosphenes, while a broad range of modelling papers have used these values and/or developed head models to estimate the resulting induced electrical field strength at the retina to induce phosphenes, with estimates typically ranging between 50-100 mV/m at a minimum (e.g., Attwell, 2003; Dimblylow, 2005, 2006; Laakso & Hirata, 2012; Saunders & Jefferys, 2007; Taki et al., 2003; Wood, 2008). The IEEE guidelines note that electrical stimulation of the occipital lobe can also induce phosphenes (Brindley & Lewin, 1968; Brindley & Rushton, 1977; Ronner, 1990); however, this requires much stronger electrical fields than those about the retina (for more

[2] At the time of writing, ICNIRP's most recent low frequency exposure guidelines (2010, p. 820) report the minimum flux density required to induce phosphenes is 5 mT. This value is much lower than the 12 mT minimum reported by Lövsund et al. (1979), however ICNIRP's guidelines do not provide a source for their claim.

information, see *1.4.2: Source Separation in tES*, p. 32). Whether considering electro- or magnetophosphenes generated by stimulating either the retina or the grey matter, the consistent causal factor is considered to be the electric field altering synaptic polarization at the stimulation site[3] (Knighton, 1975a, 1975b; Lövsund et al., 1980).

Electrically induced phosphenes are of interest for two primary reasons. First, the appearance of unintended sensory effects is typically not desired during the application of EMF (e.g., when it is being used as a treatment; see *1.3.2: tES Applications*, p. 11), therefore experimental designs involving EMF exposure will generally try to minimise the likelihood of phosphenes as they are likely to distract from or even interfere with the preferred outcome (e.g., Herring et al., 2019; Strüber et al., 2014; Vossen et al., 2015). Second, it is widely believed that electrically induced phosphenes are the result of stimulation of the retina (Laakso & Hirata, 2013; Schwiedrzik, 2009) which is part of the central nervous system. Thus, the perception of phosphenes is considered the first sign that EMF may be affecting the circuitry of the central nervous system. This possibility is considered when setting guidelines on safe levels of EMF exposure (ICNIRP, 2010; IEEE, 2019), however the biological mechanisms related to electrically induced phosphenes remain disputed as cortical exposure to electrical fields has been reported to result in phosphenes (e.g., Kanai et al., 2008; see *1.4.1: Potential Sources*, p. 25). If safety standards for exposure to EMF are influenced by the phosphene literature, then it is important to have a broad understanding of how phosphenes are generated and what influences their detection and perception.

1.3: Transcranial Electrical Stimulation (tES)

As the thesis is focused on electrophosphenes induced by transcranial electrical stimulation (**tES**), this section discusses the differences between tES and other non-invasive neurostimulation techniques (section 1.3.1), and reviews some of the different clinical and scientific applications of tES (section 1.3.2). This section will also review the methodologies

[3] The retina includes differing types of synapses compared to the grey matter which may be comparatively more sensitive to electromagnetic fields, however the wide range of cell types across both structures combined with the multiplicity of interactions between them makes it difficult to attribute sensitivity to EMF to any particular cell type in either structure.

commonly used in tES, as well as the limitations found in past studies of tES-induced phosphenes (sections 1.3.3 and 1.3.4).

1.3.1: tES, TMS and Galvanic Stimulation

A common approach to exploring neural mechanisms is to examine patients with brain damage in specific areas and observe the resulting changes in their neural function. Well-known examples of this include the linguistic changes found in Patient Tan after a stroke (Broca, 1861), and the dramatic shift in personality found in Phineas Gage after a railway spike accident removed a significant proportion of his brain (Harlow, 1848). While these studies can be revealing, researchers often prefer to explore the mechanisms of neural functionality without requiring any damage to the brain (or body). This can be achieved with the appropriate use of non-invasive brain stimulation methods (Paulus, 2011). The most common of these methods are transcranial electrical stimulation (**tES**), transcranial magnetic stimulation (**TMS**), and galvanic stimulation. Each technique can modulate neural functions by applying EMF to excite or inhibit any tissues and interconnected neural circuitry where these fields are applied. However, each stimulation method can also be used to deliberately or incidentally induce phosphenes.

Early TMS involved generating a magnetic field using an induction coil, which was placed near or around the preferred target area for stimulation (d'Arsonval, 1896). While this system produced a broad magnetic field around and within the coil, it did not allow for any degree of precision regarding what tissues were stimulated. In the case of phosphene research, this made it difficult to distinguish which part of the head was involved in phosphene perception. Modern TMS systems use multiple coils, which allow more precise targeting of specific neural regions; however, TMS is generally not used to stimulate other relevant anatomy such as the retina due to the risk of it causing retinal tears and/or vitreous detachment in the eyes, even when the eyes are not the target for stimulation (Kung et al., 2011). As a result, while magnetophosphenes induced by focused TMS can be used to assess certain specific sources of phosphene perception (see *1.4.1.3: The Visual Cortex*, p. 28), the technique is not applicable for exploring all potential phosphene sources. Although it is possible to induce

phosphenes via magnetic field exposure to the whole or broad regions of the head using an appropriate-sized coil (e.g., Lövsund et al., 1979; Souques et al., 2014), this could create multiple confounding effects such as vestibular interference (Casselman et al., 1993; Lenggenhager et al., 2006), unwanted changes in motor function (Chieffo et al., 2014), intense and lingering headaches (particularly when phosphenes are induced; IEEE, 2019; Lövsund et al., 1979, 1980), and the coil itself would limit the range of potential ambient lighting conditions tested (see *1.5: Ambient Lighting and Phosphenes*, p. 33). The use of magnetic coils also shortens potential testing times, as the coils need to be actively cooled and swapped after repeated firings (Epstein, 1998; Hallett, 2007).

EMF exposure can also be produced in a controlled fashion using galvanic stimulation, which involves a chemical action that produces a unidirectional electric current from one electrode to another (Miller-Keane, 2005). This is frequently used when probing the vestibular system (Dlugaiczyk et al., 2019; Fitzpatrick & Day, 2004), particularly the interactions between nerve activation and the resulting head, eye, and body movements (Suzuki & Cohen, 1964; 1966). However, galvanic stimulation also requires the use of low voltage, low amperage, and a very small range of frequencies (Blake et al., 2008; Stagg, 2014). This narrow range of stimulation parameters makes galvanic stimulation a highly inflexible tool to explore phosphene perception compared to electrical stimulation (see *1.3.3: tES Methodology Issues* below). As such, this thesis will focus on tES-induced phosphenes and the methodological choices that affect its outcome.

1.3.2: tES Applications

tES systems are widely available, inexpensive, simpler to operate compared to other invasive or non-invasive neurostimulation techniques (like TMS or galvanic stimulation), and safe to use when simple protocols are followed (Antal & Paulus, 2013). Once the stimulator is appropriately set up (see *1.3.3 – tES Methodology Issues* for an in-depth discussion on these details), electrodes are positioned onto the scalp and held in position using rubber straps or other form of binding apparatus (see **Figure 1.1**). The most common applications for tES are therapeutic; when tES is used to target various specific areas of the brain, the reported cognitive benefits include improvements in learning rates (Clark et al., 2012; Coffman et al.,

2012), motor sequence learning (Hashemirad et al., 2016; Nitsche et al., 2003), memory (Kadosh et al., 2010; Polanía et al., 2012; Violante et al., 2017), as well as reductions in the symptoms of depression (Bennabi et al., 2020; Loo et al., 2012) and ADHD (Bandeira et al., 2016; Breitling et al., 2016). The reported somatic benefits when applying tES include improvement in sleep quality (Acler et al., 2013; Saebipour et al., 2015), more effective stroke recovery (Baker et al., 2010; Schlaug et al., 2008), reduced symptoms of fibromyalgia (Fagerlund et al., 2015; Valle et al., 2009), and other chronic pain conditions (Fenton et al., 2009; Fregni et al., 2006). tES can also be used to explore/enhance sensory modalities, with recent findings indicating that it can improve hearing and speech perception (Riecke et al., 2015; Rufener et al., 2016) and visual perception (Laczó et al., 2012; Strüber et al., 2014). The amount of current required to induce these effects varies both across and within each study, as each individual's head will vary in terms of size and how various tissues are distributed, which changes how current is distributed about the body (see *1.3.3.4 – Volume Conduction and Current Density*, p. 18).

Figure 1.1
Example of a tES setup

Image adapted from *BNN* (https://bipolarnews.org/?p=4892), use by permission under Creative Commons Attribution-NonCommercial-ShareAlike license 4.0.

1.3.3: tES Methodology Issues

tES involves attaching electrodes to the scalp and attempting to stimulate the brain by applying electric current, which is the movement of electrons from areas with greater (positive) charge to areas with lesser (negative) charge to balance the electrical potential throughout the environment (in this case, the human head). This change in charge varies the activation state of ion channels and the current gradients between neurons in the grey matter adjacent to the electrodes, resulting in modulations of membrane potential in the brain (Fregni & Pascual-Leone, 2007). By using appropriate stimulation parameters, this means that tES can modulate the neural oscillations of parts of the brain in a controlled and non-invasive fashion (Woods et al., 2016).

It is important to consider this movement of electrons, as the overall effects of tES depend not only on what current is applied but also on how it is distributed about the body (Laakso & Hirata, 2013; Woods et al., 2016). While the intention may be to modulate electrical activity at specific parts of the brain, the electrical current is applied at the scalp (hence transcranial), and any current applied will spread throughout the body until the overall environment is electrically neutral (Woods et al., 2016). Therefore, it is essential to determine whether 1) the targeted area is being stimulated to a relevant degree; and 2) any other tissues may be stimulated to the point of activation. This requires careful consideration of the overall distribution of current density, a measure of changes in electrical flux across a given area (Paulus, 2011). Typically measured in milliamps per square meter (mA/m^2), current density (J) is directly proportional to the magnitude of the electric field (E) and the electrical conductivity of the environment (σ), as expressed in the equation:

$$J = \sigma E$$

While it is straightforward to measure and report the electric field strength at the electrode locations, the current at the actual target of stimulation will vary depending on the conductivity properties of the intervening tissues, and these quantities should be considered in order to determine 1) whether the targeted area is being stimulated to any relevant degree, and 2) if any other tissues may be stimulated to the point of activation (Laakso & Hirata, 2013).

Current density can be controlled by changing four stimulation parameters: the amount of current applied, the location of the stimulation (a.k.a., "montage"), the polarity of the stimulation, the frequency of the stimulation, and the size of the electrodes (Antal & Paulus, 2013; Woods et al., 2016). While varying the amount of current applied will determine the net quantity of current density in the body, other parameters will combine to vary how that current is distributed, as well as its effect.

Each of these parameters (montage, polarity, frequency, and electrode size) will be discussed both in terms of general tES applications, and how they can affect phosphene perception.

1.3.3.1: Montage

To stimulate specific regions of the head, an appropriate arrangement of electrodes must be selected. Since current will flow from the positive electrode (anode) to the negative electrode (cathode) through any electroconductive medium connecting them (in this case, the body), the choice of electrode locations will determine what areas will be maximally stimulated (Neuling et al., 2012). As a general rule, it is best practice to place the anode as close to the target of stimulation as possible. For example, in a past paradigm exploring the recovery of motor function where the region of interest was the precentral gyrus (Schlaug et al., 2008; see **Figure 1.2a**, p. 21), the anode was positioned on the scalp over that area of the cortex while the cathode was positioned over an area not related to motor function (in this case the supraorbital region). The cathode is typically placed at a location either near a site where stimulation is desired or over a region where activation will not affect the experiment (Antal & Paulus, 2013).

A montage does not necessarily use only one cathode or only one anode. Depending on where stimulation is intended to be delivered, any number of either cathodes or anodes can be used (e.g., Datta et al., 2009). Additionally (despite the term transcranial), the electrodes do not all need to be placed near the cranium; extracranial electrodes can be used to avoid unnecessarily changing the neuronal oscillations at multiple regions of the brain. Common alternatives used include the shoulder (e.g., Mehta et al., 2015) and the forearm (e.g., Schwarz, 1947).

In past research, subjects have reported seeing phosphenes when the montage selected involves electrodes placed close to the eyes, including the temples and any location anterior to the central vertex of the scalp (Rohracher, 1935; Schutter & Hortensius, 2010). In these studies, phosphene intensity increased as electrodes were moved closer to the eyes even while current applied was constant. This phenomenon is encountered regardless of whether the experiment is intended to produce phosphenes or not. Since the target of stimulation is usually fixed, studies wishing to avoid phosphenes will typically monitor subjects, asking them to report any perceived phosphenes and lowering the current applied until they are no longer visible (Paulus, 2010). Phosphenes have also been reported as a result of applying tES over the occipital lobe (Oz), which plays a major role in visual processing (Kanai et al., 2008). While this finding is disputed, it has not yet been clearly contradicted by experimental evidence; for more information, see *1.4.1: Potential Sources* (p. 25).

In order to examine how montage affects phosphene perception, this thesis used a range of montages that preferentially targeted either the retina (FPz-Cz), locations further away from the retina (T3-T4), the visual cortex (Oz-Cz), or both the retina and visual cortex simultaneously (FPz-Oz).

1.3.3.2: Stimulation Polarity

Electrical current comes in two basic forms: 1) alternating current (AC), where the polarity of the current periodically alternates between positive and negative at each end of the circuit, causing the direction of electron flow to also alternate; and 2) direct current (DC), where the polarity does not change and thus the direction of electron flow is constant. These types of current make up the two fundamental forms of tES: transcranial alternating current stimulation (**tACS**; Antal & Paulus, 2013), and transcranial direct current stimulation (**tDCS**; Woods et al., 2016).

At times, it may be ideal to have constant polarity effects, where it is preferred to keep specific brain regions in a constant state of hyper- or depolarisation. By using tDCS (which does not change polarity during stimulation) and placing the appropriate electrode over that part of the cortex, such polarity-specific effects can be induced (e.g., Antal et al., 2003; Jacobson et

al., 2011). Nitsche and Paulus (2000) demonstrated this may be a factor to consider by showing that anodal stimulation of the motor cortex enhanced excitability which provoked physical motion, whereas cathodal stimulation diminished the effect and increased the perceived resistance to movement. Similar findings regarding anodal and cathodal effects on motor function have replicated this effect (e.g., Fregni et al. 2006; Stagg et al. 2009). It should therefore be ascertained whether polarity-specific effects affect the outcome or outcomes of the stimulation.

Both tACS and tDCS may produce different results when attempting to induce electrophosphenes, and consideration of these effects should be taken into account when considering phosphene perception. This thesis used both tACS and tDCS to determine if there are any differences in phosphene detection thresholds resulting from manipulating polarity.

1.3.3.3: Stimulation Frequency

Electrical stimulation can vary in current strength across time, the rate of which is known as the frequency. While the EMF spectrum is theoretically limitless in terms of frequency, current applied in tES will rarely exceed 100 Hz except in specific circumstances such as experiments targeting hippocampal oscillations (Paulus, 2011). The effects of tES are often dependent on applying stimulation around specific frequencies, without which either no discernible effect is observed, or a larger quantity of current is required to produce an effect. For example, Hoy and colleagues (2015) report that tACS applied at 40 Hz significantly improved working memory performance, but no effect was found when stimulation at the same strength was delivered at zero Hz.

A common goal in neuroscience studies is to induce neural entrainment in the brain, where cortical neurons are synchronized via an externally applied stimulus, typically a rhythmic one such as a flashing light (Kim, 2004) or a repetitive sound (Tierney & Kraus, 2014). The brain has functional rhythms of electrical activity associated with specific cognitive processes (Berger, 1929), and by applying tES at the desired frequency the resulting electric field can induce similar rhythmic hyper- and depolarization of neurons. For example, stimulation can be delivered at frequencies matching the alpha band (typically defined as 8 – 12 Hz) when

exploring its role in visual perception (Helfrich et al., 2014). Alternately, rhythmic stimulation can be used to suppress specific neural rhythms associated with conditions such as Parkinson's Disease (Del Felice et al., 2019). By matching the stimulation frequency to the desired neural frequency, tES can induce, enhance, or suppress specific neural effects (Schmidt et al., 2014). While tES is typically applied using sinusoidal waveforms, various studies have also used square-wave or sawtooth waveforms to rhythmically apply stimulation (e.g., Dowsett & Hermann, 2016; Jaberzadeh et al., 2014; Marshall et al., 2006). These forms of stimulation are better suited towards applications that require a more rapid increase or decrease in voltage applied, as this can either negatively or positively affect the likelihood of neural firing in specific entrainment paradigms (e.g., Frölich & McCormick, 2010; Reato et al., 2013). However, these waveforms are also associated with greater reports of discomfort or electrical pain due to the comparatively more rapid changes in voltage (Dowsett & Hermann, 2016), and as such are generally restricted to applications that require relatively low levels of current to be applied.

Stimulation frequency options are not limited to a single frequency; multiple frequencies can be applied simultaneously, or stimulation can have no frequency at all. Stimulation can be provided across a wide band of frequencies to enhance multiple weak signals in the brain (van der Groen & Wenderoth, 2016). Alternately, a zero Hz signal is more effective in activating some neural functions, such as those of the motor cortex (Schlaug et al., 2008), or those in certain cognitive domains where no frequency component is required (Jacobson et al., 2011). While any zero Hz stimulations will be DC, there is a common misconception that tDCS cannot have a frequency component. This is not always the case. In AC, the electrodes alternate between cathode and anode, while in DC the cathode and anode do not alternate. So long as the current continues to flow in the same direction, the current strength itself can vary in any way the experimenter wishes (Paulus, 2011).

Electrophosphenes are more easily perceived at specific stimulation frequencies; however, the optimal frequencies for phosphene detection also appear to be determined by the lighting conditions in which tES is applied. While phosphenes appear to be more readily detectable under well-lit conditions with 20 Hz tES (Kanai et al., 2008; Lövsund et al., 1980, Schutter & Hortensius, 2010; Schwarz, 1947), they appear more detectable in dark conditions with 10 Hz tES (Kanai et al., 2008; Schwarz, 1947). Electrophosphene detection thresholds under dim

(a.k.a., mesopic) lighting conditions have not been reported. However, Lövsund and colleagues (1979) report that magnetophosphenes appear to be more readily detectable at 20 Hz in lighting levels of 1.2 candela per square meter. These lighting conditions could be considered mesopic; however, no statistical comparisons were reported in this study. For more on the interaction between stimulation frequency and lighting conditions, see *1.5: Ambient Lighting and Phosphenes* (p. 33).

This thesis used a broad range of stimulation frequencies to attempt to replicate the findings of previous research on phosphene detection in well-lit and dark conditions and explore the frequency dynamics involved in phosphene detection under mesopic lighting conditions.

1.3.3.4: Volume Conduction and Current Density

For any of the above methodology choices to have the desired effect, it is necessary for the targeted area to be sufficiently stimulated. As the purpose of tES is to change current density in specific parts of the brain, the simplest approach to ensure that sufficient current density is reaching the intended target would be to increase the current applied. However, this is not always practical for two reasons.

Firstly, even low levels of current density can cause sensory side effects, such as unpleasant or painful crawling/tickling sensations in the skin (Fish & Geddes, 2009). Dalziel (1961) reports that the median perceivable electrical current is as low as 700 μA, with subjects reporting feeling an electrical shock at 1200 μA. Increasing the current above these levels can lead to loss of motor control, paralysis of respiratory muscles, and ventricular fibrillation (Ahlbom et al., 2001).

Secondly, increasing overall current density makes it more likely that a broader region of tissues will be activated. Merely ensuring that there is no sign of discomfort is not sufficient, as the absence of sensory side effects does not guarantee that there are no other effects (cf. Popper, 1963; Sagan, 1986; Wright et al., 1887).

Any current that is applied via tES will be distributed via volume conduction, a phenomenon where EMF is transmitted from a source and distributed through biological tissue to nearby

regions with negative charge (Schutter & Hortensius, 2010; Wagner et al., 2012). As electric current will typically follow the path of least resistance, the distribution of current density through tES is largely determined by the geometry of tissues in the head and their relative electroconductivity properties. In order for tES to stimulate the brain, current must pass through the skin on the scalp, the skull, and the cerebrospinal fluid (**CSF**) before reaching grey matter. Compared to saline (1 Siemen/meter), skin is a poor conductor of electricity (0.47 S/m; Wagner et al., 2004). However, since the skull has relatively poor levels of electrical conductivity (0.01 S/m; Wagner et al., 2004) much of the current will spread through the skin. What current does penetrate the skull will readily spread through the highly conductive CSF (1.65 S/m; Wagner et al., 2004) until reaching the grey matter. As a result, the distribution of current density will be much broader than a relatively straight line between the cathode and anode. It is therefore necessary to strike a balance between applying sufficient current to maximally stimulate the targeted area, but not so much as to stimulate too much of the brain or cause unwanted side effects.

Whether deliberate or otherwise, volume conduction can also result in the retina being activated. Electrodes placed on the frontal half of the scalp are particularly likely to cause this, as the path of least resistance between cathode/anode can bypass the skull and instead flow via the skin through the eyes (Laakso & Hirata, 2013; Schwiedrzik, 2009), which have similar conductive properties to the skin (0.5 S/m vs. 0.46 S/m; Opitz et al, 2015).

One way to control the current density around each electrode during tES is by selecting different electrode sizes. Varying the size of each electrode can induce greater current density around one electrode compared to others in the montage, as the absolute current strength must be equal across the surface area of the cathode and anode for the electrical circuit to remain electrically neutral (i.e., positive charge must equal negative charge; Moliadze et al., 2010). As a result, using a smaller electrode produces greater current density around the targeted area, while using a larger return electrode can spread the same current density across a wider area, avoiding unnecessary stimulation of surrounding tissues (Moliadze et al., 2010). This helps improve the specificity and effectiveness of tES, helping to achieve more reliable outcomes.

This can be seen in the modelled estimates of current density derived from SimNIBS 3.1 (Thielscher et al., 2015) in **Figure 1.2** (p. 21), which shows the tDCS-induced current density across the grey matter based on four different sets of electrode sizes. All simulations have the same 500 μA current applied and the same FPz-Cz montage, with the centre of the anode placed on the scalp at FPz (left column of **Figure 1.2**) and the center of the cathode on the scalp at Cz (right column of **Figure 1.2**). The electrode sizes are based on studies using tES: 30 x 40 mm (A; Evans et al., 2021; see Chapter 3), 30 x 40 mm anode and 90 x 60 mm cathode (B; Kanai et al., 2008), 17.5 mm diameter circle (C; Adrian, 1977), and 76.2 mm diameter circle (D; Kar & Krekelberg, 2012). While only the grey matter is displayed here, the models also consider electroconductive differences in the scalp, skull, and CSF when calculating the distribution of current density. Since the purpose of tES is (usually) to stimulate the brain itself, the current density in the grey matter of the brain is presented.

Each example in **Figure 1.2** shows varying distributions of current density with the same strength of current being used. In all montages, current density is increased across much of the dorsal frontal lobe between the two electrodes; however, each montage shows a degree of variance in how current density is spread throughout the brain, including at the electrode sites. As any current applied is (ideally) distributed across the entire surface area of the electrode, larger electrodes result in the same amount of current being spread across a wider area. This is seen in **Figure 1.2d**, where very little current density is found at the actual site of each electrode; it is instead distributed more broadly throughout the grey matter (even as far from the electrodes as the brainstem). The smaller electrodes (as used in **Figure 1.2a** and **1.2c**) will result in the greatest current density in the targeted grey matter at both FPz and Cz.

Using different sized electrodes can be advantageous in effectively distributing current density. By using a larger cathode placed in a relatively neutral location (such as that used in **Figure 1.2b**), stimulation may not generate sufficient current density in any tissues that would affect the experiment. It is clear in this montage that comparatively little current density is present about Cz, whereas the targeted area at FPz receives relatively high amounts of current density.

Figure 1.2

SimNIBS-derived estimates of the normal component current density in the grey matter with an FPz-Cz montage using four different sets of electrode sizes. Black outline is the outline of the electrode as positioned on the scalp. Electrode size is to scale with the brain.

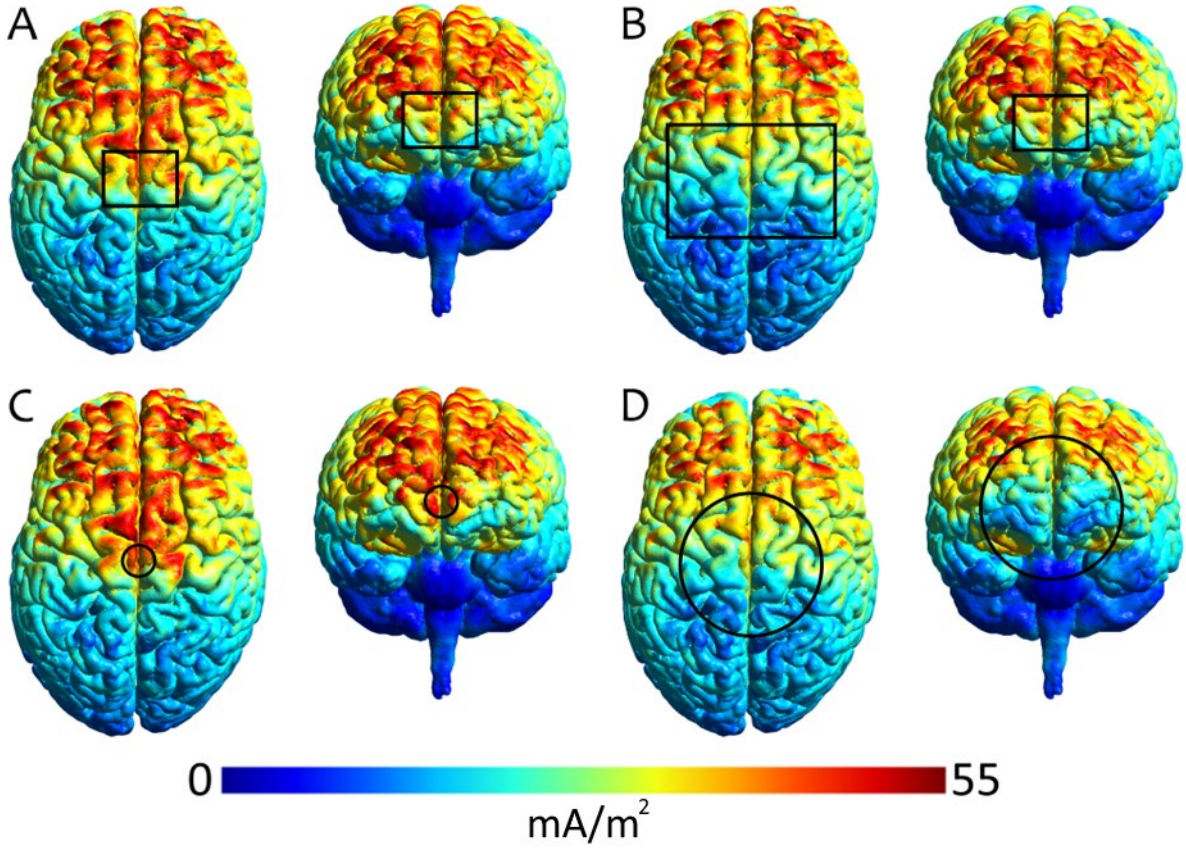

That said, there are limits to how effective varying electrode sizes can be. Each montage in **Figure 1.2** also shows greater current density in both hemispheres of the inferior frontal gyrus, located at the lower front of the brain. These areas of increased current density are a result of current flowing through the eyes (which are just in front of the inferior frontal gyrus) and into the brain. The minimal differences in current density here across each montage show that regardless of electrode size, any montage using electrodes sufficiently close to the eyes will result in retinal stimulation.

Any arrangement of electrodes must also consider the balance between current density at the target region, and the current density distributed elsewhere. This balance between stimulation at targeted areas versus stimulation at non-targeted areas is an important consideration for tES paradigms, not only due to the possibility of unwittingly activating

unintended regions of the brain, but also the likelihood of delivering current to the eyes which can induce phosphenes.

Depending on the preferred outcome, phosphenes can be made more or less likely by choosing a montage that distributes current density to preferred tissues. This thesis examined the effects of volume conduction on electrophosphene induction and detection by estimating current density in the brain and the retina across multiple montages (FPz-Cz, T3-T4, Oz-Cz, and FPz-Oz). The experiment in Chapter 2 preferentially targeted either the retina (FPz) or the cortex (Oz) in each montage, and therefore used a larger electrode at the anode over Cz to minimise distribution of current density to where it is not intended (similar to **Figure 1.2b**). As the experiment in Chapter 3 examined the effects of applying similar levels of current nearby both the retina and the visual cortex, identical sized electrodes were used in each montage. The current density modelling in Chapter 3 examined how current density is distributed in each montage and whether volume conduction in these montages could result in retinal and/or cortical activation, which could in turn generate phosphenes (for more information, see 1.4.2: Source Separation in tES, p. 32).

1.3.4: tES Methodology – Limitations of the Literature on Phosphenes

A survey of the electrophosphene literature (1956) pointed out the difficulty in reaching a firm conclusion on the electrical dynamics of phosphenes due to the use of inconsistent methodology and low sample sizes, resulting in a lack of repeatable findings to base any conclusions upon. These issues remain in electrophosphene research 60 years later; **Table 1.1** (p. 24) provides a summary of relevant methodological choices used in recent or widely cited tES studies that focused on measuring the minimum amount of current necessary to produce phosphenes (i.e., the phosphene detection threshold). These include sample size, electrode size and montage, stimulation frequency, ambient lighting, and a summary of the study's results. Sample sizes are consistently low, which may explain why many of the studies listed do not report statistical analyses. Electrode sizes are inconsistent, therefore the variance in thresholds cannot be easily compared across studies as the actual current density at the retina or cortex will vary (see *1.3.3.4: Volume Conduction and Current Density*, p. 18). Lighting conditions vary broadly (if they are reported at all), while luminance is often inconsistent

across the subject's field of view. The frequencies examined in these studies also vary between a broad/narrow range and a high/low number of frequencies tested.

These methodological inconsistencies have likely contributed to the broad range of phosphene detection thresholds reported. For example, montages targeting the occipital lobe report phosphene thresholds between approximately 100 µA (Kar & Krekelberg, 2012) and 900 µA (Rohracher, 1935). Schutter & Hortensius (2010) only applied two levels of current strength in their study (250/1000 µA) making the actual threshold value for occipital stimulation indeterminable, while Lövsund et al. (1980) report all thresholds as "*normalised with regard to strength of current at 20 Hz*", with no indication as to what this value is. The frequency sensitivity in all lighting conditions is reported to be between 8-20 Hz, but these values are not consistent across studies. This may be a result of inconsistent and non-uniform lighting conditions, where mesopic lighting can be anything from a partially lit computer monitor (Kar & Krekelberg, 2012; Schutter & Hortensius, 2010) to having subjects "*look at your own shadow on the wall*" (Schwarz, 1947).

All of these inconsistencies and areas of doubt can be resolved by conducting well-powered studies with appropriate methodology in consistent lighting conditions. This thesis will address these issues in the past research on phosphenes by using adequate sample sizes in each experiment, with appropriate electrode sizes for each montage. Stimulation frequencies were be selected to examine beliefs about the association between lighting levels and frequency-based phosphene detection thresholds, while a variety of lighting conditions were used to confirm these associations.

Table 1.1 – Commonly cited tES-induced phosphene papers and details on their methodologies

Paper	n	Electrode Size (mm)	Frequencies	Lighting	Montage	Lowest thresholds (Hz)	Lowest threshold (current)
Adrian (1977)	1	17.5 diameter	25 (5-75 Hz)	"Moderate illumination, eyes closed"	Next to eye / behind contralateral ear	18-20 Hz*	~40uA*
Kanai et al. (2008)	8	30 x 40 / 90 x 60	12 (4-40 Hz)	Office lighting	Oz-Cz	14-20 Hz	~575uA
				Dark (no adaptation)		10 Hz	~475uA
Kar & Krekelberg (2012)	5	"Surface area = 45.6cm^{2}"	6 (8-60 Hz)	Computer monitor (0.4cd/m^2)	Oz-Cz	8-20 Hz*	~100uA*
					T5-Cz	8-20 Hz*	~55uA*
					FPz-Cz	8-20 Hz*	~15uA*
Lövsund et al. (1980)	10	Not reported	36 (10-45 Hz)	3cd/m^2	Both temples	20 Hz**	Not reported*
Rohracher (1935)	1	30 x 50 / 50 x 70	14 (5-90 Hz)	Not reported	"Frontal centre / occipital centre"	20 Hz*	50uA*
					"Temporally right and left"	20-25 Hz*	200uA*
					"Occipital right and left"	15 Hz*	900uA*
					"Temporal left, occipital centre"	15 Hz*	300uA*
					"Middle occipital, right hand"	15-20 Hz*	~900uA*
Schwarz (1947)	1	"Button-sized" / "cuff"	12 (10-93 Hz)	3-9550 cd/m^2	Inside upper lip / forearm	20 Hz*	20uA*
				Dark (with adaptation)		20 Hz*	110uA*
Schutter & Hortensius (2010)	8	50 x 70	3 (2, 10, 20 Hz)	Partially 0.4 cd/m^2, mostly dark (with adaptation)	FPz-Cz	20 Hz	N/A
					Oz-Cz	10-20 Hz	N/A

Frequencies column shows the number of frequencies tested, with the range of frequencies in parentheses.

**: No statistical comparison made.*

***: Partial statistical comparison made – frequencies below 20 Hz were not compared to the peak frequency*

1.4: Biological Sources of tES-induced Phosphenes

While guidelines for non-ionizing EMF exposure are typically based on the assumption that the retina is the source of phosphenes (ICNIRP, 2010; IEEE, 2019), phosphenes can also be induced by applying EMF to parts of the brain involved in visual perception (Kammer et al., 2001; Kanai et al., 2010; Salminen-Vaparanta et al., 2014). It is known that phosphenes can be induced by applying TMS to parts of the brain (for more information, see 1.4.1.5 – EMF and the Visual Cortex, p. 30), however the question remains unresolved as to what parts of the visual system are involved in phosphene perception when tES is applied.

1.4.1: Potential Sources

Since phosphenes are a visual phenomenon, it can be assumed that the anatomical mechanisms involved in tES-induced phosphenes are parts of the visual processing stream that are particularly sensitive to electrical stimulation. The normal visual perception process begins with light entering the eye through the cornea (the transparent dome that covers the exposed section of the eyeball). This projection of light then passes through the vitreous humour in the eyeball and strikes the retina, which engages in phototransduction to convert light into low-frequency electrical signals. These signals are sent through the optic nerves to the primary visual cortex, which interacts with other regions of the brain to produce the visual perception of our surrounding environment (Goldstein, 2002). From these possibilities, the anatomical bodies that display sensitivity to electrical stimulation include the retina, the optic nerve, and the visual cortex of the brain. Their potential roles in tES-induced phosphenes are discussed below.

1.4.1.1: The Retina

The retina is a complex array of cells at the back of the eye, with multiple inputs and feedback mechanisms that together make the complexities of visual perception possible (see **Figure 1.3**, p. 26). Retinal processing begins with light hitting the photoreceptor cells, which is the first step of the phototransduction process that converts light into electrical energy. Most

photoreceptors are rod cells, which are more sensitive to light at the level of individual photons and allow vision to be possible in low-lighting conditions (Goldstein, 2002). Cones (the other type of photoreceptor) are less sensitive to light but are crucial for our chromatic (i.e., colour sensitive) and fine detail vision (Goldstein, 2002). Signals from these photoreceptors are transmitted (via the bipolar, horizontal, and amacrine cells) onto the retinal ganglion cells (which act as primitive edge detectors). These retinal ganglion cells (**RGC**) project a retinotopic map of the visual field to the visual cortex via the lateral geniculate nucleus in the thalamus (thus adjacent areas receiving input in the RGC will also be associated with the activation of adjacent neurons in the visual cortex; Goldstein, 2002).

Figure 1.3

Anatomical structure of the eye and retina

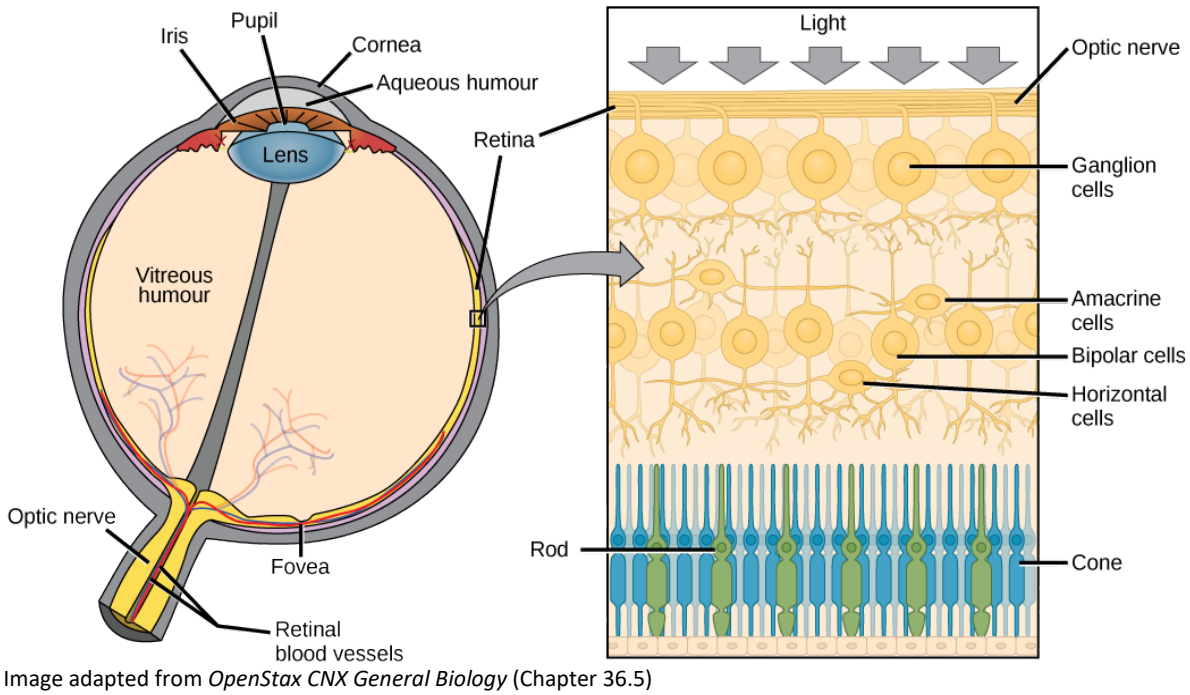

Image adapted from *OpenStax CNX General Biology* (Chapter 36.5) (https://bio.libretexts.org/Bookshelves/Introductory_and_General_Biology/General_Biology_1e_(OpenStax)), use by permission under Creative Commons license 4.0.

The electrical dynamics of the retina are complex at each stage of the retinal processing chain (see **Figure 1.3**). At rest, photoreceptor cells are more depolarized than typical neurons (-40 mV compared to the more common -60 mV; Attwell, 1990), and will respond to changes in light with graded changes in membrane potential. A photoreceptor will hyperpolarize when

excited by light, which will then depolarize a bipolar cell known as an ON-center cell, triggering an electrical response that activates any ganglion cells that it is synapsed onto. There are also OFF-center cells which are hyperpolarized by the photoreceptor and remain silent when lit. Multiple photoreceptors can be synapsed to a single bipolar cell, and horizontal cells connected to multiple networks of photoreceptors and bipolar cells can use feedback mechanisms to depolarize specific photoreceptors where those inputs are antagonistic, allowing more specific information to be passed on to the surrounding bipolar cells (Famiglietti Jr & Kolb, 1976).

Once the bipolar cells have received input (either directly from the photoreceptor or mediated via horizontal cells), the electrical response is passed on to the retinal ganglion cells (**RGCs**), either directly from the bipolar cells or mediated via amacrine cells. Like bipolar cells, RGCs can also be separated into ON-center and OFF-center activation types, based on whether they receive input from ON- or OFF-bipolar cells. Amacrine cells perform a similar function to horizontal cells where they mediate multiple inputs from bipolar cells. Amacrine cells will depolarize when input from one type of bipolar cell (ON/OFF) does not correspond with the neighbouring bipolar ON/OFF cell type that the amacrine cell is also synapsed onto, inhibiting the RGC (Solomon et al., 1993). Once this process is complete, the RGC itself does not depolarize or hyperpolarize, but instead changes the rate of action-potentials discharged through the optic nerve into the brain based on the input received from all cell types upstream (Goldstein, 2002).

This complex system of interdependent polarisation and depolarisation relationships makes the retina highly sensitive to changes in electrical current. The location of the eyes relative to the scalp also means that they are vulnerable to the spread of current across the scalp, as the current can flow through the skin and reach the eyes.

When simulating a range of tES montages, Laakso and Hirata (2013) reported that the eyes were readily stimulated by current that would flow through the relatively low resistance soft tissues of the face or the CFS surrounding the frontal lobe. As a result, regardless of the montage used, the common view of tES-induced phosphenes is that they are primarily the result of retinal stimulation (Schutter & Hortensius, 2010; Schwiedrzick, 2009).

1.4.1.2: The Optic Nerve

Bogoslovski and Ségal (1947) argued that electrically-induced phosphenes are the product of stimulating optic nerve fibres regardless of electrode placement, while acknowledging that phosphenes could also be produced by stimulating the surface of the retina in certain electrode arrangements. Countering this, Brindley (1955) observed that applying mechanical pressure to the eye increased the current required to produce phosphenes by two orders of magnitude, indicating that a structure somewhere in the eye was responsible for triggering phosphene induction. Given that manipulating the shape of the eye would not change the current density reaching the optic nerve due to tES, this conclusion appears plausible. While experiments directly stimulating the optic nerve demonstrate that phosphenes can still be produced by bypassing the eye, and that the intensity of the phosphene luminance can vary as a function of the frequency when stimulating the optic nerve (Delbeke et al., 2003; Meier-Koll, 1973), the current density required to induce phosphenes via direct optic nerve stimulation far exceeds that found in other studies where current was applied near the retina. As a result, it is generally considered that the optic nerve is not the primary anatomical mechanism driving phosphene perception from stray EMF exposure.

1.4.1.3 The Visual Cortex

Using tES with sufficient current to stimulate the retina should eventually result in phosphene perception. However, activity in the eye alone is insufficient, as it would not be possible to perceive phosphenes (or anything else) without some change in downstream visual pathways. In fact, the eye is not necessary to perceive phosphenes at all, as they can also be produced by directly stimulating the brain. Phosphenes are perceived when TMS is applied to the visual cortex (Salminen-Vaparanta et al., 2014) – with their appearance varying depending on which part of the visual cortex is stimulated (see below). Since TMS allows phosphenes to be perceived as a result of applying EMF to the cortex, it follows that EMF produced by tES might also be able to produce phosphenes by activating the grey matter of the visual cortex[4].

[4] While the white matter pathways of the brain also have a vital role in processing visual stimuli, given that grey matter tissue has relatively poor electrical conductance compared to other tissues in the brain (Wagner et al., 2004), it is unlikely that sufficient current would reach the white matter tracts in any practical tES situation before the eyes or grey matter of the visual cortex were activated first.

1.4.1.4: Functional Brain Regions

As mentioned above, each retina forms a retinotopic map of the visual field that is projected to the thalamus which synapses onto the lateral geniculate nucleus (**LGN**). The LGN combines input from both eyes into a single retinotopic map, modulated by complex inputs from the brainstem to adapt for states of consciousness (e.g., sleep) and multiple cortical regions such as the striate cortex to allow for attentional processing (Squire et al., 2012). Once these modulations are complete, the LGN projects the retinotopic map onto the visual cortex (Goldstein, 2002). The occipital lobe of the cortex is made up of several areas known to be critical for vision, referred to as visual areas 1-5 (**V1-5**; see **Figure 1.4**, below). These five areas (which will be collectively referred to here as the visual cortex[5]) have different roles to play in visual perception, and each hemisphere of the brain has its own set of visual areas due to the contralateral nature of vision, where the right hemisphere of the brain processes information from the left hemi-fields of each eye and vice-versa.

Figure 1.4
Regions of cortical grey matter and their role in the visual system

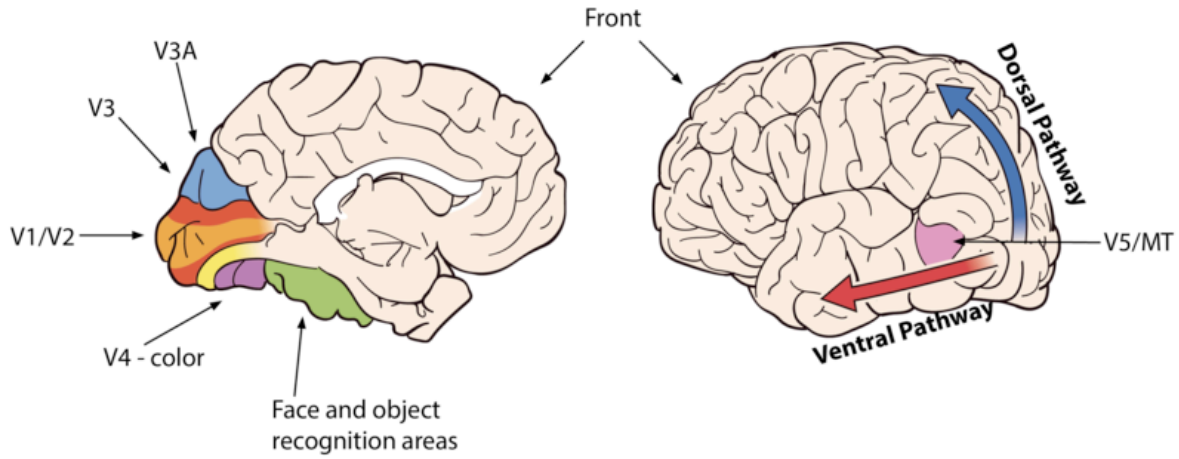

Image adapted from *Vision* by Simona Buetti and Alejandro Lleras (https://nobaproject.com/modules/vision), use by permission under Creative Commons Attribution-NonCommercial-ShareAlike license 4.0.

[5] There are other important cortical areas implicated in visual perception – regions of interest (ROIs) for vision have also been located in the frontal, parietal and temporal areas such as the inferior temporal cortex at Brodmann Area 20/21 which is important for feature binding and object recognition.

Initial cortical processing takes place in the primary visual cortex (**V1**) at the calcarine sulcus of the occipital lobe. The retinotopic mapping of the visual cortex means that the neurons across V1 are precisely arranged so that an object perceived at one position of the retina is similarly mapped across the cortex, with different cell types at various depths of the cortex responding to various features of what is perceived in that region; this can include shape, orientation, contrast, and where that object is in relation to the rest of the visual field. While V1 processes many types of visual information, further processing is required in more specialised regions of the visual cortex to allow more complex visual scenes to be perceived (Goodale, 2011). The secondary visual cortex (a.k.a. prestriate cortex; **V2**) integrates information from V1 and responds to differences in colour, basic pattern recognition, and how an object is oriented within the visual field (Anzai et al., 2007). For further processing of visual perception, V2 has feedforward connections with **V3-5** which include cortical regions with more specialised functions such as object recognition, colour, texture, spatial relations, motion, and visual-motor feedback mechanisms (Fournier et al., 2018).

1.4.1.5: EMF and the Visual Cortex

Applying TMS with sufficient strength at each region of the visual cortex (V1-V5) can induce phosphenes (e.g., Salminen-Vaparanta et al., 2014). These phosphenes change the visual field in a state-dependent manner, where the appearance of the phosphene will vary depending on the prior state of the stimulated region (Bohotin et al., 2003; Najib et al., 2016). As a result, the phosphene perceived will depend upon what is already in that area of the visual field, and the function of the section of the visual cortex being stimulated. Targeting V1 is the most reliable way to produce TMS-induced phosphenes, with increased TMS intensity producing brighter phosphenes (Kammer et al., 2005); however, reports of their perceived shape vary between subjects (Marg & Rudiak, 1994). When TMS is targeted at V1, the location of the phosphene in the field of view varies in accordance with the retinotopic organization of the cortex (Dobelle & Mladejovsky, 1974; Salminen-Vaparanta et al., 2014).

Phosphenes can also be produced by stimulating other areas of the visual cortex with TMS. Phosphenes resulting from targeting of V2 and V3 tend to be indistinguishable from those seen when stimulating V1, apart from a small drop in brightness perceived (Cowey & Walsh,

2000; Kammer et al., 2001; Salminen-Vaparanta et al., 2014). Stimulating V4 will produce a change in colour (Cowey & Walsh, 2000), while stimulating V5 will produce the perception of motion in the visual field (Guzman-Lopez et al., 2011; Hotson et al., 1994).

1.4.1.6: Cortical tES

While inducing phosphenes using TMS at the visual cortex is well established, there is less agreement about whether similar phosphenes can be produced by using tES. In an attempt to demonstrate transcranial alternating current stimulation (**tACS**) can induce neural entrainment, Kanai and colleagues (2008) applied tES over the occipital lobe (Oz-Cz montage) at a broad range of frequencies (4 - 40 Hz) in both well-lit and dark conditions. During visual perception, electroencephalography (**EEG**) over area V1 tends to measure greater spectral power in the beta frequency range (approx. 13 - 30 Hz). By contrast, in dark conditions (or with closed eyes), EEG at V1 tends to show stronger alpha band activation (approx. 8 - 12 Hz; Adrian & Matthews, 1934; Palva & Palva, 2007). In Kanai et al.'s study, not only did tACS over V1 result in phosphenes being perceived, but they were brighter and more vivid when stimulation was delivered in the frequency bands known to be dominant in V1 under each lighting condition in physiological neural processing. This alignment between the tACS frequency sensitivity and the natural rhythms of the brain under each lighting condition was interpreted as evidence that tACS was generating neural entrainment in the cortex to produce a visual phenomenon (Kanai et al., 2008).

This interpretation is widely disputed, with some researchers questioning whether direct cortical stimulation with tES can induce phosphenes. As stated above, phosphene induction with TMS is well established. However, since the focal area of stimulation in TMS is relatively small (depending on the magnetic coil used), the distribution of EMF can be directed with much greater precision than tES (Roth et al., 2007) while also requiring the application of weaker induced electric fields compared to tES, since TMS does not need to overcome the issue of volume conduction (see *1.3.3.4 – Volume Conduction and Current Density*, p. 18). Because the volume conduction effects inherent in tES result in a broader distribution of current density (see *1.3.3.4: Volume Conduction and Current Density*, p. 18), it is instead generally considered that tES-induced phosphenes are the result of retinal stimulation

regardless of the montage used, since the retina is expected to be stimulated to the point of phosphene perception before the cortex is exposed to sufficient current density to do the same (Laakso & Hirata, 2013; Schutter & Hortensius, 2010).

A common argument used to justify this position is that as the electrodes in the montage are moved closer to the retina, the current required to produce phosphenes falls (Kar & Krekelberg, 2012; Schutter & Hortensius, 2010). However, this argument only demonstrates the likelihood of retinal activation and does not exclude the possibility of cortical activation. Similarly, while the frequency-specific results of Kanai et al. (2008) correspond well with the normal frequency-based rhythms of the visual cortex, similar frequency-based findings under each lighting condition have also been found using tES montages designed to stimulate the retina but not the cortex (e.g., Brindley, 1955; Rohracher, 1935; Schwarz, 1947). Without experimental evidence that explicitly addresses cortical activation independently from retinal activation (rather than simply varying distance between the retina and the nearest electrode), we cannot rule out the possibility of phosphenes caused by tES-based cortical activation.

1.4.2: Source Separation in tES

The effects of volume conduction can make it difficult to determine whether the cortex or the retina is responsible for generating a particular phosphene. Distinguishing between these two potential sources of phosphenes is necessary if we wish to determine whether retinal phosphenes alone are the first sign of neural interference from EMF. This problem is known as source separation.

One potential way to determine which location is the source of tES-induced phosphenes involves measuring the current density at both the retina and V1 for any given montage. This has obvious complications: even if it were practical/permissible to insert probes into the retina and/or cortex *in vivo* to accurately measure current density during tES, the probes themselves would alter the electrodynamics of the tissues and (by extension) the overall distribution of current density. The closest viable alternative is modelling the spread of current from tES throughout a human skull to gather estimates of the current density at any given point. Using the DUKE head model (Christ et al., 2010), Laakso and Hirata (2013)

modelled the effect of 11 montages and showed how each montage could generate sufficient current density at the retina to produce phosphenes when sufficient and realistic levels of current were applied. One drawback of this conclusion is – much like the arguments levelled at Kanai et al. (2008) above – this only adds to the likelihood that retinal stimulation is plausible and does not directly relate to tES-induced cortical phosphenes (as no estimates of current density anywhere in the cortex were reported). Without modelled estimates of current density at the visual cortex as well as the retina, the cortical phosphene hypothesis cannot be disproven.

Previous studies attempting to determine which of these potential sources was responsible for phosphenes have compared the minimum amount of current applied near the retina to the current applied over the visual cortex when phosphenes were induced (Kar & Krekelberg, 2012; Schutter & Hortensius, 2010). However, these studies did not provide true source separation, as any montage chosen would have resulted in some change in current density at the sites being compared due to volume conduction (Laakso & Hirata, 2013).

This thesis therefore used a double dissociation technique to provide a more thorough examination of phosphene detection thresholds in relation to estimated current density at both potential source sites. Using montages that preferentially targeted the retina (FPz-Cz), the visual cortex (Oz-Cz) and both simultaneously (FPz-Oz), this thesis compared the estimated current density at these sites when phosphenes were perceived. This resulted in a more comprehensive assessment of how the retina and the visual cortex contribute to phosphene perception.

1.5: Ambient Lighting and Phosphenes

While there is debate about whether the phosphenes in the Kanai et al. (2008) study were the product of retinal or cortical activation, it is generally agreed that their detection thresholds depended on both the stimulation frequency and the ambient lighting conditions. Just as some of the effects of tES can be enhanced by stimulation at certain frequencies, varying ambient lighting conditions can affect sensitivity to tES-induced phosphenes at specific stimulation frequencies. That said, it is not the case that all lighting conditions have

been accounted for in phosphene research. There are two primary factors to consider when examining phosphenes in various lighting conditions: luminance and adaptation.

1.5.1: Environmental Background Luminance and Phosphenes

Luminance, typically measured in candelas per square meter (cd/m^2), refers to the amount of light that is emitted or reflected by a surface and then enters the eye (Lennie et al., 1993). This is distinct from illumination, which refers to the amount of light received by a surface (Shlaer, 1937). The luminance of a surface depends on the intensity of the light source and the reflectance of the surface; e.g., a surface that is highly reflective will have a higher luminance than a surface that is less reflective, when both are illuminated by the same light source (Shlaer, 1937).

Background lighting can have a significant effect on visual perception, influencing how we perceive both the colour and contrast of objects and scenes (Haldane, 1933; Jameson & Hurvich, 1964). Colour is difficult to perceive in darker conditions as the cone photoreceptors that provide chromatic information to the retinotopic map require more light to be activated compared to rods (Goldstein, 2002). Conversely, intense lighting or sudden large jumps in luminance can overexcite cone photoreceptors causing “bleaching”, which narrows the spectral sensitivity of the receptor, resulting in a shorter range of colour wavelengths that the photoreceptor responds to (Goldstein, 2002; Rushton, 1972). This effect is usually temporary, but sufficiently intense light can damage the photoreceptor permanently (Rushton & Henry, 1968).

Contrast refers to the difference in colour or luminance between an object and its background (Goldstein, 2002). This is an essential element in visual perception as it allows us to distinguish and differentiate objects and details in our visual environment (Kelly, 1977). Colour contrast is easier to identify in well-lit conditions due to the greater activation of cone photoreceptors (Cao et al., 2008; Paramei & van Leeuwen, 2016), while luminance contrast is more perceptible in low light conditions as the pupil will dilate, allowing more light to enter the eye, which increases sensitivity to differences in luminance (Beck, 1966).

Background lighting conditions affect not only the perception/detection of real objects and scenes but also the perception/detection of illusory objects (such as phosphenes). As previously mentioned, there are consistent findings showing that tES-induced phosphenes in well-lit conditions are more readily perceived with 20 Hz tES (Kanai et al., 2008; Lövsund et al., 1980; Schutter & Hortensius, 2010; Schwarz, 1947), while phosphenes in dark conditions are more readily perceived with 10 Hz tES (Kanai et al., 2008; Schwarz, 1947). However, since these studies had various methodological issues (including inconsistent ambient lighting; see *1.5.3: Ambient Lighting - Limitations of the Literature*, p. 37), these findings are in need of replication with a suitably powered and better controlled study. Additionally, there are currently no studies examining the effects of mesopic lighting on electrophosphene detection. Since EMF exposure guidelines can only consider the evidence available, it is important that this gap in the literature be filled if all common environmental conditions are to be accounted for. This thesis will comprehensively examine the effect of mesopic lighting on phosphene detection across a range of stimulation frequencies and seek to replicate the frequency-dependent effects of ambient lighting listed above.

1.5.2: Adaptation and Phosphenes

It is also important to consider how the visual system responds to changes in lighting conditions, a process known as luminance adaptation (Kalloniatus & Luu, 2007). Luminance adaptation is typically referred to as light or dark adaptation (depending on the specific lighting conditions that are being adapted to). Light adaptation is a defensive mechanism which protects the highly sensitive visual system from damage when exposed to excessive light (Goldstein, 2002). Dark adaptation occurs when the visual system returns to a state of high sensitivity, allowing visual perception to be enhanced in low light conditions (Dowling, 1960; Lamb & Pugh Jr, 2004). These processes occur primarily in the eye, however both the retina and the cortex respond differently to changes in light. During luminance adaptation, the size of the pupil is varied to control the amount of light entering the eye (more light is allowed in for dark adaptation, and less for light adaptation), whereupon the photoreceptors in the retina receive feedback from horizontal cells to control the responsiveness of each photoreceptor type in order to adapt to the lighting conditions. The overall effect of this is to

make the retina more sensitive at low lighting levels (in order to maximise visual perception under those conditions) and desensitize the retina in well-lit conditions (in order to avoid bleaching of the photoreceptors; Goldstein, 2002).

It is assumed that most luminance adaptation effects on phosphene detection originate in the retina. Applying TMS to the visual cortex, Kammer and Beck (2002) reported no differences in the minimum magnetic field strength required to induce phosphenes during four different durations of light and dark adaptation. This was presumably because adaptation occurred in the retina. As a result, cortical excitability to TMS was unchanged across all adaptation conditions (Rauschecker et al., 2004). Contrary to this, Lövsund and colleagues (1979) reported increases in the minimum magnetic flux density required to induce phosphenes as dark adaptation time increased when an electromagnet was activated over the temples. Lövsund et al. (1979) did not report the orientation of the electromagnet, meaning the distribution of the resulting magnetic field could not be precisely ascertained. However, it is widely accepted that these results were due to electrical field changes at the retina (Laakso & Hirata, 2012; IEEE, 2019).

When considering adaptation effects on tES-induced phosphenes, it was initially expected that detection thresholds would be similar when the eye was adapted to either light or dark (Müller, 1897; Nagel, 1904). However, it is now generally agreed that phosphene detection thresholds are higher when the eyes are dark-adapted (as opposed to light-adapted; Abe, 1951; Barlow et al., 1947; Bogolovski, 1935; Bogolovski et al., 1935; Bouman, 1935; Schick, 1935; Schwarz, 1940), although findings can still vary depending on the experimental methodology. Some earlier studies, which relied on condenser discharges that resulted in no frequency element to the stimulation, made the same finding of greater sensitivity to phosphenes in well-lit conditions (Bouman et al., 1951). However, by using AC stimulation, Schwarz (1947) found the reverse to be true. He found that after adaptation to well-lit conditions phosphenes were perceptible at 20 μA, but two minutes of dark adaptation increased the threshold to 110 μA, with the threshold increasing as dark adaptation time increased. Experiments using a crossover effect (where one eye was dark-adapted and the other eye was light-adapted) found similar results, with the dark-adapted eye requiring greater current to be applied in order to see phosphenes compared to the light-adapted eye (Achelis & Merkulow, 1930; Bartley, 1937; Motokawa, 1949).

As alternating current grew more widely available in the 20th century and transformers became more affordable, the ability to easily manipulate stimulation frequency opened a new line of inquiry for phosphene research. This yielded many insights into the relationship between tES-induced phosphenes and ambient lighting. Schwarz (1940; 1947) found a frequency-dependent relationship between thresholds and light adaptation, where tACS at 8 - 50 Hz increased detection thresholds as light adaptation increased, while tACS at 65 - 110 Hz decreased these thresholds as light adaptation increased. Similar AC-based findings were found during adaptation to a wide array of lighting conditions (3 - 10,000 lux; Clausen et al., 1954; Gebhard, 1952; Motokawa & Iwama, 1950); however, all the studies listed here (including Schwarz)– used low sample sizes (typically only one observer) to reach their conclusions.

Typical practice for phosphene research in well-lit conditions is to allow for at least two minutes of adaptation time, as this is usually enough time to adapt to at least 90% of the changes in contrast sensitivity (Hood & Finkelstein, 1986). Even so, the possibility that phosphene thresholds can change over time when the eyes are light-adapted may still be a factor; therefore, experiments examining the effects of different levels of ambient lighting should take this into account. When considering dark adaptation, it is generally accepted that phosphene thresholds will increase with the dark adaptation time, until the threshold stabilizes after around 15 - 40 minutes of adaptation time (depending on the intensity of light immediately prior to darkness; Abe, 1951; Barlow et al., 1947; Bogolovski, 1935; Gersuni et al., 1935; Iwama, 1949; Motokawa et al., 1948; Schwarz, 1940). Schwarz (1947) reported that phosphene detection thresholds increase with the dark adaptation period (from 2 - 500 minutes) across all frequencies tested (10 - 93 Hz). As a result, studies that wish to examine tES phosphene thresholds in dark conditions should ensure that any adaptation time is as close to zero as possible (e.g., Kanai et al., 2008). In the current study examining phosphenes in dark conditions (see Chapter 4), dark adaptation effects will be minimised by relighting the testing environment at 1.1 cd/m^2 when stimulation is not active.

1.5.3: Ambient Lighting – Limitations of the Literature

While most studies on tES phosphenes tend to be consistent regarding lighting exposure times to keep adaptation effects to a minimum, there remain inconsistencies and gaps in how luminance is accounted for (see **Table 1.1**). Ideally, the subject's field of view should remain homogenous with no changes in luminance in order to avoid changes in contrast, but this is not always the case. Schwarz (1947) used a variety of views for his test subject in order to produce varying degrees of luminance, one of which was "*look at a cloud in the sky*" to assess phosphenes at 9550 cd/m^2. More recent studies are not immune to such inconsistencies; some studies use a powered on (but mostly dark) computer monitor in a darkened room to give instructions to the subject (e.g., Kar & Krekelberg, 2012; Schutter & Hortensius, 2010). Others are vague in their overall descriptions of the lighting conditions. Some provide no quantification of luminance, e.g., "*office lighting*" (Kanai et al., 2008) or "*moderate illumination*" (Adrian, 1977). Others do not report the lighting conditions at all (e.g., Rohracher, 1935).

Similarly, the points between "well-lit" and "dark" lighting conditions are separated by a neglected area of luminance known as mesopic lighting. Typically defined as any luminance level up to 3 cd/m^2 (Stockman & Sharpe, 2006), these conditions are quite dim but commonly encountered in daily life. It is not unreasonable to assume that such lighting would be encountered by those exposed to stray EMF in their occupation, but given the dearth of evidence on the subject there is no consideration of mesopic lighting in current safety guidelines.

As mentioned above, this thesis addressed these issues by examining phosphene detection across a range of different lighting conditions with quantified luminance values and comparing the current required to induce phosphenes across each of them using a repeated measures design in a sufficiently large sample. Dark adaptation effects were minimised by keeping the subject's time in absolute darkness to a minimum and frequently re-exposing them to light. These brief exposures should have been sufficient to avoid dark adaptation, but not long or intense enough to threaten bleaching of the photoreceptors. Testing in mesopic conditions also employed stimulation at multiple frequencies to determine any frequency-dependent effects under those lighting conditions, as this combination remains largely unexplored in the literature.

1.6: Psychophysics

The study of relationships between physical stimuli and the sensory experiences that they produce is known as psychophysics. Psychophysics aims to measure and understand the psychological processes that underlie the perception of sensory information, and how their physical properties relate to subjective experience (Johnson et al., 2002; Snyder et al., 2006). In this section, we discuss how psychophysics has been used to study phosphenes in the past, and briefly review the strengths and weaknesses of different psychophysical techniques and methods.

1.6.1: How Phosphenes Are Measured

When studying electrophosphenes, psychophysics can be used to determine their perceptual detection thresholds. A threshold is the minimum amount of physical stimulation required to detect a sensory stimulus (Gescheider, 2013). In the case of tES, this corresponds to the minimum strength of electrical current applied that is necessary to induce the perception of a phosphene. Threshold estimation normally involves a binary response measure that indicates the presence/absence of the percept in question (Goldstein, 2002). In this specific case, that might be a 'yes' or 'no' response to the question "Did you see a phosphene?". "Reversal points" – e.g., where the subject's response changes from "no" to "yes" or "yes" to "no" after an increase or decrease in current strength – are therefore important in determining phosphene detection thresholds.

Psychophysics offers multiple methods for determining threshold estimates, and choosing the most appropriate one for the particular situation is important. It is common for tES studies to have small sample sizes and a limited number of testing conditions (whether frequencies or lighting conditions), and at times a combination of both (see **Table 1.1**, p. 24). This is not necessarily due to poor experimental design but is a result of the time required to estimate a reliable threshold in each testing condition. Traditional psychophysical methods often require a large number of trials (e.g., to obtain multiple "reversal points") before settling on a final

threshold estimate. Thus, using a more efficient method to estimate the threshold creates the opportunity for more stimulus conditions to be tested in the same amount of time. This should not come at the cost of unreliable data. However, it is also important to keep testing times short to minimise issues with subjects' attention, motivation, and fatigue (as well as sensitisation, adaptation, and habituation). The most appropriate psychophysical method therefore has several requirements: it must 1) require a comparatively low number of trials to determine a threshold, 2) be robust against errors in reporting, and 3) provide consistent and reliable thresholds (test-retest reliability).

1.6.2: Three Traditional Psychophysical Methods

The *method of adjustment* is a subject-directed technique for determining the threshold for detecting a stimulus. Typically used in light and sound detection paradigms (when can you see the light/hear the sound?), this technique allows the test subject to directly adjust the intensity of the stimulus until they find the point where it is just perceivable (Fechner, 1860). As the subject plays an active role in the experiment, they tend to remain attentive and motivated. Whilst this method provides threshold estimates comparatively quickly, it tends to be unreliable in most sensory testing paradigms (Ehrenstein & Ehrenstein, 1999; Gescheider, 2013; Han et al., 2016) and is considered the least accurate of the traditional psychophysical methods (Goldstein, 2002). It is unsuitable for investigating tES-induced phosphenes, as the test subject would have to operate the tES device themselves. This would be unacceptably dangerous if the subject were not trained to use it. Even if they were professionally trained in the application of tES, they would still have to move their heads repeatedly (in order to alternate between observing the phosphenes and adjusting the current strength), causing trial-to-trial inconsistencies in their field of view.

The *method of limits* is another commonly used psychophysical technique, where the intensity of the stimulation presented to the passive subject is either increased until a stimulus becomes perceptible (ascending staircase) or decreased until the stimulus is no longer perceived (descending staircase). The complete set of stimuli and the fixed step size between them are selected by the experimenter before the study. Both ascending and descending staircases are then presented to the subject in alternating order to ensure

reliability (Herrick, 1973). In the method of limits, reversals occur when an increase or decrease in stimulus intensity results in a change from a "yes" response to a "no" response or vice versa. While this technique can produce reliable results, there is the risk of practice, response bias, and habituation effects (as a result of the subject repeatedly making yes/no responses to the same stimuli; Gescheider, 2013). It can also take a long time to determine the final threshold using this method (especially when there are a large number of potential points to test in each staircase), as many staircases are usually required to obtain reliable estimates.

Another technique related to the method of limits is the *method of constant stimuli*. Like the method of limits, the stimulus set and step-size between them are again picked by the experimenter before the study. However, instead of these stimuli being presented to the subject in either an ascending or a descending order, they are presented in a random order (i.e., the stimulus intensity on each subsequent trial varies randomly rather than gradually climbing or falling). In order to detect thresholds using the method of constant stimuli, the researcher plots the function of physical stimulus intensity against the percentage of “yes” (or detect) responses directly after the experiment. The threshold corresponds to the physical stimulus intensity at which the observer detects the stimulus (e.g., the phosphene) at a rate predetermined by the experimental procedure; a 50% detection rate is common, but as this corresponds to a random guessing rate, some paradigms prefer to use higher detection rates such as 66% or 75% (Gescheider, 2013; Goldstein, 2002). While the method of constant stimuli lessens the risk of response bias and habituation effects (as each stimulus has a random current strength rather than marginally increasing or decreasing current strength), a large number of trials is required to estimate a threshold (typically more than the other two traditional psychophysical methods; Gescheider, 2013).

1.6.3: Modified Binary Search

A more recent addition to the range of psychophysical techniques is the *modified binary search* method (MBS; Tyrrell & Owens, 1988), which uses the subject’s responses to repeatedly narrow down the range of possible thresholds until the reversal point is found. Starting at the midpoint of a predetermined range of stimulation intensities, the subject’s first

response is used to reject stimulation intensities above that if they report “yes” (i.e., detect), or below that if they report “no” (i.e., do not detect). This narrowed range is then bisected, and the process is repeated until the range is limited to two points where the stimulus is perceived at one point but not at the point below it. While this method can provide a threshold estimate in relatively few trials, it works on the assumption that perception is error-free (even at the points very close to the threshold, where just noticeable differences are infinitesimally small). If the subject gives an erroneous response to a trial (e.g., because they are not sure if they perceived something; a common experience when the stimulation intensity is close to the actual threshold), this will cause their true threshold to fall into the rejected range of values, which will force the experimenter to restart the algorithm or employ an additional heuristic such as an ascending/descending staircase once the subject’s error has been discovered (Mazzi et al., 2017; Treutwin, 1995).

1.6.4: Rapid Estimation of Phosphene Thresholds

This thesis used a psychophysical method known as the *Rapid Estimation of Phosphene Thresholds* (REPT; Abrahamyan et al., 2011), which uses a Bayesian adaptive staircase system to determine the detection threshold. Bayes’ rule and information theory are used to maximize the information gained from each trial, while minimizing uncertainty in the probability distribution (Kontsevich & Tyler, 1999). The result of each trial is used to update the probability distribution function (PDF) and thus narrow the range of possible thresholds. Based on this function, REPT calculates the intensity for the next stimulation that will add the most information to the distribution based on all previous stimulation intensities and their responses (this intensity is the most probable Bayesian estimate of the threshold at that particular time). It should be noted that REPT is initially sensitive to errors made in responding, as the PDF is largely undeveloped in the early stages of the procedure. However, even in such situations, REPT’s continuous updating of the PDF means that it can still identify the true threshold (Mazzi et al., 2017). Such errors in REPT only delay the overall algorithm as opposed to requiring an entirely new one to be run (Abrahamyan et al., 2011). While untested in tES based phosphene research, the REPT algorithm has been tested in TMS research and was found to provide reliable thresholds quickly (with a relatively low number of test points

required compared to the methods listed above, while also being resistant to habituation effects; Abrahamyan et al., 2011; Mazzi et al., 2017).

For this series of experiments, the Quest algorithm (Watson & Pelli, 1983) was employed to execute REPT using Psychtoolbox in MATLAB (Kleiner et al., 2007). It uses the Weibull psychometric function:

$$p = \delta\gamma + (1-\delta) * (1 - (1-\delta) * \mathrm{e}\left(-10^{\beta*(x-x_{Threshold})}\right))$$

Where p is the probability that a given threshold will yield a positive response, δ is the likelihood that a response is random, γ is the predicted false positive response rate, β is the slope of the psychometric function, and x represents the $\log_{10}$ contrast relative to the thresholds (and their responses) recorded in the associated PDF (Watson & Pelli, 1983). By continuously updating the PDF with new data, REPT can typically narrow down the range of possible thresholds with relatively few responses. It is also generally less susceptible to response errors than other recently developed adaptive psychophysical methods.

1.7: Summary

The current view of electrophosphenes is that they are the product of retinal rather than cortical activation, with stimulation frequency-dependent characteristics dictated by ambient lighting levels. The difficulty is that this view has been formed from literature with very small sample sizes, irregular methodologies, and often no statistical analysis (see **Table 1.1**, p. 24).

For example, the view that tES at 10 Hz will result in stronger phosphenes in dark conditions is attributed to Friedrich Schwarz's study from 1947 with a single subject. Despite this, Schwarz is still being cited as the primary source for this claim; recent examples of this include: 1) the 2013 review of tACS mechanisms by Hermann and colleagues (cited by 653), 2) Lövsund and colleagues (1980, cited by 221) study of magnetophosphene thresholds, 3) Schwiedrzik's (2009) discussion paper on retinal ganglion cells being the source of tACS-induced phosphenes (cited by 99), 4) Paulus' (2010) discussion paper on separating retinal and cortical origins of phosphenes (cited by 70), 5) Kanai and colleagues' (2010, cited by 163) study on the

modulation of the cortex via tACS, and 6) Laakso and Hirata's (2013) computational analysis of how tACS stimulates the retina (cited by 105)[6].

The view that electrophosphenes are more intense at 20 Hz stimulation in well-lit conditions is also founded on poor quality legacy literature. Much like the dark condition above, this is based on a low number of studies with single digit sample sizes, often with no statistical analysis reported, questionable experimental design, and important methodological details missing (see **Table 1.1**, p. 24). As noted previously, the discussion of electrophosphenes in mesopic conditions is entirely neglected.

Similarly, the issue of whether tES phosphenes are sourced from the retina (instead of the visual cortex) has not been established. The evidence against tES-induced cortical phosphenes relies on modelled estimates (e.g., Laakso & Hirata, 2013) or varying the distance between electrodes and the retina (e.g., Rohracher, 1935), neither of which addresses the visual cortex itself. While some studies do compare montages targeting the retina or the visual cortex (e.g., Schutter & Hortensius, 2010), this is not sufficient to separate the two potential sources (because the retina and the visual cortex are not independent from each other in the visual system). An effective double dissociation analysis is required to make this source separation possible, and to date this has not been provided.

If EMF exposure guidelines are to rely (even in part) on the results of tES research, then the beliefs listed above should be confirmed using robust testing methodologies. This thesis will do so. All studies used larger sample sizes than historically found in the electrophosphene literature and employ a within-subjects design, meaning each subject was tested for every possible combination of variables. This applied to all ambient lighting conditions, all relevant frequencies in each lighting condition, and all necessary montages (in order to provide a more effective double dissociation between potential biological sources of phosphenes).

The study in Chapter 2 focused on electrophosphenes in mesopic conditions. Since little has been established regarding sensitivity to any particular frequency in mesopic conditions, phosphene detection thresholds were tested for a broad range of frequencies (fifteen frequencies between 2-30 Hz). These thresholds were determined for two montages: one

[6] Citation counts according to Google Scholar as of January 9th, 2023

preferentially targeting the retina (FPz-Cz) and another preferentially targeting the visual cortex (Oz-Cz).

The study in Chapter 3 compared the thresholds for electrophosphenes in mesopic conditions in a more narrow frequency range (seven frequencies between 6 – 32 Hz). This study tested phosphene detection using four montages rather than two (FPz-Cz, Oz-Cz, FPz-Oz, T3-T4), making a true double dissociation between retinal and cortical phosphenes possible. This investigation also compared: 1) modelled estimates of the current density at V1 and the retina for all montages; as well as 2) the relationships between those modelled current density estimates and the empirically obtained phosphene thresholds. In addition, this study examined whether stimulation polarity affects any aspect of tES phosphenes in either the retina or the cortex. In order to assess this, the polarity of stimulation was counterbalanced across the sample in all combinations of conditions to assess if polarity has an effect.

The study in Chapter 4 compared thresholds and frequency sensitivity for electrophosphenes in well-lit, mesopic, and dark conditions in the 10 – 20 Hz frequency range (already believed to be associated with phosphenes in well-lit and dark conditions). In order to determine the reliability of the REPT algorithm, thresholds for all conditions were tested twice, on two separate days, to determine test-retest reliability.

2 – EXPERIMENT ONE

Adapted from: Evans, I. D., Palmisano, S., Loughran, S. P., Legros, A. & Croft, R. J. (2019). Frequency-dependent and montage-based differences in phosphene perception thresholds via transcranial alternating current stimulation. *Bioelectromagnetics, 40,* 365-374 (2019). doi:10.1002/bem.22209

Summary: This study investigates how the location and frequency of transcranial alternating current stimulation (tACS) affects phosphene detection thresholds in mesopic conditions. We tested 24 subjects by stimulating different scalp locations (FPz-Cz vs. Oz-Cz) at different frequencies (2 – 30 Hz in 2 Hz increments) to measure their thresholds for perceiving phosphenes. Of interest, phosphene detection thresholds were substantially lower when tACS was applied over the frontal rather than occipital area of the scalp. In both cases, the lowest phosphene detection thresholds were found with a frequency of 16 Hz, which appears quite different to the minima frequencies reported in past studies using well-lit (20 Hz; Adrian, 1977; Kanai et al., 2008; Lövsund et al., 1980) and dark (10 Hz; Kanai et al., 2008; Schwarz, 1947) environmental conditions. Subsequent experiments will attempt to verify this 16 Hz frequency dependence finding under the same lighting levels (in different samples using transcranial direct current stimulation).

2.1: Introduction

Transcranial electrical stimulation (tES) is a non-invasive brain stimulation technique that allows researchers and therapists to induce localised and controlled interference in the brain by generating electrical fields at the scalp (Antal et al., 2008; Kanai et al., 2008; 2010). Its principal mechanism is the modulation of neuronal membrane potentials, which alters cortical excitability and activity depending on the current flow through the target neurons (Purpura & McMurtry, 1965). The neuromodulatory intent is to entrain brain oscillations (Antal et al., 2008) so that we may both measure the brain–function relationship in a direct manner (Hallett, 2007) and develop therapeutic techniques to manage or reverse a broad range of neural pathologies (Brittain et al., 2003; Nitsche et al., 2003). As well as altering cortical function, tES has long been found to also induce phosphenes, which are visual perceptions of flashing or shimmering light in the absence of accompanying visual input. Thresholds for phosphene generation have been used by international standards bodies to limit exposure of the head to low frequency electric and magnetic fields, with the logic being that they represent a conservative estimate of the field strength required to interfere with central nervous system function more generally (International Commission on Non-Ionizing Radiation Protection, 2010). tES has been used to study phosphene perception thresholds (Antal et al., 2003; Schwiedrzik, 2009), and from this much can be learned about the factors that affect phosphene perception. Manipulation of magnetic fields about the eye, which generates electric current as a function of the rate of change of the magnetic field, has also been used to study phosphenes (Legros et al., 2015; Lövsund et al., 1980; Souques et al., 2014). However, there is still substantial uncertainty regarding the relationship between electric current and phosphene perception thresholds, particularly in terms of stimulation location and frequency. Addressing some of this uncertainty would therefore be useful not only for phosphene-based exposure guidelines, but also for sensory neuroscience more generally.

Observational phosphene research dates back to 1755, when a boy already blinded by cataracts reported seeing a bright flash of light in the bottom half of his field of view when a Leyden jar was discharged across the orbits of his eyes (LeRoy, 1755), which would have resulted in an electric current about the eyes. Eventually, it became clear that the intensity of

these electrically-induced phosphenes was changed not only by the strength of the electrical field, but also by its frequency. The first attempts to quantify the frequency-dependent nature of phosphenes have been largely credited to Rohracher (1935). When using multiple arrangements of electrodes (known as montages) around the head, he found that phosphenes generated at 15 or 20 Hz (selected from 13 frequencies ranging between 5 – 80 Hz) consistently required the least electrical energy. Adrian (1977), testing on himself and using two orbitocontralateral ear montages, found an optimal range of 18-22 Hz (selected from 25 frequencies ranging between 0.01-75 Hz). Lövsund et al., (1980), using five subjects and testing 35 frequencies between 10-45 Hz, reported a specific threshold minimum at 20 Hz, although, as with Rohracher (1935), Schwarz (1947), and Adrian (1977), this was not statistically compared to any other frequency.

Phosphene detection thresholds have also been reported to depend on ambient lighting conditions. Schwarz (1947) tested 12 frequencies between 10 – 93 Hz with an upper jaw/forearm montage (also with a single test subject) and reported that phosphenes were most readily induced at 20 Hz in each of the lighting conditions that he tested (approx. 2.4 – 9550 cd/m^2), which is consistent with Lövsund (1980), Kanai et al. (2008) and Schutter & Hortensius (2010). By contrast, Schwarz (1947) and subsequently Kanai et al. (2008) reported that phosphenes were induced more readily at 10 Hz in the dark, suggesting that the light adaptation mechanisms of the eye might interact with phosphene perception. However, when coupled with predictions based on cellular studies of the retina and visual cortex, this luminosity function raises some questions. For example, primate retinal ganglion cell activation is most sensitive in the 14 - 18 Hz stimulation range regardless of lighting conditions (Benardete & Kaplan, 1999), whereas the visual cortex of the cat is sensitive across the 7 - 20 Hz range regardless of lighting conditions (Bringuier et al., 1997).

Given that the phosphene-frequency function would appear to better match the visual cortex rather than ganglion cell neurons, the available human data appears to be more consistent with the assumption that phosphenes are generated in the visual cortex than the retina. This is supported by results from Kanai et al. (2008) who reported that tES over occipital scalp sites resulted in phosphenes, which the authors interpreted as being due to cortical stimulation. However, there is not currently sufficient evidence to conclude on this issue, as the resultant current would also have reached the retina via volume conduction in this study (Laakso and

Hirata, 2013), and it is possible that electrophosphenes are generated at even earlier levels of retinal processing; i.e., triggered by the electrical stimulation of the horizontal, amacrine, and bipolar cells or even the photoreceptors (Attwell, 2003).

A key limitation in our understanding of tES phosphene generation is that the research underpinning this knowledge is far from complete. A combination of low sample sizes (n < 10), irregular frequencies selected for testing (and a lack of consistency in the frequencies examined across studies), irregular lighting conditions (and reporting thereof), the use of subjective measures such as "brightness ratings" to measure phosphene intensity, and the lack of within-subject experimental manipulations, all make firm conclusions difficult to draw. Given that international guidelines use phosphenes as the basis for some of their exposure limits (e.g., International Commission on Non-Ionizing Radiation Protection (ICNIRP; 2010), it is important that we develop a more complete picture of the relationship between electric current and phosphene perception.

The aim of this study was therefore to systematically examine the relationship between phosphene perception and tES-induced stimulation, while overcoming some of the limitations of the previous research. To this end, phosphene detection thresholds were obtained using transcranial alternating current stimulation (tACS) to frontal and occipital scalp sites, across a wide range of frequencies (2 - 30 Hz, in 2 Hz steps), within a relatively large sample (n = 24) and using a fully within-subjects counterbalanced design.

2.2: Method

Twenty-four healthy subjects (even gender split, aged 19-39, mean 27.9 years) completed this study after passing a modified safety screening checklist (Keel et al., 2000; for details see Appendix A, p. 157). Subjects were excluded if they reported any form of neural injury or illness, metal implant in the head or a medical implant elsewhere in the body, or non-corrected visual impairment. This research was approved by the Human Research Ethics Committee of the University of Wollongong (Approval #HE2017/454).

tES was administered using a Magstim NeuroConn Stimulator Plus MOP15-EN-01 (Magstim, Carmarthenshire, UK) operating in sinusoidal AC mode through conductive-rubber electrodes

(dimensions: 30 x 40 mm cathode, 56 mm diameter circular anode) placed on sponges saturated with a saline solution mixed with a hypoallergenic amphoteric surfactant and held in place at the appropriate montage with rubber straps. All stimulations were sinusoidal with no DC offset and no ramp-up.

The basic workflow of the experiment is provided in **Figure 2.1a** below. The experiment involved two testing sessions in which stimulation was delivered via either a frontal montage (cathode centred at FPz, anode at Cz) or an occipital montage (cathode centred at Oz, anode at Cz; see **Figure 2.1b**). The two sessions were conducted at similar times on separate days, usually within a week of each other. Session order (frontal/occipital) was counterbalanced across subjects, with each session taking approximately 90 minutes to complete. Subjects were seated on a chair in a dimly lit room with black curtains covering any walls that would appear in their field of view (including peripheral vision) to keep the field of view consistent and were asked to keep their eyes open during stimulations. Illumination at the black curtain was measured at 6 ± 0.05 cd/m^2, while luminance levels at the subjects' eyes were measured to be 0.6 ± 0.05 cd/m^2, using a J6523 Tektronix luminance probe (Tektronix, London, Canada).

Figure 2.1
A) Basic workflow for the experimental procedure. Timeframes for each phase varied, however in general the combined Setup and Familiarization phases took 20 - 30 minutes which served as the dark adaptation period.
*B) Electrode locations on the scalp (using the International 10-20 system). The rectangular electrodes (arranged lengthwise along the centre line of the scalp) were 30*40 mm, whilst the circular reference electrode at the vertex (Cz) was 56 mm in diameter.*

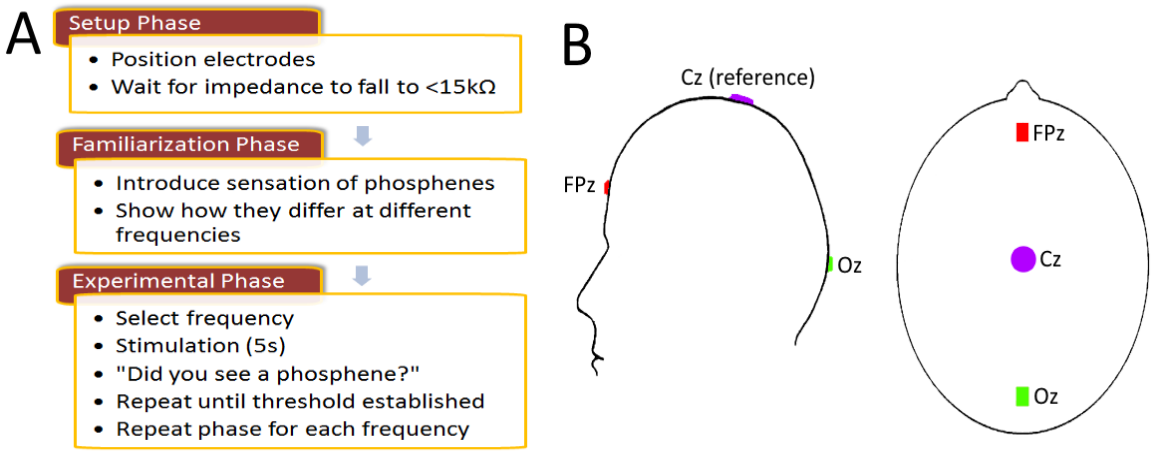

Once the electrodes were in position, subjects were verbally informed of the nature of phosphenes and what they might perceive, whilst their skin and hair were saturated from the saline in the sponges. Subjects were given 20 – 30 minutes to adapt to the lighting conditions prior to the commencement of data collection. This period included the initial experimental setup, time taken for impedance levels to fall to acceptable levels, and time necessary for the familiarization stage where subjects were first introduced to phosphenes. Once impedance between the electrodes was at 15 kΩ or below (as indicated by the stimulator), subjects were familiarized with the appearance of phosphenes using 10 seconds of transcranial alternating current stimulation (tACS) at 1000 μA, firstly at 12 Hz and then at 22 Hz, to demonstrate both the visual appearance of phosphenes and how they could change by varying only the frequency of the stimulation. Once subjects were familiarized with phosphenes, the fifteen different frequencies were tested (2 – 30 Hz) in a predetermined random order.

Thresholds for phosphene perception (in μA) were determined for each frequency by varying the tACS current using a QUEST-based Bayesian adaptive staircasing procedure (Watson & Pelli, 1983) in MATLAB's PsychToolbox (Kleiner et al., 2007), starting at 700 μA and bound between 25 μA and 1500 μA, with a step-size of 25 μA between stimulation levels. Based on the Rapid Estimation of Phosphene Threshold system validated by Mazzi et al. (2017), this adaptive threshold measurement method determined the lowest stimulation intensity that was significantly more likely than chance to evoke phosphene perceptions. When subjects did not report any phosphenes at the maximum stimulation intensity (1500 μA), a value of 1500 μA was used for the statistical analyses.

All stimulations lasted for 5 seconds, and subjects were informed when stimulation began and when it ceased. To detect false positive responses at lower stimulation levels, four sham stimulations were given at random times during each session, where the subject was given all of the audible signs of a stimulation (the usual button presses on the stimulator as well as verbal indications that the stimulation had started and finished) without actually generating an electric current. One subject was excluded from the analysis after repeated reports of phosphene perception during these sham trials. None of the 24 remaining subjects reported seeing phosphenes during any of the sham trials.

2.3: Statistical Analysis

Statistical analyses were performed using SPSS Statistics v23 (IBM, Chicago, IL). The phosphene detection thresholds obtained from our 24 subjects were examined using a two-way repeated measures ANOVA, as a function of montage (factor = montage; levels = frontal versus occipital) and the 15 different frequencies of stimulation (factor = stimulation frequency; levels = 2 – 30 Hz in steps of 2 Hz). Mean phosphene detection thresholds were calculated for each montage and for each of the 15 frequencies tested, and the stimulation frequency for each montage that required the lowest mean current for phosphenes to be perceived (i.e., the minima frequency) was identified. The phosphene thresholds for these minima frequencies were then compared to the mean phosphene thresholds at 10 Hz and 20 Hz (identified as the minima frequencies for dark and lit conditions in previous studies (Adrian, 1977; Kanai et al., 2008; Lövsund et al., 1980; Rohracher, 1935; Schwarz 1947) using planned contrasts (10 Hz versus frequency with minima, and 20 Hz versus frequency with minima) for each montage separately.

To estimate the actual frequency minima for phosphene perception (rather than restricting estimates to the 2 Hz step-size), group data regression-based curve estimates were then calculated using the Curve Fitting tool in MATLAB 2016b (Mathworks, Natick, MA). These regressions of the group data were restricted to quadratic and cubic functions to avoid overfitting, and the function with the highest R^2 value with all coefficients significant was selected as the most appropriate fit. Based on this preferred function order, fits of the same order were calculated separately for both montages. In order to test whether the two montages had different regression curves, the beta coefficients were compared using t-tests (excluding the constant).

Individual regression curves were next calculated for each of our 24 subjects separately. For these fits, the best group fit for each montage was selected based on the equation that yielded the highest adjusted R^2 value with all coefficients significant, and then regression curves were calculated for each individual subject using the same order function as selected for the montage. Because these regressions were designed to determine the most accurate estimate for an individual and not for predictions on populations, the requirement for a lower order fit was removed. This resulted in two separate regression curves for each montage per

subject. Frequencies with the minima threshold values were estimated for each subject and montage using these regression curves (as we were also interested in how minima frequencies and thresholds varied across our sample). These estimated minima frequencies were then also compared to the minima frequencies previously identified by the literature for dark and lit conditions (i.e., 10 Hz and 20 Hz respectively) using planned contrasts (10 Hz versus frequency with minima, and 20 Hz versus frequency with minima) for each montage.

2.4: Results

2.4.1: Differences in Detection Thresholds

Thresholds for all individuals in every montage and frequency can be read in Appendix B (p. 160). The Montage by Frequency repeated measures analysis of variance (ANOVA) for the phosphene detection thresholds obtained from our 24 subjects (see **Figure 2.2**, p. 54) found: A significant main effect of Montage ($F(1,23) = 271.67$, $p < 0.001$, $\eta_p^2 = 0.922$), with the thresholds lower for the FPz-Cz montage ($M = 412.36$ μA; $SD = 397.33$; $SE = 21.48$) than the Oz-Cz montage ($M = 944.10$ μA; $SD = 466.27$; $SE = 32.45$); a main effect of Frequency ($F(14,10) = 173.40$, $p < 0.001$, $\eta_p^2 = 0.996$); and an interaction between Montage and Frequency ($F(14,10) = 13.80$, $p < 0.001$, $\eta_p^2 = 0.951$). This latter result suggests that the psychophysical functions relating the frequency to phosphene detection thresholds were different for the FPz-Cz (**Figure 2.2a**) and Oz-Cz (**Figure 2.2b**) stimulations.

Of the 15 stimulation frequencies examined, the lowest thresholds for phosphene detection occurred for 16 Hz stimulation in both the FPz-Cz and Oz-Cz montages (see **Figure 2.3**, p. 55). For 16 Hz stimulation, thresholds were significantly lower than those obtained for the 10 Hz stimulations for both the FPz-Cz montage ($F(1,23) = 45.69$, $p < 0.001$, $\eta_p^2 = 0.665$) and the Oz-Cz montage ($F(1,23) = 98.61$, $p < 0.001$, $\eta_p^2 = 0.811$). The 16 Hz stimulation thresholds were also significantly lower than those obtained in the 20 Hz stimulations for the FPz-Cz montage ($F(1,23) = 11.52$, $p = 0.002$, $\eta_p^2 = 0.334$) and the Oz-Cz montage ($F(1,23) = 29.99$, $p < 0.001$, $\eta_p^2 = 0.566$).

Figure 2.2

Individual detection thresholds for tACS induced-phosphenes for our 24 subjects using either an FPz-Cz (top) or an Oz-Cz (bottom) montage, as a function of stimulation frequency. The mean thresholds across subjects for each montage lie on the solid blue line in each case. Examining the differences in variation between montages indicates that the FPz-Cz montage results in more consistent threshold values.

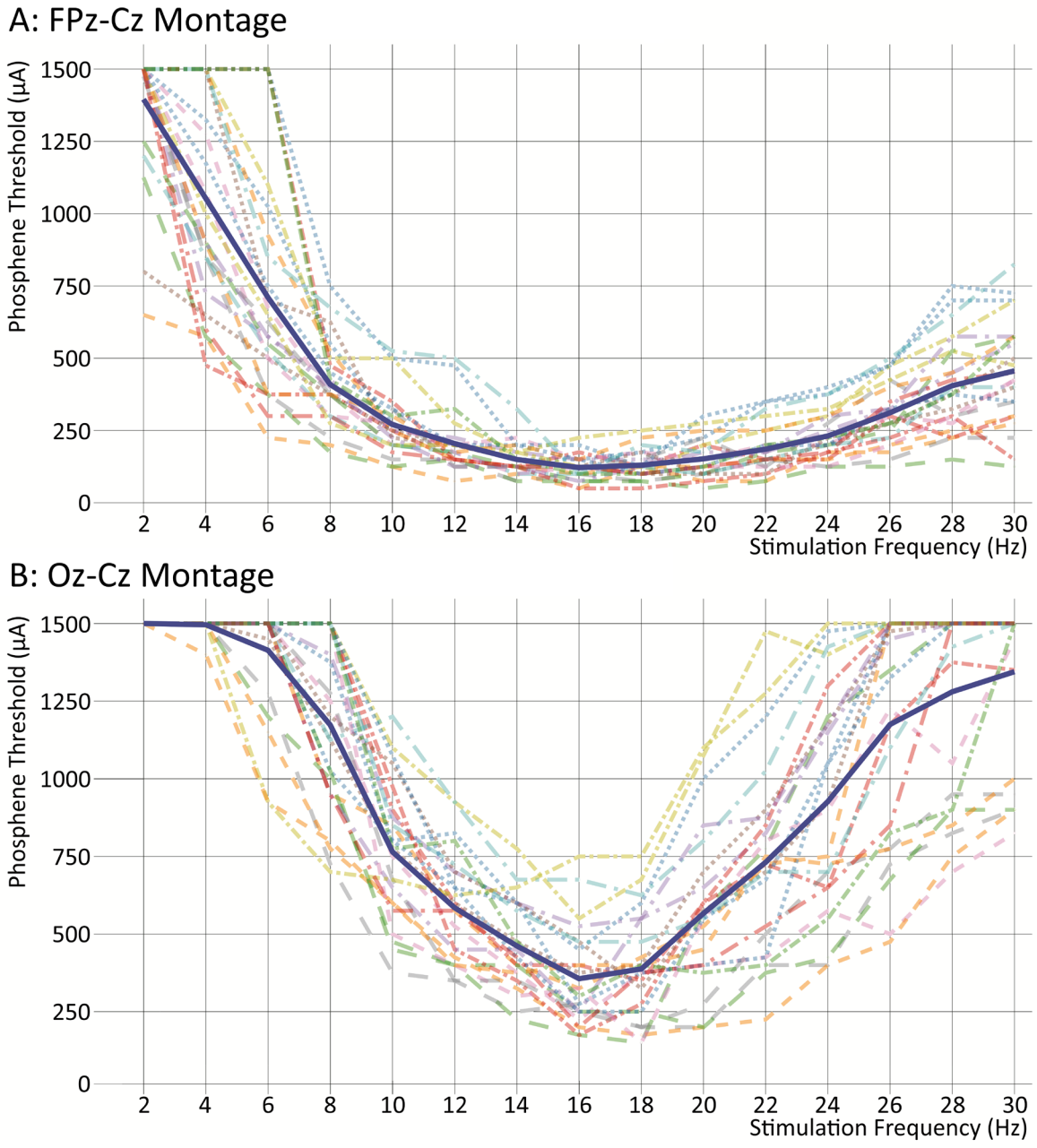

Figure 2.3

Mean phosphene detection thresholds for each frequency tested lie on the orange (FPz-Cz montage) and blue (Oz-Cz) lines respectively; standard deviation bars are shown.

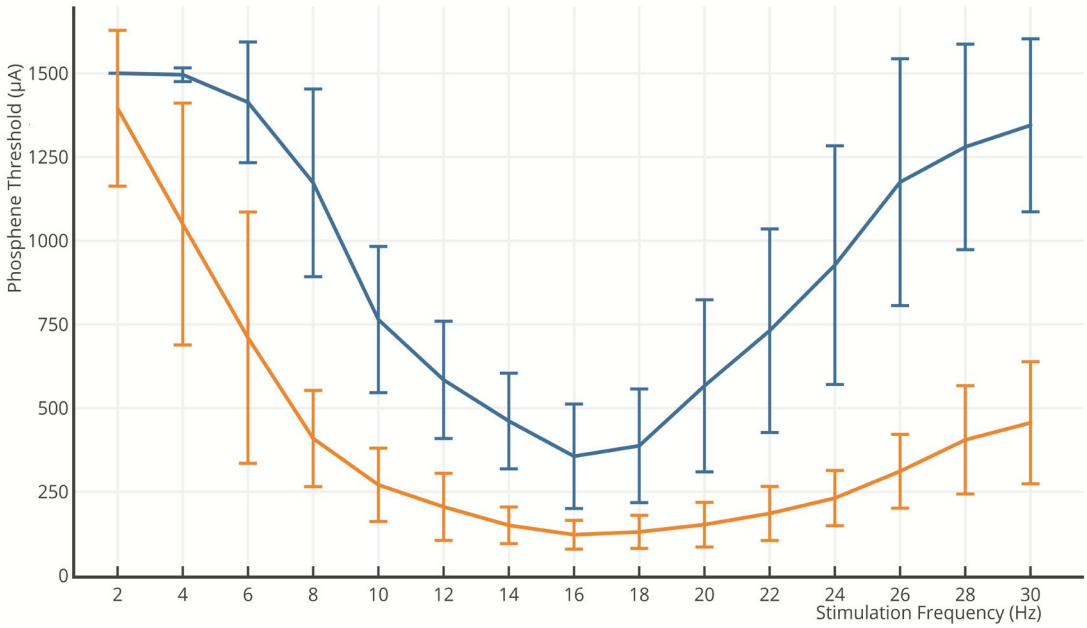

2.4.2: Group Data Regressions

Of the two types of function examined for the overall group data (both montages combined), the best fits were found to be a cubic function ($F(3,716) = 224.99$, $p < .001$, adjusted $R^2 = .487$, predicted $R^2 = 0.479$). Cubic fits were then calculated for each separate montage, where y is the phosphene detection threshold and x is the stimulation frequency in Hz (reported to two decimal places; see **Figure 2.4**, p. 56):

$$y(FPz - Cz) = -0.16x^3 + 11.90x^2 - 260.28x + 1874.59$$

$$y(Oz - Cz) = 0.03x^3 + 4.29x^2 - 169.61x + 2036.44$$

All beta coefficients were significantly different between montages; the cubic order coefficient for the Oz-Cz montage was significantly higher ($t(1,719) = 5.32$, $p < .001$), the quadratic order coefficient for the FPz-Cz montage was significantly higher ($t(1,719) = 4.46$, $p < .001$), and the linear order coefficient for the Oz-Cz montage was significantly higher ($t(1,719) = 3.79$, $p < .001$).

Figure 2.4

Cubic regression estimates for each montage. The vertical black bar on each curve shows the minima frequency.

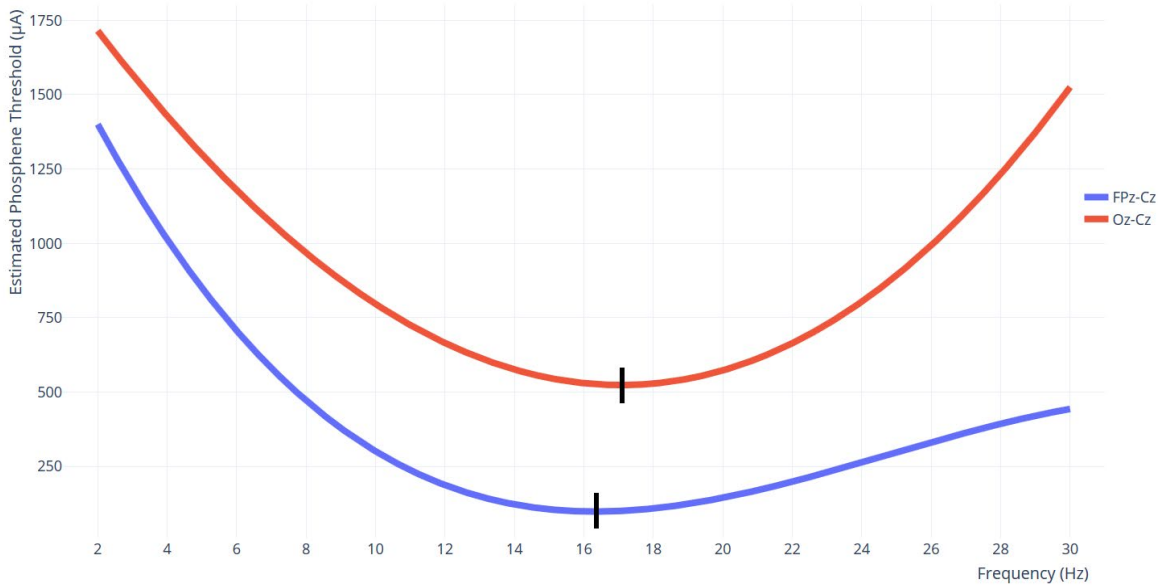

2.4.3: Individual Data Regressions

We then determined the best group fit for each montage. The best group fit for the FPz-Cz montage was a cubic function ($F(3,356) = 498.14$, $p < 0.001$, adjusted $R^2 = 0.806$, predicted $R^2 = 0.803$):

$$y(FPz - Cz) = -0.16x^3 + 11.90x^2 - 260.28x + 1874.59$$

The best group fit for the Oz-Cz montage was a quartic function ($F(4,355) = 244.94$, $p < 0.001$, adjusted $R^2 = 0.731$, predicted $R^2 = 0.727$):

$$y(Oz - Cz) = -0.038x^4 + 2.46x^3 - 46.82x^2 + 222.47x + 1229.51$$

Best fit regression curves were next calculated for each subject and montage using the same order equations as determined by these group fits. That is, cubic fits were always applied for the FPz-Cz montage, and quartic fits were always applied for the Oz-Cz montage (see **Figure 2.5**, p. 58). From these fits, the minima frequencies (and their respective threshold levels) were then estimated for each subject and for each montage.

As with the recorded data, the estimated minima frequencies for both montages were compared to the previously reported minima frequencies of 10 Hz and 20 Hz for dark and lit conditions respectively. The mean of the individually estimated frequency minima for the FPz-Cz montage (*M* = 16.30 Hz; *SD* = 1.54 Hz; *SE* = 0.31 Hz) and the Oz-Cz montage (*M* = 16.50 Hz; *SD* = 1.30 Hz; *SE* = 0.27 Hz) were both found to be significantly higher than 10 Hz (FPz-Cz: $F(1,23) = 385.94$, $p < 0.001$, $\eta_p^2 = 0.944$; Oz-Cz: $F(1,23) = 574.38$, $p < 0.001$, $\eta_p^2 = 0.961$). The frequency minima for the FPz-Cz and the Oz-Cz montages were also both significantly lower than 20 Hz (FPz-Cz: $F(1,23) = 133.03$, $p < 0.001$, $\eta_p^2 = 0.853$; Oz-Cz: $F(1,23) = 166.72$, $p < 0.001$, $\eta_p^2 = 0.879$). However, the estimated frequency minima for the two montages (16.30 Hz and 16.50 Hz) did not differ significantly from each other; $F(1,23) = 0.36$, $p = 0.554$, $\eta_p^2 = 0.015$.

The mean of the individually estimated current thresholds for the FPz-Cz montage (*M* = 87.89 µA; *SD* = 50.44 µA; *SE* = 10.30 µA) and for the Oz-Cz montage (*M* = 347.64 µA; *SD* = 161.67 µA; *SE* = 33.00 µA) were both significantly lower than at 10 Hz (FPz-Cz: $F(1,23) = 104.87$, $p < 0.001$, $\eta_p^2 = 0.820$; Oz-Cz: $F(1,23) = 233.89$, $p < 0.001$, $\eta_p^2 = 0.910$). This was also the case for the FPz-Cz montage at 20 Hz ($F(1,23) = 45.00$, $p < 0.001$, $\eta_p^2 = 0.662$) and the Oz-Cz montage at 20 Hz ($F(1,23) = 56.244$, $p < 0.001$, $\eta_p^2 = 0.710$). The estimated thresholds at the frequency minima for the FPz-Cz montage (87.89 µA) was significantly lower than for the Oz-Cz montage (347.64 µA); $F(1,23) = 72.44$, $p < 0.001$, $\eta_p^2 = 0.759$.

2.4: Discussion

Our knowledge concerning the role of tACS frequency and electrode location on phosphene thresholds has been obtained largely through extrapolation from between-subject designs using small sample sizes (n < 10) and limited frequency manipulations. The present study aimed to test the veracity of this knowledge by examining multiple tACS frequencies, and both frontal and occipital electrode montages using a fully repeated-measures design with a large sample size (n = 24). This resulted in relatively small error variance and, as a result, unambiguous relations between phosphene detection thresholds and both tACS frequency and stimulation location. Results were consistent with the existing literature in terms of the

effect of stimulation location on phosphene detection threshold, whereas some differences were found in terms of the frequency-threshold relation.

Figure 2.5

Individual regression curve estimates of phosphene detection thresholds as a function of frequency for each of the 24 subjects. The curves for the FPz-Cz montage are in the top plot and those for the Oz-Cz montage are in the bottom plot. The solid line in each plot shows the group regression curve estimate for each montage. Vertical black bar on each distribution shows the minima frequency. Similarly to the recorded data presented in Figure 2.2 (p. 54), there is comparatively lower variance in thresholds in the FPz-Cz results (≥ 10 Hz) compared to the Oz-Cz results.

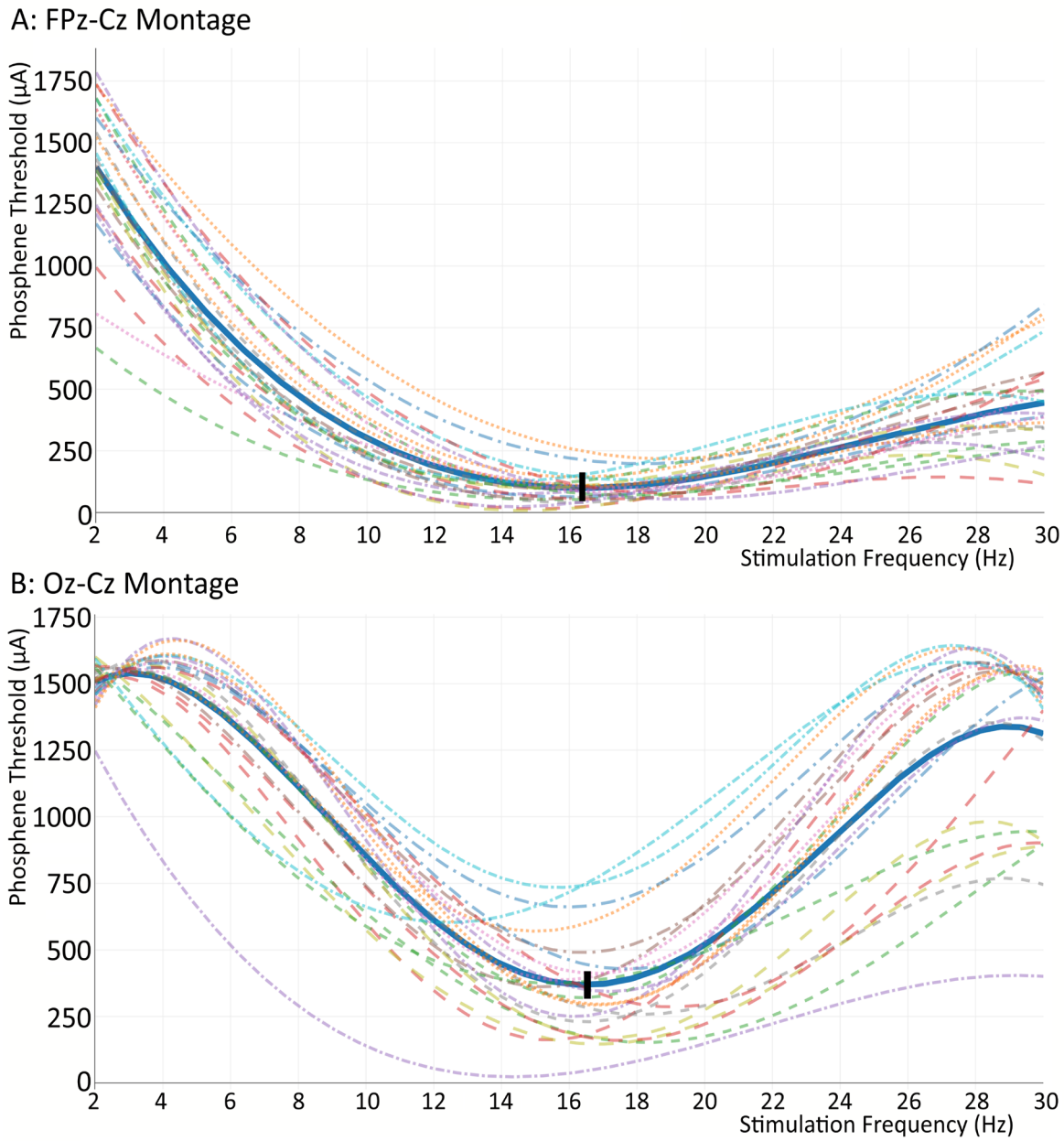

Qualitatively, phosphene appearance was reported to change consistently with stimulation intensity, regardless of montage. When stimulations were well above threshold, phosphenes typically filled the subject's entire field of view. As the amperage was reduced towards the threshold, the locations of the phosphenes became more localised; usually either at the centre of their field of view, at the periphery (or parts of the periphery), or at other locations. When stimulations were just above threshold, phosphenes were reported as indistinct; often no firm position could be identified, but the perception of flickering or a change in brightness was reported. The location of the phosphenes would (in some cases) change across frequencies, but no consistent observations were reported across the sample. Regardless of montage, and despite being blind to the stimulation frequency, subjects spontaneously reported changes in the flashing speed of the phosphenes as the frequency of stimulation changed, similar to reports in previous phosphene perception research (Turi et al., 2013). Lower frequencies (2 – 8 Hz) were typically reported as slow "pulses" of light, mid-range frequencies (10 – 24 Hz) were reported as more rapid "flashes" or "flickering" with a rate in line with the frequency, while the fastest frequencies (26 – 30 Hz) were so fast that subjects tended to report the phosphenes as a blur rather than distinct flashes of light.

Phosphene detection thresholds were substantially lower when tACS was applied over the frontal rather than occipital area of the scalp, with the current required to elicit a phosphene using the Oz-Cz montage being more than double that required for the FPz-Cz montage. This is consistent with previous reports (Kar & Krekelberg, 2012; Schutter & Hortensius, 2010). It also appears consistent with the view that phosphenes can be generated at the retina, as the current density reaching the retina is substantially higher when stimulation occurs over the frontal rather than the occipital scalp (Laakso & Hirata, 2013). However, the relationship between phosphene threshold and stimulation frequency differed between the occipital and frontal montages, with stronger frequency dependence for the occipital montage above approximately 16 Hz; this would not be expected if the occipital stimulation results in phosphenes via retinal activation. The variation in beta coefficients indicates that the stimulation of two differing sites may not necessarily result in the same activation characteristics. These differences in the threshold distributions may indicate the presence of a second (potentially occipital-based) mechanism in addition to retinal activation. However,

determining the source(s) of the phosphenes is a difficult task, and the present study was not designed to determine this.

It should be noted that the maximum stimulation used in the study was 1500 µA. This was used as the minimum estimate of the actual threshold when no phosphene was seen (as the actual phosphene threshold would necessarily have been higher than 1500 µA in this situation). However, if we had obtained the actual thresholds for these frequency conditions, the differences between the two montages would have been even larger than those shown in **Figures 2.3** (p. 55) and **2.5** (p. 58). Thus, our use of a 1500 µA ceiling cannot explain the different frequency responses that we observed for the FPz-Cz and Oz-Cz montages. Applying a different approach and removing the ceiling cap data from the analyses was not appropriate, as this resulted in: 1) lower estimates of the phosphene thresholds (when we know that the actual thresholds would be higher), 2) poorer curve fits (i.e., less variance was explained by the models), and 3) decreasing thresholds for Oz-Cz with increasing frequency (which is not consistent with what has been shown in the literature; (Adrian, 1977; Kanai et al., 2008; Lövsund et al., 1980; Rohracher, 1935; Schwarz, 1947).

Another potential explanation for the differential frequency response could be that the volume conduction of the current is frequency dependent (as a function of tissue type), with different tissues being encountered on the paths during occipital and frontal stimulation. However, as current propagation is thought to be frequency independent above 10 Hz in the cortex (Logothetis, Kayser & Oeltermann, 2007), the different frequency functions for FPz-Cz and Oz-Cz (which are primarily related to frequencies above 16 Hz) do not appear to be explicable exclusively in terms of differential volume conduction as a function of frequency from the back (versus front) of the head to the retina. There is thus no clear explanation for the different frequency-phosphene threshold relations for frontal and occipital stimulation conditions, and again the possibility of a role for the occipital cortex in phosphene perception cannot be excluded. This is consistent with Kanai et al. (2008), who argued that phosphenes can be generated at the occipital cortex.

The present study found that phosphene thresholds were lowest at approximately 16 Hz (the minima frequency), for tACS over both the frontal and occipital scalps. This differs significantly from the minima frequencies reported previously for phosphenes under both lit (20 Hz;

Adrian, 1977; Kanai et al., 2008; Lövsund et al., 1980) and dark (10 Hz; Kanai et al., 2008; Schwarz, 1947) environmental conditions. One potential explanation for this may be that the lighting conditions in the present study were in the intermediate "mesopic" range of lighting conditions between the above-mentioned lit and dark conditions. This possibility is difficult to address quantitatively given that most research has not reported the ambient lighting conditions, and there is no generally agreed definition for what luminance levels constitute mesopic lighting (Stockman & Sharpe, 2006). Of those studies that did report lighting conditions similar to the present study, Lövsund (1980) reported their minima to be at 20 Hz (with 1.2 cd/m^2 background lighting), while Kar and Krekelberg (2012) reported the lowest thresholds in the alpha range (8-15 Hz; using 0.4 cd/m^2 background lighting). A useful guide to interpreting the literature is that approximately 500 cd/m^2 is suitable lighting for typical office work, whereas 10 and 100 cd/m^2 are equivalent to twilight and low-level office lighting respectively. Thus, 'lit' conditions would be expected to be at least 100 cd/m^2, and 'dark' conditions to be below approximately 10 cd/m^2. The ambient light levels in the present study (0.6 cd/m^2) would therefore be described as dark. Thus, the present results should be compared with those of the dark conditions currently available in the literature, which primarily reported thresholds at 10 Hz. Clearly, the observed 16 Hz minima in our study do not support the previous reports of minima at 10 Hz, suggesting either: 1) a failure to replicate previous reported findings relating to dark conditions, or 2) mesopic lighting conditions cause an entirely different set of frequency-dependent effects on tACS phosphene detection compared to other lighting conditions.

Any discussion of lighting effects on phosphene induction could usefully acknowledge the issue of differential rod and cone receptor activation. Under mesopic lighting conditions, rod receptors are typically sensitive to flickering lights up to 15 Hz, whereas cone receptors are not (Conner & MacLeod, 1977; Sharpe et al., 1989). This could potentially explain the observed 16 Hz frequency minima found in the present study. However, if rod sensitivity was responsible for the frequency-dependent aspect of our findings, then phosphene perception thresholds should have been even smaller for lower frequencies, which was not the case in this study nor in any other electromagnetic-induced phosphene perception study. Further, given that testing in the present study began at least 10 minutes after entering the darkened testing area, neither light adaptation effects nor rod/cone frequency dependent interactions

are likely to have played a major role in the present study. Therefore, there is no indication that the different minima frequency for the current (16 Hz) and previous studies were due to effects of lighting.

Our findings of a 16 Hz minima frequency for phosphene perception are consistent with one of the earliest studies in this area (Rohracher, 1935), which reported the phosphene minima to be within the 15 - 20 Hz range (but lacked the frequency resolution to determine where within this range it occurred). It is also within the 14 - 18 Hz peak frequency-dependent response rate of retinal ganglion cells observed in non-human primates (Benardete & Kaplan, 1999) and within the 7 - 20 Hz expectation for the visual cortex of the cat (Bringuier et al., 1997). If indeed the cell firing rates of the cat and monkey are appropriate models for human tACS phosphene generation, this would suggest that studies reporting threshold minima at either 10 or 20 Hz (Adrian, 1977; Kanai et al., 2008; Lövsund et al., 1980; Rohracher, 1935; Schwarz, 1947) are consistent with the view that phosphenes are generated in visual cortex (given that firing rates are greater in the visual cortex at these frequencies) but are not consistent with the view that they are generated in the retina (in the sense that retinal ganglion cell firing rates are more sensitive at 14 – 18 Hz). Conversely, studies such as the present one, which reported frequency minima within the 14 – 18 Hz range, are consistent with the view that phosphenes could be generated in either the visual cortex or retina. Whether this frequency-dependent response is mediated by other retinal cells (e.g., photoreceptors, bipolar cells, amacrine cells) as well as the ganglion cells is beyond the scope of the present study.

In conclusion, the larger sample size, fully repeated-measures design, and systematic frequency sampling used in this study allowed a more thorough examination of the relationship between phosphenes generated by tACS than previous research. This resulted in relatively small error variance, enabling greater confidence in the results reported above. Of particular note, while lower phosphene perception thresholds for tACS over frontal than occipital scalp sites were replicated, the reported threshold minima at 10 Hz for dark and dim lighting conditions was not (whereas the 16 Hz minima obtained here fits more neatly with predictions based on non-human primate retinal ganglion cell firing). We also report evidence here, for the first time, that the threshold-frequency functions are different for tACS applied over the frontal and occipital regions.

3 – EXPERIMENT TWO

Adapted from: Evans, I. D., Palmisano, S., & Croft, R. J. (2021). Retinal and cortical contributions to phosphenes during transcranial electrical current stimulation. *Bioelectromagnetics*, *42*(2), 146-158. doi:10.1002/bem.22317

Summary: The previous study found that phosphenes in mesopic conditions were strongest when stimulation was set to 16 Hz. This result had never been seen before, and as a result it was considered important to replicate the finding in a different sample. The results of study 1 also raised the possibility of a second (potentially occipital-based) mechanism for phosphene generation (in addition to retinal activation). Thus, this second study was designed to examine the two most likely sources of electrophosphene generation (the retina and the visual cortex) by comparing thresholds and estimated current density using a double dissociation. In order to do so, this study compared phosphene detection thresholds using four different electrode placements: 1) an FPz-Oz montage to investigate whether prefrontal regions such as the retina contribute to phosphenes, 2) an Oz-Cz montage to investigate whether the visual cortex in the occipital lobe contributes to phosphenes, 3) an FPz-Oz montage to allow a double dissociation between the retina and visual cortex to be made possible, and 4) a T3-T4 montage for exploratory purposes. By using sinusoidal direct current with appropriate counterbalancing, each montage was also tested for any potential effect of polarity on phosphene perception. Twenty-two subjects were recruited, receiving tDCS (as distinct from tACS in Chapter 2) using each montage at frequencies ranging from 6 to 32 Hz. To estimate the differences in current density at the retina and occipital lobe across montages, we measured the current density at phosphene thresholds across twenty head models using modelling techniques. The lowest thresholds were found when both the retina and the visual cortex were stimulated rather than when either one of them was stimulated separately, strongly suggesting that tES over the visual cortex can facilitate phosphenes. No evidence of polarity affecting thresholds was found, while thresholds using tDCS were similar to those found using tACS in Chapter 2.

3.1: Introduction

Phosphenes are visual perceptions of light that are not the product of external visual stimuli. When an individual is exposed to low frequency electromagnetic fields (EMFs), phosphenes are thought to be the first observable sign of electromagnetic interference with cortical processing. Safety agencies, such as the International Commission on Non-Ionizing Radiation Protection (ICNIRP; 2010), therefore use phosphene perception thresholds to set their exposure limits. For this reason, it is important to understand the mechanisms behind EMF-induced phosphenes and determine exactly how they relate to sensory and brain function. There have been two proposed biological sources of phosphenes that are activated by electric fields, which this study will focus on: the retina, and the visual cortex in the occipital lobe. While stimulation of the retina is generally considered to be the most likely cause of EMF-based phosphene perceptions (Paulus, 2010; Schwiedrzik, 2009), there is also evidence that electrical cortical stimulation: 1) can enhance phosphene perceptions; and 2) may be responsible for inducing some phosphenes (Kanai et al., 2008). The present study was designed to determine what role (if any) direct cortical activation plays in electrophosphene perception.

Phosphenes can be induced by applying transcranial magnetic stimulation (TMS) to a number of cortical sites associated with visual processing, including V1 (the primary visual cortex) (Pascual-Leone et al., 2001; Salminen-Vaparanta et al., 2014; Silvanto et al., 2005), V2 (Kammer et al., 2001; Salminen-Vaparanta et al., 2014), V3 (Kammer, 1999; Kammer et al., 2001) and V5 (O'Shea & Walsh, 2007; Silvanto et al., 2005). Phosphenes can also be induced by transcranial electrical stimulation (tES). These tES-induced phosphenes have typically been attributed to electrical stimulation of the retina (Rohracher, 1935; Schwiedrzik, 2009; Schutter & Hortensius, 2010; Kar & Krekelberg, 2012). Detailed modelling of the current flow through the head from a range of tES studies suggests that current density at the retina could explain the phosphenes produced by several different electrode montages (Laakso & Hirata, 2013). For example, the current generated by tES over the occipital cortex will spread to other areas of the head, including the retina (Paulus, 2011), which is particularly sensitive to EMF (Bogoslowski & Ségal, 1947). The findings of several empirical studies also appear to support a retinal activation mechanism for tES-induced phosphenes (Rohracher, 1935; Adrian, 1977;

Lövsund et al., 1980; Kar & Krekelberg, 2012). However, Kanai et al. (2008) reported that phosphenes could be induced by tES applied over the occipital lobe at specific functional electroencephalogram (EEG) frequency bands known to be dominant in the visual cortex under specific lighting conditions (Palva & Palva, 2007). They argued that these phosphenes were due to cortical changes resulting from oscillatory synchrony with the external tES source. Specifically, based on the reported phosphene locations in their study, they argued that tES directly activated "the anterior visual cortex along the medial wall" (Kanai et al., 2008, p. 1841).

When assessing the possible role of the retina or the occipital cortex in phosphene perception, the usual practice is to treat each site as an independent "generator" of phosphenes (Schwiedrzik, 2009; Schutter & Hortensius, 2010; Paulus et al., 2011). These "generators" have previously been studied by comparing phosphene thresholds resulting from FPz-Cz (frontalis–vertex) and Oz-Cz (occipital–vertex) electrode montages (Schutter & Hortensius, 2010; Kar & Krekelberg, 2012), with the aim being to preferentially stimulate either the retina or the occipital cortex. One limitation with this approach is that, although it can be used to maximise current densities at the target region (e.g., the retina, using an FPz-Cz montage), it does not control for current densities at non-target regions. Since current will spread across the scalp in any montage, resulting in nonzero current density changes throughout the head (Laakso & Hirata, 2013), it follows that the phosphene induction thresholds obtained may be due to confounding electrical activity at non-target regions. This phenomenon is the basis for the view that retinal activation is the likely cause of all tES phosphenes (i.e., even when the electrodes are placed over the occipital cortex). However, since tES may result in varying levels of current density at both the retina and the occipital cortex and because there are interactions between these sites, it is plausible that the combined current density at each "generator" may contribute to phosphene perception, rather than this being due to the current density at only one generator.

The present study investigated the latter possibility by using additional stimulation conditions that provide an (approximate) double dissociation with respect to current density at the retina and occipital cortex, in order to assess the contributions of each site to phosphene perception. It included FPz-Oz (frontal midline–occipital midline), as well as FPz-Cz and Oz-Cz, electrode montages. Based on the modelling of Laakso and Hirata (2013), this should allow:

1) retinal contributions to be assessed by comparing the phosphene detection thresholds for the FPz-Oz and Oz-Cz montages (where the former results in higher current density at the retina, but similar current density at the occipital cortex to Oz-Cz); and 2) occipital contributions to be assessed by comparing phosphene detection thresholds for the FPz-Oz and FPz-Cz montages (where the former results in higher current density at the occipital cortex, but similar current density at the retina to FPz-Cz). These contributions are typically estimated by comparing the minimum current applied to each montage for phosphenes to be first perceived (Kanai et al., 2008; Schutter & Hortensius, 2010; Kar & Krekelberg, 2012). While indicative, these phosphene thresholds are not informative about the actual current densities produced by each montage at the retina or in the parts of the visual cortex known to be sensitive to electromagnetically induced phosphenes. However, estimates of the current density values at the retina and the occipital cortex can be obtained by using electromagnetic stimulation modelling software such as SimNIBS (Saturnino et al., 2019). This modelling can also be used to estimate the likely magnitude of deviations from our planned double dissociation, and how such deviations might affect the interpretation of our results.

If tES can produce phosphenes from direct occipital cortex activation, then it is plausible that tES-induced phosphene perceptions might also result from stimulating cortical areas associated with visual processing that lie outside the occipital lobe, as has been found in multiple TMS studies (Kammer, 1999; Kammer et al., 2001; O'Shea & Walsh, 2007; Salminen-Vaparanta et al., 2014; Silvanto et al., 2005). If, as Kanai et al. (2008) argued, the primary visual cortex can be directly activated when tES is delivered at Oz, then stimulating the inferotemporal cortex (known to be involved in visual processing) using a T3-T4 montage may also induce phosphenes. The present study also explored this possibility.

In addition to montage-based differences, the current density required to produce phosphenes has also been found to vary as a function of the frequency of the stimulation (e.g., Chapter 2; Kanai et al., 2008; Lövsund et al., 1980; Schwarz, 1947). The frequency associated with the lowest tES-induction thresholds appears to be 20 Hz in bright light (Lövsund et al., 1980, Kanai et al., 2008; Schutter & Hortensius, 2010; Schwarz, 1947). A similar finding was reported for 20 Hz using an electromagnet powered by alternating current (Lövsund et al., 1980). However, sensitivity to tES appears to vary across lighting levels, with the lowest phosphene induction thresholds being found for 10 Hz in the dark (Kanai et al.,

2008; Schwarz, 1947) and 16 Hz in dim lighting conditions (see Chapter 2). These lighting effects have been reported with montages targeting the face (Schwarz, 1947) and over the visual cortex at Oz-Cz (Kanai et al., 2008). However, the nature of the relationship between stimulation frequency and phosphene-induction thresholds may also depend on the tissues being stimulated. Visual stimulation results predominantly in 7 - 20 Hz activity in the primary visual cortex (Bringuier et al., 1997), which implies that electrical stimulation at these frequencies should more readily produce phosphenes (assuming tES-based entrainment is effective). However, the retina is most sensitive to electrical stimulation between 14 - 18 Hz (Bernardete & Kaplan, 1999). This implies that if phosphenes can be generated by both retinal and cortical stimulation, then such "generators" should have different frequency dependencies (in terms of the retinal or cortical stimulation frequencies that produce the lowest phosphene thresholds, or the phosphene threshold-frequency relationship more generally). As nonlinear relationships between stimulation frequency and phosphene threshold were found in the previous chapter, we also used nonlinear curve estimation to determine if the relationships between stimulation frequency and phosphene thresholds differ when the retina and cortex are differentially stimulated by tES.

The present study was designed to further clarify the mechanisms responsible for tES-induced phosphenes. It attempted to separate retinal and potential occipital cortex contributions to tES phosphenes using a double dissociation across three montages: FPz-Cz, Oz-Cz and FPz-Oz. If the retinal generator hypothesis is correct, the thresholds for phosphene perception in the FPz-Oz montage should be lower than those for the Oz-Cz montage. If the occipital cortex generator hypothesis is correct, the thresholds for phosphene perception in the FPz-Oz montage should be lower than those for the Oz-Cz montage. A T3-T4 montage was also used to explore the possibility of temporal cortex-based contributions. The frequency-dependent characteristics of these four montages were examined to determine if there might be different relations between tES frequency and phosphene induction thresholds for each of them (as would be expected if different tissues were involved in tES-based phosphene induction or modification).

Additionally, as it has not yet been established whether or not the polarity of stimulation has an effect on electrophosphene generation, this study will use sinusoidal transcranial direct current stimulation (tDCS) rather than the transcranial alternating current stimulation (tACS)

used in the previous chapter. In sinusoidal tDCS, the amplitude of the stimulation varies as a sine wave from zero to the current set by the stimulator, then back to zero and uses direct current (DC). Since the polarity of the circuit is constant and does not alternate, therefore the polarity remains positive at the anode (see **Figure 3.1b** below). By comparing the results of this study to those from Chapter 2, it can be determined whether polarity has an effect on either phosphene thresholds or the frequency dynamics of tES-induced phosphenes.

Figure 3.1
A) Basic workflow for the experimental procedure.
B) Example of a sinusoidal DC waveform as used in this study, and how it differs from other waveform types used in tES.

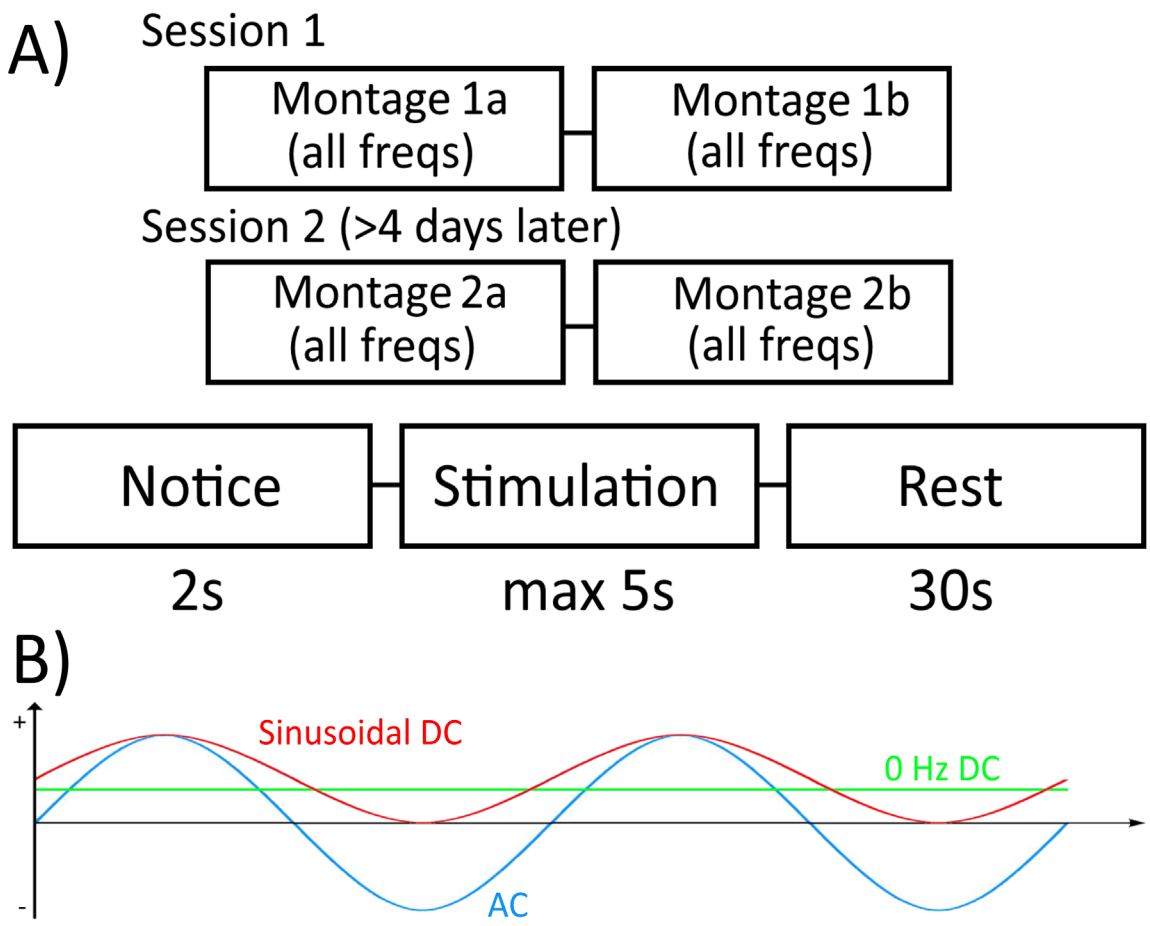

3.2: Method

Twenty-two healthy subjects (even gender split, aged 19 – 39, *M* = 27.4 years) completed this study after passing a modified safety screening checklist (Keel et al., 2000; for details see Appendix A, p. 157). Subjects were excluded if they reported any form of neural injury or illness, metal implant in the head or a medical implant elsewhere in the body, or non-corrected visual impairment. This research was approved by the Human Research Ethics Committee of the University of Wollongong (Approval #HE2017/454).

Subjects were seated on a chair in a dimly lit room with a black curtain covering any walls that would otherwise appear in their field of view (including peripheral vision) to keep the field of view consistent. Illumination at the black curtain was measured at 6 ± 0.05 cd/m^2, while luminance levels at the subjects' eyes were measured to be 0.6 ± 0.05 cd/m^2, using a J6523 Tektronix luminance probe (Tektronix, London, Canada).

tDCS was administered using a Magstim NeuroConn Stimulator Plus MOP15-EN-01 (Magstim, Carmarthenshire, UK) operating in sinusoidal DC mode through conductive-rubber electrodes (dimensions: 30 x 40 x 1mm) placed on sponges (30 x 40 x 4mm) saturated with a saline solution mixed with a hypoallergenic amphoteric surfactant and held in place at the appropriate location with rubber straps. All stimulations were sinusoidal direct current with no ramp-up.

The experiment involved two testing sessions, each of which involved stimulation using two different montages in a block design (see **Figure 3.1a**, p. 68). One session involved stimulation with FPz-Cz and Oz-Cz montages, and the other session involved stimulation with FPz-Oz and T3-T4 montages. The order of these sessions, the montages within these sessions, and which electrode was the cathode or anode within each montage, were counterbalanced across the sample. Each session took approximately 90 minutes to complete. The two sessions were conducted at similar times on separate days, usually within one week of each other.

Once the electrodes were in position, subjects were informed about phosphenes (their nature and what the subject might perceive), while their skin and hair were saturated from the saline in the sponges. They were given 20 – 30 minutes prior to the commencement of data collection to adapt to the lighting conditions. This period included the initial experimental

setup, the time taken for impedance levels to fall to 15 kΩ or below (as indicated by the stimulator), and the time necessary for the familiarization stage (where subjects were first introduced to phosphenes). Once the impedance between the electrodes was acceptable, subjects were familiarized with the appearance of phosphenes using 10 seconds of tDCS at 1000 μA, first at 16 Hz and then at 22 Hz, to demonstrate: 1) the visual appearance of phosphenes; and 2) how they could change by varying only the frequency of the stimulation. Once subjects were familiarized with phosphenes, their phosphene detection thresholds were determined at seven different frequencies (6, 10, 16, 20, 24, 28, and 32 Hz) in a predetermined random order that varied across both individual subjects and within each montage; i.e., no individual received the same order of frequencies as any other subject in any other condition. Note that to reduce any effects of the familiarization phase on the experimental phase, different frequencies were used for the different phases.

Subjects were informed when each stimulation began and when it ceased, but they were not informed of the frequency or current intensity of the stimulation. Stimulations lasted for a maximum of 5 seconds[7]. Shorter exposures were used to minimise any potential confounding effects that might occur due to their repeated exposure to these electrical currents. Subjects were instructed to keep their eyes open throughout the entire stimulation, and to verbally indicate when a phosphene was perceived, at which point stimulation ended. If the subject did not respond, stimulation continued for 5 seconds, at which point the subject was told that stimulation had ended and asked if any phosphenes were perceived. The inter-stimulus interval was 30 seconds. To detect false positive responses at lower current intensity levels, four sham stimulations were given at random points during each session, where the subject was given all the audible signs of a stimulation (the usual button presses on the stimulator as well as verbal indications that the stimulation had started and finished) without actually generating an electric current. None of the subjects reported seeing phosphenes during any of the sham trials.

Thresholds for phosphene induction (in μA) were determined for each frequency by varying the current intensity using a QUEST-based Bayesian adaptive staircasing procedure (Watson and Pelli, 1983) in MATLAB's PsychToolbox (Kleiner et al., 2007). Transcranial direct current

[7] As phosphenes tend to be immediately perceptible upon stimulation onset, the full five seconds was not always necessary.

stimulation, which started at an intensity of 700 µA, was bound between 25 µA and 1500 µA. The step-size between possible stimulation levels was 25 µA. Based on the Rapid Estimation of Phosphene Threshold system validated by Mazzi et al. (2017), this adaptive threshold measurement method determined the lowest current intensity that was significantly more likely than chance to evoke phosphene perceptions. Similar to the experiment in Chapter 2, when subjects did not report any phosphenes at the maximum stimulation intensity (1500 µA), a value of 1500 µA was used for the statistical analyses.

3.3: Statistical Analysis and Modelling

All statistical analyses were performed using SPSS Statistics v23 (IBM, Chicago, IL). As the assumption of normality was violated across several threshold values (11 out of 28), nonparametric Mann-Whitney tests were used to determine whether the position of the cathode and anode affected phosphene induction thresholds and thus whether it needed to be accounted for in subsequent statistical analyses. Tests were conducted separately for each frequency and montage, where polarity (anode, cathode) was the between-subjects factor and the phosphene induction threshold was the dependent measure. As a conservative strategy (i.e., to increase the chance of detecting a difference), no adjustment for multiple comparisons was made.

3.3.1: Retinal vs. Occipital Cortex Generator/Modifier Hypotheses

To test the hypotheses associated with the montage manipulations, data from the stimulation frequency with the lowest mean phosphene threshold was used. As the assumption of normality was violated across several of these threshold values, nonparametric statistical tests were again used. To determine whether the retina was involved in phosphene generation (or modification), a Wilcoxon signed rank test was conducted, testing for a difference in thresholds between the FPz-Oz and Oz-Cz montages, where the threshold was the dependent variable and the montage was the independent variable. Lower thresholds for the FPz-Oz condition would support retinal involvement because this montage results in

higher current densities about the retina, but similar current densities about the occipital cortex.

To determine whether the occipital cortex was involved in phosphene generation (or modification), a Wilcoxon signed rank test was conducted, testing for a threshold difference between the FPz-Oz and FPz-Cz montages, where threshold was the dependent variable and montage was the independent variable. Lower thresholds for the FPz-Oz condition would support the involvement of the occipital cortex because this montage results in higher current densities about the occipital cortex, but similar current densities about the retina.

These tests are contingent on the assumption that these combinations of montages are producing the same current density in either the retina or the occipital cortex when the same current is applied to all electrodes. To verify this, estimates of the current density were taken at both the eyes and the grey matter about Oz to determine whether any correction factor was appropriate (see 3.3.3: Modelling, p. 73).

3.3.2: Exploratory Analyses

Analyses of the relations between phosphene thresholds and tES frequency were also conducted. The experiment in Chapter 2 found different frequency-dependent functions for the FPz-Cz and Oz-Cz montages. Thus, additional analyses were performed in this study using the Curve Fitting tool in MATLAB 2016b (Mathworks, Natick, MA) to: 1) check whether this particular difference for the FPz-Cz and Oz-Cz montage functions replicated; and 2) examine the relation between thresholds and stimulation frequency for the two other montages (i.e., FPz-Oz and T3-T4). In order to account for differences across montages that might be the result of scale differences, the initial regression curve fits (of phosphene thresholds as a function of frequency) used each subject's thresholds, which had been *Z*-score normalized within montages across all frequencies. We restricted these fits to quadratic and cubic functions to avoid overfitting, and the function with the lowest *p*-value was selected as the most appropriate fit. The terms from this fit were then used to estimate the threshold-frequency curves separately for each of the four montages. In order to test whether the FPz-Cz and Oz-Cz montages had different regression curves (replication) and whether any other

montage-pairs had different regression curves, the beta coefficients (excluding the constant) were compared using *t*-tests.

To explore potential temporal cortex involvement in phosphene generation or modification, we also conducted two Wilcoxon signed rank tests, which compared the thresholds for the FPz-Oz and T3-T4 montages, and the Oz-Cz and T3-T4 montages respectively, where threshold was the dependent variable and montage was the independent variable.

3.3.3: Modelling: Confirming Adequacy of Double Dissociation

In order to check whether the magnitude of the current density differences resulting from the double dissociation was adequate, estimates of the normal component of current density in the eyes and the cortex near Oz were made using SimNIBS 3.1 (Saturino et al., 2019) on the ERNIE head model (Saturino et al., 2018) and nineteen head models from Boayue et al. (2017): 11 females; mean age 28.79, *SD* = 10.86, range 18-59. All head models included MRI-based measurements of the skin, skull, cerebrospinal fluid (CSF), grey matter, white matter, and the eyes. Tissue conductivity values were taken from Wagner et al. (2004) and Opitz et al. (2015) based on SimNIBS default settings; see **Table 3.1** (p. 74) for further details. To maximise the likelihood of measuring the activation of pyramidal neurons in the cortex, the normal component of the current density vector was used (Day et al., 1989). Using identically sized electrodes as the experiment (30 x 40 mm) at both placement sites for all montages, tDCS was simulated at the mean phosphene threshold for each montage. Phosphene studies employing TMS at the occipital cortex show that although the location of cortically-sourced phosphenes varies from person to person, they can be reliably generated by applying EM stimulation to V1 and V2 (Salminen-Vaparanta et al., 2014) or V3d and V3a close to the interhemispheric cleft (Schaeffner & Welchman, 2017). Given that sensitivity to occipital phosphenes is greatest at 40 mm below the surface of the skin but can still be produced by stimulating cortical tissue closer to the scalp (Marg and Rudiak, 1994), current density at the visual cortex was estimated by averaging current density values in the grey matter tissue within 40 mm of Oz. This would encompass any regions of the primary visual cortex previously associated with the highest sensitivity to TMS-induced phosphenes (Kanai et al., 2010; Salminen-Vaparanta et al., 2014; Schaeffner & Welchman, 2017). As the position of the retina

cannot be determined with sufficient precision within the simulated eyeball, the mean current density of the entire eyeball was used to measure retinal current density. Once these estimates had been determined, the mean current density in the eyes was compared across the FPz-Cz and FPz-Oz montages. MATLAB code for each step of this process can be found in Appendix D (p. 162).

To determine whether a correction factor was required for the retinal/occipital cortex generator analyses (see above), tDCS was simulated at the same current intensity for each montage across all 20 head models. The mean difference between current intensity in the eyes in the FPz-Oz and FPz-Cz montages was applied as a correction factor for the occipital cortex hypothesis. In a similar fashion, the mean difference between field strengths in the FPz-Oz and Oz-Cz montages was applied as a correction factor for the retinal hypothesis. Further statistical tests were conducted using these corrected values.

Table 3.1 – Tissues included in head models used in SimNIBS modelling, with their respective conductivity values (Siemens/m)

Tissue	Value (S/m)
White matter	0.126[1]
Grey matter	0.275[1]
Cerebrospinal fluid	1.654[1]
Bone	0.01[1]
Scalp	0.465[1]
Eyes	0.5[2]

1: from Wagner et al., 2004
2: from Opitz et al., 2015

3.4: Results

3.4.1: Polarity Differences

For all montages and all frequencies, no significant differences in phosphene thresholds were found based on which electrode was the cathode or the anode ($p \geq .193$). Since no

cathode/anode-based differences in phosphene thresholds were found, both arrangements were subsumed into a single dataset for the remaining analyses.

3.4.2: Retinal vs. Occipital Generator/Modifier Hypotheses

Thresholds for all individuals in every montage and frequency can be read in Appendix C (p. 161). For each montage the 16 Hz frequency produced the lowest mean phosphene threshold (see **Table 3.2** below and **Figure 3.2**, p. 76). 16 Hz thresholds were thus used to test the two hypotheses. In support of the retinal generation hypothesis, the FPz-Oz montage produced significantly lower thresholds than the Oz-Cz montage ($Z = 4.11$, $p < .001$, $r = 0.88$). However, in support of occipital cortical involvement, the FPz-Oz montage was found to produce significantly lower thresholds than the FPz-Cz montage ($Z = 2.96$, $p < .001$, $r = 0.63$). However, these statistical tests assume that both montages being compared produced the same current density in the potential generator being examined (either the retina or the occipital cortex) when the same current was applied. Thus, the correction factors for any differences were estimated using SimNIBS (see above) and then these tests were re-examined. For the retinal hypothesis, equivalent current strength from the FPz-Oz montage produced a significant 3.3% greater mean current density in the grey matter under Oz ($t(19) = 3.22$, $p = .005$, Cohen's $d = 0.23$) compared to the Oz-Cz montage. After applying this correction factor, the result remained significant: $Z = 4.11$, $p < .001$, $r = 0.88$.

Table 3.2 – Descriptive statistics for phosphene thresholds

Frequency	FPz-Oz	FPz-Cz	T3-T4	Oz-Cz
6 Hz	500 (450-625)	587.5 (500-875)	1275 (1150-1475)	1500 (x)
10 Hz	175 (125-225)	250 (225-300)	475 (325-525)	800 (700-925)
16 Hz	75 (50-100)	125 (100-175)	200 (150-250)	362.5 (275-500)
20 Hz	112.5 (100-150)	175 (125-200)	287.5 (175-325)	637.5 (475-750)
24 Hz	162.5 (125-250)	250 (200-275)	350 (275-500)	1100 (725-1325)
28 Hz	300 (250-425)	412.5 (350-575)	612.5 (525-1000)	1500 (1400-1500)
32 Hz	412.5 (275-550)	575 (425-700)	962.5 (450-1325)	1500 (x)

Medians and 1st-3rd interquartile ranges are shown for each montage and frequency. (x) indicates a value that is artificially constrained due to thresholds being higher than the maximum current density employed in this study (1500 μA), therefore no interquartile range is provided.

For the occipital cortex hypothesis, equivalent current strength in the FPz-Oz montage produced a significant 8.0% greater mean current density at the eye ($t(19) = 14.3$, $p < .001$, Cohen's $d = 0.47$) compared to the FPz-Cz montage. After applying this correction factor, the result remained significant: $Z = 2.88$, $p = .004$, $r = 0.61$.

Figure 3.2

Median threshold at each montage and stimulation frequency. Boxplots mark the median, 1st-3rd interquartile range, and full range of thresholds.

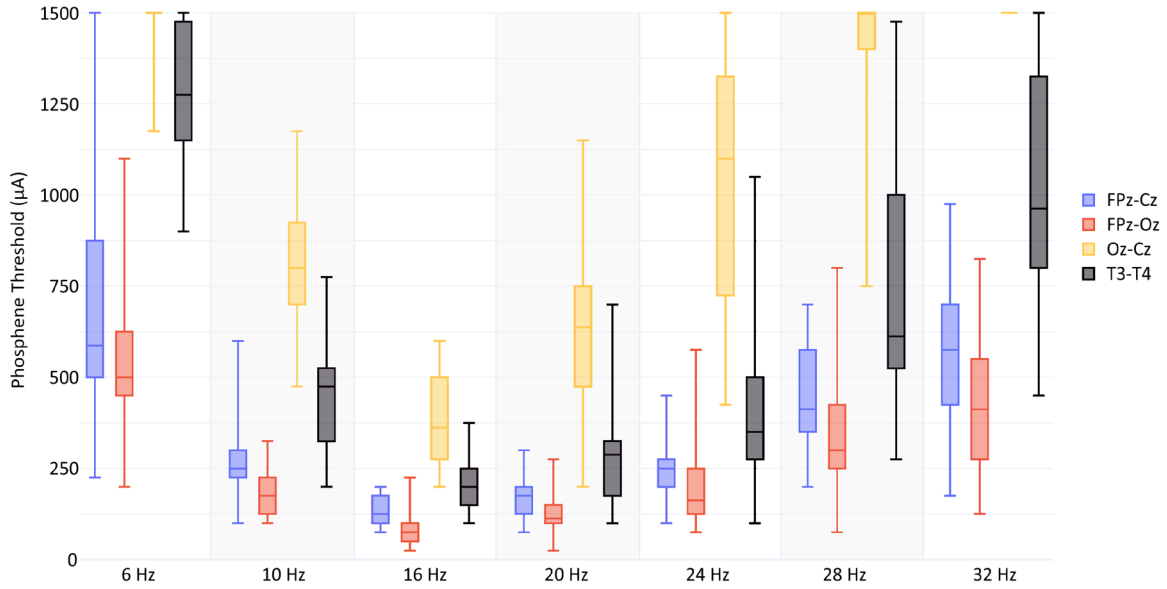

3.4.3: Exploratory Analyses

The hypothesis that the temporal lobe might be involved in phosphene perception was tested by comparing the 16 Hz threshold firstly for the T3-T4 and Oz-Cz montages, which showed that the T3-T4 montage produced significantly lower thresholds than Oz-Cz ($Z = 3.74$, $p < .001$, $r = 0.80$). A second comparison between T3-T4 and FPz-Cz also showed that the FPz-Cz montage produced significantly lower thresholds than T3-T4 ($Z = 3.48$, $p = .001$, $r = 0.74$).

Figure 3.3
Regression curves for each montage.
A) Raw threshold scores
B) Z-score normalized values

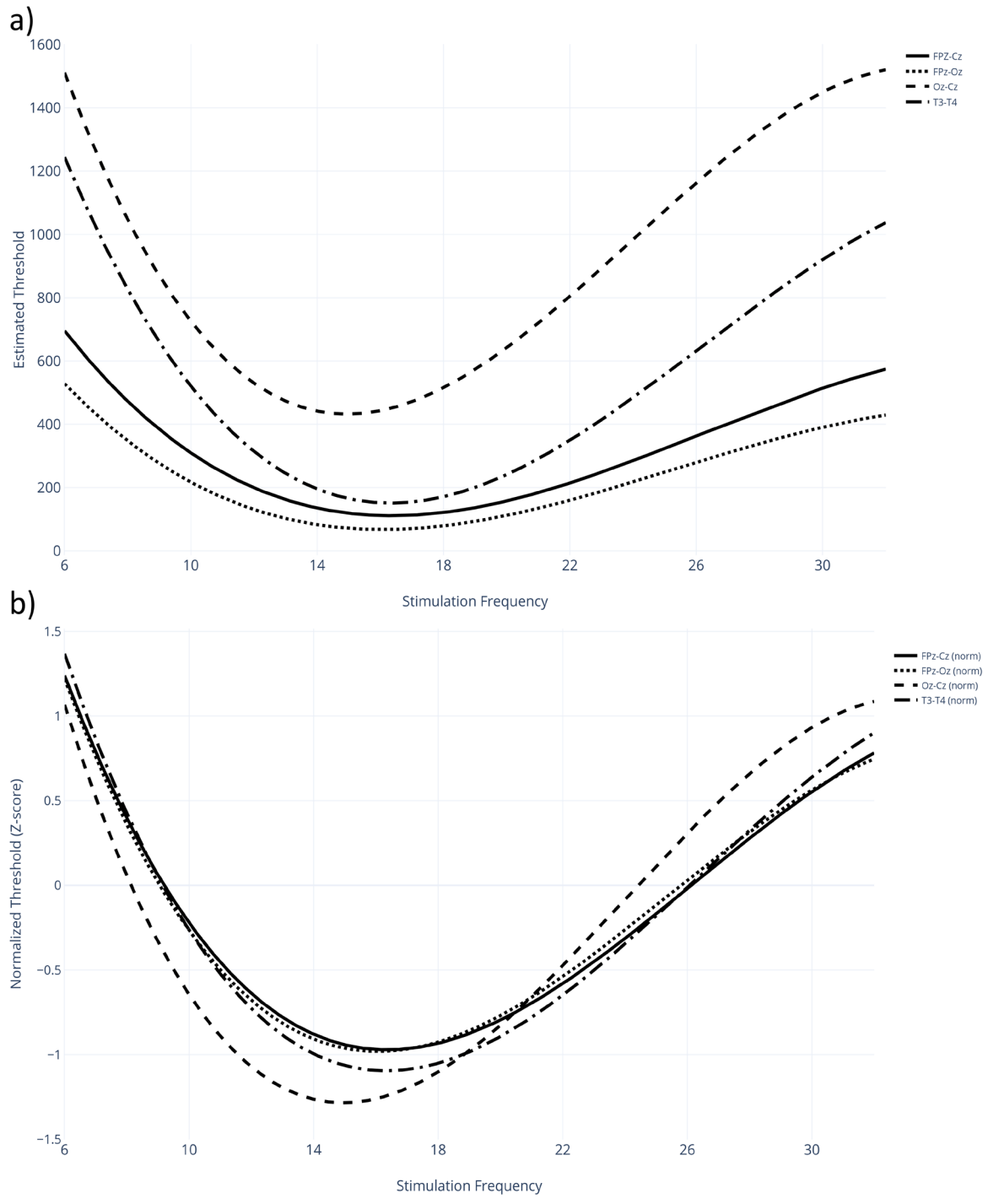

When the four montages were combined to assess the relation between stimulation frequency and phosphene threshold, the best fit was found to be a cubic function ($F(3,612) = 118.18$, $p < .001$, adjusted $R^2 = .364$). Cubic fits were accordingly calculated for each separate montage (see **Figure 3.3a**, p. 77), where y was the phosphene perception threshold and x was the stimulation frequency in Hz (raw, non-normalized regression fits):

$$y(FPz - Oz) = -0.120x^3 + 9.14x^2 - 200.42x + 1427.75, adj\ R^2 = .542$$
$$y(FPz - Cz) = -0.136x^3 + 10.72x^2 - 241.40x + 1787.41, adj\ R^2 = .558$$
$$y(T3 - T4) = -0.256x^3 + 20.15x^2 - 453.24x + 3294.00, adj\ R^2 = .709$$
$$y(Oz - Cz) = -0.374x^3 + 26.92x^2 - 553.76x + 3946.01, adj\ R^2 = .779$$

After Z-score normalization (see **Figure 3.3b**), all coefficients were compared across montages and only one significant result was found: the quadratic coefficient for the FPz-Cz montage was significantly lower than the equivalent Oz-Cz coefficient; $t(41) = 2.09$, $p = .043$, Cohen's $d = 0.62$. The minima frequencies, i.e. the estimated frequency for each montage that produced the lowest estimated phosphene threshold, were 16.37 Hz for the FPz-Cz montage, 16.06 Hz for the FPz-Oz montage, 14.95 Hz for the Oz-Cz montage, and 16.33 Hz for the T3-T4 montage.

Table 3.3 – Mean and standard deviations (n = 20) for the estimated current density values (mA/m²) and estimated electrical field strength (mV/m) within the eyes (Retina) and the grey matter 40mm around Oz when phosphene threshold current is simulated at each montage.

Montage	Threshold	Retina		Oz	
	(μA)	mA/m²	mV/m	mA/m²	mV/m
FPz-Cz	130.7	18.7 (2.69)	75.3 (10.6)	2.06 (0.273)	6.34 (0.61)
FPz-Oz	87.5	13.6 (1.95)	54.4 (7.74)	3.54 (0.517)	15.9 (2.23)
Oz-Cz	380.7	4.59 (1.12)	17.9 (4.01)	19.3 (2.47)	67.1 (9.16)
T3-T4	205.7	9.34 (1.01)	37.5 (3.98)	2.13 (0.338)	14.4 (1.55)

3.4.4: Modelling: Confirming Adequacy of Double Dissociation

Current density was modelled for the eyeball ("Ret") and the occipital grey matter near Oz ("Oz"), for each montage separately, using the phosphene thresholds obtained in the study as inputs (see **Table 3.3**, p. 78). Modelled current density estimates for each modelled head across each montage can be found in Appendix E (p. 167). This provided the best estimate of the actual current density at the retina and occipital cortex at the phosphene threshold (note that the absolute current density required at "Ret" for a phosphene decreases as the absolute current density at "Oz" increases). Current distribution about the eyes and grey matter can be seen in **Figure 3.4** (p. 80). The relative current densities for "Ret" and "Oz" can be seen to vary for FPz-Cz (**Figure 3.4a**), FPz-Oz (**Figure 3.4b**), and Oz-Cz (**Figure 3.4c**) in the manner predicted by the planned double dissociation. The statistical analysis showed no signs of non-normality in the mean current density values, therefore t-tests were appropriate for the comparison. Mean current density in the eyes at phosphene threshold was greater from the FPz-Cz montage (M = 18.7 mA/m^2, SEM = 0.601) than from the FPz-Oz montage (M = 13.6 mA/m^2, SEM = 0.436; $t(19) = 28.4$, $p < .001$, Cohen's d = 2.2)

3.5: Discussion

Consistent with the findings in Chapter 2, tES phosphene induction thresholds were found to be significantly lower for the FPz-Cz montage than the Oz-Cz montage, with the greatest difference found at 16 Hz. While this finding was not unexpected as it is widely assumed that tES-induced phosphenes are induced by retinal activation, this study extends on Chapter 2's findings by introducing the FPz-Oz montage, which allows a more thorough dissociation between retinal and occipital stimulation and added simulations of the current density differences in the relevant tissues across all montages. The FPz-Oz montage, which increased current source density at Oz while keeping it approximately constant at FPz, resulted in lower phosphene thresholds than the FPz-Cz montage (even after corrections were applied). If the retina alone was responsible for phosphene perception in both the FPz-Cz and FPz-Oz montages, then we would expect to see similar threshold levels for each montage, whereas the FPz-Oz montage required lower electrical current at the eyes to produce phosphenes

compared to the FPz-Cz montage. Thus, applying tES at scalp locations near to both the occipital cortex and the retina was found to facilitate phosphene perception in the FPz-Oz montage. Exchanging the cathode and anode electrodes had no effect on phosphene thresholds, indicating that stimulation polarity has no effect on electrophosphene perception.

Figure 3.4

SimNIBS-sourced normal component of current density distribution in the grey matter and eyes for each montage at their individual phosphene thresholds; FPz-Cz at row A, FPz-Oz at row B, Oz-Cz at row C.

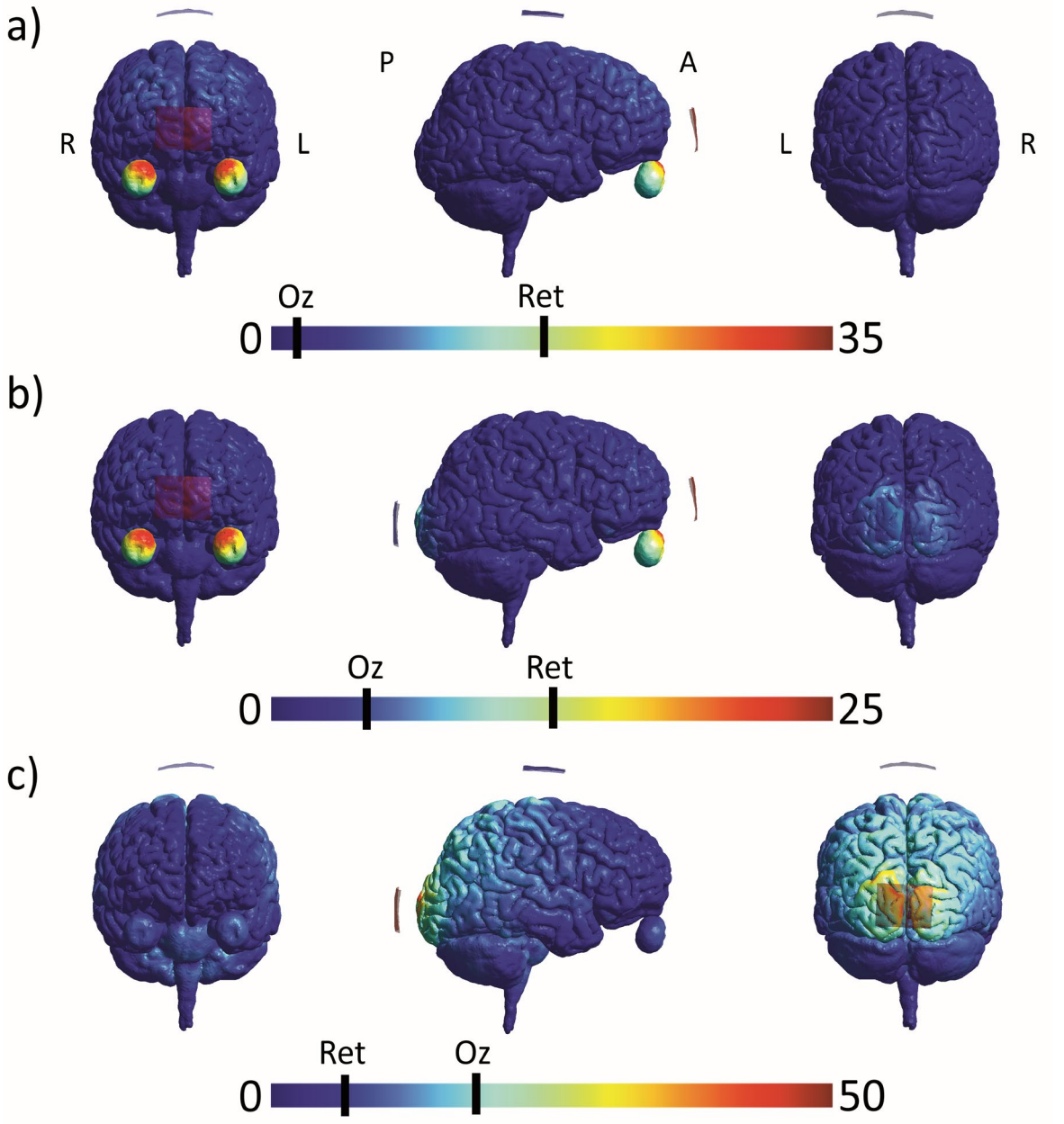

Electrode locations are displayed for each montage. ERNIE head model used. Scales are based on the maximum current density found at any individual voxel within the grey matter or eyes (mA/m^2).

Average current density within the eyes "Ret" and Oz-related grey matter ("Oz") are marked on the scale for each montage.

As noted previously, the use of the FPz-Cz, Oz-Cz, and FPz-Oz montages enables a systematic manipulation of the current source densities at the retina and the visual cortex (confirmed by our extensive modelling with SimNIBS). Several studies examining tES have proposed that regardless of the montage used, electrical activity in the retina will generate phosphenes well before the current density reaches the point where cortical activation is plausible (Laakso and Hirata, 2013; Schwiedrzik, 2009). This view is partially borne out in the current results, since the thresholds for phosphene perception were lower for the montages that included FPz (i.e., FPz-Cz and FPz-Oz) compared to those that did not (i.e., Oz-Cz and T3-T4). However, if the tES induced phosphenes in our study were solely the product of retinal stimulation, then the thresholds for the FPz-Oz montage should not have differed significantly from those for the FPz-Cz montage. However, this was not the case; the phosphenes produced by the FPz-Oz montage required even less current than those produced by the FPz-Cz montage across all of the stimulation frequencies tested, and required less current density at the eyes. It is therefore unlikely that tES produced phosphenes by directly activating only the visual cortical neurons in the FPz-Oz montage. This is because Oz-Cz resulted in higher current density in the occipital cortex than FPz-Oz, and so if only occipital cortex stimulation was relevant to the phosphenes, Oz-Cz would have produced the lowest thresholds, which it did not. Similar effects on visual perception have been reported in the TMS literature, where the combination of TMS and tES resulted in less current density being required to produce phosphenes than TMS alone (Antal et al., 2003; Antal et al., 2004; Kanai et al., 2010). Together, these findings suggest that tES applied to the visual cortex may act as a facilitator for phosphene perception rather than a direct generator of phosphenes.

In principle, it should be possible to induce phosphenes by targeting a variety of regions in the visual processing stream (ranging from specific retinal neurons/photoreceptors in the eye to the cortical areas V1, V2, V3, V5 and beyond those that have been targeted by TMS studies); however, since tES is relatively imprecise compared to other stimulation techniques like TMS, it would be highly speculative to interpret these results with sufficient precision. If one assumes that phosphenes cannot be consciously perceived until activity changes in the primary visual cortex, then cortical contributions to phosphene perception must be

considered. In the case of the FPz-Oz montage, retinal signals triggered by tES might have been facilitated by direct tES effects on neuronal activity/connectivity in the visual cortex (due to the proximity of these neurons to the Oz electrode), the result being that conscious perceptions of phosphenes were possible at lower current levels than were required for the FPz-Cz montage. Given the low estimated current density values in both the eyes and near the occipital cortex for the T3-T4 montage compared to other montages (see **Table 3.3**, p. 78), it is plausible that cortical regions outside the occipital visual cortex could also play a role in phosphene perception, and therefore the role of more anterior cortical structures in the visual system should be considered in the future. While some suggest that tES may stimulate peripheral/cranial nerves (such as the optic nerves in the cerebrum) which could indirectly affect cortical excitability, this seems unlikely given the lack of changes in current density found in the cerebrum and brainstem (see **Figure 3.4**). Given that studies attempting to alter the function of cranial nerves consistently need to apply at least double the current strengths compared to the thresholds reported here, even when the electrode montage is as close to the cerebrum or brainstem as possible (for a review, see Adair et al., 2020), it is highly unlikely that sufficient current density to affect visual perception in the cerebrum in any montage used here. If the application of tES using these montages were able to affect the function of the optic nerve found in the cerebrum, it follows that there would also be changes in function involving other cranial nerves found in the cerebrum and brainstem such as the vagus nerve (which regulates heart rate), the olfactory nerve (sense of smell), the facial nerve (facial expressions and sense of taste), the auditory nerve (hearing), and the vestibular nerve (balance) amongst others (Laine & Smoker, 1998; Monkhouse, 2005; Rea, 2014). Since there were zero reports of change or discomfort related to any of these functions, combined with the absence of estimated current density changes in these anatomical regions, there is little evidence to suggest that indirect stimulation of cranial nerves facilitates the perception of electrophosphenes.

The results suggest that some direct tES-induced change in the visual cortex contributes to the perception of phosphenes from the FPz-Oz montage. When the tES-induced retinal stimulation is eventually processed by the visual cortex, it makes sense that there would be an interaction in the activity produced by direct tES stimulation of these two regions. In this case, the tES induced phosphenes might also have been a product of retinal activation

modulated by cortical priming (i.e., priming by external tES based cortical stimulation). The mechanism for this interaction could possibly have involved the magnocellular parts of the lateral geniculate nucleus (LGN), since these cells display frequency-dependent responses to visual stimulation as opposed to parvocellular neurons (Benardete & Kaplan, 1999).

Results from animal in vivo studies might also be important in shedding light on the role that cortical stimulation plays in phosphene induction or modification. Specifically, it has been shown that retinal and visual cortical tissues have different frequency-dependent responses to electrical stimulation: retinal ganglion cells appear most sensitive to 14 – 18 Hz stimulation (Benardete and Kaplan, 1999), while cortical neurons in the visual cortex appear to be sensitive to stimulation across the 7 – 20 Hz range (Bringuier et al., 1997). Based on these findings, one might expect retinally and cortically induced phosphenes to display quite different frequency-dependent relationships, however we did not find this in our results. The regression curves showed only one difference in coefficients between montages, and all curves indicated peak sensitivity at around 16 Hz, which fits neatly into both the predicted retinal ganglion range of 14-18 Hz and the 7-20 Hz range of the cortex. This indicates that the attempt to dissociate retinal and cortical phosphenes by frequency dependence did not succeed. Although difficult to examine statistically, the trend in the minima frequency (the estimated frequency for each montage that produced the lowest estimated phosphene threshold) showed signs of falling as cortical targeting was introduced, with the FPz-Cz montage producing the highest minima frequency (16.33 Hz) and the Oz-Cz montage producing the lowest (14.95 Hz). The drop to 16.06 Hz in the FPz-Oz montage may reflect the theoretically lower cortical component of the frequency dependent relationship changing the minima frequency; however, this possibility remains speculative. If this argument has validity, it would mean that phosphenes from the T3-T4 montage are more likely to be stimulating the retina, given the similar minima frequency (16.33 Hz) to FPz-Cz. It is plausible that frequency–dependent cells within both the retina and visual cortex play a role in the phosphene perception process, but such specific interactions are beyond the scope of this paper.

The typical mechanistic studies of phosphene perception are focused on retinal activation via magnetophosphenes (ICNIRP, 2020; IEEE, 2019), while this study shows a cortical influence in electrophosphene perception. Taking a univariate approach which only considers either the retinal substrate or the occipital lobe may limit our ability to understand the phosphene

perception process. Further, if there is occipital involvement in phosphenes, then this may be relevant for exposure guidelines. For example, if there is no cortical role in phosphene perception, then exposure guidelines could potentially recommend higher current densities at the back of the head, relative to the front, whereas if phosphenes are affected by currents in the occipital cortex, at levels similar to those known to stimulate the retina, then magnetic fields at the back of the head would also be important. The results of this study suggest the latter situation. If we expand our examination to include electrical fields (V/m) as well as current density (A/m^2), our results are generally consistent with both ICNIRP recommendations from 2010 and IEEE recommendations from 2019, which advise that exposure should be limited to fields that induce electrical field strengths in CNS tissue (i.e., retina and the brain) of less than approximately 50 mV/m (ICNIRP, 2010; IEEE, 2019). The FPz-Cz threshold generated 75.3 mV/m at the retina (see **Table 3.3**, p. 78), while the FPz-Oz montage generated 54.4 mV/m at the retina. Turning to the cortex, the Oz-Cz montage generated 67.1 mV/m in the grey matter adjacent to the Oz electrode. While the T3-T4 montage did not meet the 50 mV/m threshold at either the retina or the occipital cortex, it is certain to have resulted in some parts of the brain being exposed to electrical fields exceeding the recommended exposure limits. Given that the electrical field strength values for each montage listed above are based on simulations applying the *average* current thresholds across the sample, this suggests that almost half the subjects were perceiving phosphenes with electrical field strengths of less than 50 mV/m somewhere within the head using the FPz-Oz montage. Thus, while the recommended exposure limits at present may be appropriate for an "average" member of the community, they would not necessarily be appropriate for all members of the broader population.

Figure 3.5

Left hemisphere sagittal view of SimNIBS-sourced current density distribution in the full ERNIE head model for FPz-Cz, FPz-Oz and Oz-Cz montages at their respective thresholds, with additional transverse view of T3-T4.

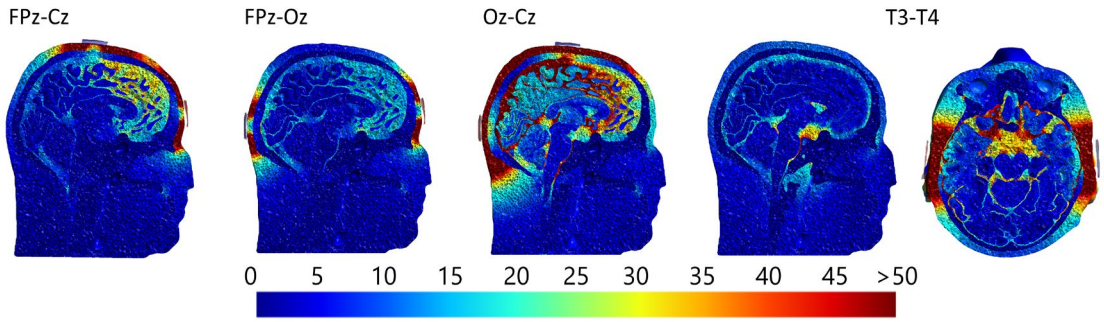

Current density was modelled at each montage's own phosphene threshold for 16 Hz. All available tissues included: skin, skull, CSF, grey matter, white matter, and eyes. Scale is in mA/m^2

The modelling of tES provided some insights into how current reaches the regions likely to produce phosphenes. As **Figure 3.5** above shows, the modelled tES has varying distributions of current density across montages while also showing some commonalities. Across all montages, current appears to flow between electrodes either via the skin or by penetrating the skull and forming a circuit via the CSF. **Figure 3.5** also shows that the vast majority of highlighted areas of current density in the modelling within the skull was in the CSF, with only the Oz-Cz montage producing broad changes in current density in the grey matter. The skull primarily acts as a resistor between the skin and the CSF, and very little change in current density is found in the grey or white matter outside the Oz-Cz montage. Even so, some changes in current density were seen in the grey matter about Oz in the FPz-Oz montage (see **Table 3.3**, p. 78), and this stimulation of the cortex combined with the retinal activation from the FPz electrode appear to have combined to produce phosphenes, given the drop in current density at the eyes compared to FPz-Cz.

It is noteworthy that this study found that cathode/anode selection did not affect phosphene thresholds across any montage or stimulation frequency. The tDCS used in the current study was found to produce similar phosphene thresholds to the tACS used in Chapter 2, which tested FPz-Cz and Oz-Cz montages under comparable conditions. This study also observed very similar frequency-dependent relations to those in the previous chapter, with 16 Hz tES producing the lowest phosphene induction thresholds for all montages in both studies. Both tDCS and tACS produce cyclic polarization/depolarizations of the tissues stimulated (whether this be retinal or otherwise). While a constant 0 Hz signal can affect changes in the body over

extended periods (Antal et al., 2003), the instantaneous change caused by a modulated signal is clear, whether it is AC or DC. As a result, the use of tDCS in the treatment or exploration of electrophysiological responses to frequency dependent stimuli (or frequency-sensitive tissue) can be considered a viable alternative for those who only have access to DC stimulators.

3.6: Conclusion

This study found that applying tES over the occipital cortex can influence phosphene perception, independent of retinal activation. While it is unlikely that these phosphenes were the product of direct (or primarily the result of) cortical stimulation alone, it does show that stimulation targeting the visual cortex contributes to phosphene perception.

4 – EXPERIMENT THREE

Adapted from: Evans, I. D., Palmisano, S., & Croft, R. J. (2022). Effect of ambient lighting on frequency dependence in transcranial electrical stimulation-induced phosphenes. *Scientific Reports*, *12*(1), 7775. doi:10.1038/s41598-022-11755-y

Summary: The previous two experiments were focused on mesopic lighting conditions and the contributions of the retina and the visual cortex to electrophosphene perception. This study focuses on the relationship between ambient lighting conditions and frequency-dependence in transcranial electric stimulation (tES) induced phosphenes to determine whether ambient lighting is an important factor in the detection of tES-induced phosphenes. Using a within-subjects design across each lighting condition (dark, mesopic, and photopic) and tACS stimulation frequency (10, 13, 16, 18, and 20 Hz), this study determined phosphene detection thresholds in 24 subjects receiving tES using an FPz-Cz montage. Phosphenes in photopic conditions were strongest at 20 Hz stimulation, while dark conditions resulted in the strongest phosphenes being detected at 10 Hz. Consistent with the previous two experiments, phosphenes in mesopic conditions were strongest at 16 Hz, with thresholds significantly lower compared to photopic or dark conditions All thresholds were tested twice (on separate days) to measure the test-retest reliability of the REPT psychophysics algorithm, which showed strong test-retest reliability across all conditions tested.

4.1: Introduction

Many aspects of neural processing rely on frequency-specific oscillations in the cortex (Buzsáki & Draguhn, 1929). As a result, the possibility of exploring and/or manipulating these frequency-based neural functions using a non-invasive technique such as transcranial electric stimulation (tES) has proven popular. Applying electric current to the brain using tES has been demonstrated to be successful in modulating cognitive, sensory, and motor functions in a frequency-dependent manner across the surface of the cortex (for reviews, see Bosman et al., 2014; Herrmann et al., 2010). Although tES can modulate cortical activity, it can also induce phosphenes; i.e., perceptions of light that are not the product of external visual stimuli (Kar & Krekelberg, 2012; Schutter & Hortensius, 2010; Schwiedrzik, 2009). These phosphenes are generally considered to be a product of electrical stimulation of the retina (Brindley, 1955; Kar & Krekelberg, 2012; Meier-Koll, 1973; Rohracher, 1935; Adrian, 1977; Lövsund et al., 1980; Attwell, 2003).

It is important to understand both the biological mechanisms responsible for inducing phosphenes and any environmental factors that influence their appearance, as these can confound tES studies, interventions, and interpretations (Schutter, 2016). For example, the threshold for inducing phosphenes is currently used by the International Commission on Non-Ionizing Radiation Protection (ICNIRP) for deriving exposure restrictions (ICNIRP, 2010), and that information can only be obtained if the effect of stimulation frequency and ambient lighting conditions are also known. Without that knowledge, experimentally derived threshold estimates may merely represent the lowest stimulation levels required to induce phosphenes in a particular *insensitive* scenario, which would limit the ability of exposure restrictions based on them to protect against phosphenes in other situations. Indeed, recent research suggests that our understanding of phosphenes may be particularly limited in terms of their relationship with stimulation frequency and ambient lighting conditions.

It has commonly been held that thresholds for phosphenes induced by transcranial alternating current stimulation (tACS) are lowest when stimulation is applied at 20 Hz in photopic (i.e., intense) lighting conditions, and at 10 Hz in complete darkness (Kanai et al., 2008). These sensitivities closely match the dominant frequencies of the visual cortex oscillations observed under these respective lighting conditions (e.g., Jasper, 1936; Palva &

Palva, 2007). These findings have been taken as evidence that tES, tuned to the dominant cortical oscillation frequency, can be used to maximally modify cortical activity at similar rhythms.

However, the studies in Chapters 2 and 3 indicate that tES-induced phosphenes are induced with a considerably lower current using 16 than 20 Hz under mesopic (dim) lighting conditions (found in different groups of subjects both when tACS or tDCS were applied). This opens the possibility that 20 Hz may not necessarily provide the lowest stimulation level required to induce phosphenes. The only research available for comparison explicitly testing phosphene threshold levels in mesopic conditions is the Schwarz (1947) study. Schwarz reported lower phosphene detection thresholds for 20 Hz stimulation in both photopic (i.e., 8 – 9550 candela per square meter; cd/m^2) and mesopic (i.e., 2.4 cd/m^2) conditions. However, those findings were based on only a single subject and used poorly controlled lighting conditions; e.g. the 2.4 cd/m^2 condition was produced by having the subject look at "*her own shadow on the wall*", and the 9550 cd/m^2 condition was produced by having the subject look at "*a white cloud in the sky*". This makes it difficult to draw conclusions from such a comparison. In contrast to Schwarz's (1947) research, the experiments in Chapters 2 and 3 used considerably larger samples (either 24 or 22 subjects) with tightly controlled lighting (consistent 0.6 cd/m^2 lighting across the entire field of view). Furthermore, the consistent findings of these experiments suggest that their results are indeed reliable. This conclusion, however, would appear (at face value) to contradict the view that the greatest sensitivity to tES occurs at the stimulation frequency that matches the dominant cortical oscillation frequency. That is, whereas the dominant cortical oscillation frequencies for dark and photopic conditions are approximately 10 and 20 Hz respectively, and the lowest current required to induce phosphenes is also at 10 and 20 Hz respectively, there is no corresponding dominant frequency for mesopic conditions established outside of the studies in this thesis.

One potential explanation for lower thresholds at 16 Hz stimulation is that this represents an overlap point between the threshold-stimulation frequency relations for photopic and dark conditions. That is, as a dim lighting condition represents a degree of photic energy that is greater than in the dark but less than in a photopic scenario, it may be relevant to the threshold-stimulation frequency of both the dark and photopic conditions. To test this

possibility, threshold-stimulation frequency relations need to be assessed under each of the dark, mesopic, and photopic conditions.

Differences in frequency dependence found in tES-induced phosphenes across lighting conditions may be explained by differences in temporal contrast sensitivity functions, i.e., the visual system's sensitivity to changes in luminance over time (de Lange Dzn, 1958; Goldstein, 2002). Temporal contrast sensitivity is typically measured using a homogenous visual stimulus that changes sinusoidally in luminance (from a minimum to a maximum value) as a function of time. While this stimulus should be perceived to flicker with higher levels of luminance contrast, it will become progressively more difficult to see this flicker as the luminance contrast decreases. However, the threshold level of luminance contrast at which this flicker is just noticeable also depends critically on the temporal frequency of the stimulus. Research has shown that rod and cone photoreceptors each have their own temporal contrast sensitivity functions, which may relate to differences in tES-related frequency dependence found in different lighting conditions.

Rod photoreceptors are more sensitive to stimulation (and thus more likely to be activated) in darker conditions, where there is insufficient input to activate cones (Barlow, 1972). In dark and mesopic conditions, temporal contrast sensitivities are largely driven by inputs from rod photoreceptors (Umino et al., 2019) particularly when exposed to stimuli flickering at 5 – 15 Hz while showing little to no activation at 19 – 23 Hz (Dai et al., 2015; Kelly, 1961). On the other hand, cone photoreceptors are more sensitive to stimulation in brighter conditions, where rod cells are saturated and do not contribute significantly to visual perception (Adelson, 1982). Temporal contrast sensitivity in these photopic conditions trends towards higher frequencies, with greatest sensitivity found at around 15 – 25 Hz and no ability to discern stimuli flickering at or above approximately 80 Hz (Dai et al., 2015; Kelly, 1961; Stockman & Sharpe, 2006). If the perception of tES-induced phosphenes is similar to, or functionally equivalent to, external flickering visual stimuli (Kar & Krekelberg, 2012), it would follow that darker conditions would result in greater sensitivity to low-frequency stimulation, and brighter conditions would result in greater sensitivity to higher frequencies.

The present study was designed to determine the following: 1) By testing the threshold-frequency stimulation relation in each of the dark, mesopic, and photopic conditions, it

examined whether the overall lowest phosphene detection threshold occurs at 16 Hz stimulation, rather than 20 Hz; 2) it compared thresholds across all lighting conditions to determine whether ambient lighting can facilitate stronger phosphene perception; and 3) it determined whether the phosphene threshold-stimulation frequency relation under mesopic conditions could be explained by the overlap of that relation across dark and photopic conditions.

4.2: Method

Twenty-four healthy subjects (even gender split, age range 20 – 40 years, *M* = 25.2 years, *SD* = 5.4) completed this study after passing a modified safety screening checklist (Keel et al., 2000; for details see Appendix A, p. 157). Subjects were excluded if they reported any form of neural injury or illness, metal implants in the head or medical implants elsewhere in the body, or non-corrected visual impairment. No subjects reported using contact lenses, while three subjects typically wore glasses but removed them during the testing phase to ensure the frames did not alter the periphery of their field of view. After being informed about the experimental procedure as well as the potential adverse effects of tES, subjects gave written and informed consent prior to any participation. This research was conducted in accordance with the guidelines of the Declaration of Helsinki and approved by the Human Research Ethics Committee of the University of Wollongong (approval #HE2017/454).

Phosphene thresholds were obtained as a function of stimulation frequency ("Frequency": 10, 13, 16, 18, and 20 Hz) and lighting condition ("Lighting Condition": dark, mesopic, photopic), using a repeated measures design. Testing was conducted over two, 70-minute sessions (on separate days) at similar times of day, usually within one week of each other. The order of these sessions, the order of the tES frequencies within these sessions, and which electrode was the cathode or anode, were counterbalanced across sessions for all subjects (see **Figure 4.1b**, p. 92). The choice of which electrode was the cathode or anode alternated across sessions for each subject. The order of the lighting conditions was randomised for each subject using a Latin square system, as was the order of stimulation frequency within each lighting condition.

Figure 4.1

A) Positioning of lighting and test subject. The test subject was seated so that the front wall filled their entire field of view (no parts of either side wall were visible). The light stand was positioned so that no shadows were visible in the subject's field of view. The photopic lighting condition was achieved by activating the fixed fluorescent ceiling light with no light stand used, while all other lighting conditions (the mesopic condition and the brief periods requiring light in the dark condition) were achieved using the light stand only.

B) Example sequence of the block design across both sessions. For the first session, each lighting condition block was presented in a random order, as were the frequencies within it. In order to account for potential within-subject order effects due to possible light adaptation, the order of the lighting blocks was reversed in the second session and the frequencies within those blocks were reversed.

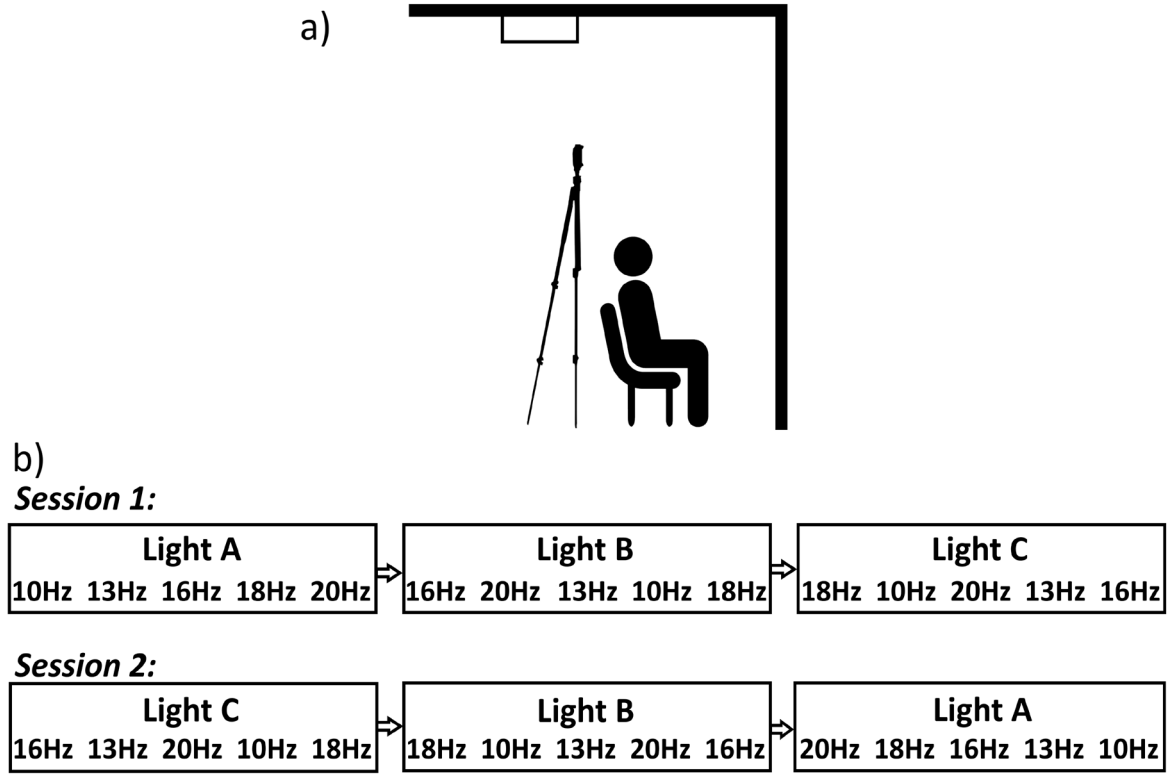

tES was administered using a Magstim NeuroConn Stimulator Plus MOP15-EN-01 (Magstim, Carmarthenshire, UK) which applied sinusoidal DC with no ramp-up, meaning that the amplitude of the stimulation varied as a sine wave from zero to the current set by the stimulator then back to zero. As such, the polarity of the electrodes did not alternate. Current was delivered to the scalp through conductive-rubber electrodes (dimensions: 30 x 40 mm) placed on sponges saturated with a saline solution mixed with a hypoallergenic amphoteric surfactant and held in place at FPz and Cz with rubber straps. This electrode montage was chosen as it is effective at stimulating the retinas (Laakso & Hirata, 2013) while also ensuring

the subjects' entire field of view was not occluded by any of the apparatus. Both previous studies in this thesis consistently found greatest sensitivity at 16 Hz using a wide range of montages (FPz-Cz, Oz-Cz, FPz-Oz, T3-T4), suggesting that the choice of montage does not appreciably affect the frequency-dependent nature of tES-induced phosphenes, provided that the retina is adequately stimulated.

The photopic lighting condition was generated by using typical ceiling-mounted fluorescent lights, positioned outside the subjects' direct line of sight. Under these lighting conditions, luminance at the eye was measured at 77.1 ± 0.05 cd/m^2 using a J6523 Tektronix luminance probe (Tektronix, London, Canada). This lighting level was chosen due to its applicability to everyday experience, as it represents the luminance typically found in office environments. The mesopic lighting condition was created using the Neewer T120 dimmable LED panel, which illuminated the areas in front of the subject (see **Figure 4.1a**, p. 92), resulting in luminance at the eye measured at 0.6 ± 0.05 cd/m^2. This lighting level was chosen in order to match the studies in Chapters 2 and 3, thus enabling a possible replication of their results. No light entered the testing room during the dark condition, resulting in zero cd/m^2. In order to prevent dark adaptation effects during the trials in the dark condition, lighting was set to 1.1 cd/m^2 while the stimulator was not active; lighting was turned off 2 seconds prior to stimulation onset and turned on immediately after the stimulation had ended.

Subjects were seated on a chair facing a 1.8 meter wide by 2.62 meter high white wall, in a position that ensured that the wall in front of them filled their entire field of view, and lighting was arranged so that no shadows were visible to the subject (see **Figure 4.1a**). When subjects were comfortable and the electrodes were put in position, they were informed about phosphenes (their nature and what they might perceive) while their skin and hair were saturated from the saline in the sponges. Once the impedance between the electrodes was at 15 kΩ or below (as indicated by the stimulator), lighting was set to 2 ± 0.05 cd/m^2 and subjects were familiarized with the appearance of phosphenes using 10 s of sinusoidal tDCS at 1000 μA, firstly at 11 Hz and then at 22 Hz, to demonstrate both the visual appearance of phosphenes and how their appearance changes by simply varying the stimulation frequency. These frequencies were chosen to avoid using the same stimulation frequencies as in the experiment itself.

Once subjects were familiarized with phosphenes, their phosphene detection thresholds were determined at each stimulation frequency in each lighting condition. They were informed when each stimulation began and when it ceased, but they were not informed of the frequency or current intensity of the stimulation. Stimulations lasted for 5 seconds, and subjects were instructed to keep their eyes open throughout the entire stimulation. Throughout the experiment, subjects were asked how bright the phosphenes appeared to be compared to the background lighting, and where the phosphenes appeared in their field of view. Many subjects also spontaneously volunteered information concerning their experience during the interval between trials. To detect false positive responses at lower current intensity levels, six sham stimulations (one in each lighting condition for each session) were given at a frequency determined in advance using a MATLAB-based random number generator. In these sham trials, the subject was given all the audible signs of stimulation (the usual button presses on the stimulator as well as verbal indications that the stimulation had started and finished) without actually generating an electric current. None of the subjects reported seeing phosphenes during any of the sham trials.

Thresholds for phosphene induction (in μA) were determined for each frequency by varying the current intensity using a QUEST-based Bayesian adaptive staircasing procedure (Watson & Pelli, 1983) in MATLAB's PsychToolbox (Kleiner et al., 2007). The tDCS, which started at 700 μA, was bound between 25 μA and 1500 μA. The step-size between possible stimulation levels was 25 μA. Based on the Rapid Estimation of Phosphene Threshold system validated by Mazzi et al. (2017), this adaptive threshold measurement method determined the lowest current intensity that was significantly more likely than chance to evoke phosphene perceptions. Each of the two sessions provided a threshold for each lighting and frequency condition, and for each combination of lighting condition and stimulation frequency, the average threshold across both sessions was taken as the final threshold.

4.3: Statistical Analysis

As significant levels of skewness, kurtosis, or heterogeneity of variance were not found, parametric analyses were conducted. Huynh-Feldt adjustments were used to account for

violations of sphericity (Frequency; Frequency by Lighting Condition), with the adjusted degrees of freedom shown.

To assess threshold reliability across the two testing sessions, for each of the Lighting Condition (photopic, mesopic, and dark) by Frequency (10, 13, 16, 18, and 20 Hz) combinations, Pearson's *r* was determined. To determine if order effects were distorting the results, thresholds were arranged in chronological order and repeated measures ANOVA was used where threshold was the dependent variable and testing order within each lighting condition (separately for each session) and across each entire session were the independent variables.

To describe the relations between phosphene thresholds, lighting conditions, and stimulation frequency, a repeated measures ANOVA was used, where threshold was the dependent variable and Lighting Condition and Frequency the independent variables. Where significant, data were further explored using repeated measures t-tests with Bonferroni comparison-wise adjustments (Lighting Condition: each level was compared to each other level; Frequency: each level was compared to each other level; Interaction: for each frequency, each level of Lighting Condition was compared to each other level). Adjusted *p*-values are shown.

To determine the lowest absolute phosphene thresholds across the lighting conditions, a repeated measures ANOVA was used where Lighting Condition was the independent variable and the dependent variable was the lowest algebraic threshold across the frequencies, for each lighting condition separately. Where the main effect was significant, *t*-tests with Bonferroni comparison-wise adjustments (Lighting Condition: each level was compared to each other level) were conducted. Adjusted *p*-values are shown.

To determine whether the phosphene threshold-stimulation frequency relation in the mesopic condition could be adequately explained by the summation of the relations in the dark and photopic conditions, regression equations were calculated as follows: To provide an estimate of the phosphene threshold-stimulation frequency relation for each of the lighting conditions separately, regression analyses were conducted for each lighting condition separately, where threshold was the dependent variable (normalized across all tested frequencies, within each subject and lighting condition separately), and Frequency the independent variable. Corrected Akaike's Information Criteria (AICc; Akaike, 1973) were used

to determine whether a linear or quadratic fit was the best model for each lighting condition. Data for each subject was used for all frequencies and lighting conditions, resulting in 72 data points per frequency.

4.4: Results

Thresholds at each Frequency/Lighting Condition combination can be seen in **Figure 4.2a** (p. 98). The interpolated regression functions relating threshold to Frequency, for each lighting condition separately, can be seen in **Figure 4.2b**. Corresponding means and standard errors are given in **Table 4.1** (p. 99). Thresholds for all individuals in every lighting condition and frequency for both testing sessions can be read in Appendix F (p. 169).

Phosphene detection thresholds were highly reliable across the two testing sessions, with Pearson's r coefficient values ranging from .91 to .99 (all $p < .001$) across the 15 Frequency/Lighting Condition combinations. No signs of learning or fatigue effects were found within either session (p between .707 - .883) or within each lighting condition (p between .472 - .940). Mean thresholds for all (30) testing points ranged between 313.5 – 407.3 µA, with standard deviations between 166.3 – 246.4 µA.

Phosphene detection thresholds were affected by lighting condition (main effect: $F(1.96,45.16) = 59.15$, $p < .001$, $\eta_p^2 = .720$), with post hoc analyses showing that this was due to lower thresholds in the dim lighting condition relative to both the photopic ($F(1, 23) = 116.4$, $p < .001$, $\eta_p^2 = .835$) and dark ($F(1, 23) = 93.93$ $p < .001$, $\eta_p^2 = .803$) conditions; no difference was observed between the photopic and dark conditions ($p > .999$). Phosphene thresholds (for the combined lighting conditions) were also affected by Frequency (main effect: $F(1.69,38.91) = 26.46$, $p < .001$, $\eta_p^2 = .535$). The frequency with the lowest threshold (16 Hz) was lower than each other frequency (all $p < .049$), and the frequency with the highest threshold (10 Hz) was higher than each other frequency ($p < .004$). Of the remaining comparisons, thresholds for 13 Hz were higher than 18 Hz ($F(1, 23) = 10.34$, $p = 0.038$, $\eta_p^2 = .310$) but did not differ from 20 Hz ($p = .795$), and 18 Hz was lower than 20 Hz ($F(1, 23) = 17.75$, $p = 0.003$, $\eta_p^2 = .436$).

The interaction between Frequency and Lighting Condition was also significant $F(4.63,106.50) = 117.60$, $p < .001$). Follow-up analyses for the significant interaction demonstrated the following:

10 Hz Stimulation. Thresholds were lower for both the mesopic ($t(23) = 13.77$, $p < .001$, Cohen's $d = 2.81$) and dark ($t(23) = 8.85$, $p < .001$, $d = 1.81$) conditions than photopic conditions, whereas mesopic and dark conditions did not differ ($t(23) = 2.25$, $p = .102$, $d = 0.46$).

13 Hz Stimulation. Thresholds were lower for mesopic than both dark ($t(23) = 7.58$, $p < .001$, $d = 1.55$) and photopic ($t(23) = 12.31$, $p < .001$, $d = 2.51$) conditions, and lower for dark compared to photopic conditions ($t(23) = 4.73$, $p < .001$, $d = 0.97$).

16 Hz Stimulation. Thresholds were lower for mesopic than both the photopic ($t(23) = 9.64$, $p < .001$, $d = 1.97$) and dark ($t(23) = 10.27$, $p < .001$, $d = 2.10$) conditions, whereas dark and photopic conditions did not differ ($t(23) = 2.54$, $p = .055$, $d = 0.52$).

18 Hz Stimulation. Thresholds were lower for the mesopic than both photopic ($t(23) = 7.98$, $p < .001$, $d = 1.63$) and dark ($t(23) = 11.65$, $p < .001$, $d = 2.38$) conditions, and photopic less than the dark condition ($t(23) = 4.12$ $p = .001$, $d = 0.84$).

20 Hz Stimulation. Thresholds were lower for the mesopic than both photopic ($t(23) = 3.25$, $p = .009$, $d = 0.67$) and dark ($t(23) = 10.71$, $p < .001$, $d = 2.19$) conditions, and photopic less than dark condition ($t(23) = 7.29$, $p < .001$, $d = 1.49$).

The lowest thresholds within each lighting condition (across all frequencies) differed as a function of Lighting Condition (main effect: $F(2,46) = 34.84$, $p < .001$, $\eta_p^2 = .602$), with lower thresholds found in the mesopic condition (at 16 Hz) relative to each of the dark (at 10 Hz; $F(1, 23) = 54.88$, $p < .001$, $\eta_p^2 = .705$) and light (at 20 Hz; $F(1, 23) = 66.42$, $p < .001$, $\eta_p^2 = .743$) conditions. No difference was found between the lowest light and dark condition thresholds ($p = .772$).

Figure 4.2

A) Phosphene thresholds and standard errors for each ambient lighting condition at each frequency tested (10, 13, 16, 18 and 20 Hz).

B) Regression-based estimates of normalised phosphene thresholds, as a function of stimulation frequency, for each ambient lighting condition.

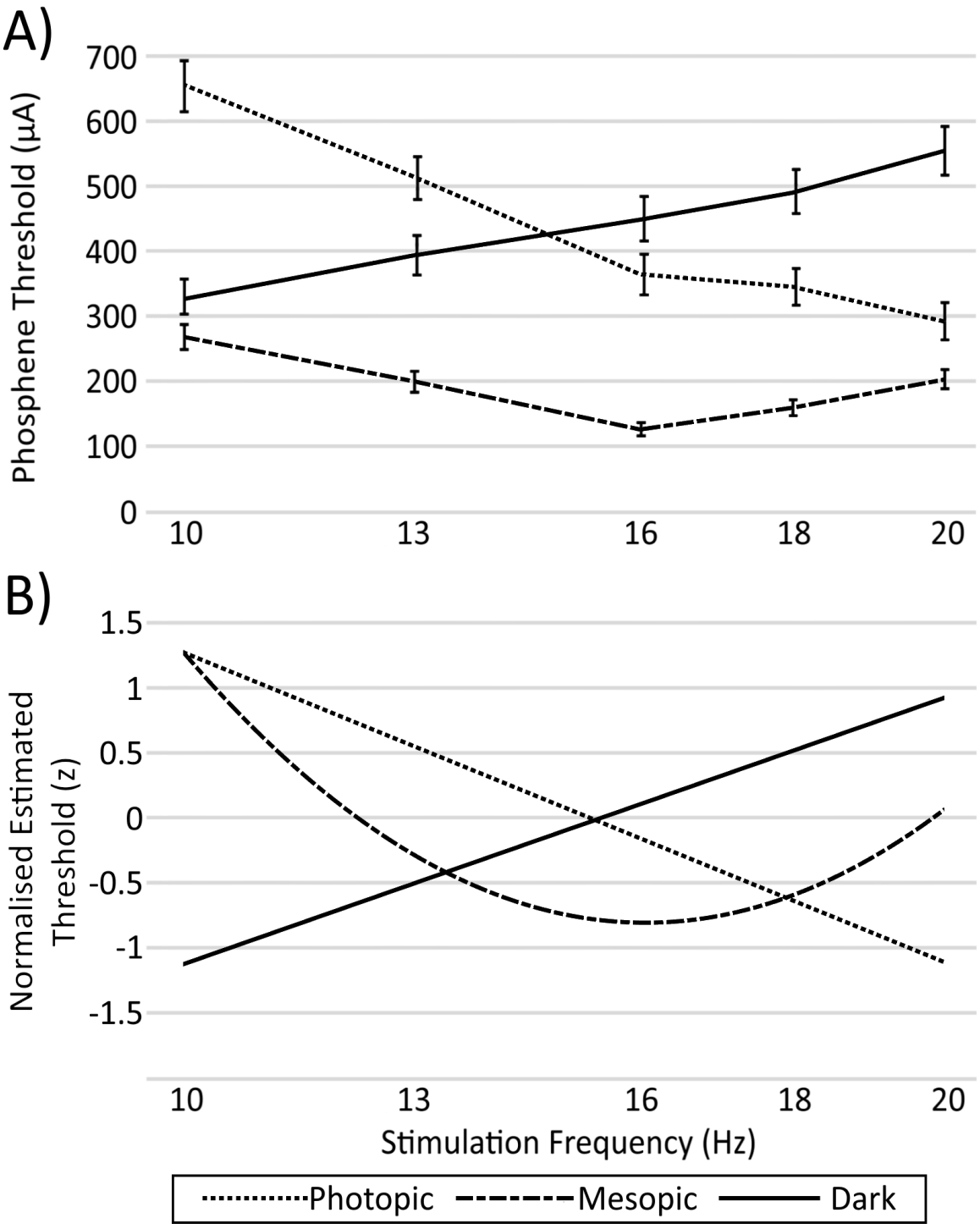

Table 4.1 – Means (and standard errors) of phosphene thresholds for each frequency and lighting condition tested (n = 24)

Frequency (Hz)	Photopic	Mesopic	Dark
10	655.2 (39.2)	270.8 (19.2)	328.1 (26.9)
13	516.1 (32.7)	203.6 (16.0)	394.3 (30.6)
16	366.1 (31.0)	130.2 (10.2)	449.0 (34.5)
18	347.4 (28.3)	163.0 (12.5)	490.1 (33.8)
20	294.3 (28.6)	206.3 (14.9)	553.6 (37.5)

For the dark condition, a linear model (AICc = 193.02) produced a better fit than the quadratic model (AICc = 194.34). For the mesopic condition, a quadratic model (AICc = 199.46) produced a better fit than the linear model (AICc = 289.71). For the photopic condition, a quadratic model (AICc = 37.02) produced a better fit than the linear model (AICc = 64.34).

The regression analyses (predicting threshold as a function of frequency) resulted in the following equations where y was the phosphene perception threshold and x was the stimulation frequency in Hz (normalized regression fits; see **Figure 4.2b**, p. 98):

$$y(Dark) = 0.203x - 3.130, adj\ R^2 = .650, p < .001$$
$$y(Mesopic) = 0.056x^2 - 1.800x + 13.682, adj\ R^2 = .634, p < .001$$
$$y(Photopic) = 0.014x^2 - 0.655x + 6.587, adj\ R^2 = .905, p < .001$$

Subjects consistently reported that phosphenes in mesopic and dark conditions increased in luminosity (compared to their backgrounds) as the stimulation intensity increased. Under photopic conditions, subjects consistently reported that the flashing of the phosphene appeared to make their field of view seem darker compared to pre-stimulation perceived luminance levels, where the flashing alternated between a visible flash and the previous level of general luminosity. This distinction became stronger as stimulation intensity increased. Four subjects reported seeing coloured phosphenes; however, these reports were not consistent across those individuals or within individuals across sessions.

4.5: Discussion

The aim of the study was to determine the relationships between phosphene detection thresholds and both ambient lighting and tES stimulation frequency. Those relations enabled us to test whether: 1) the findings from Chapters 2 and 3 of greater sensitivity to tES-induced phosphenes at 16 Hz were valid (as opposed to the standard view that sensitivity is greatest at 20 Hz; Lövsund et al., 1980; Rohracher, 1935; Schutter & Hortensius, 2010; Schwarz, 1947); and 2) this apparent contradiction in the literature was due to ambient lighting.

As can be seen in **Figure 4.2** (p. 98), each of the ambient lighting conditions had a unique phosphene threshold relation with stimulation-frequency, whereby thresholds increased with frequency in the dark condition, decreased with frequency in the photopic condition, and reduced with frequency from 10 Hz to 16 Hz and increased from 16 Hz to 20 Hz in the mesopic condition. Corresponding to this, threshold minima under dark, mesopic, and photopic conditions were found at 10 Hz, 16 Hz and 20 Hz respectively. This demonstrates that both ambient lighting conditions and stimulation frequency are important for determining the minimum current required to induce phosphenes. Correlation analyses showed consistent phosphene thresholds across sessions, indicating that order effects and the choice of which electrode was the cathode or anode had no significant effect on the results.

The lowest thresholds overall were found under mesopic conditions (at 16 Hz), with thresholds significantly higher under both dark (at 10 Hz) and photopic (at 20 Hz) conditions across all frequencies tested. This means that threshold estimates obtained using the standard photopic or dark conditions, regardless of frequency, will overestimate the current required to induce phosphenes. It follows that guidelines using phosphene detection to set exposure restrictions based on data obtained in dark or photopic conditions (e.g., ICNIRP, 2010), may underestimate the effect of electric current on neural processes (by 56 – 60%). It is important to note that even though such exposure guidelines typically rely on research using magnetic fields (rather than tES) to induce phosphenes, in both cases the cause of the phosphene is the current flowing through neural tissue (Lövsund et al., 1980), which stimulates the same physiological processes. It follows that the present results are also

applicable to research using magnetic fields to induce phosphenes and thus to low frequency electromagnetic field exposure guidelines.

The present data also resolve the apparent discrepancy between the 16 Hz sensitivity found recently in Thiele et al. (2021) following the studies in Chapters 2 and 3, and also in studies reporting thresholds at either 10 or 20 Hz (e.g. Kanai et al., 2008; Schwarz, 1947). That is, the present findings confirm that mesopic conditions result in the greatest sensitivity at 16 Hz, whereas dark and photopic conditions (similar to those in past studies) result in the greatest sensitivity at 10 and 20 Hz tES respectively. There is thus no inconsistency, only predictable differences due to the differing ambient lighting conditions used. Overall, the results of this study relating to ambient lighting and frequency dependence are consistent across multiple forms of tES, whether using tACS as shown in Chapter 2 or sinusoidal tDCS as shown in Chapter 3. While there are differences in the levels of current required to induce phosphenes across studies (e.g., Kanai et al., 2008; Thiele et al., 2021), this is likely a product of different methodological choices, as there are a multitude of variables that can change this threshold. As shown in **Figure 1.2** (p. 21), even when using the same montage on the same sample, the current density in the eyes and brain can vary based on the size, shape, and surface area of the electrodes, the material from which the electrode is made, and the conductivity medium selected (e.g., conductive gel, electrolyte-soaked sponges). Changing any of these variables will change the volume conduction characteristics of the overall circuit, resulting in different levels of current density at the retina (Laakso & Hirata, 2013). As a result, while the comparison of thresholds across studies is of little value, the findings relating to frequency and lighting remain consistent despite any variations in stimulation methodology.

Although it is tempting to suggest that different physiological processes are being engaged during tES in the mesopic relative to dark and photopic conditions, a simpler explanation may be sufficient to explain these results. As can be seen in **Figure 4.2** (p. 98), the shape of the estimated distribution of thresholds in the mesopic condition matched that of the dark condition at frequencies below the approximate crossover point at 16 Hz, and also matched that of the photopic condition at frequencies above the 16 Hz crossover point. Taken together, it would thus appear that the mesopic condition may simply represent the combination of physiological processes normally engaged in each of the dark and photopic conditions.

Consistent with this hypothesis, there is evidence that the observed frequency dependence in tES-induced phosphene research can be explained by differences in the relative activity of rod-based and cone-based vision (Motokawa & Iwama, 1950; Neftel, 1878). Cells related to rod vision, which are primed to respond in dark conditions, are maximally sensitive to stimulation at circa 10 Hz (Benardete et al., 1992; Kaplan & Benardete, 2001; Lee et al., 1994), whereas cells related to cone vision, which are primed to respond in photopic conditions, are maximally sensitive to stimulation at circa 20 Hz (Adelson, 1982; Motokawa & Iwama, 1950). In itself, this would not explain the magnitude of threshold reduction in the mesopic condition (60% and 56%, relative to the dark and photopic conditions respectively), particularly given that 16 Hz is far from the ideal stimulation frequency for either rod- or cone-related cells. However, when coupled with what is known about the rod-cone processing delay, this would appear a viable hypothesis. That is, there is a delay between rod- and cone-related cell processing under mesopic conditions (MacLeod, 1972), but as the stimulation frequency reaches approximately 15 Hz, rods and cones start to fire in phase, which increases the signal at both rods and cones and enhances the perceptibility of the stimulation (Sharpe et al., 1989). This critical 15 Hz frequency also approximates the crossover point of the dark and photopic regression estimates (see **Figure 4.2b**, p. 98), indicating that the rod-cone phase delay mechanism may be behind the lower overall thresholds at the nearby 16 Hz frequency in mesopic conditions. Further research would be required to test this hypothesis.

While high levels of current can result in discomfort or pain at the site of stimulation (World Health Organization, 2007), these effects are typically found at stimulation strengths exceeding the maximum used in this study. The maximum strength of stimulation (1500 μA) in the present study was selected in order to avoid such side effects. One subject reported an unpleasant itching-like sensation at stimulation levels above 900 μA; however, the sensation immediately ceased upon termination of the stimulation. Despite multiple inquiries during each testing session, no other subject reported any negative side effects, either during or after stimulation. Indeed, as the study deliberately kept current levels low to identify thresholds, this reduced the opportunity to obtain meaningful information about the phosphene experience more generally, which may otherwise have helped shed light on the underlying physiology responsible for phosphene induction. Of particular relevance is the degree to which phosphenes were perceived in chromatic (as opposed to achromatic) colour,

as that could provide evidence for the relative mechanistic roles of rods and cones, as a function of frequency and lighting condition. However, given the low current strengths used in the study, only four subjects reported seeing chromatic colour, and reports were not consistent across those individuals or within each individual across sessions. We thus do not believe that these anecdotal reports are sufficient to enable interpretation.

4.6: Conclusion

The present study has shown that the apparent contradiction in the literature, in terms of tES stimulation frequency and phosphene detection threshold, was due to the different ambient lighting conditions used across past studies. That is, whereas thresholds under dark and photopic conditions are lowest for 10 and 20 Hz stimulation respectively, they do not represent overall thresholds, which occur at 16 Hz in mesopic conditions. The magnitude of threshold overestimation was very large (60 and 56% for dark and photopic conditions respectively), and thus important for the application of tES research. Physiological considerations suggest that the lower thresholds in mesopic conditions, and particularly at 16 Hz stimulation, may be due to the involvement of both rod and cone photoreceptors, but further research is required to determine this. Importantly, our research also shows (for the first time) that dark, mesopic, and photopic lighting conditions each have their own unique phosphene threshold relationship with stimulation-frequency.

5 – GENERAL DISCUSSION

The overarching purpose of this thesis was to shed light on long-held assumptions and fill various gaps in our understanding of tES-phosphenes, in order that there can be a better understanding of the effects of EMF on the body. As improvements in technology result in the expanded use of non-ionizing radiation in the environment, exposure guidelines should take any plausible exposure situation into account. To that end, this thesis had three primary aims:

1) To confirm previous findings on the frequency-dependence of tES-induced phosphenes in multiple ambient lighting conditions;
2) To determine the effect of mesopic lighting on tES-induced phosphenes; and
3) To separate two possible biological sources of tES-induced phosphenes.

Overall, these experiments show that ambient lighting has a strong effect on the current strength required to induce electrophosphenes, and on which stimulation frequencies make phosphenes easier to detect. Each lighting condition tested had its' own frequency dependence characteristics regarding how much current was required to induce phosphenes, most of which were consistent with previous research findings. That said, these results show that mesopic lighting caused a sharp decrease in the current strength required to induce phosphenes compared to other lighting conditions, with different stimulation frequency-dependent effects compared to other lighting conditions. The double dissociation analysis contradicted previously held views by showing that increasing current density in the visual cortex causes an increase in sensitivity to phosphenes generated at the retina compared to retinal stimulation alone.

This chapter is separated into four sections: 1) a summary of the findings of each experiment; 2) a discussion section where all experimental findings are synthesized into their key points with the existing literature; 3) the limitations of these experiments and how future experiments could address these issues; and 4) some concluding remarks.

5.1: Summary of Findings

This section provides an overall summary of each individual experiment. This will include a description of the purpose and methodology of the experiment, any explicit hypotheses and/or expected outcomes that influenced the experimental design, and a summary of the experiment's findings. This will be followed by a synthesis of the findings across all experiments and how they relate to the primary aims of the thesis listed above.

5.1.1: Experiment One

Description: The experiment in Chapter 2 explored two aspects of electrophosphene detection that had not yet been examined in the literature: 1) the effect of stimulation frequency on phosphene detection under mesopic lighting conditions, and 2) differences in frequency sensitivity and phosphene thresholds between retinal (FPz-Cz) and cortically-targeting (Oz-Cz) montages. tACS-induced phosphene detection thresholds were compared across fifteen frequencies (2, 4, 6, …28, and 30 Hz) with consistent 0.6 cd/m^2 luminance in the subject's entire field of view, using two montages that preferentially targeted the retina (FPz-Cz) and the visual cortex (Oz-Cz) respectively.

Expectations and Hypotheses: Outcomes for this study were difficult to predict as there are only two previous studies that examined phosphenes in mesopic conditions using both montages, and they offer limited insights into mesopic phosphene perception (Kar & Krekelberg, 2012; Schutter & Hortensius, 2010). Both studies used inconsistent lighting across the subject's field of view (a partially lit computer monitor in a darkened room), and neither provided (or was intended to provide) an adequate analysis of phosphene thresholds or frequencies to reach a conclusion with any confidence. Kar and Krekelberg (2012) tested phosphene thresholds at seven frequencies but reported only four (8, 10, 15, and 20 Hz), while the phosphene thresholds were only presented on five individual line charts (one for each subject). No numerical threshold values were reported for individual subjects or averaged across the sample, and no statistical analysis examining differences in thresholds between conditions or montages was reported. Schutter and Hortensius (2010) compared subjective phosphene intensity at three frequencies (2, 10, and 20 Hz) using two fixed degrees

of current strength (250 and 1000 μA), reporting more intense phosphenes at 1000 μA in the FPz-Cz montage at 10 and 20 Hz. Both of these studies reported greater intensity of phosphenes in the FPz-Cz montage, which was also expected to be the case in the current study.

Experimental Findings: Consistently lower thresholds were found in the FPz-Cz montage compared to Oz-Cz across all frequencies; these thresholds were lowest at 16 Hz in both the FPz-Cz and Oz-Cz montages. Regression analyses showed differences in the shapes of the frequency distribution between montages, but no significant difference in the frequency producing minimum thresholds between montages. Recorded thresholds at 16 Hz were significantly lower in both montages compared to frequencies commonly reported as sensitive to phosphene perception in lit (20 Hz) and dark environmental conditions (10 Hz). This suggests that the frequency dynamics of tES phosphene thresholds in mesopic conditions are unlike those of any other ambient lighting condition previously reported.

5.1.2: Experiment Two

Description: The second study was designed to address three issues that need to be resolved for a greater understanding of electrophosphenes: 1) the source separation issue between retinal and cortical electrophosphenes; 2) to determine if the 16 Hz sensitivity found in the previous study can be replicated in a different sample; and 3) whether stimulation polarity has any effect on electrophosphene detection. Electrophosphene thresholds were compared across seven frequencies of tDCS (6, 10, 16, 20, 24, 28, and 32 Hz) with consistent 0.6 cd/m^2 luminance in the subject's entire field of view, using four montages that preferentially targeted the temporal lobe (T3-T4), the retina (FPz-Cz), the visual cortex (Oz-Cz), and both the retina and visual cortex simultaneously (FPz-Oz). A double dissociation employing both phosphene thresholds and modelled estimates of current density in MRI images of twenty real head models was used to consider the effects of stimulating the cortex and/or stimulating the retina. Polarity effects were assessed by counterbalancing which electrode was the cathode across the entire sample for each montage.

Expectations and Hypotheses: The previous study found that tACS at 16 Hz was most likely to produce the lowest thresholds in mesopic conditions, and it was expected that this finding would be replicated. That said, little confidence could be held in that expectation until this unprecedented result could be replicated in a different sample. Similar to previous studies using multiple montages, it was hypothesized that thresholds would fall as electrodes were arranged closer to the retina. There was no expectation that polarity would have a significant effect on phosphene thresholds, however, this potential confound should be tested by using tDCS since 1) this allows polarity to be consistent and controllable; and 2) any potential effect of polarity on phosphene thresholds (null or otherwise) has not been established in the literature. The only previous study that examined current density modelling in these montages (Laakso & Hirata, 2013) used different sized electrodes for each montage their modelling was based on, which would cause differences in how current density is distributed throughout the head (see *1.3.3.4: Volume Conduction and Current Density*, p. 18) making it difficult to predict any likely outcome regarding current density modelling.

Experimental Findings: Consistent with the findings of the tACS study in Chapter 2, tDCS at 16 Hz produced the lowest thresholds across all montages. Changing stimulation polarity had no effect on phosphene thresholds in any condition or combination of conditions. Thresholds fell as electrodes were arranged closer to the retina as expected, with the exception of the FPz-Oz montage, which produced the lowest thresholds in all frequencies compared to any other montage. Current density modelling showed that stimulation at the phosphene threshold in the FPz-Oz montage produced less current density in the eyes compared to stimulation at the phosphene threshold in the FPz-Cz montage, showing that tACS delivered over the visual cortex can facilitate phosphene perception.

5.1.3: Experiment Three

Description: While the previous two studies have established the frequency dynamics of tES-induced phosphenes in mesopic conditions, it is important to see how they compare to other lighting conditions. The third study compared phosphene thresholds across five frequencies (10, 13, 16, 18, and 20 Hz) of tDCS using an FPz-Cz montage in three separate lighting conditions: photopic (77.1 cd/m^2), mesopic (0.6 cd/m^2) and dark (0 cd/m^2). All possible

combinations of conditions were tested twice on separate days to assess the test-retest reliability of the REPT algorithm. Polarity effects were again assessed by counterbalancing which electrode was the cathode across the entire sample for each condition.

Expectations and Hypotheses: As seen in **Table 1.1** (p. 24), past estimates of the stimulation frequencies that produce the lowest phosphene thresholds appear to be inconsistent for both photopic lighting and dark conditions. However, it was considered most likely that the commonly reported sensitivities (20 Hz in photopic conditions and 10 Hz in dark conditions with minimal dark adaptation time) would produce the lowest thresholds. As in the previous two studies, 16 Hz was predicted to produce the lowest thresholds in the mesopic condition.

Previous studies on how phosphene thresholds compare across lighting conditions report that phosphene thresholds are higher in dark conditions compared to lit conditions (Schwarz, 1947; Kanai et al., 2008). There was little reason to expect a different finding in Experiment 3. However, as these two past studies did not form a strong evidence base, it was important to confirm that these reported differences between lighting conditions could be replicated. The dearth of studies in mesopic conditions made it difficult to estimate how thresholds in mesopic conditions would compare to other lighting conditions; the only study employing all three lighting conditions is Schwarz' (1947) single person case study that used inconsistent fields of view for each lighting condition (see *1.5.3: Ambient Lighting – Limitations of the Literature*, p. 37), which does not provide sufficient predictive value to form a plausible hypothesis.

Experimental Findings: REPT showed strong test-retest reliability across all combinations of conditions tested. Like the previous study, changing stimulation polarity had no effect on phosphene thresholds. Both photopic and dark conditions resulted in the lowest phosphene thresholds at the expected 20/10 Hz stimulation frequencies, while mesopic conditions again resulted in the lowest phosphene thresholds at 16 Hz. Mesopic conditions resulted in the lowest phosphene thresholds across all frequencies tested compared to photopic or dark conditions, indicating that mesopic conditions (which are not presently considered in exposure guidelines) provide the worst-case scenario for electrophosphene detection.

5.2: Synthesis of Findings

5.2.1: Phosphene Thresholds Are Affected by the Interaction Between Ambient Lighting and Stimulation Frequency

Guidelines on EMF exposure use experimental thresholds for phosphene perception as a conservative estimate for the potential of EMF to interfere with the central nervous system (**CNS**; ICNIRP, 2010; IEEE, 2019). The electric field strength required to induce electrophosphenes can be estimated by determining the minimum phosphene threshold across a variety of plausible conditions and using these values to generate modelled estimates of the electric field strength throughout the head. When comparing all three lighting conditions in Chapter 4, phosphene thresholds were lowest across all frequencies tested (10 - 20 Hz) in the mesopic condition, with the lowest mesopic threshold measured at 56 - 60% lower than any threshold found in photopic or dark conditions. Even this comparison may be underestimating the differences in thresholds when the visual cortex is stimulated as well as the retina: the FPz-Oz montage used in Chapter 3 produced mean thresholds of 87.5 μA, 70 - 74% lower than those found in any other lighting condition in Chapter 4 using the FPz-Cz montage (294.3 μA in photopic conditions, 328.1 μA in dark conditions).

The modelling estimates of mean phosphene thresholds in Chapter 3 showed electric field strength was higher than the 50 mV/m exposure limit recommended by ICNIRP (2010) at some point within the head across all montages. While the mean electric field strength may have been consistently above the 50 mV/m recommendation, it remains the case that a considerable proportion of the sample tested were detecting phosphenes with lower electric field strength than current guidelines recommend. As research into EMF-induced phosphenes in mesopic conditions is relatively new and thus unavailable for consideration, this indicates that current exposure guidelines are using particularly insensitive scenarios to inform estimates for EMF exposure restrictions.

Previously reported sensitivities to phosphenes at 20 Hz in photopic conditions and 10 Hz in dark conditions were confirmed in Chapter 4, while the sensitivity to phosphenes at 16 Hz in mesopic conditions was consistent across all three studies. It remains unclear why these specific frequencies caused such effects, but adding the mesopic lighting evidence provides

further insights into the potential mechanisms behind phosphene perception. When considering cortically-induced electrophosphenes, it is frequently reported that EEG recordings of the visual cortex in normal operation show greater spectral band power in the alpha band (typically 8 – 12 Hz) in dark conditions, a range that includes the 10 Hz sensitivity to phosphenes in dark conditions (Palva & Palva, 2007). Similarly, EEG in the visual cortex shows greater spectral band power in the beta band (typically 12 – 30 Hz) in lit conditions, again including the 20 Hz sensitivity to phosphenes in photopic conditions (Gale et al., 1971). No such association between EEG in the visual cortex and spectral power in mesopic conditions at 16 Hz has been reported, although this may be a consequence of using frequency bands to describe cortical activation differences rather than specific frequencies.

Considering retinally-induced electrophosphenes, the sensitivity to stimulation at 10 Hz fits well with previous findings that rod photoreceptors are maximally sensitive to activation both in dark conditions and when stimulated at around 10 Hz (Benardete et al., 1992; Kaplan & Benardete, 2001; Lee et al., 1994), while cone photoreceptors are maximally sensitive to activation both in well-lit conditions and when stimulated at around 20 Hz (Adelson, 1982; Motokawa & Iwama, 1950). The mesopic sensitivity at 16 Hz fits well with the rod-cone phase delay mechanisms under mesopic conditions, where both photoreceptor types will fire in phase at 15 Hz and strengthen visual perception in that region (Stockman & Sharpe, 2006).

5.2.2: tES Over the Occipital Lobe Can Enhance Phosphene Perception

Examining the differences in thresholds across the range of montages used (and the modelled estimates of current density for each montage) makes it clear that the retina is the structure most sensitive to electrophosphenes. That said, there is now evidence that cortical stimulation can contribute to phosphene detection even when comparatively low levels of current density are applied. The claim by Kanai and colleagues (2008) that tES over the visual cortex could induce cortical phosphenes has met with consistent pushback (e.g., Laakso & Hirata, 2013; Schutter & Hortensius, 2010; Schwiedrzik, 2009). These researchers have argued that Kanai's results were more likely to be caused by retinal activation via volume conduction. While this was likely the case in Kanai et al. (2008), a follow-up study by Kanai and colleagues in 2010 reported that thresholds for retinal phosphenes were lowered when TMS was applied

to the visual cortex. This demonstrated the possibility that the visual cortex could play a role in phosphene perception; however, the question remained whether tES applied to the visual cortex could produce the same result. The double dissociation in Chapter 3 showed that a small amount of current delivered over the visual cortex lowered the current required at FPz to produce phosphenes in a similar fashion to Kanai and colleagues 2010 study using TMS. In addition, current density analysis confirmed that the same phosphene phenomenon was produced in the FPz-Oz montage by generating *less* current density in the eyes compared to the FPz-Cz montage. If retinal stimulation alone was sufficient to produce phosphenes, then based on the estimated current density in the eyes, the FPz-Cz montage results should have been indistinguishable from those of the FPz-Oz montage, but this was not the case. Contradicting the commonly held view that "the closer electrodes get to the retina, the stronger the phosphenes are", moving one electrode from the vertex of the scalp (Cz) to the very back of the head (Oz) actually decreased the current required to produce phosphenes.

It should be made clear that this finding does not mean that tES can produce phosphenes solely by stimulating the cortex; rather, tES applied to the visual cortex can facilitate phosphene perception. While the Oz-Cz montage used in Chapter 3 resulted in comparably low current density in the eye compared to other montages (see **Table 3.3**, p. 78), this result cannot be said to demonstrate phosphenes can be induced solely from direct cortical stimulation. Even so, it should be acknowledged that comparatively little current needs to reach the occipital lobe in the FPz-Oz montage to enable this facilitation to occur. At the average phosphene threshold for the FPz-Oz montage, the mean electrical field strength (based on the modelled estimates shown in Chapter 3) in the grey matter within 40mm of Oz (15.9 mV/m), compared to 67.1 mV/m in the Oz-Cz montage at its' own phosphene threshold. For reference, it is estimated that moving into a 4T MRI at 0.5 m/second can generate peak electrical field changes in the body of approximately 1800 mV/m (Liu et al., 2003).

The 15.9 mV/m electric field strength for phosphene detection in the Oz-Cz montage is comparable to the electrical field strength in the same region created by the T3-T4 montage at its' own phosphene threshold (14.4 mV/m). Interestingly, the T3-T4 montage produced phosphenes at lower levels of estimated electric field strength in the eyes (37.5 mV/m) compared to FPz-Cz (75.3 mV/m) or FPz-Oz (54.4 mV/m). It may be the case that current being spread to the occipital cortex via volume conduction may be facilitating phosphene

perception, in the same way that phosphenes can be generated via volume conduction to the retina. This tentative hypothesis would require further validation.

This finding demonstrates that discussions on the effects of tES should consider the univariate fallacy. Multiple studies and commentaries treat the retinal/cortical phosphene source discussion as an either/or matter regarding the retinal and cortical phosphenes (e.g., Kar & Krekelberg, 2012; Schutter & Hortensius, 2010; Schwiedrzik, 2009), overlooking that the brain is an interactive set of networks and modules where no two functions are completely independent. The visual system is no exception; the effects of bottom-up mechanisms from the eyes will interact with the top-down processes of the visual cortex and later functional areas like the inferior temporal cortex (Mechelli et al., 2004; McMains & Kastner, 2011; Zeki, 2015), often making the eyes and the cortex inseparable. Examining the effects of tES should always consider interaction effects across the relevant functional network being manipulated, not just individual nodes within that network.

The counterbalancing of which electrode was the cathode/anode in Chapters 3 and 4 showed stimulation polarity had no effect on phosphene thresholds, nor did the use of either tACS (Chapter 2) or tDCS (Chapters 3 and 4) measurably affect thresholds. This means that the effect of tES was the same whether stimulated cells were subject to relative changes in polarity (i.e., becoming increasingly hyperpolarized or depolarized) or if polarity was reversed (from negative to positive). Neither the retina nor the grey matter of the visual cortex requires a complete reversal of polarity to change activation state; photoreceptors in the retina have a resting potential of -40 mV which hyperpolarizes to -80 mV when activated (Attwell, 1990), while neuronal cell bodies in the occipital grey matter only require a shift from approximately -70 mV to approximately -55 mV to trigger an action potential (Squire et al., 2012). As such, the findings on polarity do not rule out either the retina or the cortex as potential phosphene sources, however, they do indicate that the use of both tACS and tDCS can be effective in producing phosphenes.

5.2.3: REPT Is Effective in Assessing Phosphene Thresholds

Chapter 4 examined the test-retest reliability of REPT and found it to be a reliable algorithm for phosphene perception, with *r* values ranging between .91 and .99 across the 15 combinations of five frequencies and three lighting conditions tested (Frequency * Lighting) using the FPz-Cz montage. Given that significant differences in thresholds were at times less than 50 μA, these *r* values could be improved by using a stimulator with a smaller step-size in current than the 25 μA allowed by the stimulator used in this thesis, allowing greater precision in identifying the approximate threshold.

This finding is of particular value for researchers using tES, TMS or galvanic stimulation to examine sensory thresholds in many fields of study. Most stimulators are not designed to change stimulation parameters quickly or during stimulation, as sudden changes in current density in the body can result in harm. As a result of this, testing times for sensory thresholds using EMF can take a lot longer than other forms of sensory stimulation such as light or sound, as those forms of sensation are generally safer to manipulate quickly even during stimulation. The REPT testing algorithm has demonstrated that it can provide reliable thresholds using a comparatively low number of trials, allowing for a broader range of conditions to be tested on the same sample.

5.3: Limitations and Future Research

The initial study in Chapter 2 used a broad range of frequencies (2 – 30 Hz) that were considered likely to produce phosphenes in mesopic conditions based on the limited literature available; however, given the time required to collect tES phosphene thresholds (even using REPT), only fifteen specific frequencies could be used. The resulting frequency dependent effects in mesopic conditions (including finding the lowest threshold at 16 Hz) had never been reported before, therefore it was important to ensure the finding could be replicated in following studies. After producing the same 16 Hz result under mesopic lighting in three studies, it can now be said with more confidence (and precision) that tES-induced phosphenes in such conditions are more likely to be perceived when stimulation is delivered at *around* 16 Hz. We cannot be certain about the exact frequency value, as frequencies such as 15 Hz or 17 Hz were not tested. If the rod-cone phase delay mechanism is driving this

sensitivity to phosphenes in mesopic conditions, this can be established by testing at a narrower set of frequencies in this range. One option would involve keeping the current applied constant, while using frequency as an independent variable. A drawback to this is that it would require using a subjective measure such as phosphene intensity as a dependent variable, which may prove unreliable when comparing the intensity of phosphenes being delivered anything up to 30 seconds apart. Alternately, the rod-cone phase delay mechanism could also be examined by using mesopic ambient lighting at specific wavelengths of light that only activate rods or cones (e.g., Benimoff et al., 1982; Frumkes et al., 1972) as well as both.

Time limitations for each study meant only three specific levels of luminance could be tested: dark (0 cd/m^2), mesopic (0.6 cd/m^2) and photopic (77.1 cd/m^2). The division between each category is arbitrary; there is no specific value that separates scotopic (dark) from mesopic or a value that separates mesopic from photopic. Nor is there any estimate of how the phosphene frequency sensitivity shifts between these lighting conditions; in other words, it is not known how frequency sensitivity changes *as a function* of luminance. This could be measured by using luminance as the dependent variable, keeping current applied constant, and using frequency as an independent variable.

Advocates for tES phosphenes induced via occipital lobe stimulation (e.g., Kanai et al., 2008) note that stimulation matching alpha- and beta-bands, already linked with dominant EEG frequencies at the occipital lobe during light and dark conditions, produces stronger phosphenes. This observation cannot be extended to phosphenes in mesopic conditions, since there have been no EEG studies that examine how EEG spectral band power changes as ambient lighting gradually shifts between light and dark (and vice-versa). Measuring these luminance-based EEG frequency dynamics and comparing them to phosphene thresholds at those specific frequencies would provide further insight into the nature of cortex-based phosphenes. Similarly, comparing the frequency-luminance interaction of occipital EEG to the results of the frequency-luminance interaction of retinal phosphene perception experiment described in the previous paragraph would provide further insight into the relationship between retinally- and occipitally-induced electrophosphenes.

A recurring issue with EMF research is determining how changes in current density affect the brain and the CNS. This is complicated by the difficulties inherent in measuring changes in a

living, dynamic system; inserting a probe that measures changes in EMF itself causes changes in the electrodynamics of the body, therefore creating a confound that makes obtaining actual changes in current density difficult. Modelling estimates of current density provide a healthy alternative, however, error variance will inevitably increase when 1) there is subject-wise variability in phosphene thresholds across the sample, and 2) the estimation procedure uses different head models compared to the sample. When determining phosphene thresholds in an actual population, the distribution of tissue types throughout the head (and the resulting electroconductivity properties) varies between individuals, resulting in varying distributions of current density from subject to subject. As this distribution will determine the current density at the retina and visual cortex, the distribution of tissues will influence the phosphene thresholds subjects report. If modelling estimates of current density are to accurately reflect the sample, it is ideal that the head models used match the sample as closely as possible. The optimal approach would be to record a T2-weighted MRI image of the test subject's head (ideally without fat suppression; Nielsen et al., 2018), so that the current density resulting from the phosphene thresholds of that individual subject can be modelled on the subject's actual head. An alternative is to use TMS to induce phosphenes where the current density at a particular site can be more accurately calculated, however TMS applied to the retina carries a risk of causing retinal tears and/or vitreous detachment in the eyes (Kung et al., 2011), and the considerably longer testing times required (Epstein, 1998; Hallett, 2007) means that less data can be recorded in a given timeframe (for more information, see *1.3.1: tES, TMS and Galvanic Stimulation*, p. 10).

5.4: Conclusion

Overall, this thesis demonstrated that tES-induced phosphenes in mesopic conditions required considerably less current to be applied for phosphenes to be perceived. Phosphenes in mesopic conditions were most perceivable at 16 Hz, closely aligning with the rod-cone phase delay mechanism in the retina. This frequency sensitivity differed from the previously reported frequency dynamics found in dark and photopic lighting conditions, and each of

these findings was observed regardless of stimulation polarity. While most tES phosphenes appear to have a retinal origin, differences in current applied and modelled current density estimates indicate that tES applied over the visual cortex can make phosphenes more perceptible, contradicting the commonly reported view that cortical tES does not influence phosphene perception. REPT was demonstrated to be a reliable and efficient algorithm for estimating phosphene thresholds, with high test-retest reliability across a wide range of conditions.

LIST OF REFERENCES

Abe, Z. (1951). Influence of adaptation on the strength-frequency curve of human eyes, as determined with electrically produced flickering phosphenes. *The Tohoku Journal of Experimental Medicine*, *54*(1), 37-44. doi:10.1620/tjem.54.37

Abrahamyan, A., Clifford, C. W. G., Ruzzoli, M., Phillips, D., Arabzadeh, E., Harris J. A. (2011). Accurate and rapid estimation of phosphene thresholds (REPT). *PLoS One, 6*, 19554. doi:10.1371/journal.pone.0022342

Achelis, J. D. & Merkulow, J. (1930). Die elektrische Erregbarkeit des menschlichen Auges während der Dunkeladaptation (The electrical excitability of the human eye during dark adaptation.). *Z. Sinnesphysiol., 60*, 95-125.

Acler, M., Bocci, T., Valenti, D., Turri, M., Priori, A. & Bertolasi, L. (2013). Transcranial direct current stimulation (tDCS) for sleep disturbances and fatigue in patients with post-polio syndrome. *Restorative Neurology and Neuroscience, 31*(5), 661-668. doi:10.3233/RNN-130321

Adair, D., Truong, D., Esmaeilpour, Z., Gebodh, N., Borges, H., Ho, L., Bremner, J. D., Badran, B. W., Napadow, V., Clark, V. P. & Bikson, M. (2020). Electrical stimulation of cranial nerves in cognition and disease. *Brain Stimulation, 13(3)*, 717-750. doi:10.1016/j.brs.2020.02.019

Adelson, E. H. (1982). Saturation and adaptation in the rod system. *Vision Research*, *22*(10), 1299-1312. doi:10.1016/0042-6989(82)90143-2

Adey, W. R. (1981). Tissue interactions with nonionizing electromagnetic fields. Physiological Reviews, 61(2), 435-514. doi:10.1152/physrev.1981.61.2.435

Adrian, D. J. (1977). Auditory and visual sensations stimulated by low-frequency electric currents. *Radio Science, 12*(6S), 243-250. doi:10.1029/RS012i06Sp00243

Adrian, E. D. & Matthews, B. H. C. (1934). The Berger rhythm: potential changes from the occipital lobes in man. *Brain, 57*(4) 355–385.

Ahlbom, I. C., Cardis, E., Green, A., Linet, M., Savitz, D., Swerdlow, A. & ICNIRP (International Commission for Non-Ionizing Radiation Protection) Standing Committee on Epidemiology. (2001). *Review of the epidemiologic literature on EMF and Health. Environmental health perspectives, 109*(6), 911-933. doi:10.1289/ehp.109-1240626

Akaike, H. (1973). Theory and an extension of the maximum likelihood principal (*sic*). In: *International Symposium on Information Theory*. Budapest, Hungary: Akademiai Kaiado.

Anderson, A. J. & Johnson, C. A. (2006). Comparison of the ASA, MOBS, and ZEST threshold methods. Vision research, 46(15), 2403-2411. doi:10.1016/j.visres.2006.01.018

Andreuccetti, D., Contessa, G. M., Falsaperla, R., Lodato, R., Pinto, R., Zoppetti, N. & Rossi, P. (2013). Weighted-peak assessment of occupational exposure due to MRI gradient fields and movements in a nonhomogeneous static magnetic field. *Medical Physics, 40*(1), 011910. doi:10.1118/1.4771933

Angelucci, A. (1890). *Untersuchungen über die Sehthätigkeit der Netzhaut und des Gehirns* (Investigations into the visual activity of the retina and the brain). (Vol. 14). E. Roth.

Antal, A. & Paulus, W. (2013). Transcranial alternating current stimulation. *Frontiers in Human Neuroscience, 7*, 317. doi:10.3389/fnhum.2013.00317

Antal, A., Boros, K., Poreisz, C., Chaieb, L., Terney, D. & Paulus, W. (2008). Comparatively weak after-effects of transcranial alternating current stimulation (tACS) on cortical excitability in humans. *Brain Stimulation, 1,* 97–105. doi:10.1016/j.brs.2007.10.001

Antal, A., Kincses, T. Z., Nitsche, M. A. & Paulus, W. (2003). Modulation of moving phosphene thresholds by transcranial direct current stimulation of V1 in human. *Neuropsychologia, 41*(13), 1802-1807. doi:10.1016/S0028-3932(03)00181-7

Antal, A., Kincses, T. Z., Nitsche, M. A., & Paulus, W. (2003). Manipulation of phosphene thresholds by transcranial direct current stimulation in man. *Experimental Brain research*, *150*, 375-378. doi:10.1007/s00221-003-1459-8

Antal, A., Nitsche, M. A., & Paulus, W. (2006). Transcranial direct current stimulation and the visual cortex. *Brain Research Bulletin*, *68*(6), 459-463. doi:10.1016/j.brainresbull.2005.10.006

Antal, A., Varga, E. T., Kincses, T. Z., Nitsche, M. A., & Paulus, W. (2004). Oscillatory brain activity and transcranial direct current stimulation in humans. *Neuroreport*, *15*(8), 1307-1310. doi:10.1097/01.wnr.0000127460.08361.84

Anzai, A., Peng, X. & van Essen, D. C. (2007). Neurons in monkey visual area V2 encode combinations of orientations. *Nature Neuroscience, 10*(10), 1313-1321. doi:10.1038/nn1975

Attwell, D. (1990). The photoreceptor output synapse. *Progress in Retinal Research, 9*, 337-362. doi:10.1016/0278-4327(90)90010-F

Attwell, D. (2003). Interaction of low frequency electric fields with the nervous system: the retina as a model system. *Radiation Protection Dosimetry, 106*(4), 341-348. doi:10.1093/oxfordjournals.rpd.a006370

Baker, J. M., Rorden, C. & Fridriksson, J. (2010). Using transcranial direct-current stimulation to treat stroke patients with aphasia. *Stroke, 41*(6), 1229-1236. doi:10.1161/STROKEAHA.109.576785

Bandeira, I. D., Guimarães, R. S. Q., Jagersbacher, J. G., Barretto, T. L., de Jesus-Silva, J. R., Santos, S. N., Argollo, N. & Lucena, R. (2016). Transcranial direct current stimulation in children and adolescents with attention-deficit/hyperactivity disorder (ADHD) a pilot study. *Journal of Child Neurology, 31*(7), 918-924. doi:10.1177/0883073816630083

Barlow, H. B. (1972). Dark and light adaptation: Psychophysics. In: *Visual Psychophysics* (Vol. 7, pp. 1-28). Springer Berlin.

Barlow, H. B., Kohn, H. I. & Walsh, E. G. (1947). Visual sensations aroused by magnetic fields. *American Journal of Physiology, 148*, 372-375.

Bartley, S. H. (1937). Fusion of flickers of light induced by electrical stimulation of the eye. *Bulletin of experimental biology and medicine URSS, 3*, 303-306.

Beck, J. (1966). Contrast and assimilation in lightness judgments. *Perception & Psychophysics, 1*(5), 342-344.

Benardete, E. A., & Kaplan, E. (1999). The dynamics of primate M retinal ganglion cells. Visual Neuroscience, 16(2), 355-368. doi:10.1017/S0952523899162151

Benardete, E. A., Kaplan, E., & Knight, B. W. (1992). Contrast gain control in the primate retina: P cells are not X-like, some M cells are. *Visual Neuroscience*, *8*(5), 483-486. doi:10.1017/S0952523800004995

Bennabi, D., Carvalho, N., Bisio, A., Teti Mayer, J., Pozzo, T., & Haffen, E. (2020). Influence of Transcranial Direct Current Stimulation on Psychomotor Symptoms in Major Depression. *Brain Sciences, 10*(11), 792. doi:10.3390/brainsci10110792

Berger, H. (1929). Über das Elektrenkephalogramm des Menschen (On the electroencephalogram in humans). *Archiv für Psychiatrie und Nervenkrankheiten, 87*, 527-570.

Blake, E., McMakin, C., Lewis, D. C., Buratovich, N. & Neary Jr, D. E. (2008). Electrotherapy Modalities. In: *Naturopathic Physical Medicine* (pp. 539-562). Churchill Livingstone. doi:10.1016/B978-044310390-2.50017-1

Boayue, N. M., Csifcsák, G., Puonti, O., Thielscher, A. & Mittner, M. (2018). Head models of healthy and depressed adults for simulating the electric fields of non-invasive electric brain stimulation. *F1000 Research, 7*, 704. doi:10.12688/f1000research.15125.2.

Bogolovski, A. I. (1935). Ueber die Abhängigkeit der elektrischen Empfindlichkeit des Auges von den verschiedenen Adaptationsbedingungen (About the dependence of the electrical sensitivity of the eye on the various adaptation conditions). *Albrecht von Graefes Archiv für Ophthalmologie, 133*(1), 105-114.

Bogolovski, A. I., Kravkov, S. V. & Semenovskaia, E. N. (1935). L'Effet de l'excitation lumineuse spéciale préalable de la rétine sur la sensibilité lumineuse et éléctrique suivante de l'oeil (The effect of the prior special light excitation of the retina on the following light and electrical sensitivity of the eye). *Journal of Physiology U. S. S. R., 19*, 814-825.

Bogoslovski A. I. & Segal J. (1947). Analyse de facteurs physiques et physiologiques dans l'excitabilite electrique de l'organe visual (Analysis of physical and physiological factors in the electrical excitability of the visual organ). *Journal of Physiology (Paris), 39*, 101.

Bohotin, V., Fumai, A., Vandenheede, M., Bohotin, C. & Schoenen, J. (2003). Excitability of visual V1-V2 and motor cortices to single transcranial magnetic stimuli in migraine: a reappraisal using a figure-of-eight coil. *Cephalalgia, 23*(4), 264-270. doi:10.1046/j.1468-2982.2003.00475.x

Bosman, C. A., Lansink, C. S., & Pennartz, C. M. (2014). Functions of gamma-band synchronization in cognition: From single circuits to functional diversity across cortical and subcortical systems. *European Journal of Neuroscience*, *39*(11), 1982-1999. doi:10.1111/ejn.12606

Bouman, H. D. (1935). Experiments on the electrical excitability of the eye. *Netherlands Archives of Physiology (Nijhoff), 20*, 430-445.

Bouman, M. A., ten Doesschate, J. & van der Velden, H. A. (1951). Electrical stimulation of the human eye by means of periodical rectangular stimuli. *Documenta Ophthalmologica, 5*(1), 151-168.

Breitling, C., Zaehle, T., Dannhauer, M., Bonath, B., Tegelbeckers, J., Flechtner, H. H. & Krauel, K. (2016). Improving interference control in ADHD patients with transcranial direct current stimulation (tDCS). *Frontiers in Cellular Neuroscience, 10*, 72. doi:10.3389/fncel.2016.00072

Brindley, G. S. (1955). The site of electrical excitation of the human eye. *The Journal of Physiology*, *127*(1), 189. doi:10.1113/jphysiol.1955.sp005248

Brindley, G. S. & Lewin, W. S. (1968) The sensations produced by electrical stimulation of the visual cortex, *Journal of Physiology, 196*, 479–493. doi:10.1113/jphysiol.1968.sp008519

Brindley, G. S. & Rushton, D. N., Observations of the representation of the visual field of the human occipital cortex. In: Hambrecht, F. T., and Reswick, J. B. (eds.), *Functional Electrical Stimulation.* New York: Marcel Decker, 1977, pp. 261–276.

Bringuier, V., Fregnac, Y., Baranyi, A., Debanne, D. & Shulz, D. E. (1997). Synaptic origin and stimulus dependency of neuronal oscillatory activity in the primary visual cortex of the cat. *The Journal of Physiology*, *500*(3), 751-774. doi:10.1113/jphysiol.1997.sp022056

Bringuier, V., Fregnac, Y., Baranyi, A., Debanne, D. & Shulz, D. E. (1997). Synaptic origin and stimulus dependency of neuronal oscillatory activity in the primary visual cortex of the cat. *The Journal of Physiology*, *500*(3), 751-774. doi:10.1113/jphysiol.1997.sp022056

Brittain, J. S., Probert-Smith, P., Aziz, T. Z., & Brown, P. (2013). Tremor suppression by rhythmic transcranial current stimulation. *Current Biology*, *23*(5), 436-440. doi:10.1016/j.cub.2013.01.068

Broca, P. (1861). Remarques sur le siège de la faculté du langage articulé, suite à une observation d'aphémie (perte de la parole) (Remarks on the seat of the faculty of articulated language, following an observation of aphemia (loss of speech)). *Bulletin de la Société Anatomique, 6*, 330-357.

Buetti, S. & Lleras, A. (2023). Vision. In: R. Biswas-Diener & E. Diener (Eds), *Noba Textbook series: Psychology*. Champaign, IL: DEF publishers. Retrieved from http://noba.to/ngkr7ebh

Buzsaki, G. & Draguhn, A. (2004). Neuronal oscillations in cortical networks. *Science*, *304*(5679), 1926-1929. doi:10.1126/science.1099745

Cao, D., Pokorny, J., Smith, V. C., & Zele, A. J. (2008). Rod contributions to color perception: linear with rod contrast. *Vision Research, 48*(26), 2586-2592. doi:10.1016/j.visres.2008.05.001

Casselman, J. W., Kuhweide, R., Deimling, M., Ampe, W., Dehaene, I. & Meeus, L. (1993). Constructive interference in steady state-3DFT MR imaging of the inner ear and cerebellopontine angle. *American Journal of Neuroradiology, 14*(1), 47-57.

Chieffo, R., De Prezzo, S., Houdayer, E., Nuara, A., Di Maggio, G., Coppi, E., Ferrari, L., Straffi, L., Spagnolo, F., Velikova, S., Sessa, M., Comola, M., Zangen, A., Comi, G. & Leocani, L. (2014). Deep repetitive transcranial magnetic stimulation with H-coil on lower limb motor function in chronic stroke: a pilot study. *Archives of Physical Medicine and Rehabilitation, 95*(6), 1141-1147. doi:10.1016/j.apmr.2014.02.019

Christ, A., Kainz, W., Hahn, E. G., Honegger, K., Zefferer, M., Neufeld, E., Rascher, W., Janka, R., Boutz, W., Chen, J. Kiefer, B., Schmitt, P., Hollenbach, H. P., Shen, J., Oberle, M., Szcherba, D., Kam, A., Huag, J. W. & Kuster, N. (2009). The Virtual Family—development of surface-based anatomical models of two adults and two children for dosimetric simulations. *Physics in Medicine & Biology, 55*(2), N23. doi:10.1088/0031-9155/55/2/N01

Clark, V. P., Coffman, B. A., Mayer, A. R., Weisend, M. P., Lane, T. D., Calhoun, V. D., Raybourn, E. M., Garcia, C. M. & Wassermann, E. M. (2012). TDCS guided using fMRI significantly accelerates learning to identify concealed objects. *Neuroimage, 59*(1), 117-128. doi:10.1016/j.neuroimage.2010.11.036

Clausen, J., Urdal, A. & Gjesvik, A. (1954). Relation between the sensitivity for electrical stimuli and adaptation state of the eye. *The Journal of General Psychology, 51*(2), 251-260

Coffman, B. A., Trumbo, M. C., Flores, R. A., Garcia, C. M., van der Merwe, A. J., Wassermann, E. M., Weisend, M. P. & Clark, V. P. (2012). Impact of tDCS on performance and learning of

target detection: interaction with stimulus characteristics and experimental design. *Neuropsychologia, 50*(7), 1594-1602. doi:10.1016/j.neuropsychologia.2012.03.012

Conner, J. D., & MacLeod, D. I. (1977). Rod photoreceptors detect rapid flicker. *Science*, *195*(4279), 698-699. doi:10.1126/science.841308

Cowey, A. & Walsh, V. (2000). Magnetically induced phosphenes in sighted, blind and blindsighted observers. *Neuroreport, 11*(14), 3269-3273.

Crozier, S., Trakic, A., Wang, H. & Liu, F. (2007). Numerical study of currents in workers induced by body-motion around high-ultrahigh field MRI magnets. *Journal of Magnetic Resonance Imaging: An Official Journal of the International Society for Magnetic Resonance in Medicine, 26*(5), 1261-1277. doi:10.1002/jmri.21160

d'Arsonval, A. (1896). *Dispositifs pour la mesure des courants alternatifs de toutes fréquences* (Devices for measuring alternating currents of all frequencies). *Comptes rendus hebdomadaires de la Société de Biologie*, 450–451.

Dai, X., Zhang, H., He, Y., Qi, Y., Chang, B. & Pang, J. (2015). The frequency-response electroretinogram distinguishes cone and abnormal rod function in rd12 mice. *PLoS ONE, 10*(2), e0117570. doi:10.1371/journal.pone.0117570

Dalziel, C. F. (1961) Deleterious Effects of Electric Shock. In: *Meeting of experts on electrical accidents and related matters, World Health Office and International Electrotechnical Commission*. Geneva, Switzerland.

Datta, A., Bansal, V., Diaz, J., Patel, J., Reato, D. & Bikson, M. (2009). Gyri-precise head model of transcranial direct current stimulation: improved spatial focality using a ring electrode versus conventional rectangular pad. *Brain Stimulation, 2*, 201–207. doi:10.1016/j.brs.2009.03.005

Day, B. L., Dressler, D., Maertens de Noordhout, A. C. D. M., Marsden, C. D., Nakashima, K., Rothwell, J. C. & Thompson, P. (1989). Electric and magnetic stimulation of human motor cortex: surface EMG and single motor unit responses. *The Journal of Physiology*, 412(1), 449-473. doi:10.1113/jphysiol.1989.sp017626

de Lange Dzn, H. (1958). Research into the dynamic nature of the human fovea→ cortex systems with intermittent and modulated light. I. Attenuation characteristics with white and colored light. *Journal of the Optical Society of America*, *48*(11), 777-784. doi:10.1364/JOSA.48.000777

Delbeke, J., Oozeer, M. & Veraart, C. (2003). Position, size and luminosity of phosphenes generated by direct optic nerve stimulation. *Vision Research, 43*(9), 1091-1102. doi:10.1016/S0042-6989(03)00013-0

Del Felice, A., Castiglia, L., Formaggio, E., Cattelan, M., Scarpa, B., Manganotti, P., Scarpa, B., Magnanotti, P., Tenconi, E. & Masiero, S. (2019). Personalized transcranial alternating current stimulation (tACS) and physical therapy to treat motor and cognitive symptoms in Parkinson's disease: a randomized cross-over trial. *NeuroImage: Clinical, 22*, 101768. doi:10.1016/j.nicl.2019.101768

Dimbylow, P. (2005). Development of the female voxel phantom, NAOMI, and its application to calculations of induced current densities and electric fields from applied low frequency

magnetic and electric fields. *Physics in Medicine & Biology*, *50*(6), 1047. doi:10.1088/0031-9155/50/6/002

Dimbylow, P. (2006). Development of pregnant female, hybrid voxel-mathematical models and their application to the dosimetry of applied magnetic and electric fields at 50 Hz. *Physics in Medicine & Biology*, *51*(10), 2383. doi:10.1088/0031-9155/51/10/003

Dlugaiczyk, J., Gensberger, K. D. & Straka, H. (2019). Galvanic vestibular stimulation: from basic concepts to clinical applications. *Journal of Neurophysiology, 121*(6), 2237-2255. doi:10.1152/jn.00035.2019

Dobelle, W. H. & Mladejovsky, M. G. (1974). Phosphenes produced by electrical stimulation of human occipital cortex, and their application to the development of a prosthesis for the blind. *The Journal of Physiology, 243*(2), 553-576. doi:10.1113/jphysiol.1974.sp010766

Dowling, J. E. (1960). Chemistry of visual adaptation in the rat. *Nature, 188*, 114-118. doi:10.1038/188114a0

Dowsett, J. & Herrmann, C. S. (2016). Transcranial alternating current stimulation with sawtooth waves: simultaneous stimulation and EEG recording. *Frontiers in Human Neuroscience, 10*, 135. doi:10.3389/fnhum.2016.00135

Du Bois-Reymond, E. H. (1848). *Untersuchungen über thierische Elektricität* (Investigations into animal electricity). Berlin: Reimer.

Ehrenstein, W. H., Ehrenstein, A. (1999). Psychophysical Methods. In: Windhorst, U., Johansson, H. (eds), *Modern Techniques in Neuroscience Research*. Springer, Berlin, Heidelberg. doi:10.1007/978-3-642-58552-4_43

Epstein, C. M. (1998). Transcranial magnetic stimulation: language function. *Journal of Clinical Neurophysiology, 15*(4), 325-332.

Fagerlund, A. J., Hansen, O. A. & Aslaksen, P. M. (2015). Transcranial direct current stimulation as a treatment for patients with fibromyalgia: a randomized controlled trial. *Pain, 156*(1), 62-71. doi:10.1016/j.pain.0000000000000006

Famiglietti Jr, E. V. & Kolb, H. (1976). Structural basis for ON-and OFF-center responses in retinal ganglion cells. Science, 194(4261), 193-195. doi:10.1126/science.959847

Fechner, G. T. (1860) *Elemente der Psychophysik* (Elements of psychophysics). Breitkopf & Härtel, Leipzig.

Fehr, O. (1911). Die Anwendung der Elektrazität in der Augenheilkunde (The application of electricity in ophthalmology). In: *Handbuch der gesamten medizinkchen Anwendung der Elektrazität* (The Manual of the Entire Medical Application of Electricity), Vol. 2 pp. 735-799. Leipzig: Klinkhardt.

Fenton, B. W., Palmieri, P. A., Boggio, P., Fanning, J. & Fregni, F. (2009). A preliminary study of transcranial direct current stimulation for the treatment of refractory chronic pelvic pain. *Brain stimulation, 2*(2), 103-107. doi:10.1016/j.brs.2008.09.009

Fick, A. E. (1892). Entgegnung an E. Hering in Sachen der Netzhauterholung (Reply to E. Hering regarding retinal recovery). *Albrecht von Graefes Archive for Ophthalmology, 38*(4), 300-304.

Fish, R. M. & Geddes, L. A. (2009). Conduction of electrical current to and through the human body: a review. *Eplasty*, 9. PMCID: PMC2763825

Fitzpatrick, R. C. & Day, B. L. (2004). Probing the human vestibular system with galvanic stimulation. *Journal of Applied Physiology, 96*(6), 2301-2316. doi:10.1152/japplphysiol.00008.2004

Fournier, J., Müller, C. M., Schneider, I. & Laurent, G. (2018). Spatial information in a non-retinotopic visual cortex. *Neuron, 97*(1), 164-180. doi:10.1016/j.neuron.2017.11.017

Fregni, F., Boggio, P. S., Lima, M. C., Ferreira, M. J., Wagner, T., Rigonatti, S. P., Castro, A. W., Souza, D. R., Riberto, M., Freedman, S. D., Nitsche, M. A. & Pascual-Leone, A. (2006). A sham-controlled, phase II trial of transcranial direct current stimulation for the treatment of central pain in traumatic spinal cord injury. *Pain, 122(1-2)*, 197-209. doi:10.1016/j.pain.2006.02.023

Fröhlich, F. & McCormick, D. A. (2010). Endogenous electric fields may guide neocortical network activity. *Neuron, 67*(1), 129-143. doi:10.1016/j.neuron.2010.06.005

Gale, A., Coles, M., & Boyd, E. (1971). Variation in visual input and the occipital EEG: II. *Psychonomic Science*, *23*(1), 99-100. doi:10.3758/BF03336026

Gersuni, G. W., Lebedinsky, A. W., Wolochow, A. A. & Zagoruljko, L. T. (1935). Veränderungen der elektrischen Erregbarkeit des Sehapparates während der Dunkeladaptation (Changes in the electrical excitability of the visual apparatus during dark adaptation). *Fiziol. Zuhr S.S.S.R., 19*, 1115-1123

Gescheider, G. A. (2013). *Psychophysics: The Fundamentals*. Psychology Press, New York. doi:10.4324/9780203774458

Goldstein, E. B. (2002). *Sensation and perception* (6th ed.). Pacific Grove, CA: Wadsworth Group.

Goodale, M. A. (2011). Transforming vision into action. *Vision Research, 51*(13), 1567- 1587. doi:10.1016/j.visres.2010.07.027

Grüsser, O. J. & Hagner, M. (1990). On the history of deformation phosphenes and the idea of internal light generated in the eye for the purpose of vision. In: *History of Ophthalmology* (pp. 57-85). Springer, Dordrecht.

Guzman-Lopez, J., Silvanto, J. & Seemungal, B. M. (2011). Visual motion adaptation increases the susceptibility of area V5/MT to phosphene induction by transcranial magnetic stimulation. *Clinical Neurophysiology, 122*(10), 1951-1955. doi:10.1016/j.clinph.2011.03.009

Haldane, J. S. (1933). The physiological significance of Weber's law and colour contrast in vision. *The Journal of Physiology, 79*(2), 121. doi:10.1113/jphysiol.1933.sp003034

Hallett, M. (2007). Transcranial magnetic stimulation: a primer. *Neuron, 55*(2), 187-199. doi:10.1016/j.neuron.2007.06.026

Hallett, M. (2007). Volitional control of movement: the physiology of free will. *Clinical Neurophysiology*, *118*(6), 1179-1192. doi:10.1016/j.clinph.2007.03.019

Han, J., Waddington, G., Adams, R., Anson, J., & Liu, Y. (2016). Assessing proprioception: a critical review of methods. *Journal of Sport and Health Science, 5*(1), 80-90. doi:10.1016/j.jshs.2014.10.004

Harlow, J. M. (1848). Passage of an iron rod through the head. *The Boston Medical and Surgical Journal (1828-1851), 39*(20), 1.

Hashemirad, F., Zoghi, M., Fitzgerald, P. B. & Jaberzadeh, S. (2016). The effect of anodal transcranial direct current stimulation on motor sequence learning in healthy individuals: a systematic review and meta-analysis. *Brain and Cognition, 102*, 1-12. doi:10.1016/j.bandc.2015.11.005

Helfrich, R. F., Schneider, T. R., Rach, S., Trautmann-Lengsfeld, S. A., Engel, A. K. & Herrmann, C. S. (2014). Entrainment of brain oscillations by transcranial alternating current stimulation. *Current Biology, 24*(3), 333-339. doi:10.1016/j.cub.2013.12.041

Herrick, R. M. (1973). Psychophysical methodology: VI. Random method of limits. Perception & Psychophysics, 13(3), 548-554. doi:10.3758/BF03205818

Herring, J. D., Esterer, S., Marshall, T. R., Jensen, O. & Bergmann, T. O. (2019). Low-frequency alternating current stimulation rhythmically suppresses gamma-band oscillations and impairs perceptual performance. *Neuroimage, 184*, 440-449. doi:10.1016/j.neuroimage.2018.09.047

Herrmann, C. S., Fründ, I. & Lenz, D. (2010). Human gamma-band activity: a review on cognitive and behavioral correlates and network models. *Neuroscience & Biobehavioral Reviews*, *34*(7), 981-992. doi:10.1016/j.neubiorev.2009.09.001

Herrmann, C. S., Rach, S., Neuling, T. & Strüber, D. (2013). Transcranial alternating current stimulation: a review of the underlying mechanisms and modulation of cognitive processes. *Frontiers in Human Neuroscience, 7*, 279. doi:10.3389/fnhum.2013.00279

Hood, D. C. & Finkelstein, M. A. (1986). Sensitivity to light. In: *Handbook of Perception and Human Performance (Vol. 1: Sensory Processes and Perception)*. Wiley and Sons, New York.

Hotson, J., Braun, D., Herzberg, W. & Boman, D. (1994). Transcranial magnetic stimulation of extrastriate cortex degrades human motion direction discrimination. *Vision Research, 34*(16), 2115-2123. doi:10.1016/0042-6989(94)90321-2

Hoy, K. E., Bailey, N., Arnold, S., Windsor, K., John, J., Daskalakis, Z. J. & Fitzgerald, P. B. (2015). The effect of γ-tACS on working memory performance in healthy controls. *Brain and Cognition, 101*, 51-56. doi:10.1016/j.bandc.2015.11.002

Institute of Electrical and Electronics Engineers (2019). C95.1: IEEE standard for safety levels with respect to human exposure to electric, magnetic and electromagnetic fields, 0 Hz to 300 GHz. *The Institute of Electrical and Electronics Engineers.* doi:10.1109/IEEESTD.2019.8859679

International Commission on Non-Ionizing Radiation Protection (2010). Guidelines for limiting exposure to time-varying electric and magnetic fields (1 Hz to 100 kHz). *Health Physics, 99*(6), 818-836. doi:10.1097/HP.0b013e3181f06c86

International Commission on Non-Ionizing Radiation Protection. (2014). Guidelines for limiting exposure to electric fields induced by movement of the human body in a static magnetic field and by time-varying magnetic fields below 1 Hz. *Health Physics, 106*(3), 418-425. doi:10.1097/HP.0b013e31829e5580

International Commission on Non-Ionizing Radiation Protection. (2020). Gaps in knowledge relevant to the "Guidelines for limiting exposure to time-varying electric and magnetic fields (1 Hz–100 kHz)". *Health Physics*, *118*(5), 533-542. doi:10.1097/HP.0000000000001261

Jaberzadeh, S., Bastani, A. & Zoghi, M. (2014). Anodal transcranial pulsed current stimulation: a novel technique to enhance corticospinal excitability. *Clinical Neurophysiology, 125*, 344–351. doi: 10.1016/j.clinph.2013.08.025

Jacobson, L., Koslowsky, M. & Lavidor, M. (2012). tDCS polarity effects in motor and cognitive domains: a meta-analytical review. *Experimental Brain Research, 216*(1), 1-10. doi:10.1007/s00221-011-2891-9

Jameson, D., & Hurvich, L. M. (1964). Theory of brightness and color contrast in human vision. *Vision Research, 4*(1-2), 135-154. doi:10.1016/0042-6989(64)90037-9

Jasper, H. H. (1936). Cortical excitatory state and variability in human brain rhythms. *Science*, *83*(2150), 259-260. doi:10.1126/science.83.2150.259

Johnson, C. C., & Guy, A. W. (1972). Nonionizing electromagnetic wave effects in biological materials and systems. Proceedings of the IEEE, 60(6), 692-718. doi:10.1109/PROC.1972.8728

Johnson, K. O., Hsiao, S. S., & Yoshioka, T. (2002). Neural coding and the basic law of psychophysics. *The Neuroscientist, 8*(2), 111-121. doi:10.1177/107385840200800207

Kadosh, R. C., Soskic, S., Iuculano, T., Kanai, R. & Walsh, V. (2010). Modulating neuronal activity produces specific and long-lasting changes in numerical competence. *Current Biology, 20*(22), 2016-2020. doi:10.1016/j.cub.2010.10.007

Kalloniatis, M., & Luu, C. (2007). Visual acuity. In: Kolb, H., Fernandez, E. & Nelson, R. (Eds.) *Webvision: The Organization of the Retina and Visual System*. University of Utah Health Sciences Center, Utah. Bookshelf ID: NBK11509 PMID: 21413375

Kammer, T. (1998). Phosphenes and transient scotomas induced by magnetic stimulation of the occipital lobe: their topographic relationship. *Neuropsychologia*, *37*(2), 191-198. doi:10.1016/S0028-3932(98)00093-1

Kammer, T., & Beck, S. (2002). Phosphene thresholds evoked by transcranial magnetic stimulation are insensitive to short-lasting variations in ambient light. *Experimental Brain Research, 145*, 407-410. doi:10.1007/s00221-002-1160-3

Kammer, T., Beck, S., Erb, M. & Grodd, W. (2001). The influence of current direction on phosphene thresholds evoked by transcranial magnetic stimulation. *Clinical Neurophysiology, 112*(11), 2015-2021. doi:10.1016/S1388-2457(01)00673-3

Kammer, T., Puls, K., Erb, M. & Grodd, W. (2005). Transcranial magnetic stimulation in the visual system. II. Characterization of induced phosphenes and scotomas. *Experimental Brain Research, 160*(1), 129-140. doi:10.1007/s00221-004-1992-0

Kanagasabay, S. (1982). Non-ionizing radiation. In: *Current Approaches to Occupational Health* (pp. 134-168). Butterworth-Heinemann. doi:10.1016/B978-0-7236-0618-5.50013-9

Kanai, R., Chaieb, L., Antal, A., Walsh, V. & Paulus, W. (2008). Frequency-dependent electrical stimulation of the visual cortex. Current Biology, 18(23), 1839-1843. doi:10.1016/j.cub.2008.10.027

Kanai, R., Paulus, W. & Walsh, V. (2010). Transcranial alternating current stimulation (tACS) modulates cortical excitability as assessed by TMS-induced phosphene thresholds. *Clinical Neurophysiology, 121(9)*, 1551–1554. doi:10.1016/j.clinph.2010.03.022

Kaplan, E., & Benardete, E. (2001). The dynamics of primate retinal ganglion cells. *Progress in Brain Research*, *134*, 17-34. doi:10.1016/S0079-6123(01)34003-7

Kar, K. & Krekelberg, B. (2012). Transcranial electrical stimulation over visual cortex evokes phosphenes with a retinal origin. Journal of Neurophysiology 108:2173–2178. doi:10.1152/jn.00505.2012

Karpowicz, J. & Gryz, K. (2013). The pattern of exposure to static magnetic field of nurses involved in activities related to contrast administration into patients diagnosed in 1.5 T MRI scanners. *Electromagnetic Biology and Medicine, 32*(2), 182-191. doi:10.3109/15368378.2013.776428

Keel, J. C., Smith, M. J., & Wassermann, E. M. (2001). A safety screening questionnaire for transcranial magnetic stimulation. *Clinical Neurophysiology*, *112*(4), 720. doi:10.1016/s1388-2457(00)00518-6

Kelly, D. H. (1961). Visual responses to time-dependent stimuli. *Journal of the Optical Society of America*, *51*(4), 422-429. doi:10.1364/JOSA.51.000422

Kelly, D. H. (1977). Visual contrast sensitivity. *Optica Acta: International Journal of Optics, 24*(2), 107-129. doi:10.1080/713819495

Kim, D. (2004). A spiking neuron model for synchronous flashing of fireflies. *Biosystems, 76*(1-3), 7-20. doi:10.1016/j.biosystems.2004.05.035

Kleiner, M., Brainard, D. & Pelli, D. (2007). What's new in Psychtoolbox-3? *Perception (ECVP Abstract Supplement). 36*(14), 1.

Kleiner, M., Brainard, D. & Pelli, D. (2007). What's new in Psychtoolbox-3? *Perception (ECVP Abstract Supplement). 36*(14), 1.

Knighton, R. W. (1975a). An electrically evoked slow potential of the frog's retina, I: Properties of response. Journal of Neurophysiology, 38, 185–197. doi:10.1152/jn.1975.38.1.185

Knighton, R. W. (1975b). An electrically evoked slow potential of the frog's retina, II: Identification with PII component of electroretinogram. Journal of Neurophysiology, 38, 198–209. doi:10.1152/jn.1975.38.1.198

Kohata, T., Komatsu, M. & Motokawa, K. (1956). After-effects of electrical test shocks as a factor affecting retinal color effects. *The Japanese Journal of Physiology, 6*, 236-248.

Kontsevich, L. L. & Tyler, C.W. (1999) Bayesian adaptive estimation of psychometric slope and threshold. *Vision Research, 39*, 2729-2737.

Kung, S., Ahuja, Y., Iezzi, R., & Sampson, S. M. (2011). Posterior vitreous detachment and retinal tear after repetitive transcranial magnetic stimulation. *Brain Stimulation, 4*(4), 218-221. doi:10.1016/j.brs.2011.08.007

Laakso, I., & Hirata, A. (2012). Computational analysis of thresholds for magnetophosphenes. *Physics in Medicine & Biology*, *57*(19), 6147. :10.1088/0031-9155/57/19/6147

Laakso, I. & Hirata, A. (2013). Computational analysis shows why transcranial alternating current stimulation induces retinal phosphenes. *Journal of Neural Engineering, 10*, 046009. doi:10.1088/1741-2560/10/4/046009

Laczó, B., Antal, A., Niebergall, R., Treue, S. & Paulus, W. (2012). Transcranial alternating stimulation in a high gamma frequency range applied over V1 improves contrast perception but does not modulate spatial attention. *Brain Stimulation, 5*(4), 484-491. doi:10.1016/j.brs.2011.08.008

Laine, F. J. & Smoker, W. R. (1998). Anatomy of the cranial nerves. *Neuroimaging Clinics of North America, 8(1)*, 69-100.

Lamb, T. D., & Pugh Jr, E. N. (2004). Dark adaptation and the retinoid cycle of vision. *Progress in Retinal and Eye Research, 23*(3), 307-380. doi:10.1016/j.preteyeres.2004.03.001

Lee, B. B., Pokorny, J., Smith, V. C., & Kremers, J. (1994). Responses to pulses and sinusoids in macaque ganglion cells. *Vision Research*, *34*(23), 3081-3096. doi:10.1016/0042-6989(94)90074-4

Legros, A., Modolo, J., Brown, S., Roberston, J., & Thomas, A. W. (2015). Effects of a 60 Hz magnetic field exposure up to 3000 μT on human brain activation as measured by functional magnetic resonance imaging. *PloS one*, *10*(7), e0132024. doi:10.1371/journal.pone.0132024

Lenggenhager, B., Smith, S. T. & Blanke, O. (2006). Functional and neural mechanisms of embodiment: importance of the vestibular system and the temporal parietal junction. *Reviews in the Neurosciences, 17*(6), 643-657. doi:10.1515/REVNEURO.2006.17.6.643

Lennie, P., Pokorny, J., & Smith, V. C. (1993). Luminance. *Journal of the Optical Society of America, 10*(6), 1283-1293.

LeRoy, C. (1755). Où l'on rend compte de quelques tentatives que l'on a faites pour guérir plusieurs maladies par l'électricité (Where we report on some attempts that have been made to cure several diseases with electricity). *Histoire de l'Academie Royale des Sciences - Mémoires Math et Physics*, 60, 87–95.

Liu, F., Zhao, H. & Crozier, S. (2003). Calculation of electric fields induced by body and head motion in high-field MRI. *Journal of Magnetic Resonance*, *161*(1), 99-107. doi:10.1016/S1090-7807(02)00180-5

Logothetis, N. K., Kayser, C., & Oeltermann, A. (2007). In vivo measurement of cortical impedance spectrum in monkeys: implications for signal propagation. *Neuron*, *55*(5), 809-823. doi:10.1016/j.neuron.2007.07.027

Loo, C. K., Alonzo, A., Martin, D., Mitchell, P. B., Galvez, V. & Sachdev, P. (2012). Transcranial direct current stimulation for depression: 3-week, randomised, sham-controlled trial. *The British Journal of Psychiatry, 200*(1), 52-59. doi:10.1192/bjp.bp.111.097634

Lövsund, P., Öberg, P. Å., & Nilsson, S. E. G. (1979). Quantitative determination of thresholds of magnetophosphenes. *Radio Science*, *14*(6S), 199-200. doi:10.1029/RS014i06Sp00199

Lövsund, P., Öberg, P. Å., Nilsson, S. E. G. & Reuter, T. (1980). Magnetophosphenes: a quantitative analysis of thresholds. *Medical and Biological Engineering and Computing, 18*(3), 326-334. doi:10.1007/BF02443387

MacLeod, D. I. (1972). Rods cancel cones in flicker. *Nature*, *235*(5334), 173-174. doi:10.1038/235173a0

Magnusson, C. E. & Stevens, H. C. (1911). Visual sensations caused by changes in the strength of a magnetic field. *American Journal of Physiology, 29*(2), 124-136. doi:10.1152/ajplegacy.1911.29.2.124

Magnusson, C. E. & Stevens, H. C. (1914). Visual sensations caused by a magnetic field. *The London, Edinburgh, and Dublin Philosophical Magazine and Journal of Science, 28*(164), 188-207. doi:10.1080/14786440808635200

Mann, L. (1911). Elektrodiagnostik der Erkrankungen der Sinnesnerven (Electrodiagnostics of diseases of the sensory nerves). In: *Handbuch der gesamten medizinkchen Anwendung der Elektrazität* (The Manual of the Entire Medical Application of Electricity), Vol. 2 pp. 330-336. Leipzig: Klinkhardt.

Marg, E. & Rudiak, D. (1994). Phosphenes induced by magnetic stimulation over the occipital brain: description and probable site of stimulation. *Optometry and Vision Science: Official Publication of the American Academy of Optometry, 71*(5), 301-311. doi:10.1097/00006324-199405000-00001

Marshall, L., Helgadóttir, H., Mölle, M. & Born, J. (2006). Boosting slow oscillations during sleep potentiates memory. *Nature*, *444*, 610–613. doi: 10.3410/f.1052838.504764

Maxwell, J. C. (1873). A Treatise on Electricity and Magnetism. *Nature, 7*, 478–480. doi:10.1038/007478a0

Mazzi, C., Savazzi, S., Abrahamyan, A. & Ruzzoli, M. (2017). Reliability of TMS phosphene threshold estimation: Toward a standardized protocol. *Brain Stimulation, 10*(3), 609-617. doi:10.1016/j.brs.2017.01.582

Mehta, A.R., Pogosyan, A., Brown, P. & Brittain, J. (2015). Montage matters: the influence of transcranial alternating current stimulation on human physiological tremor. *Brain Stimulation, 8*(2), 260-268. doi:10.1016/j.brs.2014.11.003

Meier-Koll, A. (1973). Elektrostimulation der Netzhaut zur opthalmologischen Differentialdiagnose (Electric stimulation of the retina in ophthalmologic differential diagnosis). Biomedizinische Technik, 18, 92–97. doi:10.1515/bmte.1973.18.3.92

Miklavčič, D., Pavšelj, N. & Hart, F. X. (2006). Electric properties of tissues. In: *Wiley Encyclopedia of Biomedical Engineering*. John Wiley & Sons.

Miller-Keane, O. T. (2005). *Miller-Keane Encyclopedia & Dictionary of Medicine. Nursing & Allied Health-Revised Reprint* (7th edition). Saunders Ed.

Moliadze, V., Antal, A. & Paulus, W. (2010). Electrode-distance dependent after-effects of transcranial direct and random noise stimulation with extracephalic reference electrodes. *Clinical Neurophysiology, 121*, 2165-2171. doi:10.1016/j.clinph.2010.04.033

Monkhouse, S. (2005). *Cranial Nerves: Functional Anatomy*. Cambridge University Press.

Motokawa, K. & Ebe, M. (1952). Selective stimulation of color receptors with alternating currents. *Science, 116*(3004), 92-94.

Motokawa, K. & Iwama, K. (1950). Resonance in electrical stimulation of the eye. *Tohoku Journal of Experimental Medicine, 53*, 201-206. doi:10.1620/tjem.53.201

Motokawa, K. (1949). Visual function and the electrical excitability of the retina. *Tohoku Journal of Experimental Medicine, 51*, 145-153. doi:10.1620/tjem.51.145

Müller, G. E. (1897). Ueber die galvanischen Gesichtsempfindungen (About galvanic facial sensations). *Z. Psychology and Physiology Sinnesorg., 14*, 329-374.

Nagel, W. A. (1904). Einige Beobachtungen über die Wirkung des Druckes und des galvanischen Stromes auf das dunkeladaptierte Auge (Some observations about the effect of pressure and galvanic current on the dark-adapted eye). *Z. Psychology and Physiology Sinnesorg., 34*, 285-290.

Najib, U., Horvath, J. C., Silvanto, J. & Pascual-Leone, A. (2016). State-dependency effects on TMS: a look at motive phosphene behavior. *Journal of Visualized Experiments, 46*, e2273. doi:10.3791/2273

Narayanan, D. L., Saladi, R. N. & Fox, J. L. (2010). Ultraviolet radiation and skin cancer. International Journal of Dermatology, 49(9), 978-986. doi:10.1111/j.1365-4632.2010.04474.x

National Aeronautics and Space Administration (2013, March). The Electromagnetic Spectrum. *Imagine The Universe: Astronomer's Toolbox.* https://imagine.gsfc.nasa.gov/science/toolbox/emspectrum1.html

Neftel, W.B. (1878). Ein Fall von vorübergehender Aphasie mit bleibender medialer Hemiopie des rechten Auges, nebst einem Beitrage zur galvanischen Reaction des optischen Nervenapparates im gesunden und kranken Zustande (A case of temporary aphasia with permanent medial hemiopia of the right eye, together with a contribution to the galvanic reaction of the optical nervous apparatus in healthy and diseased states). *Arch. Psychiat. Nervenkr, 8*, 409-431.

Neuling, T., Wagner, S., Wolters, C. H., Zaehle, T. & Herrmann, C. S. (2012). Finite-element model predicts current density distribution for clinical applications of tDCS and tACS. *Frontiers in Psychiatry, 3*, 83. doi:10.3389/fpsyt.2012.00083

Nitsche M.A. & Paulus, W. (2000) Excitability changes induced in the human motor cortex by weak transcranial direct current stimulation. *Journal of Physiology, 527*(3), 633–639. doi:10.1111/j.1469-7793.2000.t01-1-00633.x

Nitsche, M. A., & Paulus, W. (2001). Sustained excitability elevations induced by transcranial DC motor cortex stimulation in humans. *Neurology*, *57*(10), 1899-1901. doi:10.1212/WNL.57.10.1899

Nitsche, M. A., Schauenburg, A., Lang, N., Liebetanz, D., Exner, C., Paulus, W. & Tergau, F. (2003). Facilitation of implicit motor learning by weak transcranial direct current stimulation of the primary motor cortex in the human. *Journal of Cognitive Neuroscience, 15*(4), 619-626. doi:10.1162/089892903321662994

Omer, H. (2021). Radiobiological effects and medical applications of non-ionizing radiation. *Saudi Journal of Biological Sciences*, 28(10), 5585-5592. doi:10.1016/j.sjbs.2021.05.071

Opitz, A., Paulus, W., Will, S., Antunes, A., & Thielscher, A. (2015). Determinants of the electric field during transcranial direct current stimulation. *Neuroimage, 109*, 140-150. doi:10.1016/j.neuroimage.2015.01.033

O'Shea, J., & Walsh, V. (2007). Transcranial magnetic stimulation. *Current Biology*, *17*(6), 196-199. doi:10.1016/j.cub.2007.01.030

Ouypornkochagorn, T., & Ouypornkochagorn, S. (2019). In vivo estimation of head tissue conductivities using bound constrained optimization. *Annals of Biomedical Engineering*, *47*, 1575-1583. doi:10.1007/s10439-019-02254-9

Palva, S. & Palva, J. M. (2007). New vistas for α-frequency band oscillations. *Trends in Neurosciences, 30*(4), 150-158. doi:/10.1016/j.tins.2007.02.001

Panich, U., Sittithumcharee, G., Rathviboon, N. & Jirawatnotai, S. (2016). Ultraviolet radiation-induced skin aging: the role of DNA damage and oxidative stress in epidermal stem cell damage mediated skin aging. *Stem Cells International*, Article ID 7370642. doi:10.1155/2016/7370642

Paramei, G. V., & van Leeuwen, C. (2016). Color and form perception: Straddling the boundary. *Frontiers in Psychology, 7*, 104. doi.org/10.3389/fpsyg.2016.00104

Pascual-Leone, A., & Walsh, V. (2001). Fast backprojections from the motion to the primary visual area necessary for visual awareness. *Science*, *292*(5516), 510-512. doi:10.1126/science.1057099

Paulus, W. (2010). On the difficulties of separating retinal from cortical origins of phosphenes when using transcranial alternating current stimulation (tACS). *Clinical Neurophysiology, 121*(7), 987–991. doi:10.1016/j.clinph.2010.01.029

Paulus, W. (2011). Transcranial electrical stimulation methods. *Neuropsychological Rehabilitation, 21*, 602–617. doi:10.1080/09602011.2011.557292

Pflüger, E. F. W. (1865). *Untersuchungen aus dem physiologischen Laboratorium zu Bonn* (Investigations from the physiological laboratory in Bonn). Hirschwald.

Polanía, R., Nitsche, M. A., Korman, C., Batsikadze, G. & Paulus, W. (2012). The importance of timing in segregated theta phase-coupling for cognitive performance. *Current Biology, 22*(14), 1314-1318. doi:10.1016/j.cub.2012.05.021

Popper, K. R. (1963). Science as falsification. *Conjectures and refutations, 1*, 33-39.

Purpura, D. P., & McMurtry, J. G. (1965). Intracellular activities and evoked potential changes during polarization of motor cortex. *Journal of Neurophysiology*, *28*(1), 166-185. doi:10.1152/jn.1965.28.1.166

Rauschecker, A. M., Bestmann, S., Walsh, V., & Thilo, K. V. (2004). Phosphene threshold as a function of contrast of external visual stimuli. *Experimental Brain Research, 157*, 124-127. doi:10.1007/s00221-004-1910-5

Rea, P. (2014). *Clinical Anatomy of the Cranial Nerves*. Academic Press, London. doi:10.1016/C2013-0-19192-1

Reato, D., Rahman, A., Bikson, M. & Parra, L. C. (2013). Effects of weak transcranial alternating current stimulation on brain activity—a review of known mechanisms from animal studies. *Frontiers in Human Neuroscience, 7*, 687. doi:10.3389/fnhum.2013.00687

Reilly, J. P. & Hirata, A. (2016). Low-frequency electrical dosimetry: research agenda of the IEEE International Committee on Electromagnetic Safety. *Physics in Medicine & Biology, 61*(12), R138. doi:10.1088/0031-9155/61/12/R138

Reuter, T. (2011). Fifty years of dark adaptation 1961–2011. *Vision Research, 51*(21-22), 2243-2262.

Riecke, L., Formisano, E., Herrmann, C. S. & Sack, A. T. (2015). 4-Hz transcranial alternating current stimulation phase modulates hearing. *Brain Stimulation, 8*(4), 777-783. doi:10.1016/j.brs.2015.04.004

Rohracher, H. (1935). *Ueber subjektive Lichterscheinungen bei Reizung mit Wechselströmen* (On subjective light phenomena in case of irritation with alternating stresses). *Zeitschrift für Sinnesphysiologie, 66*, 164-181.

Ronner, S. F. (1990). Electrical excitation of CNS neurons. In: *Neural Prostheses: Fundamental Studies*. Englewood Cliffs, NJ: Prentice Hall, 170-96.

Rosenkranz, K., Nitsche, M. A., Tergau, F., & Paulus, W. (2000). Diminution of training-induced transient motor cortex plasticity by weak transcranial direct current stimulation in the human. *Neuroscience Letters*, *296*(1), 61-63. doi:10.1016/S0304-3940(00)01621-9

Roth, Y., Amir, A., Levkovitz, Y. & Zangen, A. (2007). Three-dimensional distribution of the electric field induced in the brain by transcranial magnetic stimulation using figure-8 and deep H-coils. *Journal of Clinical Neurophysiology, 24*(1), 31-38. doi:10.1097/WNP.0b013e31802fa393

Rufener, K. S., Zaehle, T., Oechslin, M. S. & Meyer, M. (2016). 40 Hz-Transcranial alternating current stimulation (tACS) selectively modulates speech perception. *International Journal of Psychophysiology, 101*, 18-24. doi:10.1016/j.ijpsycho.2016.01.002

Rushton, W. A. H. (1972). Review lecture. Pigments and signals in colour vision. *The Journal of Physiology, 220*(3), 1P. doi:10.1113/jphysiol.1972.sp009719

Rushton, W. A. H., & Henry, G. H. (1968). Bleaching and regeneration of cone pigments in man. *Vision Research, 8*(6), 617-631. doi:10.1016/0042-6989(68)90040-0

Saebipour, M. R., Joghataei, M. T., Yoonessi, A., Sadeghniiat-Haghighi, K., Khalighinejad, N. & Khademi, S. (2015). Slow oscillating transcranial direct current stimulation during sleep has a sleep-stabilizing effect in chronic insomnia: a pilot study. *Journal of Sleep Research, 24*(5), 518-525. doi:10.1111/jsr.12301

Sagan, C. (1986). *Dragons of Eden: Speculations on the evolution of human intelligence*, pp. 7. Ballantine Books.

Salminen-Vaparanta, N., Vanni, S., Noreika, V., Valiulis, V., Móró, L. & Revonsuo, A. (2014). Subjective characteristics of TMS-induced phosphenes originating in human V1 and V2. *Cerebral Cortex, 24*(10), 2751-2760. doi:10.1093/cercor/bht131

Saturnino, G. B., Puonti, O., Nielsen, J. D., Antonenko, D., Madsen, K. H., & Thielscher, A. (2019). SimNIBS 2.1: a comprehensive pipeline for individualized electric field modelling for transcranial brain stimulation. *Brain and human body modeling: computational human modeling at EMBC 2018*, 3-25. doi:10.1007/978-3-030-21293-3

Saturnino, G. B., Siebner, H. R., Thielscher, A., & Madsen, K. H. (2019). Accessibility of cortical regions to focal TES: Dependence on spatial position, safety, and practical constraints. *NeuroImage*, *203*, 116183. doi:10.1016/j.neuroimage.2019.116183

Saunders, R. D., & Jefferys, J. G. (2007). A neurobiological basis for ELF guidelines. *Health Physics*, *92*(6), 596-603. doi:10.1097/01.HP.0000257856.83294.3e

Schaeffner, L. F., & Welchman, A. E. (2017). Mapping the visual brain areas susceptible to phosphene induction through brain stimulation. *Experimental Brain Research*, *235*(1), 205-217. doi:10.1007/s00221-016-4784-4

Schick, L. L. (1935). Schwelle des galvanischen Phosphenes bei Licht und in der Dunkelheit (Threshold of galvanic phosphenes in light and in the dark). *Journal of Physiology U.S.S.R., 18*, 231-236.

Schlaug, G., Renga, V. & Nair, D. (2008). Transcranial direct current stimulation in stroke recovery. *Archives of Neurology, 65*(12), 1571-1576. doi:10.1001/archneur.65.12.1571

Schmidt, S. L., Iyengar, A. K., Foulser, A. A., Boyle, M. R. & Fröhlich, F. (2014). Endogenous cortical oscillations constrain neuromodulation by weak electric fields. *Brain Stimulation, 7*(6), 878-889. doi:10.1016/j.brs.2014.07.033

Schutter, D. J. (2016). Cutaneous retinal activation and neural entrainment in transcranial alternating current stimulation: a systematic review. *Neuroimage*, *140*, 83-88. doi:10.1016/j.neuroimage.2015.09.067

Schutter, D.J. & Hortensius, R. (2010). Retinal origin of phosphenes to transcranial alternating current stimulation. *Clinical Neurophysiology, 121*, 1080–1084. doi:10.1016/j.clinph.2009.10.038

Schwarz, F. (1940). Quantitative Untersuchungen ueber die optische Wirkung sinusförmiger Wechselströme (Quantitative studies on the optical effect of sinusoidal alternating currents). *Z. Sinnesphysiologie, 69*, 1-26.

Schwiedrzik, C. M. (2009). Retina or visual cortex? The site of phosphene induction by transcranial alternating current stimulation. *Frontiers in Integrative Neuroscience 3*, 6. doi:10.3389/neuro.07.006.2009

Sharpe, L. T., Fach, C., Nordby, K., & Stockman, A. (1989). The incremental threshold of the rod visual system and Weber's law. *Science*, *244*(4902), 354-356. doi:10.1126/science.2711186

Sharpe, L. T., Stockman, A., & MacLeod, D. I. (1989). Rod flicker perception: scotopic duality, phase lags and destructive interference. *Vision Research*, *29*(11), 1539-1559. doi:10.1016/0042-6989(89)90137-5

Shlaer, S. (1937). The relation between visual acuity and illumination. *The Journal of General Physiology, 21*(2), 165-188. doi:10.1085/jgp.21.2.165

Silvanto, J., Cowey, A., Lavie, N., & Walsh, V. (2005). Striate cortex (V1) activity gates awareness of motion. *Nature Neuroscience*, *8*(2), 143-144. doi:10.1038/nn1379

Snyder, D. J., Prescott, J., & Bartoshuk, L. M. (2006). Modern psychophysics and the assessment of human oral sensation. *Taste and Smell, 63*, 221-241. doi:10.1159/000093762

Solomon, J. A., Sperling, G. & Chubb, C. (1993). The lateral inhibition of perceived contrast is indifferent to on-center/off-center segregation, but specific to orientation. Vision research, 33(18), 2671-2683. doi:10.1016/0042-6989(93)90227-N

Souques, M., Plante, M., Ostiguy, G., Goulet, D., Deschamps, F., Mezei, G., Modolo, J., Lambrozo, J. & Legros, A. (2014). Anecdotal report of magnetophosphene perception in 50 mT 20, 50 and 60 Hz magnetic fields. *Radioprotection*, *49*(1), 69-71. doi:10.1051/radiopro/2013088

Squire, L., Berg, D., Bloom, F. E., Du Lac, S., Ghosh, A. & Spitzer, N. C. (Eds.). (2012). *Fundamental Neuroscience*. Academic Press.

Stagg, C. J. (2014). The physiological basis of brain stimulation. In: *The Stimulated Brain*, 145-177. Academic Press. doi:10.1016/B978-0-12-404704-4.00006-5

Stagg, C. J., O'Shea, J., Kincses, Z. T., Woolrich, M., Matthews, P. M. & Johansen-Berg, H. (2009). Modulation of movement-associated cortical activation by transcranial direct current stimulation. *European Journal of Neuroscience, 30*(7), 1412-1423. doi:10.1111/j.1460-9568.2009.06937.x

Stockman, A., & Sharpe, L. T. (2006). Into the twilight zone: the complexities of mesopic vision and luminous efficiency. *Ophthalmic and Physiological Optics*, *26*(3), 225-239. doi:10.1111/j.1475-1313.2006.00325.x

Strüber, D., Rach, S., Trautmann-Lengsfeld, S. A., Engel, A. K. & Herrmann, C. S. (2014). Antiphasic 40 Hz oscillatory current stimulation affects bistable motion perception. *Brain Topography, 27*(1), 158-171. doi:10.1007/s10548-013-0294-x

Survey of the Phosphene Literature (1956). *Acta Psychiatrica Scandinavica, 30*(S94). doi:10.1111/j.1600-0447.1955.tb04280.x

Suzuki, J. I. & Cohen, B. (1964). Head, eye, body and limb movements from semicircular canal nerves. *Experimental Neurology, 10*(5), 393-405. doi:10.1016/0014-4886(64)90031-7

Suzuki, J. I. & Cohen, B. (1966). Integration of semicircular canal activity. *Journal of Neurophysiology, 29*(6), 981-995. doi:10.1152/jn.1966.29.6.981

Taki, M., Suzuki, Y. & Wake, K. (2003). Dosimetry considerations in the head and retina for extremely low frequency electric fields. *Radiation Protection Dosimetry*, *106*(4), 349-356. doi:10.1093/oxfordjournals.rpd.a006371

Thiele, C., Zaehle, T., Haghikia, A., & Ruhnau, P. (2021). Amplitude modulated transcranial alternating current stimulation (AM-TACS) efficacy evaluation via phosphene induction. *Scientific Reports*, *11*(1), 22245. doi:10.1038/s41598-021-01482-1

Thielscher, A., Antunes, A. & Saturnino, G. B. (2015). Field modeling for transcranial magnetic stimulation: A useful tool to understand the physiological effects of TMS? In: *2015 37th annual international conference of the IEEE engineering in medicine and biology society (EMBC)* (pp. 222-225). IEEE. doi:10.1109/EMBC.2015.7318340

Thompson, S.P. (1910). A physiological effect of an alternating magnetic field. *Proceedings of the Royal Society of London. Series B, Containing Papers of a Biological Character, 82*(557), 396-398. doi:10.1098/rspb.1910.0032

Tierney, A. & Kraus, N. (2014). Neural entrainment to the rhythmic structure of music. *Journal of Cognitive Neuroscience, 27*(2), 400-408. doi:10.1162/jocn_a_00704

Treutwein, B. (1995). Adaptive psychophysical procedures. Vision research, 35(17), 2503-2522. doi:10.1016/0042-6989(95)00016-X

Tukahara, S. & Abe, Z. (1951). Resonance phenomena of photopic and scotopic receptors. *Tohoku Journal of Experimental Medicine, 54*(2), 189-196. doi:10.1620/tjem.54.189

Turi, Z., Ambrus, G. G., Janacsek, K., Emmert, K., Hahn, L., Paulus, W., & Antal, A. (2013). Both the cutaneous sensation and phosphene perception are modulated in a frequency-specific manner during transcranial alternating current stimulation. *Restorative Neurology and Neuroscience*, *31*(3), 275-285. doi:10.3233/RNN-120297

Tyrrell, R. A. & Owens, D. A. (1988). A rapid technique to assess the resting states of the eyes and other threshold phenomena: the Modified Binary Search (MOBS). *Behavior Research Methods, Instruments & Computers, 20*, 137-141. doi:10.3758/BF03203817

Umino, Y., Guo, Y., Chen, C. K., Pasquale, R., & Solessio, E. (2019). Rod photoresponse kinetics limit temporal contrast sensitivity in mesopic vision. *Journal of Neuroscience*, *39*(16), 3041-3056. doi:10.1523/JNEUROSCI.1404-18.2019

Valle, A., Roizenblatt, S., Botte, S., Zaghi, S., Riberto, M., Tufik, S., Boggio, P. S. & Fregni, F. (2009). Efficacy of anodal transcranial direct current stimulation (tDCS) for the treatment of fibromyalgia: results of a randomized, sham-controlled longitudinal clinical trial. *Journal of Pain Management, 2*(3), 353. PMCID: PMC3002117

van der Groen, O. & Wenderoth, N. (2016). Transcranial random noise stimulation of visual cortex: stochastic resonance enhances central mechanisms of perception. *Journal of Neuroscience, 36*(19), 5289-5298. doi:10.1523/JNEUROSCI.4519-15.2016

Violante, I. R., Li, L. M., Carmichael, D. W., Lorenz, R., Leech, R., Hampshire, A., Rothwell, J. C. & Sharp, D. J. (2017). Externally induced frontoparietal synchronization modulates network dynamics and enhances working memory performance. *eLife, 6*, e22001. doi:10.7554/eLife.22001

von Helmholtz, H. & Southall, J. P. C. (1924). *Physiological Optics* (English edition, Vol. 2). Wisconsin: Optical Society of America.

Vossen, A., Gross, J. & Thut, G. (2015). Alpha power increase after transcranial alternating current stimulation at alpha frequency (α-tACS) reflects plastic changes rather than entrainment. *Brain Stimulation, 8*(3), 499-508. doi:10.1016/j.brs.2014.12.004

Wagner, A., Zahn, M., Grodzinsky, A. J. & Pascual-Leone, A. (2004). Three-dimensional head model Simulation of transcranial magnetic stimulation. *IEEE Transactions on Biomedical Engineering, 51*(9), 1586-1598.

Wagner, S., Rampersad, S., Oostendorp, T. F., Aydin, Ü., Vorwerk, J., Neuling, T., Hermann, C.S., Stegeman, D.F. & Wolters, C. H. (2012). Investigation of tDCS/tACS volume conduction effects in a highly realistic head model. *Journal of Neural Engineering, 11*(1), 016002. doi:10.1088/1741-2560/11/1/016002

Walz, D. (Ed.). (1995). *Bioelectrochemistry of Cells and Tissues (Vol. 2)*. Springer Science & Business Media.

Watson, A. B. & Pelli, D. G. (1983). QUEST: A Bayesian adaptive psychometric method. Perception & Psychophysics, 33(2), 113-120. doi:10.3758/BF03202828

Wood, A. W. (2008). Extremely low frequency (ELF) electric and magnetic field exposure limits: rationale for basic restrictions used in the development of an Australian standard. *Bioelectromagnetics: Journal of the Bioelectromagnetics Society, The Society for Physical Regulation in Biology and Medicine, The European Bioelectromagnetics Association*, *29*(6), 414-428. doi:10.1002/bem.20412

Woods, A. J., Antal, A., Bikson, M., Boggio, P. S., Brunoni, A. R., Celnik, P., Cohen, L. G., Fregni, F., Herrmann, C. S., Kappenman, E. S., Knotkova, H., Liebetanz, D., Miniussi, C., Miranda, P. C., Paulus, W., Priori, A., Stagg, C., Wenderoth, N. & Nitsche, M. A. (2016). A technical guide to tDCS, and related non-invasive brain stimulation tools. Clinical neurophysiology, 127(2), 1031-1048. doi:10.1016/j.clinph.2015.11.012

World Health Organization (2017). *Extremely Low Frequency Fields*. Geneva, Switzerland: WHO Press. Available from https://apps.who.int/iris/rest/bitstreams/51837/retrieve

Wright, W., Sayce, A. H. & Rylands, W. H. (1886). *The Empire of the Hittites*, pp. 59. James Nisbet & Company.

APPENDIX A

Adaptation of tES safety protocol from Keel et al. (2008) conducted via phone interview.

Hello, this is Ian Evans from the University of Wollongong returning your call about the transcranial stimulation study. Is this a good time for you to discuss it? (*If Yes, then proceed. If No, then schedule another time to call.)*

Good, well I'll start by giving you some details about the study. If you have any questions, feel free to ask them at any time. First, a little background: You may have noticed sometimes when you close your eyes you can still see some blobs of light, especially after you've been looking at a light. These are called phosphenes, and they can also be induced by very mild electromagnetic fields. This study is trying to determine the smallest strength of electromagnetic field required to generate a phosphene.

To do this, we use a technique known as transcranial alternating current stimulation. This involves attaching a sponge to either the forehead or the back of the scalp over the visual processing area of the brain, and applying a brief, mild electrical current at varying strengths until you see a phosphene. We will do this for five different frequencies of stimulation to test whether the threshold is affected by the frequency of stimulation. The entire study is expected to take two hours split into sessions of a little under one hour each, with a break in between. We can do this on separate days if it fits in with your schedule. To compensate for your time, you will receive either two credit points for the SONA program or a $30 gift voucher. All data collected will be anonymised, so there will be no way to identify you from the results. Do you wish to participate in the study?

(If Yes, then proceed. If No, "That's fine, thanks for your interest. Goodbye." and terminate the call.)

Very good. Now before enrolling you in this study, I need to determine if you are eligible to participate. I'm just going to ask a few questions in order to make sure there are no safety concerns. The questions focus on your vision and any history of head injury. If you do not wish to disclose any information, feel free to decline to answer the question. Are you happy to proceed?

(If Yes, then proceed. If No, "That's fine, thanks for your interest. Goodbye." and terminate the call.)

Okay then. First of all, have you ever had an adverse reaction to any type of brain scan or stimulation? (*If Yes, the subject is ineligible. Continue with the questions.)*

Do you have normal or corrected vision? (such as glasses or contact lenses)? *(If No, the subject is ineligible. Continue with the questions.)*

Have you ever had a seizure? *(If Yes, inquire about the nature of the seizure. If the condition is serious, recurring or recent (i.e. within the previous year), the subject is ineligible. If the subject does not wish to discuss it, proceed to the next question and the subject is ineligible.)*

Have you ever had a stroke? (*If Yes, the subject is ineligible. Continue with the questions.)*

Have you ever had a head injury (include neurosurgery)? *(If Yes, continue. This question is here to prompt any memory of metal or other medical implants relating to the next question)*

Do you have any metal in your head (outside of the mouth), such as shrapnel, surgical clips, or fragments from welding or metalwork? (*If Yes, the subject is ineligible. Continue with the questions.)*

Do you have any implanted devices such as cardiac pacemakers, medical pumps, or intracardiac lines? (*If Yes, the subject is ineligible. Continue with the questions.)*

Do you suffer from frequent or severe headaches? *(If Yes, inquire about the nature of the headaches. If the condition is serious, recurring or recent (i.e. within the previous year), the subject is ineligible. If the subject does not wish to discuss it, proceed to the next question and the subject is ineligible.)*

Have you ever had any other brain-related condition? *(If Yes, inquire about the nature of the condition. If the condition is serious, recurring or recent (i.e. within the previous year), the subject is ineligible. If the subject does not wish to discuss it, proceed to the next question and the subject is ineligible.)*

Have you ever had any illness that caused brain injury? *(If Yes, inquire about the nature of the condition. If the condition is serious, recurring or recent (i.e. within the previous year), the subject is ineligible. If the subject does not wish to discuss it, proceed to the next question and the subject is ineligible.)*

Are you taking any medications? *(If Yes, ask if the medication is psychoactive and clearly say "Please just answer Yes or No". If Yes, the subject is eligible to participate but this should be noted in the dataset as a possible confound).*

Do you need further explanation of transcranial alternating current stimulation?

If the subject is eligible:

Right, well based on your answers, you are eligible to participate in the study. Would you like to take part? *(If Yes, then proceed. If No, "That's fine, thanks for your interest. Goodbye." and terminate the call.)*

Would you like to schedule a time to take part in the experiment? (*If Yes, schedule an appointment and make sure they know how to get to the laboratory. Give directions as necessary, and advise them about parking arrangements for subjects. If No, set up a time to call back and schedule an appointment).*

In addition, would you like me to send you information about the study? (*If Yes, ask for their email address and send them the Subject Information Sheet.)*

Right, well thank you for your time, and I'll see you on (*day of experiment*). Goodbye.

If the subject is ineligible:
Right, well based on your answers, I'm afraid you are not eligible to participate in the study. (*Explain why the contraindications are an issue. Apologise for troubling them, and terminate the call*).

APPENDIX B

Table A.1: Individual subject thresholds (in µA) for each montage and frequency from Experiment One (Chapter 2)

FPz-Cz Montage

ID	2	4	6	8	10	12	14	16	18	20	22	24	26	28	30
1	1500	1325	1025	550	275	200	150	150	175	225	350	375	475	750	725
2	650	575	225	200	125	75	100	50	125	75	75	175	175	225	275
3	1125	575	375	175	125	150	75	75	75	100	175	200	250	525	575
4	1500	475	375	375	250	150	125	175	125	200	150	150	300	225	300
5	1500	725	575	425	250	225	175	150	150	150	175	250	325	450	550
6	800	650	500	375	250	200	150	125	100	100	150	200	275	375	500
7	1500	1275	675	375	200	200	225	150	175	150	200	200	300	275	425
8	1500	850	375	225	150	150	75	100	75	100	150	125	150	225	225
9	1500	1500	1100	500	500	275	175	125	100	200	250	300	475	575	700
10	1200	850	525	300	200	175	100	100	125	100	150	200	225	400	400
11	1500	1500	1500	750	500	475	200	200	125	300	350	400	475	700	700
12	1500	1500	925	525	250	150	125	100	125	125	150	150	200	250	300
13	1250	900	550	375	200	175	125	75	75	50	75	125	125	150	125
14	1500	1500	1500	475	350	150	125	50	50	75	100	175	225	300	150
15	1500	900	575	400	225	125	125	75	125	175	175	300	325	575	575
16	1500	1500	700	625	225	200	150	125	175	100	100	225	275	325	400
17	1500	1075	500	300	275	175	100	125	100	125	125	125	200	300	425
18	1475	850	625	375	325	125	125	125	150	225	125	275	425	300	350
19	1500	1000	650	275	200	200	175	225	250	275	300	325	425	525	475
20	1500	1500	850	675	525	500	325	100	200	175	325	375	500	650	825
21	1500	1175	750	450	325	200	200	150	100	125	200	200	325	375	350
22	1500	900	375	375	300	175	200	150	225	250	250	300	400	450	575
23	1500	1500	1500	425	300	325	150	100	100	125	200	225	275	375	575
24	1500	600	300	300	175	150	125	125	100	125	150	175	350	425	450

Oz-Cz Montage

ID	2	4	6	8	10	12	14	16	18	20	22	24	26	28	30
1	1500	1500	1500	1025	800	825	600	450	600	1000	1200	1475	1500	1500	1500
2	1500	1500	1500	950	850	575	400	325	425	525	725	750	1500	1500	1500
3	1500	1500	1200	1000	475	400	225	175	150	575	775	1200	1350	1500	1500
4	1500	1500	1500	1500	900	600	400	400	350	600	725	650	1175	1375	1350
5	1500	1500	1500	1400	875	700	600	525	550	650	825	1150	1450	1500	1500
6	1500	1500	1450	1125	775	600	475	375	400	700	900	1175	1475	1500	1500
7	1500	1500	1500	1250	750	525	375	225	375	400	425	575	500	700	825
8	1500	1500	1275	725	375	350	250	275	200	200	400	400	725	825	900
9	1500	1500	1500	1500	1100	925	775	550	675	1075	1475	1400	1500	1500	1500
10	1500	1500	1500	1125	1200	925	675	675	625	800	1025	1425	1500	1500	1500
11	1500	1500	1500	1375	800	650	600	275	375	400	425	1050	1500	1500	1500
12	1500	1500	1150	775	600	425	325	200	175	200	225	400	475	750	900
13	1500	1500	1500	1025	450	400	400	250	250	200	375	425	675	900	900
14	1500	1500	1500	1500	975	450	350	175	275	600	850	1300	1500	1500	1500
15	1500	1500	1500	950	650	450	450	250	550	850	875	1175	1500	1500	1500
16	1500	1500	1500	1200	1050	700	600	475	325	575	700	925	1500	1500	1500
17	1500	1500	1500	1500	500	400	300	325	150	550	800	900	1225	1050	1450
18	1500	1500	1500	1275	675	350	350	250	200	275	500	700	775	950	950
19	1500	1500	925	700	675	625	650	750	750	1100	1275	1500	1500	1500	1500
20	1500	1500	1500	1500	850	725	575	475	475	550	700	700	1100	1425	1500
21	1500	1500	1500	1500	1075	650	425	250	250	550	675	1050	1325	1500	1500
22	1500	1400	925	800	600	400	375	400	400	450	750	725	775	850	1000
23	1500	1500	1500	1500	775	800	475	300	400	375	400	550	825	900	1500
24	1500	1500	1500	950	575	575	425	200	375	400	525	650	850	1500	1500

APPENDIX C

Table A.2: Individual subject thresholds (in μA) for each montage and frequency from Experiment Two (Chapter 3)

	FPz-Cz Montage							Oz-Cz Montage						
ID	**6**	**10**	**16**	**20**	**24**	**28**	**32**	**6**	**10**	**16**	**20**	**24**	**28**	**32**
1	975	300	100	250	450	675	975	1500	700	525	925	1500	1500	1500
2	225	100	75	125	250	300	475	1500	800	250	475	775	1400	1500
3	550	250	150	175	250	425	625	1500	875	525	625	1175	1500	1500
4	500	250	125	125	200	375	550	1500	775	400	700	1150	1500	1500
5	650	200	175	200	250	375	900	1500	700	325	475	650	800	1500
6	375	150	75	100	100	275	275	1250	475	275	300	525	950	1500
7	1075	600	175	200	350	675	900	1500	1175	525	1125	1425	1500	1500
8	575	200	150	175	250	500	600	1500	1100	600	750	1325	1500	1500
9	1475	500	200	300	400	700	875	1500	800	275	400	1050	1500	1500
10	900	225	100	75	150	200	300	1175	550	200	200	425	750	1500
11	550	250	100	75	125	225	175	1500	550	325	325	550	1000	1500
12	1500	275	100	175	200	400	350	1500	900	250	700	1350	1500	1500
13	575	300	100	275	350	675	550	1500	725	250	825	1200	1500	1500
14	675	225	75	100	125	275	200	1500	975	450	500	825	1500	1500
15	600	225	100	125	275	400	650	1500	625	200	225	600	950	1500
16	800	425	125	175	275	550	675	1500	925	450	550	800	1500	1500
17	850	425	175	225	275	475	425	1500	1150	325	675	1175	1500	1500
18	325	225	200	200	250	425	800	1500	550	275	500	725	1500	1500
19	400	175	125	150	425	575	500	1500	1100	575	1150	1500	1500	1500
20	875	525	200	175	275	700	700	1500	875	475	750	1400	1500	1500
21	550	250	150	175	250	400	600	1500	850	500	650	1125	1500	1500
22	500	225	100	125	200	350	525	1500	750	400	650	1075	1450	1500
	FPz-Oz Montage							**T3-T4 Montage**						
ID	**6**	**10**	**16**	**20**	**24**	**28**	**32**	**6**	**10**	**16**	**20**	**24**	**28**	**32**
1	750	125	175	175	325	800	825	1475	375	200	350	1050	1375	1500
2	200	125	25	25	100	150	325	1150	450	225	175	350	575	925
3	500	200	100	125	175	350	575	1300	550	275	300	350	550	850
4	450	175	75	100	150	275	425	1250	525	250	300	350	525	800
5	200	125	75	125	125	200	300	1050	250	175	150	200	475	600
6	550	175	50	75	125	200	250	1400	425	225	325	475	725	1250
7	1100	300	100	150	250	650	700	1500	775	150	450	925	1450	1500
8	600	325	225	275	575	750	775	1475	525	275	525	775	1475	1500
9	425	100	50	100	125	250	400	1125	200	175	100	100	400	775
10	750	225	50	50	75	75	125	1125	325	100	100	175	275	450
11	500	125	75	100	125	150	150	900	425	125	100	200	425	1200
12	825	325	75	100	200	300	250	1500	500	375	700	850	1300	1500
13	625	250	100	175	275	500	375	1150	225	150	200	475	1000	900
14	500	150	50	75	125	250	200	1325	500	150	200	275	575	875
15	525	100	50	125	175	300	425	1150	200	175	100	100	400	775
16	450	200	100	125	175	300	575	1425	550	200	200	350	650	1050
17	825	225	75	75	150	275	275	1500	475	150	250	300	1000	1000
18	275	150	125	175	275	500	550	900	475	325	400	575	900	1225
19	275	175	50	175	300	425	525	1500	300	150	275	475	1125	1500
20	550	300	125	100	125	350	475	1450	600	200	300	500	750	1325
21	500	200	100	125	175	325	550	1250	550	250	300	350	550	825
22	450	175	75	100	150	250	400	1200	525	225	300	350	525	775

APPENDIX D

MATLAB code used to create current density modelling (see Chapter 3), then extract current density in the eyes and all grey matter within 40mm of that individual head model's location on the scalp for Oz.

```
% Preload Oz coordinates as matrix "OZ" from F:/Nibs/B_Oz.xlsx
% Comment in/out ERNIE lines as necessary

for subj = 1:19 % Remove leading zeros where needed
   if subj < 10
     sLead = ['0' num2str(subj)];
   else
     sLead = num2str(subj);
   end

s = sim_struct('SESSION');
% Name of head mesh
s.fnamehead = ['F:/Nibs/s' num2str(subj) '/sub-control' sLead '.msh'];
s.pathfem = ['F:/Nibs/s' num2str(subj) '/0/']; % Output folder
s.fields = 'eEjJ';

% FPz-Cz montage
s.poslist{1} = sim_struct('TDCSLIST');

% Set current (mA) at [cathode, anode] - must sum to zero
s.poslist{1}.currents = [-0.1307, 0.1307];
% Cathode details
s.poslist{1}.electrode(1).channelnr = 1;
s.poslist{1}.electrode(1).dimensions = [40, 30]; % In mm
% Electrode Shape
s.poslist{1}.electrode(1).shape = 'rect';
% Thickness in mm; [depth of saline/sponge, rubber electrode]
s.poslist{1}.electrode(1).thickness = [4, 1];
s.poslist{1}.electrode(1).centre = 'Fpz'; % Electrode position
s.poslist{1}.electrode(1).pos_ydir = 'Cz'; % Electrode orientation
% Anode details
s.poslist{1}.electrode(2).channelnr = 2;
s.poslist{1}.electrode(2).dimensions = [40, 30]; % In mm
s.poslist{1}.electrode(2).shape = 'rect';
s.poslist{1}.electrode(2).thickness = [4, 1]; % In mm
s.poslist{1}.electrode(2).centre = 'Cz';
s.poslist{1}.electrode(2).pos_ydir = 'Fpz';

% FPz-Oz montage
s.poslist{2} = sim_struct('TDCSLIST');
s.poslist{2}.currents = [-0.0875, 0.0875];
s.poslist{2}.electrode(1).channelnr = 1;
s.poslist{2}.electrode(1).dimensions = [40, 30];
s.poslist{2}.electrode(1).shape = 'rect';
s.poslist{2}.electrode(1).thickness = [4, 1];
s.poslist{2}.electrode(1).centre = 'Fpz';
s.poslist{2}.electrode(1).pos_ydir = 'Cz';
s.poslist{2}.electrode(2).channelnr = 2;
s.poslist{2}.electrode(2).dimensions = [40, 30];
s.poslist{2}.electrode(2).shape = 'rect';
s.poslist{2}.electrode(2).thickness = [4, 1];
```

```
s.poslist{2}.electrode(2).centre = 'Oz';
s.poslist{2}.electrode(2).pos_ydir = 'Cz';

% Oz-Cz montage
s.poslist{3} = sim_struct('TDCSLIST');
s.poslist{3}.currents = [-0.3807, 0.3807];
s.poslist{3}.electrode(1).channelnr = 1;
s.poslist{3}.electrode(1).dimensions = [40, 30];
s.poslist{3}.electrode(1).shape = 'rect';
s.poslist{3}.electrode(1).thickness = [4, 1];
s.poslist{3}.electrode(1).centre = 'Oz';
s.poslist{3}.electrode(1).pos_ydir = 'Cz';
s.poslist{3}.electrode(2).channelnr = 2;
s.poslist{3}.electrode(2).dimensions = [40, 30];
s.poslist{3}.electrode(2).shape = 'rect';
s.poslist{3}.electrode(2).thickness = [4, 1];
s.poslist{3}.electrode(2).centre = 'Cz';
s.poslist{3}.electrode(2).pos_ydir = 'Oz';

% T3-T4 montage (called T7/8)
s.poslist{4} = sim_struct('TDCSLIST');
s.poslist{4}.currents = [-0.2057, 0.2057];
s.poslist{4}.electrode(1).channelnr = 1;
s.poslist{4}.electrode(1).dimensions = [40, 30];
s.poslist{4}.electrode(1).shape = 'rect';
s.poslist{4}.electrode(1).thickness = [4, 1];
s.poslist{4}.electrode(1).centre = 'T7';
s.poslist{4}.electrode(1).pos_ydir = 'Cz';
s.poslist{4}.electrode(2).channelnr = 2;
s.poslist{4}.electrode(2).dimensions = [40, 30];
s.poslist{4}.electrode(2).shape = 'rect';
s.poslist{4}.electrode(2).thickness = [4, 1];
s.poslist{4}.electrode(2).centre = 'T8';
s.poslist{4}.electrode(2).pos_ydir = 'Cz';

% Run simulation
run_simnibs(s)
end

% Process simulation, select tissue type and extract descriptives
for subj = 1:19
   if subj < 10 % Remove leading zeros if necessary
     sLead = ['0' num2str(subj)];
   else
     sLead = num2str(subj);
   end

% Read the simulation results for grey matter, remove leading zero if
necessary
 if subj < 10
  head_mesh = mesh_load_gmsh4(['F:\Nibs\s' num2str(subj) '\90500\sub-
control0' num2str(subj) '_TDCS_1_scalar.msh']);
 else
  head_mesh = mesh_load_gmsh4(['F:\Nibs\s' num2str(subj) '\90500\sub-
control' num2str(subj) '_TDCS_1_scalar.msh']);
 end
%head_mesh = mesh_load_gmsh4('F:\Nibs\Ernie\7\ernie_TDCS_1_scalar.msh');
% Select appropriate tissue type; 2 for Ernie & Boayue
gray_matter = mesh_extract_regions(head_mesh, 'region_idx', 2);
% Define the ROI
%coords = [-4.2, -119, 20.2]; Oz for ERNIE - if Boayue dataset, use below
```

```
coords = OZ(subj,:);
r = 40; % Sphere radius in mm
elm_centers = mesh_get_tetrahedron_centers(gray_matter);
roi = sqrt(sum(bsxfun(@minus, elm_centers, coords).^2, 2)) < r;
elm_vols = mesh_get_tetrahedron_sizes(gray_matter);
field_name = 'normJ'; % normE for V/m, normJ for mA/m^2
field_idx = get_field_idx(gray_matter, field_name, 'elements');
field = gray_matter.element_data{field_idx}.tetdata;
% Selects points within the ROI and removes all others
VconA=roi.*field;
toss=nonzeros(VconA); % Removes grey matter voxels outside the sphere
% Extract descriptives
ValOut(subj,1) = mean(toss);
ValOut(subj,2) = median(toss);
ValOut(subj,3) = max(toss);
ValOut(subj,4) = min(toss);
ValOut(subj,5) = std(toss);
ValOut(subj,6) = (std(toss))/sqrt(length(toss));

 if subj < 10
  head_mesh = mesh_load_gmsh4(['F:\Nibs\s' num2str(subj) '\90500\sub-
control0' num2str(subj) '_TDCS_2_scalar.msh']);
 else
  head_mesh = mesh_load_gmsh4(['F:\Nibs\s' num2str(subj) '\90500\sub-
control' num2str(subj) '_TDCS_2_scalar.msh']);
 end
%head_mesh = mesh_load_gmsh4('F:\Nibs\Ernie\7\ernie_TDCS_2_scalar.msh');
gray_matter = mesh_extract_regions(head_mesh, 'region_idx', 2);
elm_centers = mesh_get_tetrahedron_centers(gray_matter);
roi = sqrt(sum(bsxfun(@minus, elm_centers, coords).^2, 2)) < r;
elm_vols = mesh_get_tetrahedron_sizes(gray_matter);
field_name = 'normJ';
field_idx = get_field_idx(gray_matter, field_name, 'elements');
field = gray_matter.element_data{field_idx}.tetdata;
VconA=roi.*field;
toss=nonzeros(VconA);
ValOut(subj,7) = mean(toss);
ValOut(subj,8) = median(toss);
ValOut(subj,9) = max(toss);
ValOut(subj,10) = min(toss);
ValOut(subj,11) = std(toss);
ValOut(subj,12) = (std(toss))/sqrt(length(toss));

 if subj < 10
  head_mesh = mesh_load_gmsh4(['F:\Nibs\s' num2str(subj) '\90500\sub-
control0' num2str(subj) '_TDCS_3_scalar.msh']);
 else
  head_mesh = mesh_load_gmsh4(['F:\Nibs\s' num2str(subj) '\90500\sub-
control' num2str(subj) '_TDCS_3_scalar.msh']);
 end
%head_mesh = mesh_load_gmsh4('F:\Nibs\Ernie\7\ernie_TDCS_3_scalar.msh');
gray_matter = mesh_extract_regions(head_mesh, 'region_idx', 2);
elm_centers = mesh_get_tetrahedron_centers(gray_matter);
roi = sqrt(sum(bsxfun(@minus, elm_centers, coords).^2, 2)) < r;
elm_vols = mesh_get_tetrahedron_sizes(gray_matter);
field_name = 'normJ';
field_idx = get_field_idx(gray_matter, field_name, 'elements');
field = gray_matter.element_data{field_idx}.tetdata;
VconA=roi.*field;
toss=nonzeros(VconA);
ValOut(subj,13) = mean(toss);
```

```
ValOut(subj,14) = median(toss);
ValOut(subj,15) = max(toss);
ValOut(subj,16) = min(toss);
ValOut(subj,17) = std(toss);
ValOut(subj,18) = (std(toss))/sqrt(length(toss));

 if subj < 10
  head_mesh = mesh_load_gmsh4(['F:\Nibs\s' num2str(subj) '\90500\sub-
control0' num2str(subj) '_TDCS_4_scalar.msh']);
 else
  head_mesh = mesh_load_gmsh4(['F:\Nibs\s' num2str(subj) '\90500\sub-
control' num2str(subj) '_TDCS_4_scalar.msh']);
 end
%head_mesh = mesh_load_gmsh4('F:\Nibs\Ernie\7\ernie_TDCS_4_scalar.msh');
gray_matter = mesh_extract_regions(head_mesh, 'region_idx', 2);
elm_centers = mesh_get_tetrahedron_centers(gray_matter);
roi = sqrt(sum(bsxfun(@minus, elm_centers, coords).^2, 2)) < r;
elm_vols = mesh_get_tetrahedron_sizes(gray_matter);
field_name = 'normJ';
field_idx = get_field_idx(gray_matter, field_name, 'elements');
field = gray_matter.element_data{field_idx}.tetdata;
VconA=roi.*field;
toss=nonzeros(VconA);
ValOut(subj,19) = mean(toss);
ValOut(subj,20) = median(toss);
ValOut(subj,21) = max(toss);
ValOut(subj,22) = min(toss);
ValOut(subj,23) = std(toss);
ValOut(subj,24) = (std(toss))/sqrt(length(toss));

end


% Read the simulation results for eyes

reg = 6; % Region Eyes = 6 for Ernie, 8 for Boayue
pow = 0; % Directory name - usually amperage, 0 for thresholds

% Remove leading zero if necessary
for subj = 1:19
   if subj < 10
     sLead = ['0' num2str(subj)];
   else
     sLead = num2str(subj);
   end

faff = ['F:\Nibs\s' num2str(subj) '\' num2str(pow) '\90500\sub-control'
sLead '_TDCS_1_scalar.msh'];
%faff = ['F:\Nibs\Ernie\7\ernie_TDCS_1_scalar.msh'];
surf = mesh_load_gmsh4(faff);
m = mesh_extract_regions(surf, 'region_idx', reg);
[vol,edg] = mesh_get_tetrahedron_sizes(m);
field_name = 'normJ';
field_idx = get_field_idx(m, field_name, 'elements');
field = m.element_data{field_idx}.tetdata;
eValOut(subj,1) = mean(field);
eValOut(subj,2) = median(field);
eValOut(subj,3) = max(field);
eValOut(subj,4) = min(field);
eValOut(subj,5) = std(field);
eValOut(subj,6) = (std(field))/sqrt(length(field));
```

```
faff = ['F:\Nibs\s' num2str(subj) '\' num2str(pow) '\90500\sub-control'
sLead '_TDCS_2_scalar.msh'];
%faff = ['F:\Nibs\Ernie\7\ernie_TDCS_2_scalar.msh'];
surf = mesh_load_gmsh4(faff);
m = mesh_extract_regions(surf, 'region_idx', reg);
[vol,edg] = mesh_get_tetrahedron_sizes(m);
field_name = 'normJ';
field_idx = get_field_idx(m, field_name, 'elements');
field = m.element_data{field_idx}.tetdata;
eValOut(subj,7) = mean(field);
eValOut(subj,8) = median(field);
eValOut(subj,9) = max(field);
eValOut(subj,10) = min(field);
eValOut(subj,11) = std(field);
eValOut(subj,12) = (std(field))/sqrt(length(field));

faff = ['F:\Nibs\s' num2str(subj) '\' num2str(pow) '\90500\sub-control'
sLead '_TDCS_3_scalar.msh'];
%faff = ['F:\Nibs\Ernie\7\ernie_TDCS_3_scalar.msh'];
surf = mesh_load_gmsh4(faff);
m = mesh_extract_regions(surf, 'region_idx', reg);
[vol,edg] = mesh_get_tetrahedron_sizes(m);
field_name = 'normJ';
field_idx = get_field_idx(m, field_name, 'elements');
field = m.element_data{field_idx}.tetdata;
eValOut(subj,13) = mean(field);
eValOut(subj,14) = median(field);
eValOut(subj,15) = max(field);
eValOut(subj,16) = min(field);
eValOut(subj,17) = std(field);
eValOut(subj,18) = (std(field))/sqrt(length(field));

faff = ['F:\Nibs\s' num2str(subj) '\' num2str(pow) '\90500\sub-control'
sLead '_TDCS_4_scalar.msh'];
%faff = ['F:\Nibs\Ernie\7\ernie_TDCS_4_scalar.msh'];
surf = mesh_load_gmsh4(faff);
m = mesh_extract_regions(surf, 'region_idx', reg);
[vol,edg] = mesh_get_tetrahedron_sizes(m);
field_name = 'normJ';
field_idx = get_field_idx(m, field_name, 'elements');
field = m.element_data{field_idx}.tetdata;
eValOut(subj,19) = mean(field);
eValOut(subj,20) = median(field);
eValOut(subj,21) = max(field);
eValOut(subj,22) = min(field);
eValOut(subj,23) = std(field);
eValOut(subj,24) = (std(field))/sqrt(length(field));

roll = roll + 1;
end
```

APPENDIX E

Table A.3: Individual subject statistics for current density within the eyes in each montage and frequency from Experiment Two (Chapter 3). All values in mA/m^2

	FPz-Cz Montage						Oz-Cz Montage					
ID	**Mean**	**Median**	**Max**	**Min**	**SD**	**SE**	**Mean**	**Median**	**Max**	**Min**	**SD**	**SE**
1	16.6	15.4	33.1	9.3	4.35	0.051	3.69	3.64	5.78	2.37	0.49	0.006
2	15.1	14.5	26.2	9.2	2.90	0.034	3.09	3.07	4.06	2.10	0.30	0.003
3	19.7	18.8	36.7	7.4	4.24	0.049	4.24	4.20	7.72	0.69	0.69	0.008
4	17.4	17.1	32.4	7.7	4.53	0.053	4.89	4.86	7.54	3.30	0.49	0.006
5	12.7	12.2	23.0	8.0	2.68	0.026	3.09	3.08	4.40	1.93	0.38	0.004
6	16.6	16.0	29.9	8.3	4.34	0.052	4.70	4.69	6.60	3.20	0.62	0.007
7	23.1	22.6	40.0	9.4	5.92	0.081	6.62	6.52	9.32	4.14	0.81	0.011
8	17.0	15.5	36.7	9.5	4.85	0.048	2.96	2.95	4.42	1.94	0.33	0.003
9	21.0	19.7	41.6	11.5	4.96	0.052	4.27	4.28	6.01	2.43	0.47	0.005
10	21.2	20.7	34.0	13.2	4.03	0.053	5.00	5.01	6.64	3.79	0.36	0.005
11	17.3	16.0	37.3	9.0	5.26	0.050	4.70	4.48	8.85	2.49	1.00	0.009
12	19.1	18.4	35.4	6.6	5.34	0.068	5.85	5.76	10.49	2.16	1.01	0.013
13	21.5	21.3	43.0	6.2	6.39	0.081	5.73	5.63	8.33	3.12	0.80	0.010
14	20.7	19.2	47.5	9.0	6.32	0.068	3.58	3.58	5.27	2.09	0.48	0.005
15	18.3	17.1	43.2	5.9	5.87	0.070	5.40	5.33	7.83	3.15	0.60	0.007
16	20.8	20.5	41.8	7.0	5.30	0.062	4.68	4.69	7.94	2.22	0.46	0.005
17	19.4	18.3	39.1	10.1	4.61	0.046	3.82	3.75	6.30	2.54	0.59	0.006
18	22.9	22.1	47.0	11.6	5.80	0.070	5.29	5.32	7.20	3.72	0.55	0.007
19	16.9	15.7	32.6	9.2	4.07	0.040	3.53	3.54	5.60	2.07	0.46	0.005
20	16.6	15.4	33.1	9.3	4.35	0.051	3.69	3.64	5.78	2.37	0.49	0.006

	FPz-Oz Montage						T3-T4 Montage					
ID	**Mean**	**Median**	**Max**	**Min**	**SD**	**SE**	**Mean**	**Median**	**Max**	**Min**	**SD**	**SE**
1	12.0	11.2	23.6	6.87	3.01	0.035	8.7	8.7	11.5	5.84	0.76	0.009
2	10.6	10.2	18.2	6.63	1.94	0.023	8.3	8.2	14.1	5.90	0.89	0.010
3	14.1	13.5	25.9	5.09	2.94	0.034	10.5	10.5	16.8	4.43	1.38	0.016
4	13.0	12.7	23.5	5.88	3.16	0.037	8.8	8.9	14.6	5.07	1.29	0.015
5	9.1	8.7	16.1	5.73	1.81	0.018	7.6	7.6	10.7	4.89	0.82	0.008
6	12.5	12.1	21.9	6.38	3.08	0.037	9.1	9.1	13.8	5.06	1.35	0.016
7	17.1	16.8	29.2	7.34	4.13	0.056	10.9	10.8	15.4	7.30	1.32	0.018
8	12.1	11.1	25.7	6.94	3.33	0.033	8.7	8.6	13.2	5.61	1.03	0.010
9	15.0	14.1	29.0	8.46	3.35	0.035	9.9	9.9	14.5	5.85	1.14	0.012
10	15.3	14.9	24.0	9.70	2.73	0.036	10.1	10.1	13.6	7.35	0.85	0.011
11	12.9	11.9	27.1	6.96	3.77	0.036	8.9	9.0	14.0	5.16	1.27	0.012
12	14.0	13.5	25.4	5.18	3.74	0.048	10.2	10.1	15.1	6.18	1.40	0.018
13	15.6	15.4	30.5	4.94	4.40	0.056	10.9	10.8	24.1	5.56	1.95	0.025
14	14.5	13.6	32.8	6.64	4.28	0.046	9.8	9.9	12.4	6.34	0.96	0.010
15	13.6	12.8	31.2	4.80	4.08	0.048	10.7	10.5	17.5	6.31	1.64	0.019
16	14.8	14.5	28.8	5.23	3.53	0.041	8.4	8.4	15.9	3.81	1.28	0.015
17	13.9	13.2	27.7	7.35	3.15	0.032	8.8	8.5	18.0	4.66	1.75	0.018
18	16.6	16.0	33.1	8.60	3.96	0.048	10.1	9.9	16.2	5.63	1.69	0.020
19	11.9	11.1	22.6	6.47	2.74	0.027	7.9	7.9	11.4	5.42	0.83	0.008
20	12.0	11.2	23.6	6.87	3.01	0.035	8.7	8.7	11.5	5.84	0.76	0.009

Table A.4: Individual subject statistics for current density in all grey matter within 40mm of Oz in each montage and frequency from Experiment Two (Chapter 3). All values in mA/m^2

	FPz-Cz Montage						Oz-Cz Montage					
ID	**Mean**	**Median**	**Max**	**Min**	**SD**	**SEM**	**Mean**	**Median**	**Max**	**Min**	**SD**	**SEM**
1	2.11	2.06	6.29	0.47	0.48	0.002	17.67	17.64	38.61	3.75	4.02	0.021
2	2.02	1.95	3.35	0.98	0.38	0.007	16.44	16.26	28.76	7.87	3.33	0.057
3	2.13	2.08	4.40	0.53	0.46	0.002	21.68	21.54	46.59	5.78	4.89	0.024
4	1.81	1.78	3.49	0.72	0.31	0.003	19.75	19.19	41.48	5.71	4.58	0.039
5	2.01	1.95	4.67	0.66	0.42	0.002	16.70	16.52	43.71	3.75	4.22	0.022
6	2.28	2.22	4.69	0.68	0.51	0.004	22.71	22.61	48.10	5.97	5.30	0.038
7	1.96	1.89	4.35	0.63	0.42	0.003	18.67	18.31	43.71	5.25	4.39	0.028
8	2.41	2.33	4.88	0.84	0.54	0.003	22.53	22.26	62.78	5.13	5.45	0.029
9	2.52	2.49	4.31	1.30	0.46	0.006	22.59	22.28	40.58	8.65	4.48	0.056
10	2.44	2.43	3.45	1.38	0.39	0.012	21.64	21.06	33.93	11.33	4.25	0.132
11	2.25	2.23	3.91	0.68	0.53	0.006	18.10	17.89	32.44	5.26	3.39	0.039
12	1.90	1.88	5.43	0.56	0.38	0.002	17.82	17.49	39.26	4.45	4.59	0.029
13	2.11	2.05	4.23	0.46	0.44	0.002	19.31	19.29	41.80	4.10	4.88	0.025
14	1.93	1.91	4.66	0.59	0.36	0.003	20.52	20.57	41.34	3.61	4.57	0.043
15	2.06	2.00	4.05	0.68	0.45	0.003	18.64	18.49	43.35	6.14	3.95	0.028
16	2.45	2.30	4.67	0.66	0.61	0.011	23.19	22.36	37.04	9.57	4.70	0.084
17	1.65	1.64	3.15	0.37	0.39	0.004	14.85	14.74	28.93	3.48	3.70	0.033
18	1.69	1.65	3.52	0.54	0.37	0.003	15.84	15.95	28.52	4.07	3.77	0.028
19	1.80	1.77	3.55	0.54	0.32	0.002	18.74	17.78	41.62	4.97	5.40	0.039
20	1.61	1.56	3.92	0.52	0.34	0.002	18.41	17.79	51.32	2.98	5.39	0.027

	FPz-Oz Montage						T3-T4 Montage					
ID	**Mean**	**Median**	**Max**	**Min**	**SD**	**SEM**	**Mean**	**Median**	**Max**	**Min**	**SD**	**SEM**
1	3.46	3.38	6.90	0.92	0.79	0.004	2.11	2.06	6.29	0.47	0.48	0.007
2	2.75	2.58	5.80	1.31	0.73	0.013	2.02	1.95	3.35	0.98	0.38	0.002
3	4.20	4.18	9.52	1.08	1.09	0.005	2.13	2.08	4.40	0.53	0.46	0.003
4	3.74	3.52	8.82	0.85	1.01	0.009	1.81	1.78	3.49	0.72	0.31	0.002
5	3.08	3.01	7.13	0.78	0.86	0.004	2.01	1.95	4.67	0.66	0.42	0.004
6	4.27	4.18	10.41	0.92	1.09	0.008	2.28	2.22	4.69	0.68	0.51	0.003
7	3.60	3.50	9.05	1.02	0.88	0.006	1.96	1.89	4.35	0.63	0.42	0.003
8	4.13	3.95	11.29	1.01	1.10	0.006	2.41	2.33	4.88	0.84	0.54	0.006
9	3.75	3.61	7.84	1.13	0.83	0.010	2.52	2.49	4.31	1.30	0.46	0.012
10	3.46	3.36	5.54	1.98	0.64	0.020	2.44	2.43	3.45	1.38	0.39	0.006
11	2.98	2.96	4.96	1.03	0.52	0.006	2.25	2.23	3.91	0.68	0.53	0.002
12	3.32	3.21	7.67	0.61	0.90	0.006	1.90	1.88	5.43	0.56	0.38	0.002
13	3.68	3.59	8.31	0.69	1.04	0.005	2.11	2.05	4.23	0.46	0.44	0.003
14	4.01	3.92	8.31	0.78	0.99	0.009	1.93	1.91	4.66	0.59	0.36	0.003
15	3.31	3.30	8.43	0.73	0.72	0.005	2.06	2.00	4.05	0.68	0.45	0.011
16	3.84	3.70	6.46	1.57	0.80	0.014	2.45	2.30	4.67	0.66	0.61	0.004
17	2.53	2.50	5.33	0.62	0.61	0.005	1.65	1.64	3.15	0.37	0.39	0.003
18	2.84	2.79	5.99	0.65	0.71	0.005	1.69	1.65	3.52	0.54	0.37	0.002
19	3.52	3.31	8.74	1.06	1.17	0.008	1.80	1.77	3.55	0.54	0.32	0.004
20	4.28	4.13	11.73	0.86	1.17	0.006	3.09	3.06	6.79	0.96	0.75	0.003

APPENDIX F

Table A.5: Individual subject thresholds (in μA) for each lighting condition and frequency from Experiment Three (Chapter 4). Separate thresholds for each testing session are provided.

	Session One														
	Photopic					Mesopic					Dark				
ID	10	13	16	18	20	10	13	16	18	20	10	13	16	18	20
1	750	650	450	525	400	225	250	150	225	200	675	750	750	750	975
2	475	325	225	200	175	175	150	75	125	150	300	225	300	375	350
3	525	275	225	300	200	200	125	100	125	175	200	75	100	125	125
4	350	425	200	225	100	175	175	75	50	75	275	350	450	425	500
5	350	225	225	300	200	125	100	100	100	100	325	250	500	575	600
6	900	750	500	475	475	350	150	175	225	300	475	575	700	700	650
7	825	525	325	250	225	375	300	150	125	150	400	425	400	450	525
8	525	400	175	175	175	275	200	50	125	150	400	400	450	450	400
9	850	725	600	600	600	225	250	125	125	125	225	250	250	275	375
10	825	550	375	300	250	200	200	100	125	150	300	525	475	475	400
11	500	400	300	350	300	175	175	125	125	125	150	200	250	250	350
12	950	750	700	525	525	475	375	200	200	175	375	550	575	650	700
13	975	725	600	675	575	450	350	250	275	275	575	550	675	700	875
14	625	425	125	300	150	225	125	150	125	125	125	275	225	225	375
15	800	725	500	475	425	325	250	150	175	225	475	575	625	700	725
16	825	550	350	275	225	425	350	200	250	300	375	425	475	525	600
17	525	400	325	250	200	200	150	100	150	275	275	325	425	450	475
18	575	450	325	250	225	250	200	125	150	225	325	425	500	550	675
19	800	625	425	375	350	250	175	100	200	225	325	450	475	575	650
20	575	475	325	300	275	175	150	100	175	225	150	225	275	350	475
21	850	700	625	550	525	425	325	225	300	350	375	525	625	675	775
22	700	525	375	300	225	300	175	100	175	225	125	275	325	375	475
23	400	350	250	225	150	275	175	100	175	250	300	450	475	525	600
24	350	325	225	200	175	125	125	75	125	200	325	350	450	550	650

	Session Two														
	Photopic					Mesopic					Dark				
ID	10	13	16	18	20	10	13	16	18	20	10	13	16	18	20
1	775	675	450	525	425	275	250	150	275	200	675	750	800	750	925
2	425	350	275	200	175	225	125	75	100	125	300	250	275	450	375
3	525	300	200	275	175	225	125	75	100	200	225	100	75	125	125
4	375	425	250	225	125	200	150	75	50	100	300	350	475	425	500
5	300	225	225	275	225	125	100	75	75	125	350	275	425	550	625
6	825	800	525	475	475	300	150	200	300	325	500	575	700	700	575
7	875	525	300	250	200	425	375	150	100	175	400	425	475	425	500
8	600	400	175	150	175	250	200	75	100	125	350	475	450	450	400
9	800	725	675	600	525	225	200	175	125	100	250	250	225	200	350
10	825	600	375	250	250	250	150	100	125	150	300	475	475	475	450
11	500	450	300	325	350	175	125	150	125	125	125	200	175	250	350
12	875	750	625	500	550	400	325	200	150	225	425	550	650	650	650
13	925	800	600	675	500	400	325	250	225	325	575	550	725	675	800
14	675	425	125	300	150	225	125	100	125	125	125	275	225	225	325
15	800	650	500	475	400	300	250	150	225	300	475	575	625	675	775
16	900	525	350	275	225	425	300	200	250	325	325	425	475	500	600
17	500	400	300	250	175	250	150	100	150	225	275	325	350	450	550
18	525	450	300	325	225	300	175	125	150	225	300	425	500	625	675
19	800	600	425	375	325	250	200	100	175	275	325	450	550	575	725
20	575	475	350	300	300	175	125	100	175	275	150	225	275	400	425
21	800	725	625	550	500	475	350	225	300	375	375	550	625	750	825
22	625	525	400	300	225	300	175	125	175	250	150	275	325	400	475
23	400	400	250	200	150	275	225	100	175	250	300	375	475	525	625
24	400	300	225	200	175	150	100	75	125	200	325	375	450	575	650

APPENDIX G

Statement of Contribution of Others

As co-authors of the following publications:

Chapter 2: Evans, I. D., Palmisano, S., Loughran, S. P., Legros, A. & Croft, R. J. (2019). Frequency-dependent and montage-based differences in phosphene perception thresholds via transcranial alternating current stimulation. *Bioelectromagnetics, 40*, 365-374 (2019). doi:10.1002/bem.22209

Chapter 3: Evans, I. D., Palmisano, S., & Croft, R. J. (2021). Retinal and cortical contributions to phosphenes during transcranial electrical current stimulation. *Bioelectromagnetics, 42*(2), 146-158. doi:10.1002/bem.22317

Chapter 4: Evans, I. D., Palmisano, S., & Croft, R. J. (2022). Effect of ambient lighting on frequency dependence in transcranial electrical stimulation-induced phosphenes. *Scientific Reports, 12*(1), 7775. doi:10.1038/s41598-022-11755-y

I declare that the greater part of the work is directly attributable to the PhD Candidate, that the candidate contributed to the research design, data collections, processing and analysis, and the writing and editing of the manuscripts.

Principle Supervisor: Senior Professor Rodney Croft

Signature:

Date: 23/03/2023

Co-Supervisor: Professor Stephen Palmisano

Signature:

Date: 20/03/2023

APPENDIX H

PDF proofs of published manuscripts, in order of their publication.

Article removed for copyright reasons, please refer to the citation:

Evans, I. D., Palmisano, S., Loughran, S. P., Legros, A. & Croft, R. J. (2019). Frequency-dependent and montage-based differences in phosphene perception thresholds via transcranial alternating current stimulation. Bioelectromagnetics, 40, 365-374. doi:10.1002/bem.22209

Article removed for copyright reasons, please refer to the citation:

Evans, I. D., Palmisano, S., Loughran, S. P., Legros, A. & Croft, R. J. (2019). Frequency-dependent and montage-based differences in phosphene perception thresholds via transcranial alternating current stimulation. Bioelectromagnetics, 40, 365-374. doi:10.1002/bem.22209

Article removed for copyright reasons, please refer to the citation:

Evans, I. D., Palmisano, S., Loughran, S. P., Legros, A. & Croft, R. J. (2019). Frequency-dependent and montage-based differences in phosphene perception thresholds via transcranial alternating current stimulation. Bioelectromagnetics, 40, 365-374. doi:10.1002/bem.22209

Article removed for copyright reasons, please refer to the citation:

Evans, I. D., Palmisano, S., Loughran, S. P., Legros, A. & Croft, R. J. (2019). Frequency-dependent and montage-based differences in phosphene perception thresholds via transcranial alternating current stimulation. Bioelectromagnetics, 40, 365-374. doi:10.1002/bem.22209

Article removed for copyright reasons, please refer to the citation:

Evans, I. D., Palmisano, S., Loughran, S. P., Legros, A. & Croft, R. J. (2019). Frequency-dependent and montage-based differences in phosphene perception thresholds via transcranial alternating current stimulation. Bioelectromagnetics, 40, 365-374. doi:10.1002/bem.22209

Article removed for copyright reasons, please refer to the citation:

Evans, I. D., Palmisano, S., Loughran, S. P., Legros, A. & Croft, R. J. (2019). Frequency-dependent and montage-based differences in phosphene perception thresholds via transcranial alternating current stimulation. Bioelectromagnetics, 40, 365-374. doi:10.1002/bem.22209

Article removed for copyright reasons, please refer to the citation:

Evans, I. D., Palmisano, S., Loughran, S. P., Legros, A. & Croft, R. J. (2019). Frequency-dependent and montage-based differences in phosphene perception thresholds via transcranial alternating current stimulation. Bioelectromagnetics, 40, 365-374. doi:10.1002/bem.22209

Article removed for copyright reasons, please refer to the citation:

Evans, I. D., Palmisano, S., Loughran, S. P., Legros, A. & Croft, R. J. (2019). Frequency-dependent and montage-based differences in phosphene perception thresholds via transcranial alternating current stimulation. Bioelectromagnetics, 40, 365-374. doi:10.1002/bem.22209

Article removed for copyright reasons, please refer to the citation:

Evans, I. D., Palmisano, S., Loughran, S. P., Legros, A. & Croft, R. J. (2019). Frequency-dependent and montage-based differences in phosphene perception thresholds via transcranial alternating current stimulation. Bioelectromagnetics, 40, 365-374. doi:10.1002/bem.22209

Article removed for copyright reasons, please refer to the citation:

Evans, I. D., Palmisano, S., Loughran, S. P., Legros, A. & Croft, R. J. (2019). Frequency-dependent and montage-based differences in phosphene perception thresholds via transcranial alternating current stimulation. Bioelectromagnetics, 40, 365-374. doi:10.1002/bem.22209

Evans, I. D., Palmisano, S., & Croft, R. J. (2021). Retinal and cortical contributions to phosphenes during transcranial electrical current stimulation. Bioelectromagnetics, 42(2), 146-158. doi:10.1002/bem.22317

Article removed for copyright reasons, please refer to the citation:

Evans, I. D., Palmisano, S., & Croft, R. J. (2021). Retinal and cortical contributions to phosphenes during transcranial electrical current stimulation. Bioelectromagnetics, 42(2), 146-158. doi:10.1002/bem.22317

Article removed for copyright reasons, please refer to the citation:

Evans, I. D., Palmisano, S., & Croft, R. J. (2021). Retinal and cortical contributions to phosphenes during transcranial electrical current stimulation. Bioelectromagnetics, 42(2), 146-158. doi:10.1002/bem.22317

Article removed for copyright reasons, please refer to the citation:

Evans, I. D., Palmisano, S., & Croft, R. J. (2021). Retinal and cortical contributions to phosphenes during transcranial electrical current stimulation. Bioelectromagnetics, 42(2), 146-158. doi:10.1002/bem.22317

Article removed for copyright reasons, please refer to the citation:

Evans, I. D., Palmisano, S., & Croft, R. J. (2021). Retinal and cortical contributions to phosphenes during transcranial electrical current stimulation. Bioelectromagnetics, 42(2), 146-158. doi:10.1002/bem.22317

Article removed for copyright reasons, please refer to the citation:

Evans, I. D., Palmisano, S., & Croft, R. J. (2021). Retinal and cortical contributions to phosphenes during transcranial electrical current stimulation. Bioelectromagnetics, 42(2), 146-158. doi:10.1002/bem.22317

Article removed for copyright reasons, please refer to the citation:

Evans, I. D., Palmisano, S., & Croft, R. J. (2021). Retinal and cortical contributions to phosphenes during transcranial electrical current stimulation. Bioelectromagnetics, 42(2), 146-158. doi:10.1002/bem.22317

Article removed for copyright reasons, please refer to the citation:

Evans, I. D., Palmisano, S., & Croft, R. J. (2021). Retinal and cortical contributions to phosphenes during transcranial electrical current stimulation. Bioelectromagnetics, 42(2), 146-158. doi:10.1002/bem.22317

Article removed for copyright reasons, please refer to the citation:

Evans, I. D., Palmisano, S., & Croft, R. J. (2021). Retinal and cortical contributions to phosphenes during transcranial electrical current stimulation. Bioelectromagnetics, 42(2), 146-158. doi:10.1002/bem.22317

Article removed for copyright reasons, please refer to the citation:

Evans, I. D., Palmisano, S., & Croft, R. J. (2021). Retinal and cortical contributions to phosphenes during transcranial electrical current stimulation. Bioelectromagnetics, 42(2), 146-158. doi:10.1002/bem.22317

Article removed for copyright reasons, please refer to the citation:

Evans, I. D., Palmisano, S., & Croft, R. J. (2021). Retinal and cortical contributions to phosphenes during transcranial electrical current stimulation. Bioelectromagnetics, 42(2), 146-158. doi:10.1002/bem.22317

Article removed for copyright reasons, please refer to the citation:

Evans, I. D., Palmisano, S., & Croft, R. J. (2021). Retinal and cortical contributions to phosphenes during transcranial electrical current stimulation. Bioelectromagnetics, 42(2), 146-158. doi:10.1002/bem.22317

Article removed for copyright reasons, please refer to the citation:

Evans, I. D., Palmisano, S., & Croft, R. J. (2021). Retinal and cortical contributions to phosphenes during transcranial electrical current stimulation. Bioelectromagnetics, 42(2), 146-158. doi:10.1002/bem.22317

scientific reports

Check for updates

OPEN

Effect of ambient lighting on frequency dependence in transcranial electrical stimulation-induced phosphenes

Ian Evans[1,2,3,4]✉, Stephen Palmisano[1,2] & Rodney J. Croft[1,2,3,4]

Inconsistencies have been found in the relationship between ambient lighting conditions and frequency-dependence in transcranial electric stimulation (tES) induced phosphenes. Using a within-subjects design across lighting condition (dark, mesopic [dim], photopic [bright]) and tES stimulation frequency (10, 13, 16, 18, 20 Hz), this study determined phosphene detection thresholds in 24 subjects receiving tES using an FPz-Cz montage. Minima phosphene thresholds were found at 16 Hz in mesopic, 10 Hz in dark and 20 Hz in photopic lighting conditions, with these thresholds being substantially lower for mesopic than both dark (60% reduction) and photopic (56% reduction), conditions. Further, whereas the phosphene threshold-stimulation frequency relation increased with frequency in the dark and decreased with frequency in the photopic conditions, in the mesopic condition it followed the dark condition relation from 10 to 16 Hz, and photopic condition relation from 16 to 20 Hz. The results clearly demonstrate that ambient lighting is an important factor in the detection of tES-induced phosphenes, and that mesopic conditions are most suitable for obtaining overall phosphene thresholds.

Many aspects of neural processing rely on frequency-specific oscillations in the cortex[1]. As a result, the possibility of exploring and/or manipulating these frequency-based neural functions using a non-invasive technique like transcranial electric current stimulation (tES) has proven popular. Applying electric current to the brain using tES has been demonstrated to be successful in modulating cognitive, sensory, and motor functions in a frequency-dependent manner across the surface of the cortex (for reviews see[2,3]). Although tES can modulate cortical activity, it can also induce phosphenes (i.e., perceptions of light that are not the product of external visual stimuli[4–6]). These phosphenes are generally considered to be a product of electrical stimulation of the retina[6–12].

It is important to understand both the biological mechanisms responsible for inducing phosphenes, and any environmental factors that influence their appearance, as these can confound tES studies, interventions and interpretations[13]. For example, the threshold for inducing phosphenes is currently used by the International Commission on Non-Ionizing Radiation Protection (ICNIRP) for deriving exposure restrictions[14], and that information can only be obtained if the effect of stimulation frequency and ambient lighting conditions are also known. Without that knowledge, experimentally-derived threshold estimates may merely represent the lowest stimulation levels required to induce phosphenes in a particular *insensitive* scenario, which would limit the ability of exposure restrictions based on them to protect against phosphenes in other situations. Indeed, recent research suggests that our understanding of phosphenes may be particularly limited in terms of their relation with stimulation frequency and ambient lighting conditions.

It has commonly been held that thresholds for phosphenes induced by transcranial alternating current stimulation (tACS) are lowest when stimulation is applied at 20 Hz in photopic (i.e., intense) lighting conditions and at 10 Hz in complete darkness[15]; sensitivities that closely match the dominant frequencies of the visual cortex oscillations observed under these respective lighting conditions (e.g.[16,17]). These findings have been taken as evidence that tES, tuned to the dominant cortical oscillation frequency, can be used to maximally modify cortical activity at similar rhythms.

[1]School of Psychology, University of Wollongong, Wollongong, Australia. [2]Illawarra Health and Medical Research Institute, University of Wollongong, Wollongong, NSW 2522, Australia. [3]Australian Centre for Electromagnetic Bioeffects Research, Wollongong, Australia. [4]Centre for Population Health Research On Electromagnetic Energy, Monash University, Melbourne, Australia. ✉email: ievans3@une.edu.au

However, recent research suggests that under mesopic (dim) lighting conditions, tES phosphenes are induced with considerably less current using 16 than 20 Hz stimulations[18,19], which suggests that 20 Hz does not provide the lowest stimulation level required to induce phosphenes. This raises concerns about the relative veracity of these new reports. The only research available for comparison explicitly testing phosphene threshold levels in mesopic conditions is the Schwarz[20] study. Schwarz[20] reported lower phosphene detection thresholds for 20 Hz stimulation in both photopic (i.e., 8–9550 cd per square meter; cd/m^2) and mesopic (i.e., 2.4 cd/m^2) conditions. However, those findings were based on only a single subject and used poorly controlled lighting conditions; e.g. the 2.4 cd/m^2 condition was produced by having the subject look at "her own shadow on the wall", and the 9550 cd/m^2 condition was produced by having the subject look at "a white cloud in the sky". This makes it difficult to draw conclusions from such a comparison. In contrast to Schwarz's[20] research, more recent studies[18,19] used considerably larger samples (either 24 or 22 participants in each of these studies) with tightly controlled lighting (consistent 0.6 cd/m^2 lighting across the entire field of view). Furthermore, the consistency of the initial[18] and replication[19] study suggests that their results are indeed reliable. This conclusion, however, would appear (at face value) to contradict the view that the greatest sensitivity to tES occurs at the stimulation frequency that matches the dominant cortical oscillation frequency. That is, whereas the dominant cortical oscillation frequencies for photopic and dark conditions are approximately 20 and 10 Hz respectively, and the lowest current required to induce phosphenes is at 20 and 10 Hz respectively, there is no corresponding dominant frequency for mesopic conditions.

One potential explanation for lower thresholds at 16 Hz stimulation is that this represents an overlap point between the threshold-stimulation frequency relations for photopic and dark conditions. That is, as a dim lighting condition represents a degree of photic energy that is greater than in the dark, but less than in a photopic scenario, it may be relevant to the threshold-stimulation frequency of both the dark and photopic conditions. To test this possibility, threshold-stimulation frequency relations need to be assessed under each of dark, mesopic and photopic conditions.

Differences in frequency dependence found in tES-induced phosphenes across lighting conditions may be explained by differences in temporal contrast sensitivity functions (i.e., the visual system's sensitivity to changes in luminance over time[21,22]). Temporal contrast sensitivity is typically measured using a homogenous visual stimulus that changes sinusoidally in luminance (from a minimum to a maximum value) as a function of time. While this stimulus should be perceived to flicker with larger levels of luminance contrast, it will become progressively more difficult to see this flicker as this luminance contrast decreases. However, the threshold level of luminance contrast at which this flicker is just noticeable also depends critically on the temporal frequency of the stimulus. Research has shown that rod and cone photoreceptors each have their own temporal contrast sensitivity functions, which may relate to differences in tES-related frequency dependence found in different lighting conditions.

Rod photoreceptors are more sensitive to stimulation (and thus more likely to be activated) in darker conditions, where there is insufficient input to activate cones[23]. In dark and mesopic conditions, temporal contrast sensitivities are largely driven by inputs from rod photoreceptors[24] particularly when exposed to stimuli flickering at 5–15 Hz while showing little to no activation at 19–23 Hz[25,26]. On the other hand, cone photoreceptors are more sensitive to stimulation in brighter conditions, where rod cells are saturated and do not contribute significantly to visual perception[27]. Temporal contrast sensitivity in these photopic conditions trends towards higher frequencies, with greatest sensitivity found at around 15–25 Hz and no ability to discern stimuli flickering at or above approximately 80 Hz[25,26,28]. If the perception of tES-induced phosphenes is similar or functionally equivalent to external flickering visual stimuli[6], it would follow that darker conditions would result in greater sensitivity to low-frequency stimulation, and brighter conditions would result in greater sensitivity to higher frequencies.

The present study was designed to determine the following. First, by testing the threshold-frequency stimulation relation in each of dark, mesopic and photopic conditions, it examined whether the overall phosphene detection threshold occurs at 16 Hz stimulation, rather than 20 Hz. Second, it extended the results of previous studies[18,19], which found lower thresholds at 16 Hz stimulation in mesopic conditions (and which increased for higher and lower frequencies), compared to dark and photopic lighting conditions. Third, it determined whether the phosphene threshold-stimulation frequency relation under mesopic conditions could be explained by the overlap of that relation across dark and photopic conditions.

Method

Twenty-four healthy participants (even gender split, age range 20–40 years, $M = 25.2$ years, $SD = 5.4$) completed this study after passing a modified safety screening checklist[29]. Participants were excluded if they reported any form of neural injury or illness, metal implants in the head or medical implant elsewhere in the body, or non-corrected visual impairment. No participants reported using contact lenses, while three participants typically wore glasses but removed them during the testing phase to ensure the frames did not alter the periphery of their field of view. After being informed about the experimental procedure as well as potential adverse effects of tES, subjects gave written and informed consent prior to any participation. This research was conducted in accordance with the guidelines of the Declaration of Helsinki, and approved by the Human Research Ethics Committee of the University of Wollongong (approval #HE2017/454).

Phosphene thresholds were obtained as a function of stimulation frequency ("Frequency": 10, 13, 16, 18, and 20 Hz) and lighting condition ("Lighting Condition": dark, mesopic, photopic), using a repeated measures design. Testing was conducted over two, 70-min sessions (on separate days) at similar times of day and usually within one week of each other. The order of these sessions, the order of the tES montages within these sessions, and which electrode was the cathode or anode within each montage, were counterbalanced across sessions for all participants (see Fig. 1b). The choice of which electrode was cathode/anode alternated across sessions for each

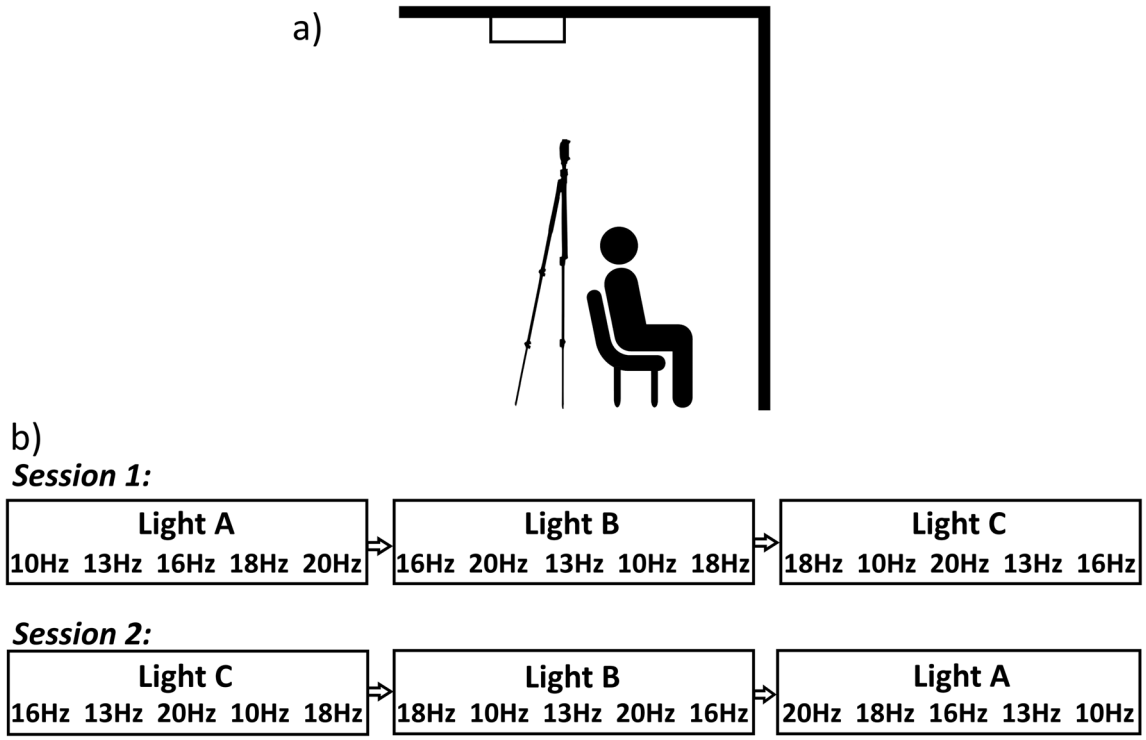

Figure 1. (**a**) Positioning of lighting and test subject. The test subject was seated so that the front wall filled their entire field of view (no parts of either side wall were visible). The light stand was positioned so that no shadows were visible in the subject's field of view. The photopic lighting condition was achieved by activating the fixed fluorescent ceiling light with no light stand used, while all other lighting conditions (the mesopic condition and the brief periods requiring light in the dark condition) were achieved using the light stand only. (**b**) Example sequence of the block design across both sessions. For the first session, each lighting condition block was presented in a random order, as were the frequencies within it. In order to account for potential within-subject order effects due to possible light adaptation, in the second session the order of the lighting blocks was reversed and the frequencies within those blocks were reversed.

subject. The order of the lighting conditions was randomised for each participant using a Latin square system, as was the order of stimulation frequency within each lighting condition.

tES was administered using a Magstim NeuroConn DC Stimulator Plus MOP15-EN-01 (Magstim, Carmarthenshire, UK) which applied sinusoidal DC with no ramp-up, meaning that the amplitude of the stimulation varied as a sine wave from zero to the current set by the stimulator then back to zero. As such, the polarity of the electrodes did not alternate. Current was delivered to the scalp through conductive-rubber electrodes (dimensions: 3×4 cm) placed on sponges saturated with a saline solution mixed with a hypoallergenic amphoteric surfactant and held in place at FPz and Cz with rubber straps. This electrode montage was chosen as it is effective at stimulating the retinas[30] while also ensuring the participants' entire field of view was not occluded by any of the apparatus. Previous tES studies under mesopic lighting conditions[18,19] all consistently found greatest sensitivity at 16 Hz using a wide range of montages (FPz-Cz, Oz-Cz, FPz-Oz, T3-T4), suggesting that the choice of montage does not appreciably affect the frequency-dependent nature of tES-induced phosphenes providing that the retina is adequately stimulated.

The photopic lighting condition was generated by using typical ceiling-mounted fluorescent lights, positioned outside the participants' direct line of sight. Under these lighting conditions, luminance at the eye was measured at 77.1 ± 0.05 cd/m^2 using a J6523 Tektronix luminance probe (Tektronix, London, Canada). This lighting level was chosen due to its applicability to everyday experience, as it represents the luminance typically found in office environments. The mesopic lighting condition was created using the Neewer T120 dimmable LED panel illuminating the areas in front of the participant (see Fig. 1a), resulting in luminance at the eye measured at 0.6 ± 0.05 cd/m^2. This lighting level was chosen in order to match that of previous studies[18,19] and thus to enable replication of their results. No light entered the testing room during the dark condition, resulting in zero cd/m^2. In order to prevent dark adaptation effects during the trials in the dark condition, lighting was set to 1.1 cd/m^2 while the stimulator was not active; lighting was turned off 2 s prior to stimulation onset and turned on immediately after the stimulation had ended.

Participants were seated on a chair facing a 1.8 m wide by 2.62 m high white wall, in a position that ensured that the wall in front of them filled their entire field of view, and lighting was arranged so that no shadows were visible to the participant (see Fig. 1a). When participants were comfortable and the electrodes put in position, they were informed about phosphenes (their nature and what they might perceive) whilst their skin and hair were saturated from the saline in the sponges. Once impedance between the electrodes was at 15 kΩ or below

(as indicated by the stimulator), lighting was set to 2 ± 0.05 cd/m^2 and participants were familiarized with the appearance of phosphenes using 10 s of sinusoidal tES at 1000 μA, firstly at 11 Hz and then at 22 Hz, to demonstrate both the visual appearance of phosphenes, and how their appearance changes by simply varying the stimulation frequency. These frequencies were chosen to avoid using the same stimulation frequencies as in the experiment itself.

Once participants were familiarized with phosphenes, their phosphene detection thresholds were determined at each stimulation frequency and lighting condition. They were informed when each stimulation began and when it ceased, but they were not informed of the frequency or current intensity of the stimulation. Stimulations lasted for 5 s, and participants were instructed to keep their eyes open throughout the entire stimulation. Throughout the experiment participants were asked how bright the phosphenes appeared to be compared to the background lighting, and where the phosphenes appeared in their field of view. Many participants also spontaneously volunteered information concerning their experience during the interval between trials. To detect false positive responses at lower current intensity levels, six sham stimulations (one in each lighting condition for each session) were given at a frequency determined in advance using a MATLAB-based random number generator. In these sham trials, the participant was given all the audible signs of a stimulation (the usual button presses on the stimulator as well as verbal indications that the stimulation had started and finished) without actually generating an electric current. None of the participants reported seeing phosphenes during any of the sham trials.

Thresholds for phosphene induction (in μA) were determined for each frequency by varying the current intensity using a QUEST-based Bayesian adaptive staircasing procedure[31] in MATLAB's PsychToolbox[32]. The tES, which started at 700 μA, was bound between 25 and 1500 μA. The step-size between possible stimulation levels was 25 μA. Based on the Rapid Estimation of Phosphene Threshold system validated by Mazzi et al.[33], this adaptive threshold measurement method determined the lowest current intensity that was significantly more likely than chance to evoke phosphene perceptions. Each of the two sessions provided a threshold for each lighting and frequency condition, and for each combination of lighting condition and stimulation frequency, the average threshold across both sessions was taken as the final threshold.

Statistical analysis. As significant levels of skewness, kurtosis or heterogeneity of variance were not found, parametric analyses were conducted. Huynh–Feldt adjustments were used to account for violations to sphericity (Frequency; Frequency by Lighting Condition), with the adjusted degrees of freedom shown.

To assess threshold reliability across the two testing sessions, for each of the Lighting Condition (photopic, mesopic, dark)/Frequency (10, 13, 16, 18, 20 Hz) combinations, Pearson's r was determined. To determine if order effects were distorting the results, thresholds were arranged in chronological order and repeated measures ANOVA were used where threshold was the dependent variable and testing order within each lighting condition (separately for each session) and across each entire session were the independent variables.

To describe the relations between phosphene thresholds, lighting conditions and stimulation frequency, a repeated measures ANOVA was used where threshold was the dependent variable, and Lighting Condition and Frequency the independent variables. Where significant, data were further explored using repeated measures t tests with Bonferroni comparison-wise adjustments (Lighting Condition: each level was compared to each other level; Frequency: each level was compared to each other level; Interaction: for each frequency, each level of Lighting Condition was compared to each other level). Adjusted p-values are shown.

To determine the lowest absolute phosphene thresholds across the lighting conditions, a repeated measures ANOVA was used where Lighting Condition was the independent variable, and the dependent variable was the lowest algebraic threshold across the frequencies, for each lighting condition separately. Where the main effect was significant, t tests with Bonferroni comparison-wise adjustments (Lighting Condition: each level was compared to each other level) were conducted. Adjusted p-values are shown.

To determine whether the phosphene threshold-stimulation frequency relation in the mesopic condition could be adequately explained by the summation of the relations in the dark and photopic conditions, regression equations were calculated as follows. To provide an estimate of the phosphene threshold-stimulation frequency relation for each of the lighting conditions separately, regression analyses were conducted for each lighting condition separately where threshold was the dependent variable (normalized across all tested frequencies, within each subject and lighting condition separately), and Frequency the independent variable. Corrected Akaike's Information Criteria (AICc[34]) was used to determine whether a linear or quadratic fit was the best model for each lighting condition. Data for each participant was used for all frequencies and lighting conditions, resulting in 72 data points per frequency.

Results

Thresholds at each Frequency/Lighting Condition combination can be seen in Fig. 2a and in Supplementary Table 1. The interpolated regression functions relating threshold to Frequency, for each lighting condition separately, can be seen in Fig. 2b. Corresponding means and standard errors are given in Table 1.

Phosphene thresholds were highly reliable across the two testing sessions, with Pearson's r coefficient values ranging from 0.91 to 0.99 (all $p < 0.001$) across the 15 Frequency/Lighting Condition combinations. No signs of learning or fatigue effects were found within either session (p between 0.707–0.883) or within each lighting condition (p between 0.472–0.940). Mean thresholds for all (30) testing points ranged between 313.5–407.3 μA, with standard deviations between 166.3–246.4 μA.

Phosphene thresholds were affected by lighting condition (main effect: $F(1.96,45.16) = 59.15$, $p < 0.001$, $\eta_p^2 = 0.720$), with post hoc analyses showing that this was due to lower thresholds in the dim lighting condition relative to both the photopic ($F(1, 23) = 116.4$, $p < 0.001$, $\eta_p^2 = 0.835$) and dark ($F(1, 23) = 93.93$, $p < 0.001$, $\eta_p^2 = 0.803$) conditions; no difference was observed between the photopic and dark conditions ($p > 0.999$).

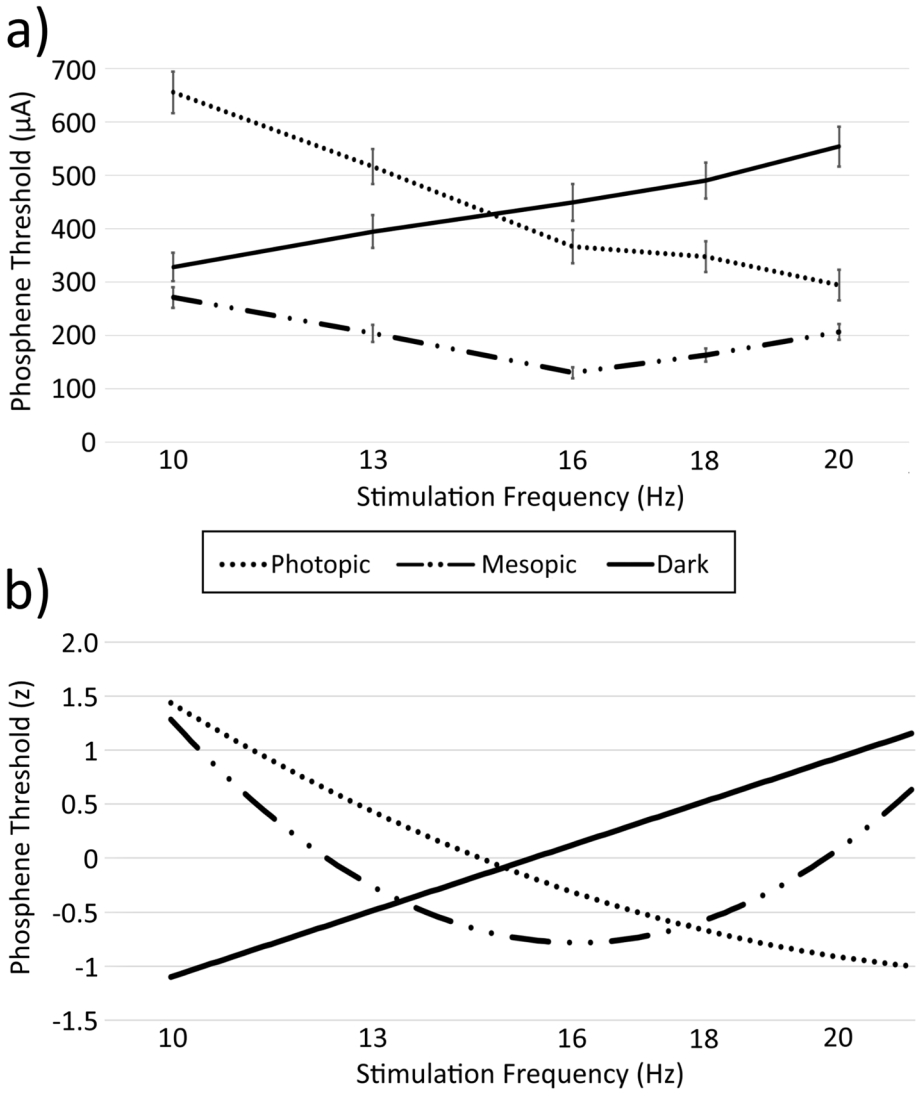

Figure 2. (**a**) Phosphene thresholds and standard errors for each ambient lighting condition at each frequency tested (10, 13, 16, 18 and 20 Hz). (**b**) Regression-based estimates of normalised phosphene thresholds, as a function of stimulation frequency, for each ambient lighting condition.

Frequency (Hz)	Photopic	Mesopic	Dark
10	655.2 (39.2)	270.8 (19.2)	328.1 (26.9)
13	516.1 (32.7)	203.6 (16.0)	394.3 (30.6)
16	366.1 (31.0)	130.2 (10.2)	449.0 (34.5)
18	347.4 (28.3)	163.0 (12.5)	490.1 (33.8)
20	294.3 (28.6)	206.3 (14.9)	553.6 (37.5)

Table 1. Means (and standard errors) of the phosphene thresholds for each frequency and lighting condition tested. n = 24.

Phosphene thresholds (for the combined lighting conditions) were also affected by Frequency (main effect: $F(1.69,38.91) = 26.46$, $p < 0.001$, $\eta_p^2 = 0.535$). The frequency with the lowest threshold (16 Hz) was lower than each other frequency (all $p < 0.049$), and the frequency with the highest threshold (10 Hz) was higher than each other frequency ($p < 0.004$). Of the remaining comparisons, thresholds for 13 Hz were higher than 18 Hz ($F(1, 23) = 10.34$, $p = 0.038$, $\eta_p^2 = 0.310$) but did not differ from 20 Hz ($p = 0.795$), and 18 Hz was lower than 20 Hz ($F(1, 23) = 17.75$, $p = 0.003$, $\eta_p^2 = 0.436$).

The interaction between Frequency and Lighting Condition was also significant $F(4.63,106.50) = 117.60$, $p < 0.001$). Follow-up analyses for the significant interaction demonstrated the following: *10 Hz Stimulation.* Thresholds were lower for both the mesopic ($t(23) = 13.77$, $p < 0.001$, Cohen's $d = 2.81$) and dark ($t(23) = 8.85$, $p < 0.001$, $d = 1.81$) conditions than photopic conditions, whereas mesopic and dark conditions did not differ ($t(23) = 2.25$, $p = 0.102$, $d = 0.46$). *13 Hz Stimulation*. Thresholds were lower for mesopic than both dark ($t(23) = 7.58$, $p < 0.001$, $d = 1.55$) and photopic ($t(23) = 12.31$, $p < 0.001$, $d = 2.51$) conditions, and lower for dark compared to photopic conditions ($t(23) = 4.73$, $p < 0.001$, $d = 0.97$). *16 Hz Stimulation.* Thresholds were lower for mesopic than both the photopic ($t(23) = 9.64$, $p < 0.001$, $d = 1.97$) and dark ($t(23) = 10.27$, $p < 0.001$, $d = 2.10$) conditions, whereas dark and photopic conditions did not differ ($t(23) = 2.54$, $p = 0.055$, $d = 0.52$). *18 Hz Stimulation.* Thresholds were lower for the mesopic than both photopic ($t(23) = 7.98$, $p < 0.001$, $d = 1.63$) and dark ($t(23) = 11.65$, $p < 0.001$, $d = 2.38$) conditions, and photopic less than the dark condition ($t(23) = 4.12$ $p = 0.001$, $d = 0.84$). *20 Hz Stimulation.* Thresholds were lower for the mesopic than both photopic ($t(23) = 3.25$, $p = 0.009$, $d = 0.67$) and dark ($t(23) = 10.71$, $p < 0.001$, $d = 2.19$) conditions, and photopic less than dark condition ($t(23) = 7.29$, $p < 0.001$, $d = 1.49$).

The lowest thresholds within each lighting condition (across all frequencies) differed as a function of Lighting Condition (main effect: $F(2,46) = 34.84$, $p < 0.001$, $\eta_p^2 = 0.602$), with lower thresholds found in the mesopic condition (at 16 Hz) relative to each of the dark (at 10 Hz; $F(1, 23) = 54.88$, $p < 0.001$, $\eta_p^2 = 0.705$) and light (at 20 Hz; $F(1, 23) = 66.42$, $p < 0.001$, $\eta_p^2 = 0.743$) conditions. No difference was found between the lowest light and dark condition thresholds ($p = 0.772$).

For the dark condition, a linear model (AICc = 193.02) produced a better fit than the quadratic model (AICc = 194.34). For the mesopic condition, a quadratic model (AICc = 199.46) produced a better fit than the linear model (AICc = 289.71). For the photopic condition, a quadratic model (AICc = 37.02) produced a better fit than the linear model (AICc = 64.34).

The regression analyses (predicting threshold as a function of frequency) resulted in the following equations (see Fig. 2b):

Dark Threshold = $-3.130 + 0.203 \times$ Frequency; adj-$R^2 = 0.650$, $p < 0.001$.
Mesopic Threshold = $13.682 - 1.800 \times$ Frequency $+ 0.056 \times$ Frequency^2; adj-$R^2 = 0.634$, $p < 0.001$.
Photopic Threshold = $6.587 - 0.655 \times$ Frequency $+ 0.014 \times$ Frequency^2; adj-$R^2 = 0.905$, $p < 0.001$.

Participants consistently reported that phosphenes in the mesopic and dark conditions increased in luminosity (compared to their background) as the stimulation intensity increased. Under photopic conditions, participants consistently reported that the flashing of the phosphene appeared to make their field of view seem darker compared to pre-stimulation perceived luminance levels, where the flashing alternated between a visible flash and the previous level of general luminosity. This distinction became stronger as stimulation intensity increased. Four participants reported seeing coloured phosphenes, however these reports were not consistent across those individuals, nor within individuals across sessions.

Discussion

The aim of the study was to determine the relations between phosphene detection thresholds and both ambient lighting and tES stimulation frequency. Those relations enabled us to test whether: (1) the recently reported evidence of greater sensitivity to tES-induced phosphenes at 16 Hz[18,19,35], as opposed to the standard view that sensitivity is greatest at 20 Hz[5,7,11,20], and (2) whether this apparent contradiction in the literature was due to ambient lighting.

As can be seen in Fig. 2, each of the ambient lighting conditions had a unique phosphene threshold relation with stimulation-frequency, whereby thresholds increased with frequency in the dark condition, reduced with frequency in the photopic condition, and reduced with frequency from 10 to 16 Hz and increased from 16 to 20 Hz in the mesopic condition. Corresponding to this, threshold minima under dark, mesopic and photopic conditions were found at 10 Hz, 16 Hz and 20 Hz respectively. This demonstrates that both ambient lighting condition and stimulation frequency are important for determining the minimum current required to induce phosphenes. Correlation analyses showed consistent phosphene thresholds across sessions, indicating that order effects and the choice of which electrode was the cathode or anode had no significant effect on the results.

The lowest thresholds overall were found under mesopic conditions (at 16 Hz), with thresholds significantly higher under both dark (at 10 Hz) and photopic (at 20 Hz) conditions. This means that threshold estimates obtained using the standard photopic or dark conditions, regardless of frequency, will overestimate the current required to induce phosphenes. It follows that guidelines using phosphene detection to set exposure restrictions based on data obtained in dark or photopic conditions (e.g.[14]), may underestimate the effect of electric current on neural processes (by 56–60%). It is important to note that even though such exposure guidelines typically rely on research using magnetic fields (rather than tES) to induce phosphenes, in both cases the cause of the phosphene is the current flowing through neural tissue[11], which stimulates the same physiological processes. It follows that the present results are also applicable to research using magnetic fields to induce phosphenes, and thus to low frequency electromagnetic field exposure guidelines.

The present data also resolve the apparent discrepancy between recent research, which found thresholds for phosphene detection at 16 Hz[18,19,35], and studies reporting thresholds at either 10 or 20 Hz (e.g.[15,20]). That is, the present findings demonstrate that mesopic conditions result in greatest sensitivity at 16 Hz[18,19], whereas dark and photopic conditions (similar to those in past studies) result in greatest sensitivity at 10 and 20 Hz tES respectively. There is thus no inconsistency, only predictable differences due to the differing ambient lighting conditions used. Overall, the results of this study relating to ambient lighting and frequency dependence are

consistent across multiple forms of tES, whether using tACS[11,15,18] or sinusoidal tDCS[19]. While there are differences in the levels of current required to induce phosphenes across studies, this is a likely product of different methodological choices, as there are a multitude of variables that can change this threshold. For example, even when using the same montage on the same sample, the threshold values can vary based on the size, shape and surface area of the electrodes, the material which the electrode is made from, and the conductivity medium selected (e.g., conductive gel, electrolyte-soaked sponges). Changing any of these variables will change the volume conduction characteristics of the overall circuit, resulting in different levels of current density at the retina[30]. As a result, while the comparison of thresholds across studies is of little value, the findings relating to frequency and lighting remain consistent despite any variations in stimulation methodology.

Although it is tempting to suggest that different physiological processes are being engaged during tES in the mesopic relative to dark and photopic conditions, a simpler explanation may be sufficient to explain the results. As can be seen in Fig. 2, the shape of the estimated distribution of thresholds in the mesopic condition matched that of the dark condition at frequencies below the approximate crossover point at 16 Hz, and also matched that of the photopic condition at frequencies above the 16 Hz crossover point. Taken together, it would thus appear that the mesopic condition may simply represent the combination of physiological processes normally engaged in each of the dark and photopic conditions.

Consistent with this hypothesis, there is evidence that the observed frequency dependence in tES-induced phosphene research can be explained by differences in the relative activity of rod-based and cone-based vision[36,37]. Cells related to rod vision, which are primed to respond in dark conditions, are maximally sensitive to stimulation at circa 10 Hz[38–40], whereas cells related to cone vision, which are primed to respond in photopic conditions, are maximally sensitive to stimulation at circa 20 Hz[27,37]. In itself this would not explain the magnitude of threshold reduction in the mesopic condition (60% and 56%, relative to the dark and photopic conditions respectively), particularly given that 16 Hz is far from the ideal stimulation frequency for either rod- or cone-related cells. However, when coupled with what is known about the rod-cone processing delay, this would appear a viable hypothesis. That is, there is a delay between rod- and cone-related cell processing under mesopic conditions[41], but as the stimulation frequency reaches approximately 15 Hz, rods and cones start to fire in phase, which increases the signal at both rods and cones and enhances the perceptibility of the stimulation[42]. This critical 15 Hz frequency also approximates the crossover point of the dark and photopic regression estimates (see Fig. 2b), indicating that the rod-cone phase delay mechanism may be behind the lower overall thresholds at the nearby 16 Hz frequency in mesopic conditions. Further research would be required to test this hypothesis.

While high levels of current can result in discomfort or pain at the site of stimulation[43], these effects are typically found at stimulation strengths exceeding the maximum used in this study. The maximum strength of stimulation (1500 μA) in the present study was selected in order to avoid such side effects. One subject reported an unpleasant itching-like sensation at stimulation levels above 900 μA, however the sensation immediately ceased upon termination of the stimulation. Despite multiple enquiries during each testing session, no other participant reported any negative side effects, either during or after stimulation. Indeed, as the study deliberately kept current levels low to identify thresholds, this reduced the opportunity to obtain meaningful information about the phosphene experience more generally, which may otherwise have helped shed light on the underlying physiology responsible for phosphene induction. Of particular relevance is the degree to which phosphenes were perceived in chromatic (as opposed to achromatic) colour, as that could provide evidence for the relative mechanistic roles of rods and cones, as a function of frequency and lighting condition. However, given the low current strengths used in the study, only four participants reported seeing chromatic colour, and reports were not consistent across those individuals, nor within each individual across sessions. We thus do not believe that these anecdotal reports are sufficient to enable interpretation.

Conclusion

The present study has shown that the apparent contradiction in the literature, in terms of tES stimulation frequency and phosphene detection threshold, was due to the different ambient lighting conditions used across past studies. That is, whereas thresholds under dark and photopic conditions are lowest for 10 and 20 Hz stimulation respectively, they do not represent overall thresholds, which occur at 16 Hz in mesopic conditions. The magnitude of threshold overestimation was very large (60 and 56% for dark and photopic conditions respectively), and thus important for application of tES research. Physiological considerations suggest that the lower thresholds in mesopic conditions, and particularly at 16 Hz stimulation, may be due to the involvement of both rod and cone photoreceptors, but further research is required to determine this. Importantly, our research also shows (for the first time) that dark, mesopic and photopic lighting conditions each have their own unique phosphene threshold relation with stimulation-frequency.

Data availability

The dataset resulting from this experiment is available from the corresponding author upon reasonable request.

Received: 10 December 2021; Accepted: 21 April 2022
Published online: 11 May 2022

References

1. Buzsáki, G. & Draguhn, A. Neuronal oscillations in cortical networks. *Science* **304**, 1926–1929 (2004).
2. Herrmann, C. S., Fründ, I. & Lenz, D. Human gamma-band activity: A review on cognitive and behavioral correlates and network models. *Neurosci. Biobehav. Rev.* **34**, 981–992 (2010).
3. Bosman, C. A., Lansink, C. S. & Pennartz, C. M. Functions of gamma-band synchronization in cognition: From single circuits to functional diversity across cortical and subcortical systems. *Eur. J. Neurosci.* **39**, 1982–1999 (2014).

4. Schwiedrzick, C. Retina or visual cortex? The site of phosphene induction by transcranial alternating current stimulation. *Front. Integr. Neurosci.* **3**(6), 1–2 (2009).
5. Schutter, D. J. & Hortensius, R. Retinal origin of phosphenes to transcranial alternating current stimulation. *Clin. Neurophysiol.* **121**, 1080–1084 (2010).
6. Kar, K. & Krekelberg, B. Transcranial electrical stimulation over visual cortex evokes phosphenes with a retinal origin. *J. Neurophysiol.* **108**, 2173–2178 (2012).
7. Rohracher, H. Über subjective Lichterscheinungen bei Reizung mit Wechselströmen [About subjective light effects when stimulated with alternating currents]. *Z. Sinnesphysiology.* **66**, 164–181 (1935).
8. Brindley, G. S. The site of electrical excitation of the human eye. *J. Physiol.* **127**, 189–200 (1955).
9. Meier-Koll, A. Elektrostimulation der Netzhaut zur opthalmologischen Differentialdiagnose [Electrostimulation of the retina in ophthalmic differential diagnosis]. *Biomed. Technol.* **18**(3), 92–97 (1973).
10. Adrian, D. J. Auditory and visual sensations stimulated by low-frequency electric currents. *Radio Sci.* **12**(6S), 243–250 (1977).
11. Lövsund, P., Öberg, P. Å., Nilsson, S. E. G. & Reuter, T. Magnetophosphenes: A quantitative analysis of thresholds. *Med. Biol. Eng. Comput.* **18**(3), 326–334 (1980).
12. Attwell, D. Interaction of low frequency electric fields with the nervous system: The retina as a model system. *Radiat. Prot. Dosim.* **106**, 341–348 (2003).
13. Schutter, D. J. Cutaneous retinal activation and neural entrainment in transcranial alternating current stimulation: A systematic review. *Neuroimage* **140**, 83–88 (2016).
14. International Commission on Non-Ionizing Radiation Protection. Guidelines for limiting exposure to time-varying electric and magnetic fields (1 Hz to 100 kHz). *Health Phys.* **99**(6), 818–836 (2010).
15. Kanai, R., Chaieb, L., Antal, A., Walsh, V. & Paulus, W. Frequency-dependent electrical stimulation of the visual cortex. *Curr. Biol.* **18**(23), 1839–1843 (2008).
16. Jasper, H. H. Cortical excitatory state and variability in human brain rhythms. *Science* **83**, 259–260 (1936).
17. Palva, S. & Palva, J. M. New vistas for alpha-frequency band oscillations. *Trends Neurosci.* **30**, 150–158 (2007).
18. Evans, I. D., Palmisano, S., Loughran, S. P., Legros, A. & Croft, R. J. Frequency-dependent and montage-based differences in phosphene perception thresholds via transcranial alternating current stimulation. *Bioelectromagnetics* **40**, 365–374 (2019).
19. Evans, I. D., Palmisano, S. & Croft, R. J. Retinal and cortical contributions to phosphenes during transcranial electrical current stimulation. *Bioelectromagnetics* **42**(2), 146–158 (2021).
20. Schwarz, F. Über die elektrische Reizbarkeit des Auges bei Hell- und Dunkeladaptation [About the electrical sensitivity of the eye in light and dark adaptation]. *Pflügers Arch. Eur. J. Physiol.* **249**, 76–86 (1947).
21. de Lange, H. Research into the dynamic nature of the human fovea—Cortex systems with intermittent and modulated light. I: Attenuation characteristics with white and colored light. *J. Opt. Soc. Am.* **48**(11), 777–784 (1958).
22. Goldstein, E. B. *Sensation and Perception* 6th edn. (Wadsworth Group, 2002).
23. Barlow, H. B. Dark and light adaptation: Psychophysics. In *Visual Psychophysics*, 1–28 (Springer, 1972).
24. Umino, Y., Guo, Y., Chen, C. K., Pasquale, R. & Solessio, E. Rod photoresponse kinetics limit temporal contrast sensitivity in mesopic vision. *J. Neuro* **39**(16), 3041–3305 (2019).
25. Kelly, D. H. Visual responses to time-dependent stimuli: Amplitude sensitivity measurements. *J. Opt. Soc. Am.* **51**(4), 422–429 (1961).
26. Dai, X. *et al.* The frequency-response electroretinogram distinguishes cone and abnormal rod function in rd12 mice. *PLoS One* **10**(2), e0117570. https://doi.org/10.1371/journal.pone.0117570 (2015).
27. Adelson, E. H. Saturation and adaptation in the rod system. *Vis. Res.* **22**, 1299–1312 (1982).
28. Stockman, A. & Sharpe, L. T. Into the twilight zone: The complexities of mesopic vision and luminous efficiency. *Ophthalmic Physiol. Opt.* **26**(3), 225–239 (2006).
29. Keel, J. C., Smith, M. J. & Wassermann, E. M. A safety screening questionnaire for transcranial magnetic stimulation. *Clin. Neurophysiol.* **112**, 720 (2000).
30. Laakso, I. & Hirata, A. Computational analysis shows why transcranial alternating current stimulation induces retinal phosphenes. *J. Neural Eng.* **10**, 046009. https://doi.org/10.1088/1741-2560/10/4/046009 (2013).
31. Watson, A. B. & Pelli, D. G. QUEST: A Bayesian adaptive psychometric method. *Percept. Psychophys.* **33**(2), 113–120 (1983).
32. Kleiner, M., Brainard, D. & Pelli, D. What's new in Psychtoolbox-3?. *Perception [ECVP Abstract Supplement).* **36**(14), 1 (2007).
33. Mazzi, C., Savazzi, S., Abrahamyam, A. & Ruzzoli, M. Reliability of TMS phosphene threshold estimation: Toward a standardized protocol. *Brain Stimul.* **10**, 609–617 (2017).
34. Akaike, H. Theory and an extension of the maximum likelihood principal. In *International Symposium on Information Theory* (Akademiai Kaiado, 1973).
35. Thiele, C., Zaehle, T., Haghikia, A. & Ruhnau, P. Amplitude modulated transcranial alternating current stimulation (AM-TACS) efficacy evaluation via phosphene induction. *Sci. Rep.* **11**(1), 1–10 (2021).
36. Neftel, W. B. Ein Fall von vorübergehender Aphasie mit bleibender medialer Hemiopie des rechten Auges, nebst einem Beitrage zur galvanischen Reaction des optischen Nervenapparates im gesunden und kranken Zustande [A case of temporary aphasia with permanent medial hemiopia of the right eye, together with a contribution to the galvanic reaction of the optical nervous apparatus in healthy and diseased states]. *Archiv fur Psychiatrie und Nervenkrankheiten.* **8**, 409–431 (1878).
37. Motokawa, K. & Iwama, K. Resonance in electrical stimulation of the eye. *Tohoku J. Exp. Med.* **53**, 201–206 (1950).
38. Benardete, E. A., Kaplan, E. & Knight, B. W. Contrast gain control in the primate retina: P cells are not X-like, some M cells are. *Visual Neurosci.* **8**, 483–486 (1992).
39. Lee, B. B., Pokorny, J., Smith, V. C. & Kremers, J. Responses to pulses and sinusoids in macaque ganglion cells. *Vis. Res.* **34**, 3081–3096 (1994).
40. Kaplan, E. & Benardete, E. The dynamics of primate retinal ganglion cells. *Prog. Brain Res.* **134**, 17–34 (2001).
41. MacLeod, D. I. Rods cancel cones in flicker. *Nature* **235**(5334), 173–174 (1972).
42. Sharpe, L. T., Stockman, A. & MacLeod, D. I. Rod flicker perception: Scotopic duality, phase lags and destructive interference. *Vis. Res.* **29**(11), 1539–1559 (1989).
43. World Health Organisation. *Extremely Low Frequency Fields*. https://apps.who.int/iris/rest/bitstreams/51837/retrieve (WHO Press, 2007).

Author contributions

All authors planned the study. I.E. collected and processed the data. All authors participated in interpreting the results, writing the manuscript and have approved the final version.

Funding

Grant sponsor: Centre for Population Health Research on Electromagnetic Energy, grant number APP1060205.

Competing interests
The authors declare no competing interests.

Additional information
Supplementary Information The online version contains supplementary material available at https://doi.org/10.1038/s41598-022-11755-y.

Correspondence and requests for materials should be addressed to I.E.

Reprints and permissions information is available at www.nature.com/reprints.

Publisher's note Springer Nature remains neutral with regard to jurisdictional claims in published maps and institutional affiliations.